



Ketamine's fast antidepressant drug response: Biosignatures and pathways

Dissertation

Der Fakultät für Biologie
der Ludwig-Maximilians-Universität
München

Vorgelegt von

Katja Weckmann

München, Februar 2017

Erstgutachter: PD Dr. Mathias V. Schmidt

Zweitgutachter: Prof. Dr. Laura Busse

Promotionsgesuch eingereicht am: 20.02.2017

Tag der mündlichen Prüfung: 27.09.2017

The work presented in this thesis was performed in the laboratory of Prof. Dr. Christoph Turck, Department of Translational Psychiatry, Research Group of Proteomics and Biomarkers, Max Planck Institute of Psychiatry, Munich, Germany.

Eidesstattliche Erklärung

Ich versichere hiermit an Eides statt, dass die vorgelegte Dissertation von mir selbständig und ohne unerlaubte Hilfe angefertigt ist.

München, den 02.01.2018

.....

(Katja Weckmann)

Erklärung

Hiermit erkläre ich,

- dass die Dissertation nicht ganz oder in wesentlichen Teilen einer anderen Prüfungskommission vorgelegt worden ist.
- dass ich mich anderweitig einer Doktorprüfung ohne Erfolg nicht unterzogen habe.

München, den 02.01.2018

.....

(Katja Weckmann)

Table of contents

| | |
|--|----|
| Abstract | 7 |
| Abbreviations | 8 |
| 1.0 Introduction..... | 12 |
| 1.1 Major depressive disorder: Clinical characteristics and classification systems | 12 |
| 1.1.1 Diagnostic and Statistical Manual of Mental Disorders (DSM) | 13 |
| 1.1.2 International Statistical Classification of Diseases and Related Health Problems (ICD) | 13 |
| 1.1.3 Research domain criteria (RDoC) | 14 |
| 1.2 The functional neuroanatomy of depression..... | 15 |
| 1.3 Treatment options for MDD: Monoamines and beyond | 16 |
| 1.3.1 Monoaminergic hypothesis of depression..... | 16 |
| 1.3.2 The corticosteroid receptor hypothesis of depression | 18 |
| 1.3.3 The neuronal plasticity hypothesis of depression..... | 20 |
| 1.4 Animal models of depression | 30 |
| 1.4.1 Models of acute stress | 30 |
| 1.4.2 Hormones of the HPA-axis | 31 |
| 1.4.3 Models of chronic stress..... | 32 |
| 1.5 Biomarkers in MDD research..... | 33 |
| 2.0 Thesis project aims and objectives..... | 34 |
| 3.0 Materials and Methods | 35 |
| 3.1 Chemicals and consumables | 35 |
| 3.2 Buffers and solutions..... | 37 |
| 3.3 Software and equipment..... | 39 |
| 3.4 Animals and ketamine treatment | 39 |
| 3.5 Forced swim test (FST) | 40 |
| 3.6 Isolation of blood plasma | 40 |
| 3.7 Isolation of cytoplasmic (CF) and membrane-associated (MF) proteins | 40 |
| 3.8 Protein concentration determination with the Bradford assay..... | 41 |

| | |
|---|----|
| 3.9 Protein concentration determination with the Lowry assay | 41 |
| 3.10 Western Blot..... | 41 |
| 3.11 OxyBlot™ Protein oxidation detection..... | 42 |
| 3.12 Total antioxidant capacity (TAC) | 42 |
| 3.13 Isolation of mitochondria | 42 |
| 3.14 Blue native-polyacrylamide gel electrophoresis (BN-PAGE) | 43 |
| 3.15 Sample preparation for LC-ESI-MS/MS analyses..... | 43 |
| 3.15.1 Protein sample preparation for the identification of OXPHOS ETC protein complexes | 43 |
| 3.15.2 Protein sample preparation for quantitative proteomics analyses | 43 |
| 3.15.3 In-gel-trypsin digestion and peptide extraction..... | 44 |
| 3.16 Protein identification with LTQ Orbitrap XL™ | 44 |
| 3.17 Quantitative proteomics analyses with Q Exactive™ Hybrid Quadrupole-Orbitrap™ Mass Spectrometer..... | 45 |
| 3.18 OXPHOS protein complex in-gel-enzymatic activity measurement..... | 46 |
| 3.19 Ketamine treated mouse primary hippocampal neurons | 46 |
| 3.20 Cytotoxicity measurement through the MTT assay | 47 |
| 3.21 Isolation of polar metabolites | 47 |
| 3.21.1 Isolation of polar metabolites from mouse tissue | 47 |
| 3.21.2 Isolation of polar metabolites from mouse blood plasma..... | 47 |
| 3.21.3 Isolation of polar metabolites from PHN | 47 |
| 3.22 Targeted metabolomics analysis through selected reaction monitoring (SRM) with 5500 QTRAP triple quadrupole..... | 48 |
| 3.23 Statistics and data analyses..... | 49 |
| 3.23.1 Identification of significant metabolite and protein level alterations | 49 |
| 3.23.2 Identification of significantly enriched pathways | 49 |
| 3.23.3 Calculation of metabolite pair ratios..... | 49 |
| 3.23.4 Identification of metabolite biomarker candidates | 49 |
| 4.0 Results | 51 |
| 4.1 Investigating the antidepressant-like effect of ketamine through the FST..... | 51 |

| | |
|--|-----|
| 4.2 Metabolomics profiling of ketamine treated mice and primary hippocampal neurons..... | 52 |
| 4.2.1 Comparative Metabolomics profiling of defined mouse brain regions, the liver, blood, and mouse primary hippocampal neurons | 53 |
| 4.2.1 Time-dependent metabolomics profiling of the hippocampus | 56 |
| 4.2.3 Biomarker discovery for ketamine’s antidepressant-like effects..... | 66 |
| 4.3 Time-dependent hippocampal proteome profiling..... | 69 |
| 4.3.1 Ketamine’s effect on the glutamatergic and GABAergic system..... | 73 |
| 4.3.2 Ketamine’s impact on the mitochondrial energy metabolism, protein damage and quality control system | 78 |
| 4.3.3 A potential signaling cascade for ketamine drug action | 86 |
| 4.4 Analyses of mitochondrial OXPHOS protein complexes with blue native-polyacrylamide gel electrophoresis (BN-PAGE)..... | 87 |
| 4.4.1 Isolation of mitochondria | 87 |
| 4.4.2 Separation and identification of the OXPHOS protein complexes with BN-PAGE and LC-MS/MS analyses | 88 |
| 4.4.3 OXPHOS protein complex in-gel-enzymatic activity measurement | 89 |
| 5.0 Discussion..... | 92 |
| 5.1 Ketamine’s fast antidepressant-like effect..... | 92 |
| 5.2 A comparative metabolomics profiling analyses..... | 92 |
| 5.3 Time-dependent hippocampal metabolomics and proteomics profiling analyses..... | 94 |
| 5.3.1 Ketamine’s impact on the mitochondrial energy metabolism..... | 94 |
| 5.3.2 Ketamine’s effects on the antioxidant defense and quality control system..... | 96 |
| 5.3.3 A potential novel signaling cascade for ketamine’s antidepressant-like effects | 97 |
| 5.3.4 Ketamine’s effects on the glutamatergic and GABAergic system | 98 |
| 5.4 An additional and novel model for Ketamine’s antidepressant effect | 100 |
| 5.4 Clinical relevance..... | 102 |
| 6.0 Literature | 103 |
| 7.0 Acknowledgements | 129 |
| Curriculum Vitae..... | 130 |

Abstract

Less than 50% of all patients with major depressive disorder (MDD) treated with currently available antidepressants (ADs) show full remission. Moreover, about one third of the patients suffering from MDD does not respond to conventional ADs and develop treatment-resistant depression (TRD).

In 2000 Berman and his colleagues demonstrated for the first time a rapid antidepressant effect of a low dose of ketamine, acting within 2 hours (h) and 4h and lasting up to 10 days. Ketamine, a non-competitive, voltage-dependent N-Methyl-D-aspartate receptor (NMDAR) antagonist, is a drug that is usually used for anaesthesia. An antidepressant effect of ketamine can be observed in patients suffering from TRD. Moreover, ketamine diminished suicidal ideation. These clinical findings provide a promising basis for novel therapeutic targets and development in MDD. Previous studies showed that pharmacological treatment with ketamine results in a glutamate burst, increased brain-derived neurotrophic factor (BDNF) levels, Tropomyosin receptor kinase B (TrkB) receptor and mammalian target of rapamycin complex 1 (mTORC1) activation, elevated synaptic protein synthesis and integration of α -amino-3-hydroxy-5-methyl-4-isoxazolepropionic acid receptors (AMPA) into the synaptic membrane. These processes strengthen glutamatergic synapses resulting in synaptogenesis.

The overall aim of this thesis is to identify biosignatures and biomolecular pathways affected by ketamine treatment. Results from my research in mice can aid in the development of novel fast acting ADs with a similar mode of action as ketamine, however, with fewer side-effects.

Taken together, the results of the present study implicate the mitochondrial energy metabolism as a downstream effector of ketamine treatment in the hippocampus (HPC), which includes processes such as glycolysis, citrate cycle and oxidative phosphorylation (OXPHOS). Ketamine significantly alters protein levels of the electron transport chain (ETC) as well as the energy status measured by ATP, ADP, NADH, NAD, GTP and GDP metabolite levels and the respective ratios. Furthermore, ketamine affects the antioxidant capacity by changing enzymes and molecules; thereby finally leading to decreased carbonylated (damaged) protein levels.

In addition, ketamine impacts the gamma-aminobutyric acid (GABA)ergic and glutamatergic system by altering GABA, glutamate and glutamine metabolite levels and ratios as well as changing GABA_A and AMPAR protein levels. My proposed novel model describes an elevation of synaptic Ca^{2+} upon neuronal activation that leads to mitochondrial enrichment in the synaptic compartment. Furthermore, activated mTORC1 induces mitochondrial metabolism and promotes adenosine triphosphate (ATP) production to cope with the elevated energy demand in activated synapses.

Abbreviations

| | |
|---------------|--|
| 4E-BP1 | Eukaryotic initiation factor 4E-binding protein 1 |
| 5-HT | 5-hydroxytryptamine (serotonin) |
| ACN | Acetonitrile |
| ACTH | Adrenocorticotrophic hormone |
| AD | Antidepressant |
| ADP | Adenosine diphosphate |
| Akap1 | A-kinase anchor protein 1, mitochondrial |
| AMPA | α -amino-3-hydroxy-5-methyl-4-isoxazolepropionic acid receptors |
| AMPK | Adenosinmonophosphate-activated proteinkinase |
| APS | Ammonium persulfate |
| ATP | Adenosine triphosphate |
| ATP5a | Complex V ATP synthase subunit alpha |
| AVP | Arginine-vasopressin |
| BDNF | Brain-derived neurotrophic factor |
| BN-PAGE | Blue native-polyacrylamide gel electrophoresis |
| BP | blood plasma |
| BSA | Bovine serum albumin |
| CaMKII | Ca ²⁺ /calmodulin-dependent protein kinase II |
| cAMP | Cyclic adenosine monophosphate |
| CDP | Cytidine diphosphate |
| CF proteins | Cytoplasmic proteins |
| CMS | Chronic mild stress |
| CNQX | 6-cyano-7-nitroquinoxaline-2,3-dione |
| CoA | Coenzyme A |
| CRBL | Cerebellum |
| CREB | cAMP-response element binding protein |
| CRF | Corticotropin-releasing factor |
| CSF | Cerebrospinal fluid |
| Cyc 1 | Cytochrome c1, heme protein, mitochondrial |
| DAB | 3:30-Diaminobenzidine |
| DDM | Dodecylmaltosid |
| dGDP | Deoxyguanosine diphosphate |
| dGTP | Deoxyguanosine triphosphate |
| DMSO | Dimethyl sulfoxide |
| DNA | Deoxyribonucleic acid |
| DNPH | 2,4-Dinitrophenylhydrazine |
| DNP-hydrazone | 2,4-Dinitrophenylhydrazone |
| Drp1 | Dynammin-related protein 1 |
| DSM | Diagnostic and statistical manual of mental disorders |
| dTMP | 5-Thymidylic acid |
| DTT | Dithiothreitol |
| EAAT | Excitatory amino acid transporters |
| EDTA | Ethylenediaminetetraacetic acid |
| eEF2 | Eukaryotic elongation factor 2 |
| EPSC | Excitatory postsynaptic current |

| | |
|----------------------|--|
| ESI | Electrospray ionization |
| FA | Formic acid |
| FC | Fold change |
| FDR | False discovery rate |
| FST | Forced swim test |
| FT | Fourier transform |
| GABA | Gamma-aminobutyric acid |
| GABA _A R1 | Gamma-aminobutyric acid type A receptor subunit 1 |
| GABAR | Gamma-aminobutyric acid receptor |
| GAT1 | GABA transporter 1 |
| GDP | Guanosine diphosphate |
| GR | Glucocorticoid receptor |
| Gria | AMPA receptor subunit |
| GSK-3 β | Glycogen synthase-kinase-3 β |
| GTP | Guanosine triphosphate |
| h | Hours |
| HMDB | Human metabolome database |
| HPA | Hypothalamic pituitary adrenal |
| HPC | Hippocampus |
| IAM | Iodacetamide |
| ICD | International Statistical Classification of Diseases and Related Health Problems |
| iGluR | Ionotropic glutamate receptor |
| IPSP | Inhibitory postsynaptic potential |
| LC | Liquid chromatography |
| LH | Learned helplessness |
| LTD | Long-term depression |
| LTP | Long-term potentiation |
| MAOI | Monoamine oxidase inhibitor |
| MAPK | Mitogen activated protein kinase |
| MBP | Myelin basic protein |
| MDD | Major depressive disorder |
| MF proteins | Membrane-associated proteins |
| mGluR | Metabotropic Glutamate receptor |
| MOG | Myelin oligodendrocyte glycoprotein |
| MR | Mineralcorticoid receptor |
| mRNA | Messenger ribonucleic acid |
| Mrps15 | 28S ribosomal protein S15, mitochondrial |
| Mrps27 | 28S ribosomal protein S27, mitochondrial |
| Mrps35 | 28S ribosomal protein S35, mitochondrial |
| Mrps5 | 28S ribosomal subunit S5, mitochondrial |
| MS | mass spectrometry |
| MS/MS | tandem mass spectrometry |
| MTCOI | Complex III cytochrome C oxidase subunit I |
| mTORC1 | Mammalian target of rapamycin complex 1 |
| MTT | 3-(4,5-dimethylthiazol-2-yl)-2,5-diphenyltetrazolium |
| NAD | Nicotinamide adenine dinucleotide |

| | |
|---------------|--|
| NaSSA | Noradrenergic and specific serotonergic AD |
| NBQX | 2,3-Dihydroxy-6-nitro-7-sulfamoyl-benzo-chinoxaline-2,3-dione |
| NBT | Nitro blue tetrazolium |
| Ndufaf7 | NADH dehydrogenase [ubiquinone] complex I, assembly factor 7 |
| Ndufb8 | NADH dehydrogenase [ubiquinone] oxidoreductase subunit b8 |
| Ndufv2 | NADH dehydrogenase [ubiquinone] flavoprotein 2 |
| NMDAR | N-Methyl-D-aspartate receptor |
| NMDAR1 | N-Methyl-D-aspartate receptor subunit 1 |
| NSF | Novelty-suppressed feeding |
| Otub1 | Ubiquitin thioesterase |
| OXPHOS | Oxidative phosphorylation |
| pAMPK | phosphorylated AMPK |
| PFC | Prefrontal cortex |
| PGC1 α | Peroxisome proliferator-activated receptor gamma coactivator 1- α |
| PHN | Primary hippocampal neurons |
| PKA | cAMP-dependent proteinkinase A |
| PKC | Protein kinase C |
| PLS-DA | Partial least squares-discriminant analyses |
| PMS | Phenazine methosulfate |
| pmTORC1 | Phosphorylated mammalian target of rapamycin complex 1 |
| Prdx1 | Peroxiredoxin 1 |
| Prdx3 | Peroxiredoxin 3 |
| Prkar2a | cAMP-dependent protein kinase type II-alpha regulatory subunit |
| PSD-95 | Postsynaptic density protein 95 |
| Psmb7 | Proteasome subunit beta type-7 |
| Psmc1 | 26S proteasome non-ATPase regulatory subunit 1 |
| Psmc6 | 26S proteasome non-ATPase regulatory subunit 6 |
| Psmc8 | 26S proteasome non-ATPase regulatory subunit 8 |
| PVN | Paraventricular nucleus |
| RDoC | Research Domain Criteria |
| Rpl10 | 60S ribosomal protein L10 |
| Rpl18a | 60S ribosomal protein L18a |
| Rpl19 | 60S ribosomal protein L19 |
| Rpl28 | 60S ribosomal protein L28 |
| Rpl28 | 60S ribosomal protein L28 |
| SAM | Significance analysis of microarrays (proteins, metabolites) |
| SARI | 5-HT (serotonin) receptor antagonists/reuptake inhibitor |
| SDHA | Succinate dehydrogenase subunit A |
| SDHB | Succinate dehydrogenase subunit B |
| SDS | Sodium dodecyl phosphate |
| SNP | Single-nucleotide polymorphism |
| SNRI | Noradrenaline reuptake inhibitor |
| SRM | Selected reaction monitoring |
| SSRI | Serotonin reuptake inhibitor |
| TAC | Total antioxidant capacity |
| TCA | Tricyclic AD |
| Tfam | mitochondrial transcription factor A |

| | |
|-----------|--|
| Tim23 | Translocase of inner membrane 23 |
| TRD | Treatment-resistant depression |
| TrkB | Tropomyosin receptor kinase B |
| TST | Tail suspension test |
| Ube2h | Ubiquitin-conjugating enzyme E2 H |
| UDP | Uridine diphosphate |
| UMP | Uridine 5'-monophosphate |
| Uqcrc2 | Ubiquinol-cytochrome C reductase core protein II |
| VIP-score | Variable influence of projection score |

1.0 Introduction

Mood disorders, in particular major depressive disorder (MDD) are the 4th leading cause of disability worldwide and might become the 2nd only to cardiovascular diseases in the next two decades^{1, 2}. The prevalence for mood disorders has been estimated at 21 million people across 28 European countries at an annual cost of 106 billion Euro^{3, 4}. Globally, approximately 350 million people suffer from MDD, where women are more likely to be affected than men with a ratio of approximately 2:1. However, men are frequently suffering from more severe forms of depression. The average age of onset is 32 years^{5, 6}. The currently available medications are antidepressants (ADs) which require a chronic long-term treatment of several, but at least two weeks, until a therapeutic effect is achieved^{7, 8}. Less than 50% of all patients treated with current antidepressants show full remission⁹. Moreover, about one third of the patients suffering from MDD does not respond to conventional ADs and therefore suffer from treatment-resistant depression (TRD)¹⁰. At its worst, 15% of severely depressed individuals commit suicide and overall 800 000 people die by suicide every year. Therefore, suicide is the second leading cause of death in the ages of 15 to 29-years⁶. MDD is a highly heterogeneous disorder and results from a complex interaction of social, environmental, psychological, and biological factors; however, the underlying cause remains elusive^{11, 12}. Epidemiology studies revealed that genetic as well as environmental factors contribute to the development of depression. Family, monozygotic and dizygotic twin studies lead to heritability estimates for the genetic component of approximately 50%. An increased susceptibility was observed for environmental factors like stressful and adverse life-events¹³⁻¹⁵.

1.1 Major depressive disorder: Clinical characteristics and classification systems

MDD is diagnosed based on the patient's self-reported experiences and symptoms and/or descriptions of a person's behavior by relatives or friends as well as a mental status examination¹⁶. To date, there is no laboratory or biomarker test for MDD¹⁷. MDD, also known as unipolar depression, stays in contrast to bipolar depression, which includes manic episodes in addition to the depressive symptoms. Manic episodes are characterized by increased or irritable mood, over-activity, pressure to speak, inflated self-esteem, and a decreased need for sleep. Depression can be long-lasting or recurrent, but it always and substantially impairs the person's ability to function at work/school or cope with daily life^{16, 18-20}.

The most widely used criteria for diagnosing MDD are the American Psychiatric Association's revised fourth edition of the *Diagnostic and Statistical Manual of Mental Disorders* (DSM-IV), and the World Health Organization's *International Statistical Classification of Diseases and Related Health Problems* (ICD-10), distinguishes between depressive episode (a single episode) and recurrent depressive disorder (for repeated episodes)^{18, 19}. The ICD-10 is generally used in European countries, whereas DSM-IV is used in the USA and many other non-European nations. However, the authors of both catalogues have worked towards conforming one another. Diagnostic criteria for MDD are essentially descriptions of symptoms that fall into one of four categories:

- affective or mood symptoms including depressed mood, feelings of worthlessness, or guilt
- behavioral symptoms including social withdrawal and agitation
- cognitive symptoms, or problems in thinking including difficulty with concentration or making decisions
- somatic or physical symptoms including sleep alterations like insomnia or hypersomnia^{18, 20}

1.1.1 Diagnostic and Statistical Manual of Mental Disorders (DSM)

The first DSM was published 1952 by the American Psychiatric Association and has gone through several revisions until DSM-IV, the fourth edition, was published in 2000. It lists over 200 mental health conditions and the criteria required for each in order to make an appropriate diagnosis.

DSM-IV describes MDD as a disorder that impairs an individual's function: socially, occupationally and educationally. According to DSM-IV a patient needs to meet the criteria of at least 5 of 9 specific symptoms for a diagnosis of MDD—present nearly every day and at least for two weeks. The two main symptoms of MDD are:

- depressed mood indicated by either a patient's self-report or observations made by others
- anhedonia which describes a decreased interest or pleasure in most activities that the patient had enjoyed before

One of these main symptoms must be present to meet the criteria for a diagnosis for MDD. Further symptoms can be:

- significant weight change (5%) or a change in appetite
- sleep alterations like Insomnia or hypersomnia
- fatigue or loss of energy
- change in activity like psychomotor agitation or retardation
- feelings of worthlessness or excessive or inappropriate guilt
- diminished ability to think, concentrate or being more indecisive
- suicidality with thoughts of death, suicide attempts, and suicide plans

Furthermore, the described symptoms must be present without being the direct physiological effects of a substance (e.g. a drug of abuse, a medication) or a general medical condition (e.g. hypothyroidism). MDD can further be divided into a single major depressive episode or recurrent, which describes the intermediate relief of depressive symptoms for at least two consecutive months²⁰.

1.1.2 International Statistical Classification of Diseases and Related Health Problems (ICD)

In the early 1960s, a programme with the Mental Health Programme of the World Health Organization started with the aim to improve the diagnosis and classification of mental disorders. In contrast to the DSM-IV, ICD-10 does not use the term MDD, however, it describes very similar criteria for the diagnosis and defines three typical depressive symptoms:

- depressed mood
- anhedonia
- reduced energy

Two of these three symptoms should be present in order to meet the criteria for depressive disorder diagnosis. Further symptoms include:

- change in appetite
- sleep alterations
- feelings of worthlessness and decreased self-confidence
- feelings of guilt

- diminished ability to think, concentrate
- lack of interest
- suicidality
- further somatic symptoms

Depending on the number and severity of symptoms a depressive episode can be mild, moderate, or severe and the term recurrent describes multiple depressive episodes without mania. In general, mild depression includes a minimum of 2 to 3 symptoms which describe a patient as generally impaired, but able to do most activities. In order to meet the criteria for moderate depression, an individual typically has to suffer from 3 or more symptoms. A diagnosis of moderate depression mostly involves great difficulties to do the daily activities. Severe depression includes even more symptoms than described for mild and moderate depression. Typically the patient loses his or her self-worth and has feelings of guilt. Suicidal ideation and suicidal attempts are often recognized and usually there are also somatic symptoms. Unlike DSM-IV, ICD-10 includes psychotic symptoms and, therefore, is differentiated in severe depression with or without psychotic symptoms¹⁸.

1.1.3 Research domain criteria (RDoC)

MDD is a highly heterogeneous brain disorder and neuroscientists, psychologists, and medical doctors in the field of psychiatry could therefore conclude that not only a single MDD exists rather than there are different subtypes of MDD. The symptoms described in DSM-IV and ICD-10 can vary from patient to patient, but would still meet the criteria for a diagnosis of MDD, however, patients might show a different set and amount of symptoms and co-morbidities. Another promoting aspect for subtypes of MDD comes from the fact that different patients respond to different AD treatments (personal communication, Thomas Kirmeier and Ulrike Schmidt, Max Planck institute of psychiatry, Munich). At present, MDD is categorized by diagnostic systems that does not incorporate neuroscience research information, and thus is suboptimal.

Another way of classification system involves the deconstruction of complex behaviors into so-called research domains or constructs to attempt the linkage of these to an underlying neurobiological system. RDoC was initiated in 2008 and developed by the National Institute of Mental Health. In contrast to DSM-IV and ICD-10, RDoC aims at understanding and categorizing the neurobiology of certain biological processes, subsequently looking to a range of the behavioral outcome, also described as domains or constructs. RDoC attempts “to create a new kind of taxonomy for mental disorders by bringing the power of modern research approaches in genetics, neuroscience, and behavioral science to the problem of mental illness.”

RDoC is based on four assumptions:

- a diagnostic approach based on the biology as well as the symptoms must not be constrained by the current DSM categories
- mental disorders are biological disorders involving brain circuits that implicate specific domains of cognition, emotion, or behavior
- each level of analysis needs to be understood across a dimension of function
- mapping the cognitive, circuit, and genetic aspects of mental disorders will yield new and better targets for treatment

The major preliminary RDoC research domains or constructs include a:

- negative valence systems (fear, anxiety, loss)
- positive valence systems (reward learning, reward valuation)
- cognitive systems (attention, perception, working memory, cognitive control),
- systems for social processes (attachment formation, social communication, perception of self, perception of others)
- arousal and modulatory systems (arousal, circadian rhythm, sleep, and wakefulness)

At the moment these domains or constructs can be studied in 8 different classes:

- genes
- molecules
- cells
- neural circuits
- physiology
- behaviors
- self-reports
- paradigms²¹

In contrast to DSM-IV and ICD-10, RDoC considers dimensions of behaviors that range from normal to abnormal and focuses on behavior-brain relationships and links them to clinical characteristics.

1.2 The functional neuroanatomy of depression

MDD involves different brain regions and neuronal connectivity networks. Clinical imaging and post-mortem studies of brains from depressed patients have revealed functional and structural alterations in several limbic and cortical brain regions, e.g. the prefrontal cortex (PFC), hippocampus (HPC), cingulate cortex, amygdala, and basal ganglia²²⁻²⁵.

The PFC is the cerebral cortex that covers the front part of the frontal lobe, which has been implicated in planning complex cognitive behaviors, personality expression, decision-making, and moderating social behavior. The basic function of the PFC is to orchestrate thoughts and actions in accordance with internal goals^{24, 25}. The HPC, cingulate cortex and the amygdala belong to the limbic system, a complex set of brain structures that supports a variety of functions including adrenaline flow, emotions, behaviors, motivation, long-term memory and olfaction. The HPC plays an important role in memory, learning, and spatial navigation²⁶. The cingulate cortex is a part of the limbic system that receives inputs from the thalamus and the neocortex and projects to the entorhinal cortex via the cingulum. It is involved in emotion formation and processing, learning and memory, which makes it highly influential in linking behavioral outcomes to motivation²⁷⁻²⁹. The amygdala regulates emotional reactions including fear responses, processing of memory, decision-making³⁰. The basal ganglia comprise multiple subcortical nuclei, which are strongly interconnected with the cerebral cortex, thalamus, and brainstem as well as several other brain areas. Their functions include the control of voluntary motor movements, procedural learning, as well as automatic behaviors such as bruxism, eye movements, cognition, and emotions. Further, they are implicated in action selection—deciding which of several possible behaviors should be executed³¹⁻³⁴.

MDD patients show neuronal atrophy and reduced volumes culminating in a decreased neuronal function of the HPC and the PFC. In contrast, the amygdala of MDD patients shows elevated activity and altered morphology³⁵⁻⁴⁶. The decreased volume of the HPC and PFC might therefore lead to several symptoms typically observed for MDD e.g. feelings of worthlessness or

excessive/inappropriate guilt, diminished ability to think and concentrate, or being more indecisive. An increased function of the amygdala may lead to a loss of control of emotions and mood, increased fear, anxiety, and hypothalamic pituitary adrenal (HPA)-axis dysregulation (also see section 1.3.2)³⁵. The altered connectivity of these regions might therefore underlie depressive symptoms.

1.3 Treatment options for MDD: Monoamines and beyond

The most common treatments for MDD are psychological treatments such as behavioral activation, cognitive behavioral therapy, and interpersonal psychotherapy. In addition, AD medication is used, such as tricyclic ADs (TCAs) and selective serotonin reuptake inhibitors (SSRIs)⁶. The first medications, therefore also called first generation of ADs, became available in the 1960s including monoamine oxidase inhibitors (MAOI) and TCAs^{47, 48}. Further research elucidating the mechanism of MAOIs and TCAs represented the main evidence for the monoamine hypothesis of depression and drove the pharmacological research for over 4 decades. In the 1980s and 1990s, several different classes of ADs, the so-called second generation of ADs were developed. These ADs include SSRIs, selective noradrenaline reuptake inhibitors (SNRIs), noradrenergic and specific serotonergic ADs (NaSSAs), and 5-hydroxytryptamine (5-HT) receptor antagonists/reuptake inhibitors (SARIs)^{49, 50}. They are based on the monoaminergic hypothesis of depression with a primary mechanism of monoamine reuptake inhibition and/or antagonism of selected monoamine receptors. Drugs acting on the monoaminergic system usually need at least 2 to 8 weeks before a therapeutic effect can be observed and each drug is only efficient in around 60–70% of patients⁸. Furthermore, the observed discrepancy between pharmacological and biochemical function of ADs (a few minutes) and their clinical mood altering responses (10–15 days) remains elusive⁵¹. A third generation of ADs is based on peptidergic, glutamatergic, or circadian rhythm-related mechanisms including corticotropin-releasing factor (CRF) 1 receptor antagonists, glutamatergic agents (N-Methyl-D-aspartate receptor (NMDAR) modulators, α -amino-3-hydroxy-5-methyl-4-isoxazolepropionic acid (AMPA)kines, metabotropic Glutamate receptor (mGluR) modulators), and melatonergic agonist/5-HT_{2c} receptor antagonist^{9, 52-57}.

Over the past 50 years different theories were developed trying to explain the pathobiology of MDD. These theories included alterations in the monoaminergic, glutamatergic, gamma-aminobutyric acid (GABA)ergic, or neurotrophin system, as well as changes in the regulation of the HPA axis and neuronal plasticity. The following sections will explain each hypothesis and the known or hypothesized underlying biomolecular mechanisms.

1.3.1 Monoaminergic hypothesis of depression

Monoamines are neurotransmitters like serotonin, noradrenaline, and dopamine, which are derived from aromatic amino acids like phenylalanine, tyrosine, tryptophan, and the thyroid hormones. The monoaminergic system is involved in the regulation of cognitive processes such as emotion, arousal, and certain types of memory^{58, 59}. Serotonin, also called 5-hydroxytryptamine (5-HT), regulates mood, appetite, sleep, but also influences some cognitive functions, including memory and learning⁶⁰⁻⁶². On the other hand, the general function of noradrenaline is to mobilize the brain and body for an action. Therefore, noradrenaline release is low during sleep and increases during wakefulness. Noradrenaline increases arousal and alertness and therefore rise during situations of stress^{63, 64}.

The basic version of the monoaminergic hypothesis of depression was developed after the discovery of TCAs and MAOIs in the 1960s^{47, 48}. MDD was recognized as a disorder with reduced availability of monoamines, in particular serotonin and noradrenaline and that ADs would simply act through an increase of extracellular synaptic monoamines⁶⁵. Afterwards, the sensitization status of monoamine receptors rather than monoamine availability was discussed to be more the reason for AD action and might therefore also play a role in the development of depression. The hypothesis was criticized after the discovery that inhibition of monoamine reuptake leads to a quick increase in synaptic monoamine availability within hours, but a delayed therapeutic effect of several weeks^{51, 66, 67}. It was proposed that slow adaptive changes in post-receptor signaling cascades and downstream mediators might be the key in explaining the delayed onset. The updated version of the hypothesis then integrated post-receptor signaling cascades with mechanism of gene expression including epigenetic mechanisms and several other processes including synaptic mechanisms, neurotrophic mechanisms and neurogenesis^{68, 69}.

In detail, the functional deficiency of serotonergic and noradrenergic neurotransmission in depression was inferred from the effects of TCAs and MAOIs at the monoamine metabolism. Both drug types increase synaptic monoamine levels. The first MAOI was recognized in the early 1950s when the antitubercular drug iproniazid showed mood-elevating properties⁷⁰. The action of MAOIs and TCAs are mediated either through inhibiting monoamine metabolism or reuptake, stimulating their release directly or indirectly through blocking presynaptic inhibitory autoreceptors⁷⁰. MAOIs are irreversible inhibitors of the main metabolic enzymes of the neurotransmitters noradrenaline, serotonin and dopamine. TCAs inhibit more or less selectively a number of membrane transporters of monoamines resulting in an increase of extracellular monoamines. Afterwards more selective ADs were developed, the so-called SSRIs, which resulted in the current mainstay of the treatment with drugs like paroxetine, which is the most commonly prescribed AD at the moment, fluoxetine, fluvoxamine, sertraline and citalopram⁷⁰. However, SSRIs seem to be less effective than TCAs in the treatment of severe depression⁷¹. For this reason SNRIs with lack of binding to monoamine receptors were developed, e.g., venlafaxine and milnacipran⁷⁰. By a screening in experimental animals, drugs with no or only weak monoamine reuptake inhibitory effect, but antagonistic effect at α_2 -adrenergic and 5-HT₂ receptors were discovered. Afterwards more specific ones were developed, but were not clinically demonstrated unambiguously. Overall, these drugs have the same effect in facilitating noradrenergic or serotonergic neurotransmission or both⁷⁰.

A subset of depressed patients showed lowered levels of noradrenaline⁷². Therefore, monoamine concentrations might be altered through disrupted synthesis, storage or release or postsynaptic receptors or messenger activity alterations.

Monoamine receptors account for approximately 5% of synapses in the brain⁵¹. Noradrenergic neurons have their cell bodies in the locus coeruleus in the brainstem and innervate the limbic system and neocortex⁷⁰. There are different subtypes of adrenergic receptors, which are all G-protein coupled receptors and mediate their underlying mechanism through a second messenger intercellular process. Noradrenaline seems to act on two types of receptors; postsynaptic excitatory α_1 receptors and inhibitory presynaptic α_2 autoreceptors on terminals of noradrenergic projection targets⁷⁰. Autoreceptor activation leads to an inhibition of noradrenaline release, thereby serving as a negative feedback loop to limit extracellular noradrenaline concentrations in the synaptic cleft. A second negative feedback loop lies within the locus coeruleus, where noradrenaline can also be released by local collaterals and dendrites of projection neurons^{70, 73-75}. Inhibition of α_2 autoreceptors

on noradrenergic cell bodies controls the whole noradrenergic system^{70, 73-75}. Moreover, synaptic noradrenaline concentrations in the locus coeruleus and the forebrain are controlled by reuptake of noradrenaline by membrane transporters, which is a target for ADs. The combination of a reuptake inhibitor and the simultaneous blockade of α_2 autoreceptors block both control mechanisms^{70, 76, 77}. However, a chronic treatment might desensitize α_2 autoreceptors⁷⁸⁻⁸⁰.

Serotonergic neurons have a very similar neurophysiology compared to the noradrenergic system. The cell bodies localize in the raphé nucleus of the midbrain and literally project to every brain region, but also to the same forebrain areas as noradrenergic neurons⁷⁰. The neurocircuitry of the limbic system is involved in the regulation of mood and behavior and is rich in serotonergic projections^{26, 81}. There are different kinds of 5-HT receptors, all of which are G-protein-coupled, except the 5-HT₃ receptor, which is an ion channel. The antidepressant effect targeting the serotonergic system is mainly mediated by enhancing serotonergic neurotransmission at postsynaptic 5-HT receptors. The regulatory mechanisms of this system are very similar to that observed for the noradrenergic system. However, in contrast to the noradrenergic system the autoreceptors of the cell bodies in the raphé nucleus and forebrain are different. At the cell body 5-HT autoreceptors control cell firing and at the terminals 5-HT autoreceptors regulate neurotransmitter release^{49, 70, 82-86}.

The lag-time of SSRIs and SSNIs therapeutic effect might be due to the activation of inhibitory autoreceptors at serotonergic and noradrenergic neurons to initially attenuate the effects of ADs, which upregulate the amount of serotonin and noradrenaline in the synaptic cleft⁷⁰. As a consequence, the noradrenaline and serotonin levels first decrease, however, increase again after approximately 4 weeks. This effect might be mediated by desensitization of these autoreceptors over time^{70, 87, 88}.

In the later and unified hypothesis the increase of synaptic noradrenaline and serotonin levels still seems to be critical for AD action. However, some downstream pathways like the increase of postsynaptic receptors in the cortex are probably responsible for AD drug action triggered by the elevated monoamine concentrations^{70, 89, 90}.

From the original study of neurotransmitter serotonin and noradrenaline concentrations and membrane receptor activity and sensitivity, neuroscientists started focusing more on mediated downstream signaling pathways, but also on stress regulatory system of an organism. Monoaminergic neurotransmitters, especially dopamine, serotonin, and noradrenaline regulate the HPA-axis. The latter is responsible for an individual's appropriate response to stressful situations, and regulates many body processes, including digestion, the immune system, mood and emotions, sexuality, and energy storage and expenditure^{91, 92}.

1.3.2 The corticosteroid receptor hypothesis of depression

An individual is (Human beings are) repeatedly exposed to stressful situations throughout their life and the organism reacts in order to maintain homeostasis on a biochemical, neurobiological, circadian, hormonal, and behavioral way. Disruptions in this homeostatic system can lead to depressive symptoms^{14, 15, 93-95}.

The HPA-axis integrates physical and psychosocial stimuli in order for an individual to react effectively to its environment^{14, 15}. It consists of a chain of neuronal and endocrine organs: the hypothalamus, the pituitary gland and adrenal gland. There are further anatomical connections between different brain areas such as the amygdala, HPC, and PFC which facilitate the activation of the HPA-axis⁹⁶. Sensory information arrives at the amygdala and is processed and conveyed to several brain regions involved in responses to fear. Fear-signaling inputs at the hypothalamus activate the sympathetic nervous system and the modulating systems of the HPA-axis. It is governed by secretion of CRF and arginine-vasopressin (AVP) from the hypothalamus which then activates the secretion of adrenocorticotrophic hormone (ACTH) into circulation from the pituitary gland^{94, 97}.

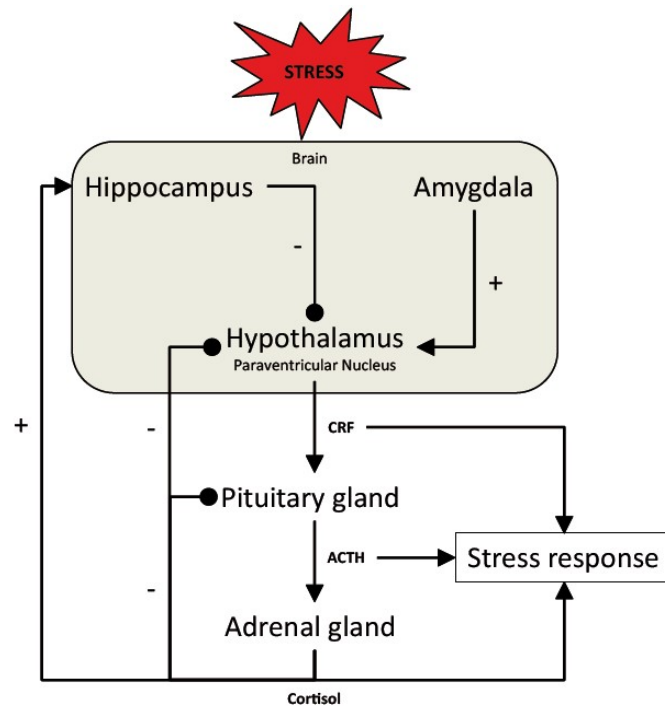


Figure 1: Schematic overview of the HPA-axis regulation in response to stress. Environmental stress is processed by the amygdala, which positively influences the paraventricular nucleus of the hypothalamus. The latter is negatively regulated by the HPC. The amygdala response to a stressful situation leads to CRF release of the hypothalamus thus activating the pituitary gland to secrete ACTH. The enhanced activity of the pituitary gland then results in cortisol secretion by the adrenal gland. Together, CRF, ACTH and cortisol regulate the organism's stress response. Furthermore, cortisol also inhibits the pituitary gland and the hypothalamus, whereas it activates the HPC.

CRF binds to CRF-receptor type 1 and type 2 with distinct functions, tissue specificity, and binding affinity^{98, 99}. ACTH activates the secretion of cortisol (cortisol in human and corticosterone in rodents), a glucocorticoid, which belongs to the class of corticosteroids. Cortisol is released from the adrenal gland and together with CRF and ACTH facilitates the stress response. Furthermore, cortisol inhibits the pituitary gland and the hypothalamus thereby forming a negative feedback loop that limits cortisol secretion, but enhances hippocampal activity (figure 1). After its release, cortisol interacts with glucocorticoid receptor (GR) and mineralcorticoid receptor (MR) throughout the body⁹⁷.

However, during chronic and sustained stress situations, continuously elevated levels of cortisol lead to neuronal atrophy and volume decline of the HPC and PFC^{35, 36, 43, 46}. The majority of depressed patients, mostly suffering from severe depression with/ or without psychotic symptoms, have a dysfunctional hyperactive HPA-axis regulation¹⁰⁰⁻¹⁰². Hyperactivity results from a deficit in the negative feedback, caused by an insufficient GR activation, which under normal conditions serves to decrease cortisol concentrations in the blood¹⁰³. Plasma cortisol levels following a higher release of

ACTH are elevated in a majority of MDD patients. Cortisol levels remain elevated in the afternoon and evening instead of the prominent cortisol peak during the morning as observed in healthy controls^{104, 105}. Furthermore, a reduced GR expression in post-mortem human brain of depressed patients was observed and a non-suppression of cortisol secretion following the administration of dexamethasone^{103, 106-110}.

Another study showed a correlation of stressful life events with increased vulnerability for affective and anxiety disorders. Stressful life-events also often precede the onset of depression and correlate with the severity of depression. Stressful life-events in childhood also predispose to the development of mood and anxiety disorders in adulthood^{14, 15}.

The HPC is a highly plastic brain region and is therefore especially sensitive to the effects of stress. Corticosterone-treated animals showed neuronal atrophy with reduction in cell body size but no differences in cell number in the HPC and PFC. Chronic stress and glucocorticoids have a negative effect on cell proliferation leading to a rapid and prolonged decrease in neurogenesis in the HPC^{43, 46}. The number of spine/synapse connections in HPC and PFC are decreased upon chronic stress. A loss of these connections might lead to a functional disconnection, so that a normal control of emotions and mood is not given. The medial PFC controls and regulates mood and emotions by input from other brain regions, mostly from the amygdala. Therefore, stress or rather the resulting neuronal atrophy and volume decline of the HPC and PFC could result in cognitive deficits and labile mood as well as emotions^{35, 36, 38, 111}. The morphological and functional effects of chronic stress can often be reversed by chronic, but not acute AD treatment¹¹¹⁻¹¹⁶.

Chronic stress and glucocorticoid treatment also reduce brain-derived neurotrophic factor (BDNF) mRNA and protein levels¹¹⁷⁻¹¹⁹. BDNF is a member of the nerve growth factor family and the most abundant neurotrophic factor in the brain. It has an important role during embryonic development in the guidance, function, and survival of neurons. But it is also expressed at high levels in adult brain and plays an important role in brain function, plasticity, and survival¹¹⁷. This knowledge links the glucocorticoid receptor hypothesis of depression to the neuronal plasticity hypothesis of depression.

1.3.3 The neuronal plasticity hypothesis of depression

Neuronal plasticity is the overall term to describe many processes where the brain senses, adapts and responds to external and internal stimuli⁹. It consists of major cellular and molecular manifestations in the adult brain like modifications of gene expression and synaptic plasticity. Modifications of gene expression include the activation of signaling cascades, activation of transcription factors, epigenetic changes, and activation/repression of different genes¹²⁰⁻¹²⁵. Modifications of synaptic plasticity are often referred to activity-dependent modifications at glutamatergic receptors. The most common long-lasting changes are long-term potentiation (LTP) and long-term depression (LTD) to selectively strengthen or weaken a synapse, respectively. LTD is an activity-dependent reduction in synaptic efficacy whereas LTP is an activity dependent increase and strengthening in of synaptic efficacy. LTD probably serves to specifically clear old memory traces in the HPC. LTD results from persistent weak synaptic activity and leads to a decrease of postsynaptic receptor density as well as probably presynaptic decrease of neurotransmitter release. In contrast to LTD, LTP is stimulated by higher persistent activity and strengthen synapses. Plasticity occurring at glutamatergic synapses allows the encoding of new information and thus, LTD and LTP play a role in learning and memory. These processes are mediated through glutamatergic excitatory and GABAergic inhibitory neurons¹²⁶⁻¹²⁹.

Synaptic plasticity leads to alterations in synaptogenesis, alterations in dendritic function, neurite extension, synaptic remodeling, and modification of synaptic neurotransmissions. Maladaptive plasticity to a pathological state can at least partly be reversed through AD treatment by inducing neuronal plasticity¹¹²⁻¹¹⁶. Upon modulation of receptors for serotonin and noradrenaline through AD treatment, different downstream pathways get activated that have a common function which is the regulation of gene expression, e.g. BDNF^{9, 130, 131}. The neuronal plasticity hypothesis of depression therefore combines different models: the neurotrophin hypothesis of depression, the glutamatergic hypothesis of depression and the GABAergic hypothesis of depression. I will describe each model and the underlying biomolecular mechanism in the following section.

1.3.3.1 The glutamatergic system

In the human brain, glutamatergic neurons project from the cortex to the subcortical regions like locus coeruleus, raphé nucleus, and substantia nigra where monoaminergic pathways are modulated¹³². The glutamatergic system controls learning, memory, cognition, emotion, neurotoxic actions, and induction of neuronal plasticity^{126, 127, 132}. In a pathological state glutamate becomes a potent excitotoxin triggering rapid or delayed neurotoxicity. Furthermore, glutamate plays a role in several neurodegenerative and neuropsychiatric diseases like Huntington's chorea, epilepsy, Alzheimer's disease, schizophrenia, anxiety disorders, and MDD^{132, 133}.

Glutamate is the major mediator of excitatory neurotransmission in mammalian brain which can be found in approximately 80% of all neurons^{132, 134}. It is synthesized by transamination of alpha-Ketoglutarate in the citrate cycle or recycled through the glutamate/glutamine cycle¹³⁴. Glutamate is transported to synaptic vesicles by vesicular glutamate transporters and is released into the synaptic cleft in a Ca²⁺-dependent manner. There, it can bind to two classes of glutamate receptors: ionotropic (iGluRs) and metabotropic (mGluRs) glutamate receptors. iGluRs consists of NMDARs, α -amino-3-hydroxy-5-methyl-4-isoxazolepropionic acid receptors (AMPA), and kainate receptors. NMDARs comprise a tetrameric complex of two NR1 and NR2 subunits. There are 8 splice variants for NR1, 4 for NR2 and two for NR3. AMPARs comprise a homomeric or heteromeric complex of 4 subunits (Gria1-4). Kainate receptors have three low-affinity subunits (GluR5-7) and two high affinity subunits (KA1 and KA2). mGluRs are classified into three groups according to their second messenger coupling system, molecular structure, sequence homology and their pharmacology. Group I mGluRs (mGluR 1 and 5 and their splice variants) are positively linked to phospholipase C and their activation is linked to increased phosphoinositide turnover and enhances glutamate excitation. Group II mGluRs (mGluR2 and mGluR3) and Group III mGluRs (mGluR4, 6, 7, 8 and their splice variants) are G_i-coupled, coupled to adenylate cyclase and upon activation inhibit cyclic adenosine monophosphate (cAMP) production and glutamate release presynaptically¹³⁵⁻¹³⁹.

High-affinity excitatory amino acid transporters (EAAT) in neighbouring glial cells clear the synaptic cleft from glutamate. In glial cells, glutamate is transformed into glutamine by glutamine synthetase and is transported back to the neurons where it is metabolized back to glutamate by glutaminase¹⁴⁰.

AMPA receptors are important for synapse maturation and the number of AMPARs and their activity is a determinant for the synaptic strength. NMDAR and AMPAR often co-localize in dendritic spines¹²³. Spines can be subdivided into three most common subtypes according to their size and relative proportion of the spine head and neck: stubby, thin, and mushroom spines. Spines are primary sites

for structural plasticity of excitatory neurotransmission. They undergo activity-dependent enlargement and stabilization and, conversely, inactive spines get eliminated. The major mechanism for expression of LTP at the hippocampal CA1 region requires NMDAR activation and therefore Ca^{2+} -influx into the postsynaptic terminal and activation of downstream signaling cascades¹²³. In detail, the presynaptically released glutamate binds to NMDARs and AMPARs. The latter gets activated first which leads to depolarization of the postsynaptic membrane. NMDARs are usually blocked by Mg^{2+} , however, a certain threshold of depolarization then causes conformational changes, eventually resulting in NMDAR opening. This in turn leads to recruitment of AMPARs to the postsynaptic membrane which is believed to mediate LTP¹²³. One extensively studied downstream cascade upon LTP is the transcription factor cAMP-response element binding protein (CREB). Generally all kinds of ADs stimulate CREB function¹⁴¹. The mechanisms that are influenced by CREB include learning and memory, outgrowth of neuronal processes, regulation of circadian rhythms, neurogenesis, pathophysiology of neuropsychiatric and neurodegenerative disorders and mechanisms of psychotropic drugs. CREB is regulated by multiple kinases of which the activation by the Ras-mitogen activated protein kinase (MAPK) and the calcium/calmodulin-dependent cascades might be the most important studied for MDD. Chronic AD treatment activates ERK-MAPK and cAMP-dependent Protein kinase A (PKA) that subsequently induce CREB phosphorylation and activation. There are more than 100 genes regulated by CREB, e.g., *Gria1*, the presynaptic protein *Synapsin1*, *CRF*, and *BDNF*^{9, 69, 142-155}. Therefore, *BDNF* is transcribed in a neuronal activity-dependent manner.

1.3.3.2 The neurotrophin hypothesis of depression

The neurotrophin hypothesis of depression arose in 2006 and postulates that a decrease in *BDNF* levels plays a major role in the pathobiology of MDD and possibly other neuropsychiatric diseases and the restoration of these levels may be critical for AD drug action^{117, 156-159}.

The *BDNF* gene can be transcribed into at least 11 different transcripts. The functional difference is not studied extensively yet, but it seems that they regulate the availability of *BDNF* at different cell compartments, like cell soma, dendrites and axons according to the needs of plasticity^{160, 161}. *BDNF* is secreted from postsynaptic spines or presynaptic terminals through a Ca^{2+} -dependent influx at NMDARs or voltage-gated Ca^{2+} -channels^{120, 121, 160, 162-164}. The secreted *BDNF* binds to and activates the Tropomyosin receptor kinase B (*TrkB*) receptor, which is localized on glutamatergic post- and presynapses and co-localizes postsynaptically with NMDARs and postsynaptic density protein 95 (*PSD-95*), a scaffolding protein that regulates activity-dependent incorporation of AMPARs into the synaptic spine membrane during experience-dependent synaptic strengthening¹⁶⁵⁻¹⁷¹. The activated *TrkB* receptor interacts with different docking proteins that regulate downstream pathways like the MAPK cascade, but also indirectly activates the ubiquitous mammalian target of rapamycin complex 1 (*mTORC1*)¹⁷². *mTORC1* is a central regulatory nexus that integrates important physiological signals from different cellular signaling cascades, thereby modulating anabolic versus catabolic pathways in response to nutrients, growth factors, and the cellular energy status¹⁷³⁻¹⁷⁷. Among other functions, *mTORC1* controls several metabolic pathways at the transcriptional, translational, and post-translational level¹⁷⁶. This includes regulation of glycolysis, the pentose phosphate pathway¹⁷⁵, and oxidative phosphorylation (*OXPHOS*) by positively modulating mitochondrial biogenesis and activity^{173, 177}. *mTORC1* positively regulates protein synthesis in an activity-dependent manner and, therefore, is required for synaptic plasticity. *BDNF*'s effect at the *mTORC1* pathway was well studied with regard to stress and synaptic plasticity^{125, 178-180}. Chronic mild stress (*CMS*, cf. section 1.4) in mice

leads to decreased protein levels of mTORC1 pathway components in the PFC including phosphorylated and activated mTORC1 and p70S6 Kinase, a serine/threonine kinase which, when phosphorylated, induces protein synthesis at the ribosome. Moreover, CMS results in decreased synaptic protein levels and the number and function of spines¹⁸¹. Acute and chronic stress decreases BDNF levels in the dentate gyrus and pyramidal cell layer of the HPC in rodents. Virtually all kinds of ADs increase BDNF levels in limbic brain regions, mainly the HPC and PFC and can prevent stress-induced decline of BDNF in the HPC^{117, 118, 182}. In order to further study the effects of BDNF different transgenic BDNF mouse-lines were generated. A homozygous deletion of BDNF is lethal, whereas heterozygous BDNF +/- mice showed reduced length and branching of apical dendrites at the CA3 region of pyramidal neurons in the HPC similar to what is observed during stress¹⁸³. The knock-in BDNF Val66Met transgenic mouse line expresses a single-nucleotide polymorphism (SNP), which is found in approximately 25% of humans. The mutation has been associated with hippocampal volume decline and an increased vulnerability to develop MDD in patients with traumatic or early life stress events. In rodents, the SNP mutant reduces the processing of pro-BDNF to BDNF, reduces BDNF transport to synaptic terminals and thereby blocks the activity-dependent release of BDNF into the synaptic cleft. BDNF Val66Met mice have decreased dendrite length, branch points of neurons and number and function of spines in the HPC and medial PFC. The observed changes are associated with increased anxiety and depression-like behaviors¹⁸⁴.

A viral-mediated mesolimbic dopamine pathway-specific knockdown of BDNF showed that BDNF is not needed for the development of depression-like behavior induced by CMS¹⁸⁵. In line with this study, knockdown of BDNF in hippocampal dentate gyrus, but not the CA1 region, attenuates the AD drug response without inducing depression-like behavior¹⁸⁶. Furthermore, the application of BDNF into the brain of rats showed synaptic plasticity as well as antidepressant-like effects in two animal stress paradigms: the forced swim test (FST) and learned helplessness (LH, cf. section 1.4)¹⁸⁷⁻¹⁸⁹.

Furthermore, BDNF is required for LTP establishment and is involved in memory acquisition and also long-term memory storage. Therefore, BDNF ultimately results in cell survival during hippocampal development, increased synaptic protein levels, presynaptic neurotransmitter release, and synapse formation^{149, 178, 183, 190-193}. BDNF also influences the monoaminergic system, thereby also connecting the neurotrophin hypothesis to the monoaminergic hypothesis of depression.

However, some findings suggest a more complex system for BDNF mediated mechanisms. Different kinds of stress paradigms increase BDNF expression or show a more complex pattern of regulation. Many inconsistent findings were produced and a partial knockout of BDNF in mice does not produce a depression-like behavior in rodents, however, it reduces AD treatment effects^{158, 186}. Furthermore, BDNF has opposing roles in the HPC and PFC versus the nucleus accumbens and ventral tegmental area¹¹⁷.

1.3.3.3 The glutamatergic hypothesis of depression

The neurotrophin hypothesis of depression is obviously linked to the glutamatergic hypothesis of depression as described in the previous section that already concentrated on the glutamatergic system. In this section, I will focus on several lines of evidence that promote a glutamatergic hypothesis of depression and explain the biomolecular mechanisms.

Neuroimaging and post-mortem brain studies of depressed patients showed ventricular enlargement, HPC and PFC volume reductions, and reduced neuron and glia density. The hippocampal volume reduction in depressed patients also correlates with length and recurrence of depressive episodes. AD treatment stimulates neurogenesis in the HPC and preclinical studies demonstrated that chronic AD treatment increases glial cell birth in the PFC^{35-43, 46, 111, 194-196}.

Different paradigms of stress or administration of corticosterone in rats induce a rapid and transient increase of extracellular glutamate in PFC, HPC, and amygdala¹⁹⁷⁻²⁰⁰. Moreover, different types of environmental stress in animals enhance glutamate release, reduce glial mediated glutamate cycling, and alter synaptic transmission in limbic and cortical areas. Chronic stress induces neuronal atrophy of apical dendrites in CA3 hippocampal area, increases the amplitude while reducing a decay of NMDAR currents, impairs LTP, and facilitates LTD^{112, 201-207}.

However, stress initially induces LTP in the HPC, but followed by a longer period where LTP is inhibited by increasing the threshold for LTP, probably to rather preserve the stressful memory than other information. Chronic stress may therefore decrease the volume of the HPC^{35, 43, 208}. On the other hand, the amygdala shows hypertrophy—an increased neuronal growth and number of spines—upon stress can be observed, probably thereby enhancing the emotional and anxious reaction to stress^{44, 45}. The neuronal atrophy at the PFC might also result from the increased inhibitory function of the amygdala projecting to the PFC.

Different studies on the plasma and brain of patients with mood disorders found altered levels of glutamate, however these findings were inconsistent. On the one hand, glutamate levels were increased in the plasma and brain of patients with mood disorders²⁰⁹⁻²¹³. AD treatment reduces plasma glutamate levels of depressed patients^{209, 214, 215}. In contrast, glutamate levels were decreased in the CSF of depressed individuals. Neuroimaging brain studies revealed elevated glutamate/glutamine levels in the frontal lobe, basal ganglia, and occipital cortex of depressed patients^{212, 216, 217}. Another study showed reduced glutamate/glutamine levels in anterior cingulate cortex²¹⁸⁻²²¹. Individuals suffering from depression showed abnormal elevation of glutamate neurotransmission and levels in cortical and limbic brain areas. Chronic, but not acute treatment with ADs markedly and significantly reduces the depolarization-evoked release of glutamate, but not the release of GABA in hippocampal synaptosomes affecting the readily releasable pool of vesicles—the physiological relevant pool of neurotransmitters²²². Treatment with conventional ADs acutely increases whereas and chronically administered reduces presynaptic glutamate release^{222, 223}. Therefore, the reduction of glutamate observed with chronic AD treatment might be an adaptive mechanism.

Patients suffering from MDD showed down-regulated glutamine synthetase transcripts in anterior cingulate cortex, dorsolateral PFC, and amygdala²²⁴. Vesicular glutamate transporters, that transport glutamate into synaptic vesicles were unchanged, however, repeated AD treatment increases vesicular glutamate transporters mRNA in the cortex and HPC in rats^{225, 226}. Reduced EAAT1 and EAAT2 protein levels, that are expressed in astroglia, were found in two post-mortem frontal brain tissues in patients suffering from MDD²²⁴. EAAT3 and EAAT4 are mainly localized at neurons and their mRNA levels were decreased in the striatum in mood disorders²²⁷.

A decreased NMDAR binding and NR1 subunit expression was reported in the HPC and superior temporal cortex in MDD patients²²⁸⁻²³¹. In preclinical studies, monoaminergic ADs *per se* have no effect on spine number, however, these drugs are capable of blocking the effects of chronic stress.

Chronic treatment with an SSRI (fluoxetine) resulted in up-regulation of NR2A and AMPAR subunit Gria1 and Gria2 in the forebrain. Chronic fluoxetine treatment increases the protein levels of phosphorylated Synapsin1, PSD-95, and synaptic Gria1 in a rat model of reduced synapse density. Acute AD treatment rescues LTP after acute stress²³²⁻²³⁴. Tianeptine also reverses stress induced down-regulation of MEK/ERK-MAPK signaling cascades and phosphorylation of Gria1 subunit of AMPARs²³⁵. Furthermore, chronic AD treatment increases the membrane insertion and synaptic expression of Gria1 and up-regulates Gria2/3. Therefore, an antidepressant effect might be mediated through AMPARs as activation of AMPARs increases BDNF expression and stimulation of synaptic plasticity. As a consequence AMPAKines, potentiators of AMPARs, were developed^{55, 56, 179, 236-240}. Chronic AD treatment reduces NMDAR function or expression and various ADs like imipramine and citalopram also bind to and inactivate NMDARs. Furthermore, various NMDAR antagonists showed antidepressant-like effects in animal screening tests^{179, 213, 241-243}.

Ketamine – a fast acting antidepressant

In 2000 Berman et al. demonstrated for the first time a rapid antidepressant effect of a low dose of ketamine, within 2h and 4h that last up to 7 and 10 days²⁴⁴. Ketamine, a drug usually used for anaesthesia, is a non-competitive, voltage-dependent NMDAR antagonist which blocks the NR2B- and NR2A-containing receptors equally in the presence of Mg²⁺²⁴⁵⁻²⁵⁰. An antidepressant effect of ketamine can be observed in patients suffering from TRD^{251, 252}. Moreover, ketamine diminished suicidal ideation.²⁵³ These clinical findings provide a promising basis in studying the glutamatergic system of the brain—receptors, modulators and affected pathways—for novel therapeutic targets and development in MDD. Unfortunately, ketamine cannot be used as a first-line drug due to its psychomimetic side-effects. However, it is therefore also suitable in order to study the neurobiology of schizophrenia, but also misused as a drug²⁵⁴⁻²⁵⁸.

A number of studies in animal models were published in the last years revealing an antidepressant-like effect and insights into the molecular mechanism of ketamine drug action. Several behavioral testing like LH, FST, chronic mild stress (CMS) and novelty suppressed feeding (NSF) could demonstrate the antidepressant-like effect of a single injection of ketamine in mice and rats^{179, 240, 243, 259-261}. A low dose of 10 mg kg⁻¹ ketamine seems to act through the activation of mTORC1 causing an increase of synaptic proteins as well as an elevated number of spines and their activity in the medial PFC of rats¹⁷⁹. In this study, the key regulators of protein translation and members of the mTORC1-signalling pathway eukaryotic initiation factor 4E-binding protein 1 (4E-BP1), p70S6K and mTORC1 show increased phosphorylation and therefore activation already 30 minutes after a single injection of a low dose of ketamine¹⁷⁹. Although, most recently, a study revealed that 1h after a 10 mg kg⁻¹ ketamine treatment does not increase pmTORC1 protein levels in the HPC and PFC in mice²⁶². An even lower concentration of ketamine (3 mg kg⁻¹) does not phosphorylate mTORC1 and p70S6K in the frontal cortex of mice²⁴³. Moreover, the antidepressant-like effects observed in the FST 30 minutes after ketamine administration were blocked by rapamycin, an mTORC1 inhibitor, with a ketamine concentration of 10 mg kg⁻¹ in rats, but not with 3 mg kg⁻¹ in mice^{179, 243}. Furthermore, increased levels of postsynaptic proteins required for formation, maturation, and function of new spine synapses like PSD-95, Gria1 as well as Synapsin1 were observed 2h after ketamine treatment (10 mg kg⁻¹) and lasting up to 72h in the medial PFC in rats¹⁷⁹. However, 3 mg kg⁻¹ of ketamine administration does not change Gria1 protein levels in the frontal cortex of mice²⁴³. Whereas in another study 10 mg kg⁻¹ showed an increase of Gria1 and Gria2 protein levels in the HPC, but not

the PFC of mice²⁶². Nevertheless, ketamine's (3 mg kg⁻¹ and 10 mg kg⁻¹) antidepressant-like effects are dependent on AMPARs. Receptor blockage by 2,3-Dihydroxy-6-nitro-7-sulfamoyl-benzochinoxaline-2,3-dione (NBQX) reverses the antidepressant-like behavioral effects in mice and rats^{179, 243}. Exposing rats to stress in the LH paradigm decreased the number of spines and protein levels of synaptic Gria1, PSD-95, and Synapsin1 protein levels. This could be reversed by a single injection of ketamine. Furthermore, also these effects could be blocked by rapamycin¹⁷⁹.

A single ketamine injection of 3 mg kg⁻¹ as well as 10 mg kg⁻¹ also seems to deactivate the eukaryotic elongation factor 2 (eEF2) kinase which phosphorylates eEF2 in the HPC of mice. Thus, eEF2 phosphorylation in the HPC, but not in the frontal cortex and PFC, is decreased already 30 min, 1h and 24h after ketamine administration resulting in an increased translation of BDNF in the HPC^{243, 262}. Moreover, translation, but not transcription of BDNF is necessary for ketamine drug action as indicated by unaltered BDNF mRNA levels, but increased BDNF and pro-BDNF protein levels after a single injection of ketamine. Furthermore, knock-out of BDNF and/or the TrkB receptor blocked the antidepressant-like effect of ketamine in mice²⁴³.

Inhibition of MAPK, a regulator of protein translation during neural activity, does not have an effect on FST behavior upon ketamine treatment, however, a reduction of MAPK phosphorylation in hippocampal tissue could be observed. Ketamine requires the phosphorylation and inhibition of glycogen synthase-kinase-3 β (GSK-3 β), which has a role in regulating the insertion of glutamate receptors into the postsynaptic membrane and regulation of transcription^{38, 243, 263, 264}. These findings suggest a rapid transformation of the synaptic structure and function in the PFC of rats and HPC of mice through a single injection of ketamine thereby enhancing synaptic plasticity leading to the rapid antidepressant-like effect of ketamine. Moreover, ketamine drug action is dependent on AMPAR activity, BDNF translation as well as most probably the mTORC1-signalling pathway.

There are two major hypotheses for ketamine's antidepressant effects: one postulates the direct inhibition and the other an indirect inhibition or disinhibition of inhibition of excitatory pyramidal neurons^{38, 243, 265, 266}.

The disinhibition of inhibition hypothesis is most widely discussed and suggests a selective antagonism at PFC inhibitory neurons resulting in a disinhibition of inhibition and activation of excitatory pyramidal neurons. NMDARs mediate excitatory postsynaptic potentials throughout the brain. Paradoxically, NMDAR antagonism predominately decreases the activity of putative inhibitory GABAergic interneurons, thereby increasing the firing rate of the majority of excitatory pyramidal neurons. The fact that GABAergic inhibitory interneurons of the PFC are mostly activated by NMDARs implies a mechanism by which NMDAR inhibition causes excitation by disinhibition of pyramidal neurons of the PFC^{265, 266}. Further supporting this hypothesis are results of a dose-response study in rats using microdialysis. Low doses of ketamine (10, 20, and 30 mg kg⁻¹) increase glutamate outflow in the PFC and increased glutamatergic neurotransmission²⁶⁶. In contrast, intermediate (50 mg kg⁻¹) or anaesthetic (200 mg kg⁻¹) doses of ketamine did not affect or decrease glutamate levels, respectively²⁶⁶. These effects were also blocked by intra-PFC application of the AMPA/kainate receptor antagonist 6-cyano-7-nitroquinoxaline-2,3-dione (CNQX)²⁶⁶. Furthermore, ketamine increased excitatory postsynaptic current (EPSC) frequency responses to serotonin in medial PFC pyramidal neurons which was blocked by rapamycin¹⁷⁹. Ketamine decreases the average frequency of AMPAR EPSC recorded from rat hippocampal slices at CA1 stratum radiatum interneurons. Acute application of ketamine to hippocampal slices of mice potentiated the synaptic responses measured by field potentials. Furthermore, ketamine NMDAR-EPSCs were also decreased in rat primary hippocampal neurons (PHN)^{243, 262}.

The above model provides a mechanism for MDD. It implies that MDD results from a breakdown of synaptic homeostasis and destabilization of glutamatergic synapses. Synaptic terminals are maintained and controlled by circuit activity and function including the activity-dependent release of BDNF. In case of normal mood with synaptic homeostasis glutamate is released from presynaptic terminals in an activity-dependent manner and AMPARs and NMDARs are activated leading to BDNF secretion from the postsynaptic terminal. Upon stress and during MDD glutamatergic synapses destabilize leading to neuronal atrophy and decreased synaptic connections in the PFC and HPC and reduced BDNF release and mTORC1 activity. Importantly, these processes are dependent on GABAergic inhibitory interneurons which during stress and MDD further the decline of neuronal activity of excitatory glutamatergic neurons by increased release of GABA—a process that can be described as LTD-like. Ketamine mainly blocks NMDARs at GABAergic inhibitory neurons, thereby decreasing the GABA release and its inhibitory effects on glutamatergic excitatory neurons. As a consequence, glutamate release increases, which then binds and activates AMPARs and NMDARs. The postsynaptic membrane is depolarized, which promotes BDNF secretion from glutamatergic excitatory neurons and synthesis of synaptic proteins involved in spine remodeling—an LTP-like process (figure 2)³⁸.

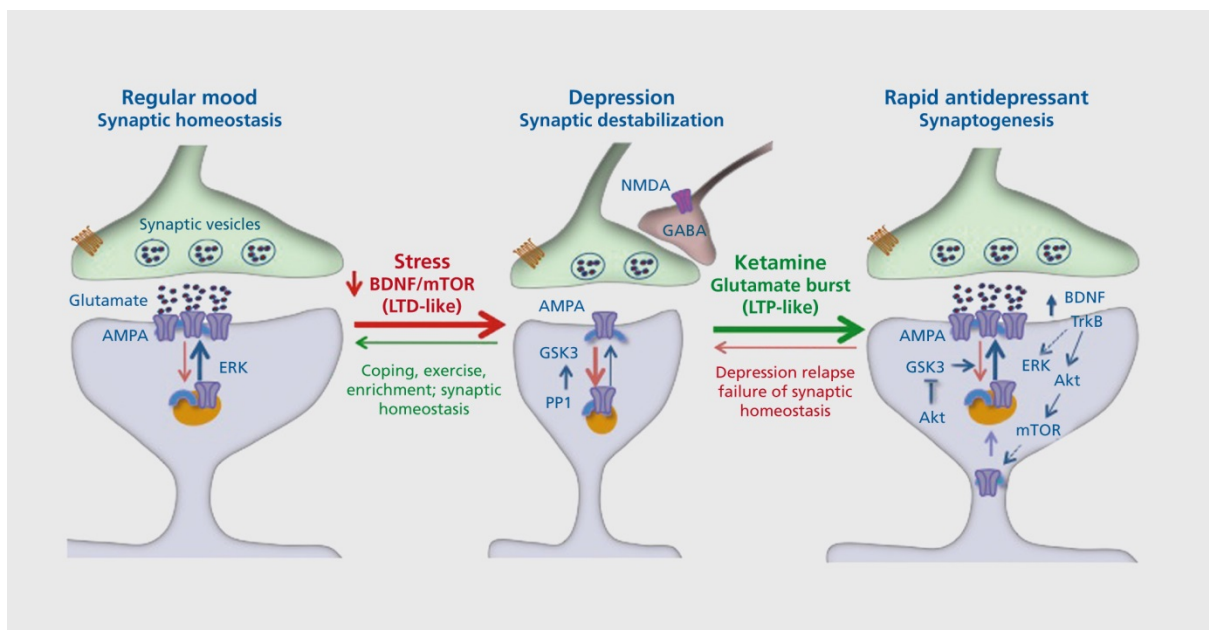


Figure 2: Model of MDD development and ketamine's antidepressant effect on excitatory glutamatergic and inhibitory GABAergic interneurons. In the case of regular mood and synaptic homeostasis pre- and postsynapses regulate their activity by presynaptic release of glutamate which binds to AMPARs and NMDARs postsynaptically. In the case of stress leading to MDD homeostasis is destabilized by increasing interference from GABAergic interneurons and inhibition of glutamatergic neuron activity. This process leads to an internalization of AMPARs into the cytoplasm and decreased BDNF levels and mTORC1 activity ultimately weakening glutamatergic synapses (LTD-like). Stress coping or exercise can reverse this effect. However, pharmacological treatment with ketamine results in a glutamate burst, increased BDNF levels, TrkB receptor and mTORC1 activation, elevated protein synthesis of synaptic proteins and integration of AMPARs into the synaptic membrane. These processes strengthen glutamatergic synapses resulting in synaptogenesis. Over time the antidepressant effect might weaken, causing a depression relapse and loss of synaptic homeostasis³⁸.

The direct model proposes a mechanism of NMDAR inhibition at excitatory pyramidal neurons. According to this model, NMDAR blockade would be in line with a homeostatic synaptic plasticity mechanism with a rapid compensatory effect and increase in mTORC1 activity as well as synaptic protein synthesis²⁶⁷. There is also evidence that ketamine mainly acts through blockade of NR2B-containing NMDARs as selective antagonists are also effective in patients and decrease the

immobility time in FST and tail suspension test (TST) in preclinical models^{179, 268, 269}. Furthermore, NR2B-, but not NR2A-containing NMDARs, when activated restrict mTORC1 activity and synaptic protein synthesis and regulate excitatory homeostatic synaptic plasticity. NR2B-containing NMDARs are more sensitive to glutamate and therefore would also be more sensitive towards ketamine blockade^{268, 270-272}. Higher concentrations of ketamine would block all NMDARs leading to psychomimetic side-effects and anaesthesia²⁶⁷. Furthermore, with higher doses ketamine might bind to other proteins like the opioid receptors²⁶⁷. The indirect hypothesis describes the different effects of ketamine by binding to NMDARs on different cell types. An anaesthetic effect is observed when ketamine also binds to NMDARs present on excitatory neurons and other receptors²⁵⁵.

Recently, Zanos et al. discovered that the fast antidepressant-like effects of ketamine seems to be dependent on a ketamine's metabolism. Deuterated ketamine at the C6 position (6,6-dideuteroketamine) is unable to metabolize, however without changing its pharmacological properties. 6,6-dideuteroketamine also decreases the immobility time in the FST, but no antidepressant-like effects in the LH paradigm.

Mice treated with the ketamine metabolite (2R, 6R)-hydroxynorketamine exhibit an antidepressant-like effect similar to ketamine, however, most probably independent of NMDAR binding, but also dependent on AMPAR activity. Pretreatment of NBQX also prevented an antidepressant-like effect of (2R, 6R)-hydroxynorketamine. Furthermore, (2R, 6R)-hydroxynorketamine also decreases pEF2 1h and 24h as well as increases BDNF protein levels 24h after the treatment in HPC, but not the PFC in mice²⁶².

1.3.3.4 The GABAergic system, alterations and treatment options of MDD

Several lines of evidence already pointed to an involvement of GABAergic neurotransmission and receptors in MDD and AD drug action. GABA is the most widely expressed inhibitory neurotransmitter in the mammalian brain and modulates neuronal function and behavioral processes like sleep, feeding, aggression, sexual behavior, pain, cardiovascular behavior, thermoregulation, locomotor activity, and mood^{195, 247, 273-278}. GABA represents approximately one third of the synapses in cerebral cortex, HPC, thalamus, basal ganglia, cerebellum, and the brain stem^{273, 279-282}. GABA neurotransmission is present in GABAergic inhibitory interneurons and modulates local neuronal circuitry such as glutamatergic, noradrenergic, dopaminergic, and serotonergic neurons²⁸³. Furthermore, the GABAergic and glutamatergic neurotransmission are interconnected with the HPA-axis. Glutamatergic and GABAergic synaptic inputs are identified in hypothalamic CRF-containing neurons^{284, 285}. The HPC, PFC, lateral septum, and amygdala regulate the HPA-axis by affecting the hypothalamic paraventricular nucleus (PVN). However, none of these regions directly innervate to the PVN, they project to PVN-projecting neurons which in turn regulate the PVN. HPC and PFC release glutamate which activate PVN-projecting neurons. On the other hand, the lateral septum and medial amygdala inhibit PVN-projecting neurons by GABA. The PVN-projecting neurons inhibit or activate the PVN by either GABA or glutamate, respectively. The activated PVN releases CRF and therefore activates the pituitary gland that releases ACTH which in turn activates the adrenal gland. The HPC, PFC, pituitary gland, and PVN are then inhibited in a feedback loop by released cortisol^{91, 286}. The regulatory roles of glutamatergic and GABAergic systems in the activity of the HPA-axis are intriguing regarding how they interact and are involved in depression.

Glutamate decarboxylase synthesizes GABA from glutamate which then is stored in synaptic vesicles and released into the synaptic cleft in a Ca^{2+} -dependent manner^{273, 287-290}. GABA binds to two classes of receptors: The ionotropic GABA_A and the metabotropic GABA_B receptors. GABA_A receptors are composed of 5 subunits belonging to several different classes. Its activation leads to Cl^- -influx into the postsynaptic cell causing a fast inhibitory postsynaptic potential (IPSP). GABA_B receptors are metabotropic autoreceptors, expressed as heterodimers with GABAB1 and GABAB2 subunits and different splice variants. Therefore, GABA_B receptors are G-protein-coupled inhibiting synaptic neurotransmission presynaptically and mediating a slow IPSP^{275, 291-297}. After release, GABA is quickly cleared from the synaptic cleft in a sodium-dependent uptake process of GABA transporters in presynaptic terminals or glia cells. Glial GABA is transformed to succinate semialdehyde by mitochondrial GABA transaminase. Succinate semialdehyde is metabolized to succinate and re-enters the citrate cycle to regenerate glutamate by alpha-Ketoglutarate. Glutamate is transferred to glutamine, which is then transported to neurons, in which it is transformed to GABA—a process also described as GABA/glutamine cycle^{282, 289, 298, 299}.

Preclinical and clinical evidence strongly associates the GABAergic system with depression. Preclinical mouse studies showed, that the knockout of the major GABA transporter 1 (GAT1) led to a reduced depression- and anxiety-like behavior in comparison to wild-type mice³⁰⁰. GABA_B receptor knockout mice exhibit an antidepressant-like effect as observed through a reduced immobility time in the FST. In contrast, chronic treatment with drugs which are known to have antidepressant properties like lithium, valproate, carbamazepine, fengabide, and probagide, increase GABA_B receptor, but not GABA_A receptor protein levels in the rat HPC and frontal cortex³⁰¹⁻³⁰³. In contrast, traditional ADs reduce GABA_A receptor protein levels in the rat HPC, cortex, and hypothalamus, albeit, not in all studies³⁰⁴⁻³¹¹. Further analyses on rats could demonstrate increased receptor binding sites for GABA_B receptors in the HPC of rats treated with conventional ADs, again, not in all studies³¹²⁻³¹⁷. LH, as a stress paradigm decreases GABA_B receptor protein levels and AD treatment reverses this effect in the frontal cortex of rats³¹⁸⁻³²¹.

Clinical studies on GABA have so far yielded conflicting results. GABA levels at the plasma and CSF of depressed patients were reduced, whereas in two other studies no alterations of GABA levels in CSF could be observed. Another study demonstrated decreased GABA levels in plasma, surprisingly, even persisting after successful AD treatment for at least 4 years whereas another study could not find any differences before and after AD administration^{283, 322-337}. Neuroimaging brain studies with depressed patients showed reduced GABA levels at the occipital cortex, anterior cingulate cortex, and medial and dorsal anterior PFC^{212, 338-340}. Furthermore, there were no correlations of GABA levels and the severity of MDD symptoms. The protein levels of glutamate decarboxylase, the enzyme transforming glutamine to GABA, were reduced in the cerebral cortex and cerebellum in MDD patients. However, higher glutamate decarboxylase protein levels were found in the dorsolateral PFC, superior temporal cortex, and HPC³⁴¹⁻³⁴³. The density of GABA_A receptors in PFC was elevated and GABA_A receptor subunit A1 and GABA_A receptor subunit B3 were up-regulated in the anterior cingulate cortex of MDD suicide victims. In contrast, GABA_A receptor subunit A mRNA levels were reduced in the frontal cortex of suicide victims^{224, 344-346}.

Modulations of GABAergic neurotransmission have proven effective in sustaining a positive response of AD treatment like progabide (an analogue and prodrug of GABA), tiagabine (a GABA reuptake inhibitor), and fengabine. The latter showed an antidepressant effect, but its biomolecular mechanism remains unknown. The effects were reversed by GABA_A receptor antagonists. In clinical

trials, fengabine's efficacy was comparable to that of the TCAs, however with a more rapid onset of action and much less side effects^{347, 348}.

1.4 Animal models of depression

A model is defined as an organism (non-human) or a particular biological state of an organism that reproduces aspects of human pathology, therefore, providing a certain degree of predictive validity³⁴⁹. Typical symptoms of MDD like depressed mood, guilt, and suicidality are difficult to model as it is either uncertain if such emotions are distinct for humans or not clear if there are present in rodents (cf. section 1.1). In general, we do not know if a mouse is depressed or can feel depressed. Other symptoms, also common in MDD, can be modelled like anhedonia, behavioral despair, and neurovegetative changes like appetite or sleep. Depression models are often evaluated by three main criteria: 1) face validity (requires a reasonable level of symptom consistency), 2) construct validity (requires causative factors and a comparable etiology) and 3) pharmacological validity (requires reversal of depressant-like symptoms by available ADs)³⁵⁰⁻³⁵³. The major problem in MDD research is the restricted availability of validated animal models as no “depression gene” was discovered yet³⁵⁴. An ideal model would lead to an understanding of the underlying biomolecular mechanisms involved in MDD and its development.

1.4.1 Models of acute stress

Forced swim test (FST) and tail suspension test (TST)

The FST is the most widely used test for AD drug action and in general more often applied as a screening test for substances with potential antidepressant-like properties. Moreover, depression-like behavior can also be tested. The FST was developed in 1977 and is also called Porsolt test. A mouse or rat is placed in a cylinder filled with water. Following an initial phase, the time the mouse or rat struggles, swims, and floats, the latter also referred to as immobility time, are measured. The immobility time is then mostly applied to describe depression-like (higher immobility time) or antidepressant-like (reduced immobility time) behavior (figure 3). The test is highly reliable in predicting the therapeutic potential of a tested compound. In general, tested substances should always also been tested for locomotion as changes in such activities might therefore have an influence on the FST. Disadvantages of the FST are the low face and construct validity. The TST was first introduced in 1985, in which mice are suspended by their tail and the time the animal stays immobile is measured (figure 3). The two different tests are interpreted as behavioral despair and the behavior is reversed by acute administration of almost all ADs³⁵⁴⁻³⁶⁴.

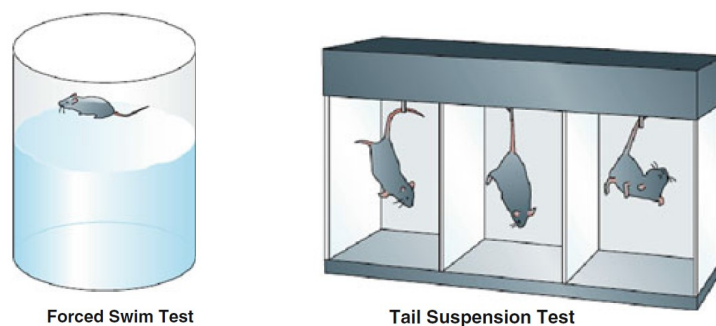


Figure 3: Simplified illustration of the forced swim test (FST) and tail suspension test (TST). In the FST, a mouse or rat that is placed in a cylinder filled with water shows three different behaviors: struggling, swimming, or floating. The latter is a measure for depressant-like behavior. In the TST, a mouse is suspended by its tail and the immobility time is a measure for depressant-like behavior³⁶⁵.

The learned helplessness (LH) Model

As described in the previous sections, individuals that have suffered from trauma or other stressful life-events are more vulnerable to develop MDD. In this context, unpredictable, uncontrollable and inescapable stress-like exposure to electric shocks might cause a state of helplessness in animals. Re-exposed to the same stress, however, with an easy escape route, will lead to either increased escape latency or a completely failure to escape. The model was first developed in the 1960s while studying classical Pavlovian conditioning. Animals develop persistent changes like weight loss, diminished sexual behavior, alterations in sleep pattern and HPA-axis activity with elevated levels of CRF and corticosterone and loss of spines in the HPC. The LH stress paradigm is short-lived in mice only persisting 2 to 3 days. The results are largely compatible with the ones gained by the FST. Only 10–80% of animals fail to develop escape deficits. These results let to breeding of helpless and non-helpless animals to create different LH-strains. Repeated AD treatment and electroconvulsive seizure therapy reduces latency to escape and decreases the number of animals that showed LH. Most strikingly, no currently available AD in clinical use, failed when testing for LH. LH seems to be a good model for AD drug action as it has excellent face validity and a high predictive value^{349, 353, 354, 359, 366-373}.

1.4.2 Hormones of the HPA-axis

The forebrain GR knockout mice display enhanced basal serum glucocorticoid levels, dexamethasone non-suppression, increased immobility in FST and TST, and the changes are reversible by AD treatment. However, overexpression of GR in forebrain of mice shows similar effects, suggesting that mood altering properties are more complex than simply changing the hormone levels. Another model is based on the fact that chronic glucocorticoid administration leads to depression. Chronic administration of corticosterone for 20 days into their drinking water leads to anhedonia, increased TST immobility which is reversible by chronic amitriptyline administration (a TCA) in mice. Increases in serum cortisol levels in MDD might be secondary to CRF synthesis and secretion. CRF's behavioral effects might be independent to adrenal function as they are not reversed by adrenalectomy. To deepen the knowledge of CRF's behavioral effects, numerous transgenic and knockout mouse lines were developed. Overexpression of CRF during mouse development leads to increased anxiety, elevated FST and TST immobility time during adulthood and, in line with this study, conditional

CRFR1 knockout mice display anxiolysis. This research led to the development of CRFR1 antagonists used in depression and anxiety disorders by pharmaceutical companies³⁷⁴⁻³⁸⁰.

1.4.3 Models of chronic stress

Models of chronic stress were developed based on clinical evidence that chronic stressful life-events in humans lead to an increased risk for a depressive episode. The main strength of these models lies in the ability to characterize neuroplasticity in association with chronic stress and/or AD treatment. The tests are composed of chronic uncontrollable and unpredictable stress that is coupled with a method measuring depression- and antidepressant-like behavior. However, low throughput rates makes them poorly suited for pharmacological validation of new compounds^{118, 365}.

Chronic mild stress (CMS)

CMS applies a variety of intermittent physical stresses like food and water deprivation, small temperature alterations, changes of cage mates over a relatively prolonged time period (1 to 7 weeks). Anhedonia can be analyzed by a sucrose preference test. Moreover, mouse behavior like grooming deficits or changes in aggressive and sexual behavior can be measured. CMS creates subtypes for anhedonia as only about 60% of mice develop anhedonia associated with increased FST immobility. However, all mice showed alterations in locomotor activity and reduced exploration. Many developed phenotypes are reversible by chronic AD treatment either during the stress or afterwards. Rats develop an AD-sensitive and AD-resistant phenotype upon CMS which makes these animals a perfect model of TRD. However, there are problems to reproduce the results in different laboratories. CMS shows a good predictive value, face validity, and construct validity^{351, 381-388}.

Psychosocial stress model

CMS mostly consists of physical stressors not considering that these forms of stress are unlikely to happen to mice and rats in the wild. Moreover, to make an animal model more comparable to the human situation where stress mostly develops from social interactions, the psychosocial stress paradigm was introduced which is also called the social defeat stress. In this stress paradigm, two or more rodents are “forced” to interact socially and physically. Thus, one resident mouse and to a later time point another intruder mouse are interacting in one cage. The intruder mouse is investigated and they start fighting; subsequently they get divided after some minutes. The resident mouse reaches a dominant status whereas the intruder is defeated. Some groups use age- and strain-matched mice whereas others use another more aggressive or larger mouse strain for defeating. In addition to physical stress, some research groups add another psychological stress where they prolong the sensory contact for usually 24h. Therefore, the experimental mouse is exposed to different aggressors for several days by holding them in the same cage without being able to physical interact. Afterwards, these mice display a reduced social interaction, exploration, locomotor activity, and anhedonia, increased FST/TST immobility time and alterations in HPA-axis activity and autonomic functions. Many symptoms can be reversed by chronic, but not acute AD treatment. The social defeat stress model should be applied for at least 20 days in order to develop depression-like symptoms. An even shorter defeat stress might rather lead to an anxiety phenotype^{185, 389-400}.

Other forms of social stress

In order to more accurately model human stressful situations, several different kinds of stress paradigm were developed. A prolonged social isolation during adulthood results in reduced sucrose drinking and alterations in sexual behavior. Early life stress induced by maternal separation during postnatal developmental periods, results in cognitive and “emotional” changes that persist into adulthood. The novelty-suppressed feeding (NSF) test elicits competing motivations: drive to eat and fear to be in the center of a bright lit arena. NSF more likely measures anxiety, however, the stress paradigm is also sensitive to chronic AD treatment⁴⁰¹⁻⁴⁰⁴.

1.5 Biomarkers in MDD research

The National Institutes of Health defines a biomarker as being “a characteristic objectively measured and evaluated as an indicator of normal biological and pathogenic processes, or biological responses to a therapeutic intervention”⁴⁰⁵. This characteristic can be physiological, pathological and anatomical and includes genes, mRNAs, proteins, metabolites, images, electroencephalography patterns, electrophysiological traces, physiological, and cognitive signals^{35, 43, 106, 107, 118, 406-414}.

Biomarkers can be used to differentiate between health and disease states and help classify disease subtypes (diagnostic biomarker) as well as treatment outcome (treatment biomarker). Moreover, biomarkers are useful in drug development efforts by providing information of a biological state or drug effect. In psychiatric research biomarkers can help to stratify patient sub-populations. Drug development would benefit from biomarkers or a biosignature to predict a treatment effect for newly developed ADs. Currently, mood disorders are symptomatically determined by a patient’s self-report or by information from others. As described in section 1.1, to date symptoms are assessed based on DSM-IV or ICD-10 without any biological parameters^{16, 17}. Biomarkers for MDD still remain elusive and are of urgent need. The development and validation of biomarkers predictive for MDD subtypes would greatly help not only in the development of novel ADs, but also in clinical trials to stratify MDD patients.

The literature describes several biomarkers that might be suitable for translation into the clinic:

- Growth factors like BDNF (cf. section 1.3)^{118, 407-409, 413}
- Pro-inflammatory markers like cytokines including tumor necrosis factor- α and interleukin-6 have altered levels in MDD^{410, 411, 414, 415}
- Endocrine markers reflecting an altered HPA-axis regulation (cf. section 1.3.2) and the dexamethasone suppression test^{106, 107, 412}. Dexamethasone is a synthetic glucocorticoid and the test is a measure for the integrity of feedback inhibition of the HPA-axis. A positive test result is reflected by elevated plasma cortisol levels. This test might reflect an MDD subtype as well as differentiate between healthy and MDD subjects
- ADs and MDD affect electroencephalography profiles which might serve as a biomarker⁴⁰⁶
- HPC volume decline in individuals suffering from MDD and reversal after AD treatment (cf. section 1.3)^{35, 43}
- Markers like neurotransmitters and (mRNA) as described in previous sections

None of these potential biomarkers are currently used in the clinic. In all likelihood a set of biomarkers will ultimately be required.

2.0 Thesis project aims and objectives

MDD is a devastating neuropsychological disorder with a high co-morbidity and risk for mortality accompanied by a dysfunctional brain circuitry involving the HPC and PFC. Conventional ADs need at least 2 to 8 weeks before a therapeutic effect results and approximately one third of the patients do not respond to traditional treatment and therefore suffer from TRD⁸. In 2000, Berman et al. discovered the fast antidepressant effect of ketamine with symptom reduction already within 2h and 4h, lasting up to 7 to 10 days and being especially effective for patients suffering from TRD. Unfortunately, ketamine's psychomimetic side-effects prevented its routine use in the clinic so far^{179, 243, 244, 251, 416}.

Ketamine is a non-competitive antagonist of the NMDAR with profound downstream effects. To date, studies on ketamine's biomolecular mechanism mainly focuses on the BDNF and mTORC1 mediated neurotrophic effects on synaptic plasticity—a process with high energy demand in form of adenosine triphosphate (ATP)^{179, 243, 262}. However, the exact mechanism and brain circuitry still remains elusive. So far, no alternative cellular targets besides and downstream of the NMDAR are known that could aid the development of alternative faster acting ADs with a similar mode of action as ketamine, but with fewer side-effects. Furthermore, no treatment biomarkers for ketamine's mode of action, especially for its antidepressant effects are known.

The fast antidepressant action of ketamine was previously reported in patients suffering from TRD. However, the actions of ketamine are afflicted with psychomimetic side effects and have prevented its clinical routine use as antidepressant drug to date. Hence, the examination of ketamine's cellular targets (other than NMDAR) and its exact mechanism of action might provide new contact points for future antidepressant drug development and biomarker research. Therefore, the overall aim of this thesis is to identify biosignatures and biomolecular pathways affected by ketamine treatment. Results from my research in mice can aid in the development of novel fast acting ADs with a similar mode of action as ketamine, however, with fewer side-effects. The specific objectives of my thesis project are:

- To investigate the time-dependent antidepressant-like effect of a low ketamine dose in mice using the FST
- To compare metabolite profiles of defined brain regions, liver, and blood from ketamine- and vehicle-treated mice as well as mouse primary hippocampal neurons (PHN) subjected to ketamine and vehicle treatment
- To determine hippocampal ketamine treatment response biomarkers, especially for the drugs' antidepressant effect
- To compare hippocampal protein expression profiles between ketamine- and vehicle-treated mice based on molecular pathways identified by metabolomic analyses

3.0 Materials and Methods

3.1 Chemicals and consumables

Table 1: Chemicals and consumables used in the present study.

| Reagent/ Consumable | Company |
|--|----------------|
| 10x TGS | Sigma-Aldrich |
| 2-Mercaptoethanol | Bio-Rad |
| 3:30-Diaminobenzidine (DAB) | Sigma-Aldrich |
| Acetic acid (HCOOH) | Sigma-Aldrich |
| Acetonitrile (ACN) | Merck |
| Acrylamide/ Bis-Acrylamide 40%, 37.5:1 | Sigma-Aldrich |
| Acrylamide/Bis-Acrylamid 30%, 37.5:1 | Serva |
| Adenosine triphosphate (ATP) | Sigma-Aldrich |
| Aminocaproic acid | Fluka |
| Ammonium bicarbonate (NH ₄ HCO ₃) | Merck |
| Ammonium persulfate (APS) | Bio-Rad |
| Bis-Tris | Sigma |
| Bovine serum albumin (BSA) | Bio-Rad |
| Bromophenol blue | Bio-Rad |
| catalase | Sigma-Aldrich |
| Coomassie brilliant Blue G250 | Serva |
| Coomassie brilliant Blue R250 | Bio-Rad |
| Costar Spin X Tubes | Millipore |
| cuvette | Biostep |
| Cytochrom c | Sigma-Aldrich |
| Digitonin | Fluka |
| Dimethyl sulfoxide (DMSO) | Sigma |
| Dipotassium phosphate (K ₂ HPO ₄) | Sigma-Aldrich |
| Dithiothreitol (DTT) | Bio-Rad |
| Dodecylmaltosid (DDM) | Sigma-Aldrich |
| Eppendorf tubes | Eppendorf |
| Ethanol | Merck |
| Ethylenediaminetetraacetic acid (EDTA) | Sigma-Aldrich |
| Formic acid (FA) | Merck |
| Glycerole | Merck |
| Glycine | Merck |
| Hepes | Sigma-Aldrich |
| Hydrogen chloride (HCl) | Merck |
| Imidazole | Fluka |
| Iodacetamide (IAM) | Bio-Rad |
| Isoflurene | Aabbott |
| Isopropanol | KMS |

| | |
|--|---------------------|
| Ketamine | Pfizer |
| Lead(II) nitrate | Sigma-Aldrich |
| Luminata Forte | Millipore |
| Magnesium chloride | Sigma-Aldrich |
| Methanol | Roth |
| Microvials PP | VWR international |
| Monopotassium phosphate (KH ₂ PO ₄) | Sigma-Aldrich |
| Nicotinamide adenine dinucleotide (NADH) | Sigma-Aldrich |
| Nitro blue tetrazolium (NBT) | Sigma-Aldrich |
| Phenazine methosulfate (PMS) | Sigma-Aldrich |
| Phosphatase inhibitor cocktail 2 and 3 | Sigma-Aldrich |
| pipettes/pipette tips 0.1-1 000µl | Eppendorf |
| Potassium acetate | Roth |
| Precision Plus Protein All Blue Standard | Bio-Rad |
| Protease inhibitor: Complete C Mini | Roche |
| Protein-Assay (Bradford reagent) | Bio Rad |
| PVDF-membrane | Millipore |
| Saccharose | Sigma-Aldrich |
| Scalpell | Feather |
| Screw cap PP blue | VWR international |
| Sodium carbonate | Merck |
| Sodium chloride (NaCl) | Merck |
| Sodium dodecyl phosphate (SDS) | Bio-Rad |
| Sodium hydroxide (NaOH) | Merck |
| Succinate | Sigma-Aldrich |
| Temed | Bio-Rad |
| Tricine | Bio-Rad |
| Tris Base | Bio-Rad |
| Tris/HCl 0.5M, pH 6.8 | Bio-Rad |
| Tris/HCl 1.5M, pH 8.8 | Bio-Rad |
| Triton X-100 | Sigma-Aldrich |
| Trypsin | Serva |
| Tween 20 | Sigma-Aldrich |
| Ultracentrifugation tube | Beckman, Nr. 326819 |
| Urea | Merck |
| Whatman-paper | Whatman |

3.2 Buffers and solutions

Table 2: Buffers and solutions used in the present study.

| Buffers and solutions | |
|--|--|
| 250-STM buffer | Loading buffer (Western Blot) - 10 ml |
| 250 mM Saccharose | 1.25 ml Tris/HCl (pH 6.8) |
| 50 mM Tris/HCL (pH 7.4) | 4.6 ml 20% SDS |
| 5 mM Magnesiumchloride | 4 ml 100% Glycerol |
| 1/100 Protease Inhibitor | 0.6g DTT |
| | 0.01% Bromphenol blue |
| Coomassie staining solution (PVDF membrane) | 10x TBS |
| 5% isopropanol | 0.2 M Tris |
| 10% acetic acid | 1.37 M NaCl |
| 0.03% Coomassie Blue R250 | pH 8.0 |
| Coomassie destaining solution (PVDF membrane) | Coomassie staining solution (gel) |
| 50% methanol | 10% methanol |
| 10% acetic acid | 5% acetic acid |
| | 0.001% Coomassie Blue R250 |
| Coomassie destaining solution (gel) | 20x BN-loading buffer |
| 10% isopropanol | 50 mM Bis-Tris |
| 10% acetic acid | 500 mM aminocaproic acid |
| | 5% Coomassie Blue G250 |
| 3x BN-buffer | HDP-buffer |
| 1.5 M aminocaproic acid | 10 mM Hepes (pH 7.9) |
| 75 mM Imidazole | 1/100 protease inhibitor |
| pH 7.0 | |
| Transfer-buffer | 1xTBS-T |
| 25 mM Tris | 1x TBS |
| 192 mM glycine | 0.05% Tween |
| 10% methanol | |
| BN-anode-buffer | BN-cathode-buffer |
| 25mM Imidazole | 50 mM tricine |
| pH 7.0 | 7.5 mM imidazole |
| | a) 0.02% Coomassie Blue G250 |
| | b) 0.002% Coomassie Blue G250 |

Activity solution complex I

1mg/mg NBT
0.1mg/ml NADH
0.1 M Tris/HCl (pH 7.4)

Activity solution complex III

50 mM phosphate buffer (pH 7.4)
0.4mg/ml DAB
1mg/ml cytochrome c

Activity solution complex V

35 mM Tris (pH 8.3)
270 mM glycine (pH 8.3)
14mM magnesium chloride
0.2% lead(II) nitrate
8 mM ATP

Activity solution complex II

50 mM phosphate buffer (pH 7.4)
84mM succinate
0.2 mM PMS
2mg/ml NBT
4.5 mM EDTA

Activity solution complex IV

50 mM phosphate buffer (pH 7.4)
1mg/ml DAB
1mg/ml cytochrome c
20µg/ml catalase
75mg/ml saccharose

Solubilization buffer

30 mM Hepes
150 mM potassium acetate
10% glycerol
pH 7.4

3.3 Software and equipment

Table 3: Software and equipment used in the present study.

| Software and equipment | Company |
|--|---|
| 5500 QTRAP triple quadrupole mass spectrometer | AB/SCIEX |
| Adobe Illustrator | Adobe |
| Centrifuge 5804 R | Eppendorf |
| ChemiDoc MP System | Bio-Rad |
| ChemiDoc™ MP Imaging System | Bio-Rad |
| Criterion™ Blotter | Bio-Rad |
| Criterion™ Gel, 1 mm, 18 wells | Bio-Rad |
| Dionex Ultimate 3000 RSLC nanoUPLC | Thermo Fisher Scientific |
| Gel-Scanner: GS-800 Calibrated Densitometer | Bio-Rad |
| Gradient gel-pouring system, Pump P-1 | Pharmacia LKB |
| Graphpad Prism 6 | GraphPad Software |
| Homogenizer PotterS | Sartorius |
| Image Lab™ | Bio-Rad |
| iMark™ Microplate Absorbance reader | Bio-Rad |
| In-house software package iSPY | Cambridge Centre for Proteomics |
| LTQ Orbitrap™ XL mass spectrometer | Thermo Fisher Scientific |
| Mascot Daemon | Matrix Sciences |
| MetaboAnalyst | Metaboanalyst (http://www.metaboanalyst.ca) |
| Microplate Manager Software | Bio-Rad |
| Microsoft office | Microsoft |
| Mini-PROTEAN | Bio-Rad |
| MultiQuant software | AB/SCIEX |
| nanoflow HPLC-2D system | Eksigent |
| PD Quest | Bio-Rad |
| pH Meter, CG803 | Schott |
| Prominence UFLC high-performance liquid chromatography system | Shimadzu |
| Q Exactive™ Orbitrap™ mass spectrometer | Thermo Fisher Scientific |
| Quantity One | Bio-Rad |
| Rex-Leuchtplatte | Roth |
| Sonifier 250 | Branson |
| Spectrophotometer DU 640 | Beckman |
| Speed Vac Plus, SC 210 A | Savant |
| SPSS statistics | IBM |
| String (http://www.string-db.org) | String (http://www.string-db.org) |
| Thermomixer 5436 | Eppendorf |
| Ultracentrifuge sw55Ti XL-90 | Beckmann |
| Ultrasound bath VSR9 | Merck |
| Xcalibur | Thermo Scientific |

3.4 Animals and ketamine treatment

Eight-week-old male C57BL/6 mice (Charles River Laboratories, Maastricht, the Netherlands) were first singly housed for 2 weeks under standard conditions (12h light/dark cycle, lights on at 06.00 am, room temperature 23 ± 2 °C, humidity 60%, tap water and food ad libitum) in the facilities of the Max Planck Institute of Psychiatry. After habituation, the mice were treated intraperitoneally with S-ketamine (3 mg kg⁻¹, Pfizer, Karlsruhe, Germany) or vehicle (0.9% saline solution). 2h, 14h, 24h and 72h after ketamine treatment, an FST was performed measuring the antidepressant-like behavior and afterwards animals were killed by an overdose of isoflurane (Forene, Abbott, Wiesbaden, Germany). Blood was taken cardiac puncture and the animals were subsequently perfused with 0.9% ice-cold saline solution. Mice were decapitated, their livers and brains were harvested and dissected. Tissues and blood were shock-frozen in liquid nitrogen and stored at -80 °C until further analysis. The

experiments were performed in accordance with the European Communities Council Directive 86/609/EEC. The protocols were approved by the committee for the Care and Use of Laboratory Animals of the Government of Upper Bavaria, Germany.

3.5 Forced swim test (FST)

Each mouse was put into a 2 liter glass beaker (diameter: 13 cm, height: 24 cm) filled with tap water (21 ± 1 °C) to a height of 15 cm, so that the mouse could not touch the bottom with its hind paws or tail. Testing duration was 6 min and at the end of the test the animals were immediately dried with a towel and returned to their home cage. The floating time was scored 2h (ketamine-treated animals: n=33, vehicle-treated animals: n=33), 14h (ketamine-treated animals: n=31, vehicle-treated animals: n=29), 24h (ketamine-treated animals: n=33, vehicle-treated animals: n=33) and 72h (ketamine-treated animals: n=31, vehicle-treated animals: n=29) after ketamine treatment by an experienced observer, blind to the condition of the animals.

3.6 Isolation of blood plasma

The animals' blood was taken by cardiac puncture and plasma was obtained by centrifuging the blood in a phosphatase inhibitor cocktail 2 and 3 (Sigma-Aldrich, Munich, Germany), EDTA and protease inhibitor cocktail Tablets 'cOmplete' (Roche Diagnostics, Mannheim, Germany) containing pre-added tube at 1 300g for 10 min. The blood plasma (supernatant) was stored in -20 °C and the pellet containing the blood cells was discarded.

3.7 Isolation of cytoplasmic (CF) and membrane-associated (MF) proteins

CF and MF were prepared by repeated tissue homogenization and extraction of non-membrane-associated proteins and solubilization of MF proteins with sodium dodecyl sulfate (SDS). In detail, tissues were homogenized for 30s in 1ml of 2 M NaCl, 10 mM Hepes/NaOH, pH 7.4, containing 1mM EDTA, phosphatase inhibitor cocktail 2 and 3 (Sigma-Aldrich, Munich, Germany), protease inhibitor cocktail Tablets 'cOmplete' (Roche Diagnostics, Mannheim, Germany), then incubated for 10 min and homogenized again for 30 s and further with a ultrasonicator for 3×10 s on ice. The homogenates were centrifuged at 16 100 g at 4 °C for 20min. The supernatant contained the CF proteins. The pellets were rehomogenized in 1 ml of 0.1 M Na_2CO_3 and 1 mM EDTA containing 1 mM EDTA, phosphatase inhibitor cocktail 2 and 3 (Sigma-Aldrich, Munich, Germany), protease inhibitor cocktail Tablets 'cOmplete' (Roche Diagnostics, Mannheim, Germany), pH 11.3, mixed at 4 °C for 30 min and collected by centrifugation (16 100g at 4 °C for 20min). Subsequently, the pellets were extracted with 5 M urea, 100 mM NaCl, 10 mM Hepes, pH 7.4 and 1 mM EDTA containing 1 mM EDTA, phosphatase inhibitor cocktail 2 and 3 (Sigma-Aldrich, Munich, Germany), protease inhibitor cocktail Tablets 'cOmplete' (Roche Diagnostics, Mannheim, Germany) and then washed twice with 0.1 M Tris/HCl, containing 1 mM EDTA, phosphatase inhibitor cocktail 2 and 3 (Sigma-Aldrich, Munich, Germany), protease inhibitor cocktail Tablets 'cOmplete' (Roche Diagnostics, Mannheim, Germany) pH 7.6. The pellets were solubilized in 20-50 μl of 2% SDS, 50 mM dithiothreitol and 0.1 M Tris/HCl, containing 1 mM EDTA, phosphatase inhibitor cocktail 2 and 3 (Sigma-Aldrich, Munich, Germany), protease

inhibitor cocktail Tablets 'cOmplete' (Roche Diagnostics, Mannheim, Germany) pH 7.6, at 90 °C for 1 min and stored at -20 °C until further analysis.

3.8 Protein concentration determination with the Bradford assay

CF protein concentrations were determined by a Bradford protein assay (Bio-Rad, Hercules, USA) based on the principles of Bradford according to the manufactures descriptions⁴¹⁷.

3.9 Protein concentration determination with the Lowry assay

MF protein concentrations were determined by a Lowry protein assay (Bio-Rad, Hercules, USA) based on the manufactures descriptions⁴¹⁸.

3.10 Western Blot

Hippocampal MF and CF proteins from 8-week-old male C57BL/6 mice treated with ketamine for 2h, 14h, 24h and 72h were fractionated by SDS-polyacrylamide gel electrophoresis and Western Blot was performed based on standard protocols. After electrophoresis, proteins were transferred to PVDF membranes (Immobilon-P, Millipore, Billerica, USA). Primary antibodies were against complex II subunit A of the succinate dehydrogenase complex (SDHA, sc98253, Santa Cruz Biotechnology, Dallas, USA), protein kinase C γ (PKC γ , Acris antibodies, Herford, Germany), Ca²⁺/calmodulin-dependent protein kinase II α (CaMKII α , Abcam, Cambridge, UK), subunit 1 of gamma-aminobutyric acid type A receptor (GABA_AR1, Abcam, Cambridge, UK), subunit 1 of N-Methyl-D-aspartate receptor 1 (NMDAR1, Abcam, Cambridge, UK), Peroxisome proliferator-activated receptor gamma coactivator 1- α (PGC1 α , Novus Biologicals, Littleton, USA), mitochondrial transcription factor A (Tfam, Abcam, Cambridge, UK), adenosinmonophosphate-activated proteinkinase (AMPK, Abcam, Cambridge, UK), phosphorylated AMPK (pAMPK, Cell Signaling, Merck, Darmstadt, Germany), peroxiredoxin 1 (Prdx1, Abcam, Cambridge, UK), Peroxiredoxin 3 (Prdx3, Abcam, Cambridge, UK), translocase of inner membrane (Tim23, BD Biosciences, Heidelberg, Germany), β -Actin (Sigma, Munich, Germany), Porin (Abcam, Cambridge, UK), myelin basic protein (MBP, Abcam, Cambridge, UK), myelin oligodendrocyte glycoprotein (MOG, Abcam, Cambridge, UK) and oxidative phosphorylation (OXPHOS) protein complexes by a premixed antibody cocktail ('MitoProfile', Abcam, Cambridge, UK) against complex I subunit NADH:ubiquinone oxidoreductase subunit B8 (NDUFB8), complex II SDHB, complex III mitochondrial cytochrome C oxidase subunit I (MTCOI), complex IV (Ubiquinol-cytochrome C reductase core protein II (UQCRC2) and complex V ATP synthase subunit alpha (ATP5a). Anti-rabbit, anti-mouse and anti-goat ECL horseradish peroxidase-linked secondary antibodies (GE Healthcare Life Sciences, Little Chalfont, Buckinghamshire, UK) were used. The densitometric analyses were performed with the Image Lab software (Bio-Rad, Munich, Germany).

3.11 OxyBlot™ Protein oxidation detection

Oxidative modification of proteins by oxygen free radicals and other reactive species (ROS) occurs in physiologic and pathologic processes. As a consequence of the modification, carbonyl groups are introduced into protein side chains by a site-specific mechanism. The OxyBlot™ Kit (Merck Millipore, Darmstadt, Germany) provides reagents for simple and sensitive immunodetection of these carbonyl groups, which is a hallmark of the oxidation status of proteins. The carbonyl groups in the protein side chains are derivatized to 2,4-Dinitrophenylhydrazone (DNP-hydrazone) by reaction with 2,4-Dinitrophenylhydrazine (DNPH). The DNP-derivatized protein samples are separated by SDS-gel electrophoresis followed by Western Blot. Afterwards, the membrane is incubated with primary antibody (Anti-DNP), specific to the DNP moiety of the proteins. This step is followed by incubation with a horseradish peroxidase-antibody conjugate directed against the primary antibody (secondary antibody: goat anti-rabbit immunoglobulin).

5µL containing 10µg of CF hippocampal protein sample is transferred into an eppendorf tube and 5µL 12% SDS is added for a final concentration of 6% SDS. The sample is derivatized by adding 10µL of 1x DNPH Solution. The mixture is incubated at room temperature for 15 min in the dark. 7.5µL of Neutralization Solution is added to stop the reaction. 1µL of 2-Mercaptoethanol is added to the sample mixture to avoid further protein oxidation. The protein mixture was then separated in an SDS-gel and Western Blot was performed based on standard protocols. After electrophoresis, proteins were transferred to PVDF membranes (Immobilon-P, Millipore, Billerica, MA, USA).

3.12 Total antioxidant capacity (TAC)

The TAC Assay Kit (BioVision, Milpitas, USA) measures antioxidant molecules and proteins by reducing Cu^{2+} to Cu^+ . Cu^+ chelates with a colorimetric probe giving a broad absorbance peak around 570 nm, proportional to the total antioxidant capacity. The lyophilized Trolox standard is dissolved in 20µL of DMSO by vortexing, then 980µL of water is added and mixed well, generating a final 1 mM solution. Antioxidants are measured by adjusting 0.25µL CF protein sample to 100µL total volume, filling the sample with water. One part of the Cu^{2+} reagent is diluted with 49 parts of the Assay diluent. 100µL of Cu^{2+} working solution is added to all standard and samples. The mixture is transferred to a 96 well plate, covered and incubated at room temperature for 1.5h. Afterwards, the signal is measured at an absorbance of 570 nm using the plate reader.

3.13 Isolation of mitochondria

Mitochondria were isolated by repeated brain tissue homogenization and centrifugation. Therefore, brain tissue of approximately 30mg were incubated in 180µL of 250-STM buffer for 15 min on ice and then homogenized, incubated for 10 min on ice and homogenized a second time. The homogenate was then centrifuged at 800g for 15 min at 4°C. The supernatant contains already mitochondria. The pellet also containing mitochondria is resuspended with 640µL 250-STM buffer and centrifuged at 800g for 15 min at 4°C. This supernatant is combined with the first one and centrifuged at 6 000g for 15 min at 4°C. The mitochondria enriched pellet is resuspended with 100µL of 250-STM buffer and centrifuged a 6 000g for 15 min at 4°C. The pellet is resuspended with 250µL 10 mM Hepes, incubated on ice for 30 min and subsequently loaded on a sucrose gradient containing 1.75ml of

50%, 1.75ml of 36% and 0.75ml of 20% sucrose and centrifuged at 25 000rpm at 4°C for 60 min. Afterwards the third fraction between the 20% and 36% sucrose contain the mitochondria and are washed twice with 1.5ml 10mM Hepes and centrifuged at 17 200g for 20 min at 4 °C. The pellet is resuspended with 50µl 10mM Hepes and the protein concentration determined with Bradford assay. Mitochondrial membrane protein complexes are solubilized with 1ml solubilization buffer without digitonin, Dodecylmaltoside (DDM) or Triton-x100 and centrifuged twice at 17 500g for 10 min at 4 °C. 50µl solubilization buffer with 2µl of a 20% Digitonin stock solution (8g Digitonin/g protein) or 0.75µl of a 20% DDM stock solution (3g DDM/g protein) or 0.75µl of a 20% Triton-x100 stock solution (3g Triton-x100/g protein) is added to the pellet and incubated for 30 min at 4 °C while gently mixing. Subsequent centrifugation at 17 500g for 10 min at 4 °C results in a supernatant containing mitochondrial membrane protein complexes. Afterwards 1x BN-loading buffer is added to the mitochondrial membrane protein complexes for the blue native-polyacrylamide gel electrophoresis (BN-PAGE).

3.14 Blue native-polyacrylamide gel electrophoresis (BN-PAGE)

Native protein complexes can be separated by BN-PAGE. Therefore, also mitochondrial membrane protein complexes are separated in a 4% to 16% gradient gel without SDS as a detergent. Coomassie contains a negative anionic charge and can binds to hydrophobic membrane proteins. Therefore, the proteins can be electrophoretic separated. BN-cathode buffer with 0.02% Coomassie is filled into the inner chamber and the BN-anode buffer into the outer chamber. Gel electrophoresis starts with 100V and is subsequently increased up to 200V. After approximately one third of the SDS-gel-electrophoresis, the BN-cathode buffer with 0.02% Coomassie is exchanged with BN-cathode buffer containing 0.002% Coomassie. Mitochondrial OXPHOS ETC protein complexes were then identified by LC-ESI-MS/MS with the LTQ Orbitrap XL™ (Thermo Fisher Scientific, Bremen, Germany).

3.15 Sample preparation for LC-ESI-MS/MS analyses

3.15.1 Protein sample preparation for the identification of OXPHOS ETC protein complexes

Identification of mitochondrial OXPHOS protein complexes requires the separation of the complexes by BN-PAGE. Separated protein complexes were then stained with Coomassie staining solution for 20 min and destained over night with Coomassie destaining solution. Each gel band of interest was cut into an approximately 2.5 mm gel slice and then further cut into smaller gel pieces.

3.15.2 Protein sample preparation for quantitative proteomics analyses

Hippocampal CF and MF proteins were mixed 1:1 with CF and MF ¹⁵N-labeled internal standard. *In vivo* ¹⁵N-labeled hippocampal proteins were derived from C57BL/6 mice mice that were raised with a ¹⁵N mouse diet (Silantes, Munich, Germany) for 12 weeks. 50 µg of the ¹⁴N/¹⁵N protein mixture were separated by SDS gel electrophoresis. Separated proteins were stained with Coomassie staining solution for 20 min and destained over night with Coomassie destaining solution. Each gel lane was

cut into 16 approximately 2.5 mm slices per biological replicate and these further cut into smaller gel pieces.

3.15.3 In-gel-trypsin digestion and peptide extraction

The gel pieces were covered with 100 μ l of 25 mM Na₄HCO₃/50% ACN in order to destain the gel pieces completely and mixed for 10 min at room temperature. The supernatant was discarded and this step repeated twice. Proteins inside the gel pieces are reduced with 75 μ l 1x DTT/25 mM NH₄HCO₃ mixed at 56 °C for 30 min in the dark. The supernatant is discarded and for alkylation 100 μ l IAM are added to the gel pieces and mixed for 30 min at room temperature. The supernatant was discarded and the gel pieces washed twice with 100 μ l 25 mM Na₄HCO₃/50% ACN and mixed for 10 min at room temperature. The supernatant is discarded and gel pieces are dried for approximately 20 min at room temperature. Proteins are digested with 50 μ l trypsin solution (5ng/ μ l trypsin/25 mM NH₄HCO₃) over night at 37 °C. Peptides were extracted from the gel pieces by mixing them in 50 μ l of 2% FA/50% ACN for 20 min at 37 °C and subsequently sonicating them for 5 min. The supernatant contains the peptides. This step is repeated twice with 50 μ l of 1% FA/50% ACN. The supernatants are then combined and the solution removed by centrifugal vacuum concentrator (Speed Vac Plus, SC 210 A, Savant) and the pellet is stored at -20 °C.

3.16 Protein identification with LTQ Orbitrap XL™

The LTQ Orbitrap XL™ is a hybrid fourier transform (FT) mass spectrometer combining a linear ion trap MS and the Orbitrap mass analyzer. Peptide ions are generated by electrospray ionization (ESI) and collected in the LTQ XL and afterwards ejected into the C-shaped storage trap. The C-trap is used to store and for collision before injecting them to the Orbitrap Mass Analyzer. Signals are amplified and transformed into a frequency spectrum by fast Fourier transformation which is finally converted into a mass spectrum. Ions can be selected in the linear ion trap and fragmented either in the ion trap (CID) or in the collision cell (HCD). For HCD (Higher Energy Collisional Dissociation) ions are passed through the C-trap into the gas-filled collision cell (figure 4)⁴¹⁹.

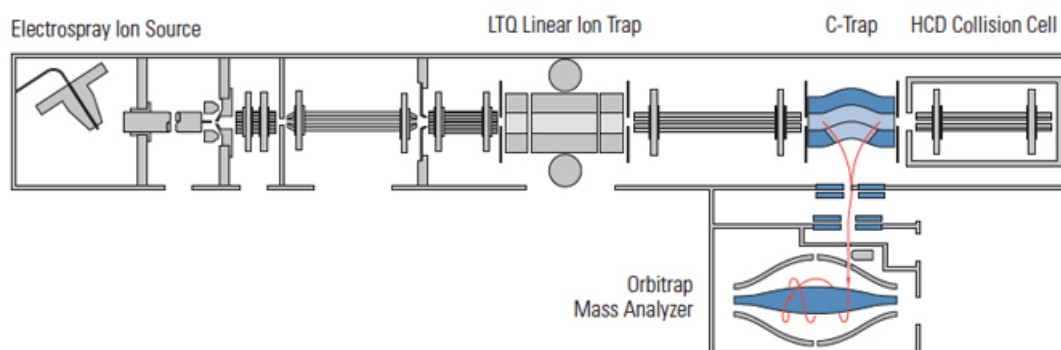


Figure 4: Schematic of the LTQ Orbitrap™. The LTQ Orbitrap XL™ consists of an ESI Ion Source, an LTQ XL Linear Ion Trap, a C-Trap, an HCD Collision Cell and an Orbitrap Mass Analyzer⁴¹⁹.

The mitochondrial membrane protein samples for MS-measurements are filtered beforehand with Costar SpinX filter tubes. They are first activated with 5 μ l of 0.1% HCOOH, centrifuged at 1 000g for 1

min at 4 °C and the flow-through was discarded. The protein samples are dissolved in 20µl 0.1% HCOOH, vortexed for 30 sec and sonicated for 10 min. 7µl of the protein samples are transferred to Costar SpinX filter tubes and centrifuged for 3 min at 1000g at 4 °C and 5µl of the filtered protein sample filled into a vial for MS-measurements. Tryptic peptides were then dissolved in 0.1% FA and analyzed with a nanoflow HPLC-2D system (Eksigent, Dublin, CA, USA) coupled online to an LTQ-Orbitrap XL™ mass spectrometer. Samples were on-line desalted for 10 min with 0.1% FA at 3 µl/min (Zorbax-C18 (5 µm) guard column, 300 µm × 5 mm, Agilent Technologies, Santa Clara, CA, USA) and separated via RP-C18 (3 µm) chromatography (in-house packed Pico-frit column, 75 µm × 15 cm, New Objective, Woburn, MA, USA). Peptides were eluted with a gradient of 95% ACN/0.1% HCOOH from 10% to 45% over 93 min at a flow rate of 200 nl/min. Column effluents were directly infused into the mass spectrometer via a nanoelectrospray ion source (Thermo Fisher Scientific). The mass spectrometer was operated in positive mode applying a data-dependent scan switch between MS and MS/MS acquisition. Full scans were recorded in the Orbitrap mass analyzer (profile mode, m/z 380–1600, resolution $R = 60000$ at m/z 400). The MS/MS analyses of the five most intense peptide ions for each scan were recorded in the LTQ mass analyzer in centroid mode. The mitochondrial OXPHOS ETC protein complexes were then identified with Mascot Daemon (Matrix Sciences London, <http://www.matrixscience.com/daemon.html>). Proteins were considered with a score ≥ 50 and ≥ 2 peptide matches and searched within the Swiss-Prot database $FDR \leq 0.052$.

3.17 Quantitative proteomics analyses with Q Exactive™ Hybrid Quadrupole-Orbitrap™ Mass Spectrometer

The Q Exactive™ Quadrupole-Orbitrap™ mass spectrometer combines high-performance quadrupole precursor selection with high-resolution and accurate mass Orbitrap detection (figure 5)⁴²⁰.

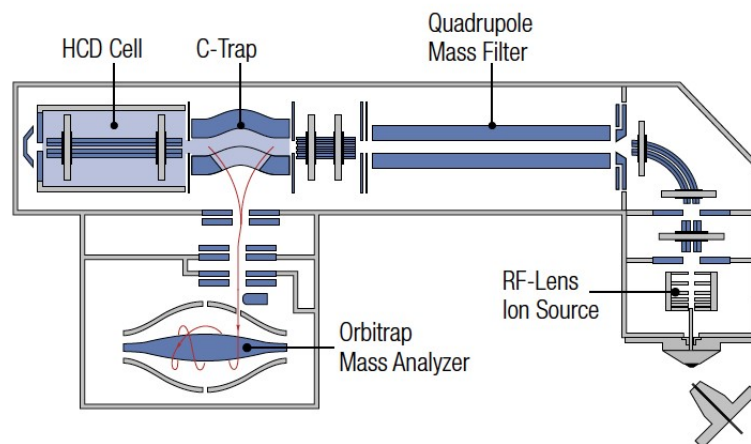


Figure 5: Schematic representation of the Q Exactive™ Quadrupole-Orbitrap™. The mass spectrometer consists of an ESI ion source, a quadrupole mass filter, a C-Trap, an HCD Collision Cell and an Orbitrap Mass Analyzer⁴²⁰.

Hippocampal MF and CF proteins were identified and quantified by a Dionex Ultimate 3000 RSLC nanoUPLC (Thermo Fisher Scientific, Waltham, USA) system and a Q Exactive™ Orbitrap™ mass spectrometer (figure 5, Thermo Fisher Scientific, Waltham, USA). Separation of peptides was performed by reverse-phase chromatography at a flow rate of 300 nl/min and a Thermo Scientific reverse-phase nano easy-spray column (Thermo Scientific PepMap C18, 2 µm particle size, 100A pore size, 75 µm x 50 cm length). Peptides were loaded onto a pre-column (Thermo Scientific PepMap 100 C18, 5 µm particle size, 100A pore size, 300 µm x 5mm length) from the Ultimate 3000 autosampler

with 0.1% FA for 3 min at a flow rate of 10 μ l/min. After this period, the column valve was switched to allow elution of peptides from the pre-column onto the analytical column. Solvent A was water + 0.1% FA and solvent B was 80% ACN, 20% water + 0.1% FA. The linear gradient employed was 2-40% B in 30 min. The LC eluant was sprayed into the MS by means of an easy-spray source (Thermo Fisher Scientific). All m/z values of eluting ions were measured in an Orbitrap mass analyzer, set at a resolution of 70 000. Data dependent scans (Top 20) were employed to automatically isolate and generate fragment ions by higher energy collisional dissociation (HCD) in the quadrupole mass analyzer and measurement of the resulting fragment ions was performed in the Orbitrap analyser, set at a resolution of 17 500. Peptide ions with charge states of 2+ to 4+ and above were selected for fragmentation.

Orbitrap™ raw files were converted to mzXML files using MSConvert software. The in-house software package iSPY, which was adapted from an earlier version of a peptide quantitation program known as iTracker, was used to identify and quantify peptides. The software was used to convert mzXML to mgf files that were then finally imported into Mascot and searched against the SwissProt Mouse database and a decoy database. The databases were searched using the following settings: variable modifications of carbamidomethyl (cys), oxidation (met); 20 ppm peptide tolerance, 0.1 Da MS/MS tolerance, 2 missed cleavages and peptide charge state of +2, +3, or +4. In iSPY, Mascot dat output files were run through Percolator for improved identification. Non-unique peptides were discarded. Only peptides with a protein type 1 error of less than 0.01 were kept in the final dataset. The heavy and light peak intensities for each peptide were calculated in iSPY using retention time and sequence information from the MS1 spectra and Mascot search, respectively. Briefly, the intensities for a pre-specified number of isotopomeric peaks were calculated by scanning through a retention window spanning a set distance either side of the maximum intensity value. The ^{14}N and ^{15}N peptide isotopic peaks from the MS1 dataset were used to compare the theoretical mass difference between the heavy and light peptides, and the typical isotopic distribution patterns. Only quantifiable peptides (those for which both a heavy and a light peak intensity were identified in five replicates) were included in the dataset.

3.18 OXPHOS protein complex in-gel-enzymatic activity measurement

The enzymatic activity of the mitochondrial membrane OXPHOS protein complexes were measured in the gel by histochemical staining through redox reactions of the OXPHOS protein complexes enzymatic activity. The gel bands of interest were cut out of the gel and for a minimum of 30 min incubated in a pre-incubation buffer. Afterwards the gel bands were incubated in activity solution different time points depending on the ETC protein complex (complex I: 3.5 min; complex II: 30 min; complex III: 50-60 min; complex IV: 40 min; complex V: 80 min). The reaction was then stopped with a stopping solution for complex I-IV containing 50% methanol/10% HCOOH and for complex V 50% methanol.

3.19 Ketamine treated mouse primary hippocampal neurons

PHN were a gift from Dr. D. Refojo and S. A. Giusti (Max Planck Institute of Psychiatry, Munich, Germany). Briefly, the PHN were prepared from CD1 mouse embryos (E17.5–E19.5) and maintained in Neurobasal-A medium with 2% B-27 and 0.5 mM GlutaMAX-I (Gibco) at 37 °C and 5% CO_2 ⁴²¹. After

3 weeks PHN maturation, cells were treated with different concentrations of ketamine for 24h (0.005 M, 0.001 M, 0.0009 M, 0.0008 M, 0.0007 M, 0.0006 M, 0.0005 M, 0.0004 M, 0.0003 M, 0.0002 M, 0.0001 M, 0.00009 M, 0.00008 M, 0.00007 M, 0.00006 M, 0.00005 M, 0.00004 M, 0.00003 M, 0.00002 M, 0.00001 M, 0.000005 M, 0.000001 M) and tested for cell viability with the 3-(4,5-dimethylthiazol-2-yl)-2,5-diphenyltetrazolium (MTT) assay. Further, mature 3 week-old PHN were treated with 0.0001 M of ketamine for 24h and metabolites were isolated for further metabolomics analyses.

3.20 Cytotoxicity measurement through the MTT assay

Cytotoxicity was measured by the MTT calorimetric assay that determines cell metabolic rate. Viable, metabolically active cells produce reduction equivalents that reduce the MTT to its insoluble formazan that shows an absorbance maximum at 570 nm. The quantity of formazan is directly proportional to the number of viable cells. PHN were grown in a 96 well plate with 150 µl of medium. 75 µl of the medium was removed and 25 µl of MTT (2mg/ml in PBS) was added and covered with the 75 µl of the remaining medium subsequently incubated for 6h at 37 °C. The formazan was solubilized by incubation of 100 µl 40 % dimethylformamide/ 10 % SDS, pH 4 over night in the dark at room temperature. The formazan dependent absorbance was then measured at 570 nm.

3.21 Isolation of polar metabolites

3.21.1 Isolation of polar metabolites from mouse tissue

Mouse tissues were homogenized (2 min × 1 200 min⁻¹, homogenizer PotterS, Sartorius, Göttingen, Germany) in 30-fold ice-cold 80% methanol. Samples were centrifuged (14 000 g, 10 min, 4 °C) and the supernatants were incubated on dry ice. Afterwards, the pellets were incubated in 6-fold ice-cold 80% methanol and then combined with the previous supernatants. The metabolite extracts were vortexed, centrifuged (14 000 g, 10 min, 4 °C), and the solution was removed by centrifugal vacuum concentrator (Speed Vac Plus, SC 210 A, Savant) and the samples stored at -80 °C.

3.21.2 Isolation of polar metabolites from mouse blood plasma

400µl of cold (stored at -80 °C) 100% methanol was added to 100µl of mouse blood plasma and vortexed for 2 min and afterwards incubated on dry ice for 2h. The mixture was then centrifuged at 2 053 g for 10 min at 4 °C. The supernatant was transferred to a new tube and subsequently centrifuged at 1 105 g for 2 min at 4 °C. The solution was removed by centrifugal vacuum concentrator (Speed Vac Plus, SC 210 A, Savant) and the samples stored at -80 °C.

3.21.3 Isolation of polar metabolites from PHN

The metabolism of the cells are slowed down by incubating the cell culture plates on ice for 10 min. Afterwards the cell were washed twice with Dulbecco's phosphate-buffered saline and incubated on

dry ice until the cells are completely frozen. Twice, 500 μ l of ice-cold 80% methanol (stored at -80 °C) was added, the plates are transferred to ice, scraped and the fluid collected and subsequently frozen in liquid nitrogen. The samples were then melt on ice, subsequently vortexed for 30s and centrifuged for 10 min at 800 g at 4 °C. The supernatant was then stored at dry ice and the pellet resolved with 500 μ l of ice-cold 80% methanol (stored at -80 °C) and the sample frozen in liquid nitrogen. The mixture was then melt again on ice, vortexed for 30s and centrifuged for 10 min at 800 g at 4 °C. The supernatants are combined, centrifuged at 15 000 rpm for 1 min subsequently transferred to a new tube and the solution was removed by centrifugal vacuum concentrator (Speed Vac Plus, SC 210 A, Savant) and the samples stored at -80 °C.

3.22 Targeted metabolomics analysis through selected reaction monitoring (SRM) with 5500 QTRAP triple quadrupole

Samples were resuspended using 20 μ l liquid chromatography-mass spectrometry grade water. 10 μ l were injected and analyzed using a 5500 QTRAP triple quadrupole mass spectrometer (AB/SCIEX, Framingham, USA) coupled to a Prominence UFLC high-performance liquid chromatography system (Shimadzu, Columbia, USA) via SRM of a total of 293 endogenous water-soluble metabolites for steady-state analyses of samples (figure 6).

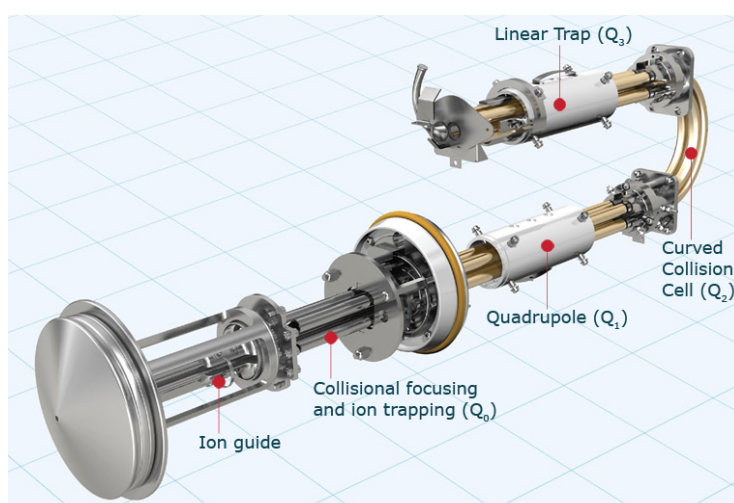


Figure 6: Schematic representation of the 5500 QTRAP triple quadrupole. The mass spectrometer consists of an ESI ion source, three quadrupoles. In targeted metabolomics research the first quadrupole Q1 selects specific ions (metabolites), the second Q2 fragment these ions and the third Q3 select the fragment ions⁴²².

Samples were delivered to the mass spectrometer via normal phase chromatography using a 4.6-mm \times 10 cm Amide Xbridge HILIC column (Waters, Milford, USA) at 350 μ l min⁻¹. Gradients were run starting from 85% buffer B (high-performance liquid chromatography grade ACN) to 42% B from 0 to 5 min; 42% B to 0% B from 5 to 16 min; 0% B was held from 16 to 24 min; 0% B to 85% B from 24 to 25 min; 85% B was held for 7 min to re-equilibrate the column. Buffer A comprised 20 mM ammonium hydroxide/20 mM ammonium acetate (pH 9.0) in 95:5 water:ACN. Some metabolites were targeted in both positive and negative ion modes for selected reaction monitoring transitions using positive/negative polarity switching. Electrospray ionization voltage was +4 900 V in positive ion mode and - 4500 V in negative ion mode. The dwell time was 4 ms per selected reaction monitoring transition and the total cycle time was 1.89 s. Approximately 9–12 data points were acquired per detected metabolite. Peak areas from the total ion current for each metabolite-selected

reaction monitoring transition were integrated using the MultiQuant v2.0 software (AB/SCIEX)⁴²³. Animals from the same cohort were used for all metabolomics analyses.

3.23 Statistics and data analyses

3.23.1 Identification of significant metabolite and protein level alterations

Metabolite intensities as well as protein ratios were median-normalized and auto-scaled for statistical analysis. Significant metabolite and protein level changes 2h, 14h, 24h and 72h upon ketamine treatment were identified by multivariate partial least squares-discriminant analyses (PLS-DA) and high-dimensional feature selection significance analysis of microarrays (SAM) using MetaboAnalyst⁴²⁴⁻⁴²⁶. The quality of the PLS-DA models were assessed for R^2 , Q^2 and accuracy values with variable influence of projection (VIP)-score ≥ 1.0 and for SAM with $q \leq 0.1$ and false discovery rate (FDR) ≤ 0.10 ⁴²⁷. We improved robustness of our data analyses and increased confidence in significantly altered metabolites and proteins as well as in the subsequent analyses of overrepresented KEGG pathways by only considering the overlap between the two different statistical methods.

3.23.2 Identification of significantly enriched pathways

Metabolomics pathway analyses were performed using MetaboAnalyst^{424, 425} applying a hypergeometric algorithm for overrepresentation analysis and relative-betweenness centrality for pathway topology analysis. Pathways were considered affected if they were significantly enriched for KEGG pathways ($P_{\text{Holm-corrected}} \leq 0.05$) for all significantly altered metabolites. Proteomic pathway enrichment for KEGG pathways was assessed by String with an FDR ≤ 0.10 ^{428, 429}.

3.23.3 Calculation of metabolite pair ratios

The median-normalized metabolite intensities before auto-scaling of selected pairs of metabolites were used to calculate metabolite ratios. For statistical analyses, Student's t-test was performed by using the metabolite ratio of interest for each ketamine- and vehicle-treated animal (for example, metabolite x/metabolite y of one ketamine-treated animal) calculated by dividing the metabolite intensity of metabolite x by the intensity of metabolite y for each time point. The final metabolite ratio of interest (for example, metabolite x/metabolite y for all ketamine- and vehicle-treated animals) was then calculated by dividing the average metabolite intensities of all ketamine-treated animals by the average metabolite intensities of all vehicle-treated animals.

3.23.4 Identification of metabolite biomarker candidates

AD treatment hippocampal metabolite biomarker candidates were detected by applying multivariate PLS-DA models taking the VIP-scores (VIP-score ≥ 1.0) and SAM with $q \leq 0.10$ and FDR ≤ 0.10 into account. The quality of the PLS-DA models was assessed in terms of R^2 , Q^2 and accuracy values. Metabolites qualified as biomarker candidates if they had a consistent VIP-score ≥ 1.0 for the 2h, 14h

and 24h time points for which good and robust PLS-DA models had been determined. In addition, they required $q \leq 0.1$ for at least one of the time points.

4.0 Results

The overall goal of the present study was to identify biosignatures and molecular pathways affected by ketamine treatment. My results aid in the development of novel fast acting ADs with a similar mode of action as ketamine, but with fewer side effects.

First, I investigated the fast antidepressant-like effects of a low dose of ketamine with the help of a behavioral test, FST. Next, I compared metabolite profiles of defined brain regions, the liver, and blood from drug- and vehicle-treated mice as well as mouse primary hippocampal neurons (PHN). In addition, the metabolomics results obtained from the HPC revealed biomarkers for ketamine's antidepressant-like effects that aid in the development of fast acting ADs. I also investigated time-dependent hippocampal proteome alterations between ketamine- and vehicle-treated mice and compared specific protein expression profiles based on the molecular pathways identified by metabolomics analyses.

4.1 Investigating the antidepressant-like effect of ketamine through the FST

To investigate ketamine's fast antidepressant activity I chose the FST, the most widely used behavioral assay to study antidepressant-like effects in mice and rats. C57BL/6 wild-type mice were assessed at different time points with regard to the antidepressant-like FST floating behavior after receiving a single injection of a low dose of ketamine (3 mg kg^{-1} ; figure 7). In order to avoid any behavioral habituation, independent groups of mice were examined for their FST floating time. A two-way analysis of variance (ANOVA) showed no statistically significant interaction between the effects of treatment and different time points on the FST floating time.

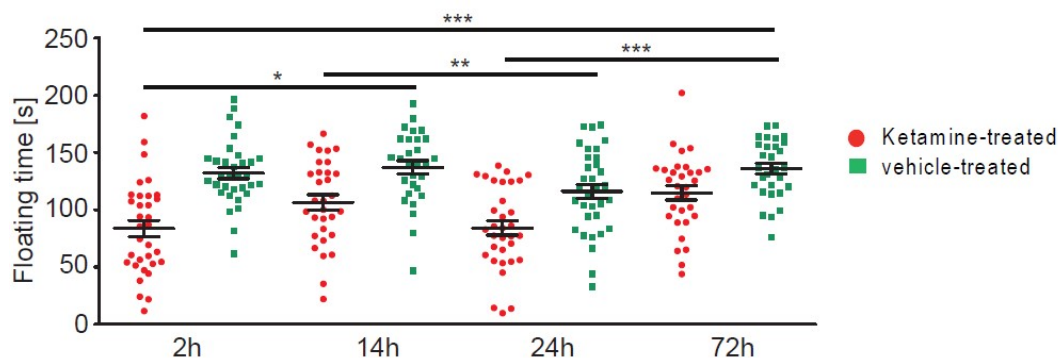


Figure 7: Antidepressant-like behavioral analysis of ketamine- (3 mg kg^{-1}) and vehicle-treated wild-type mice. Passive floating behavior was measured using FST. Independent groups of mice were used for all time points to avoid behavioral habituation. The floating time was scored 2h (ketamine-treated animals: $n=33$, vehicle-treated animals: $n=33$), 14h (ketamine-treated animals: $n=31$, vehicle-treated animals: $n=29$), 24h (ketamine-treated animals: $n=33$, vehicle-treated animals: $n=33$) and 72h (ketamine-treated animals: $n=31$, vehicle-treated animals: $n=29$) after the respective treatment. Two-way analysis of variance (ANOVA) followed by Tukey's honest significant difference (HSD) test, $F_{(1,244)}=58.75$, $p \leq 0.001$ for treatment groups; $F_{(3,244)}=7.59$, $p \leq 0.001$ for duration of response; $F_{(3,244)}=1.77$, $p=0.15$ for treatment-duration interaction. *: $p \leq 0.05$, **: $p \leq 0.01$, ***: $p \leq 0.001$. P-values were determined by two-way ANOVA and Tukey's HSD test. Error bars represent s.e.m.

The main effects analysis showed a significant reduction in FST floating time when comparing ketamine- with vehicle-treated animals and significant alterations for the different time points. Therefore, no treatment effects for the individual time points were examined. A Tukey's honest significant difference (HSD) test revealed a statistically significant difference in FST floating time

between the 2h (ketamine-treated animals: n=33, vehicle-treated animals: n=33), 14h (ketamine-treated animals: n=31, vehicle-treated animals: n=29) and 72h (ketamine-treated animals: n=31, vehicle-treated animals: n=29) time points, between the 14h and 24h (ketamine-treated animals: n=33, vehicle-treated animals: n=33) time points and between the 24h and 72h time points.

Ketamine's fast antidepressant-like effect is reflected on the behavioral level by the FST floating time. To determine the biomolecular effects of drug action I next analyzed time dependent metabolomics changes.

4.2 Metabolomics profiling of ketamine treated mice and primary hippocampal neurons

Alterations affecting the metabolome are a reflection of modified pathway activities in response to drug treatment^{430, 431}. In the present study, C57BL/6 mice as well as PHN treated with a single low dose of ketamine (3mg kg^{-1} in mice and $100\mu\text{M}$ for PHN) were analyzed in order to identify affected biomolecular pathways and to assemble treatment biomarkers with the help of a sensitive metabolomics platform (for details, cf. chapter 3). Metabolomics profiling analyses of defined mouse brain regions, liver, blood, as well as mouse PHN were performed. The analyses are focused on the HPC and PFC as these brain regions are well known for their involvement in MDD pathobiology (for details, cf. chapter 1). Besides, the cerebellum (CRBL) was included as a brain region with no significant role in MDD pathobiology. I also acquired metabolomics data for blood plasma (BP) and the liver. On the basis of the obtained FST results (cf. section 4.1) 5 mice per group and time point were chosen for the metabolomics analyses.

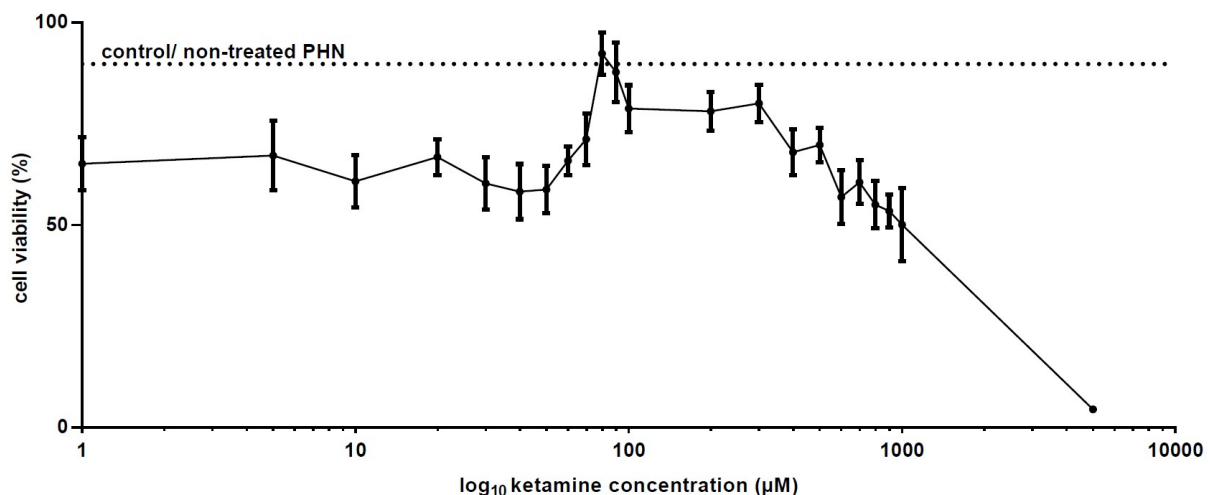


Figure 8: Cellular viability of mouse PHN treated with 22 different concentrations of ketamine measured with the MTT-assay. The dotted line indicates cell viability without ketamine treatment.

The ketamine concentration for PHN treatment was assessed with the MTT assay (figure 8). This colorimetric assay measures metabolic activity and thus indirectly cellular viability. PHN were treated with 22 different concentrations of ketamine for 24h and cellular viability was compared to control/non-treated PHN. Low doses of ketamine ($\leq 80\mu\text{M}$ of ketamine) result in decreased cellular viability of ~60–70%. The cellular viability increases again with $80\mu\text{M}$ ketamine up to control levels. However, then the cellular viability decreases again with increased ketamine concentrations resulting in a very low metabolic rate and increased cell death (figure 8). Based on these results I treated PHN

with a low dose of 100 μ M of ketamine for 24h. Cell viability was still very high at \sim 80% and only slightly below that observed for control PHN.

4.2.1 Comparative Metabolomics profiling of defined mouse brain regions, the liver, blood, and mouse primary hippocampal neurons

A total of 228, 233, 243, 233, and twice 196 metabolites were quantified in the PHN 24h, CRBL 2h, liver 2h, PFC 2h, BP 2h and BP 24h, respectively (supplemental table 1). In comparison to univariate statistical analyses like the t-test, multivariate statistical analyses consider many dependent variables in contrast to a single one. Therefore, univariate statistical analyses are generally not recommended to be used when dealing with very large variable (here: metabolites) numbers since many metabolites would appear significant just by chance. Usually this issue can also be avoided in univariate statistical analyses with many dependent variables by multiple testing like Bonferroni correction. However, this method tends to be too conservative and therefore, I used multivariate statistical analyses taking all metabolites into account. I combined two different multivariate statistical methods in order to achieve robust metabolomics results.

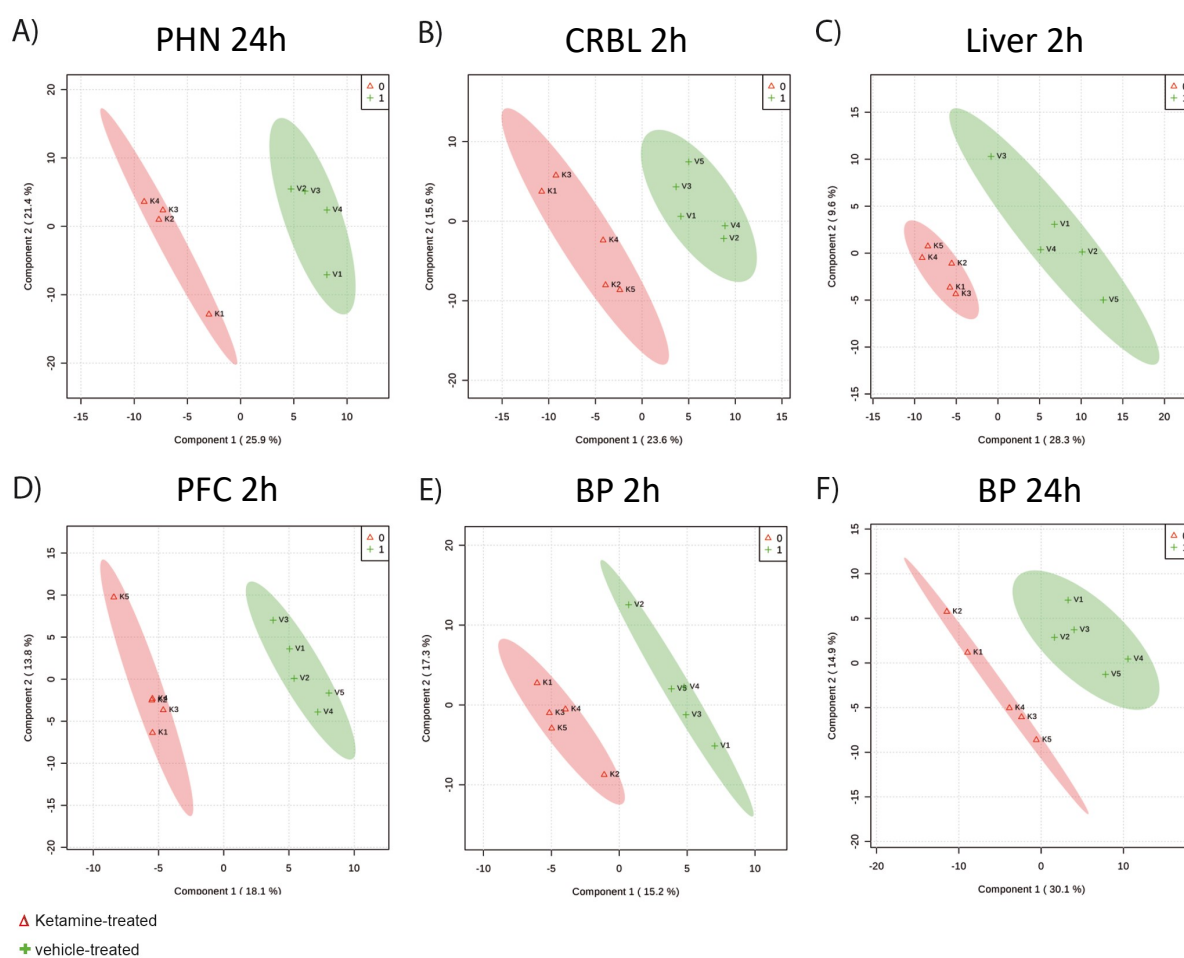


Figure 9: Multivariate partial least squares-discriminant analysis (PLS-DA) of (A) mouse primary hippocampal neurons 24h (PHN 24h), (B) cerebellum 2h (CRBL 2h), (C) liver 2h (Liver 2h), (D) prefrontal cortex 2h (PFC 2h), (E) blood plasma after 2h (BP 2h) and (F) 24h (BP 24h) after ketamine (3 mg kg⁻¹ in animals and 100 μ M in mouse PHN) and vehicle treatment or vehicle using all quantified metabolites. N=5 mice per group and time point.

First, the metabolite profiles were analyzed by multivariate partial least squares-discriminant analysis (PLS-DA) and significance analysis of Microarrays and other –omics datasets (SAM). PLS-DA is a supervised statistical method suitable for analyzing and classifying metabolomics data. However, this method is prone to overfitting. To overcome this problem cross-validation is employed in order to assess the quality criteria of the PLS-DA. Therefore, especially the R^2 and Q^2 are calculated as they describe the goodness of fit or explained variation and the predicted variation or the quality of prediction, respectively. The values indicate how well the PLS-DA model is able to mathematically reproduce the data in the dataset. In general, a poorly and well fit model is described by $R^2 \sim 0.20-0.30$ and $\sim 0.80-0.90$, respectively. Furthermore, a good and outstanding model is defined by Q^2 values of ≥ 0.50 and ≥ 0.90 , respectively. The quality criteria assessment by Q^2 values only indicate good and robust PLS-DA models for PHN 24h (figure 9A and table 4) and the liver 2h (figure 9C and table 4). The metabolite profiles separated ketamine- from vehicle-treated mice and PHN using PLS-DA (figure 9A-F).

Table 4: Quality criteria assessment (R^2 , Q^2 and accuracy values) of the multivariate data analyses using PLS-DA for mouse primary hippocampal neurons 24h (PHN 24h), cerebellum 2h (CRBL 2h), liver 2h, prefrontal cortex (PFC 2h), blood plasma 2h and 24h (BP 2h and BP 24h) after ketamine (3 mg kg^{-1} in animals and $100 \mu\text{M}$ in mouse PHN) and vehicle treatment. R^2 , Q^2 and accuracy values indicate good (PHN 24h: $R^2=1.00$, $Q^2=0.62$, accuracy=1.00; Liver 2h: $R^2=0.84$, $Q^2=0.55$, accuracy=0.90) and weak models (CRBL 2h: $R^2=1.00$, $Q^2=0.45$, accuracy=0.80; PFC 2h: $R^2=1.00$, $Q^2=0.49$, accuracy=0.90; BP 2h: $R^2=1.00$, $Q^2=-0.29$, accuracy=0.50; BP 24h: $R^2=0.95$, $Q^2=0.20$, accuracy=0.60). N=5 mice per group and time point.

| | PHN 24h | CRBL 2h | Liver 2h | PFC 2h | BP 2h | BP 24h |
|----------|---------|---------|----------|--------|-------|--------|
| Accuracy | 1.00 | 0.80 | 0.90 | 0.90 | 0.50 | 0.60 |
| R^2 | 1.00 | 1.00 | 0.84 | 1.00 | 1.00 | 0.95 |
| Q^2 | 0.62 | 0.45 | 0.55 | 0.49 | -0.29 | 0.20 |

Abbreviations: PHN, Primary hippocampal neurons; CRBL, Cerebellum; PFC, Prefrontal Cortex; BP, Blood Plasma; h, hour

On the other hand the other models of CRBL 2h (figure 9B and table 4), PFC 2h (figure 9D and table 4), BP 2h (figure 9E and table 4), and BP 24h (figure 9F and table 4) showed weak quality criteria which might therefore result in false-positives. Therefore, I restricted further statistical metabolomics profiling for PHN 24h and Liver 2h. For the identification of metabolite changes characteristic for group separation, the VIP-score was used. Metabolites with $\text{VIP-scores} \geq 1.0$ are considered important for group separation and were selected for subsequent data analysis. To further increase the robustness of the analyses, I combined the PLS-DA with results obtained from a SAM analysis, to determine a reliable list of metabolites that significantly contribute to ketamine drug action. SAM is a statistical method that was originally developed for mRNA expression analyses of microarrays. In the present study, 6 and 13 metabolites were statistically significant altered in PHN 24h and liver 2h, respectively (table 5). In PHN 24h 3 metabolites were up- and downregulated whereas in the liver 2h all metabolites showed reduced levels.

Table 5: Metabolite alterations of (A) mouse primary hippocampal neurons (PHN) treated with ketamine (100 μ M) for 24h and (B) the liver from mice treated with ketamine (3 mg kg⁻¹) 2h after treatment (PLS-DA VIP-score \geq 1.0, SAM FDR \leq 0.10 and SAM q \leq 0.10). N=5 mice per group and time point.

| Metabolite | HMDB | FC | PLS-DA, VIP-score | SAM, p-value | SAM, q-value | SAM, FDR |
|---|-----------|------|-------------------|--------------|--------------|-------------|
| A) | | | | | | |
| Carbamoyl phosphate | HMDB01096 | 2.90 | 1.91 | 0.0003 | 0.04 | \leq 0.10 |
| 2-Deoxyglucose-6-phosphate | HMDB01254 | 0.54 | 1.84 | 0.0011 | 0.09 | \leq 0.10 |
| Sarcosine | HMDB00271 | 1.57 | 1.82 | 0.0023 | 0.09 | \leq 0.10 |
| N6-Acetyl-L-lysine | HMDB00206 | 1.78 | 1.80 | 0.0026 | 0.09 | \leq 0.10 |
| Phenylpropionate | HMDB02359 | 0.51 | 1.80 | 0.0028 | 0.09 | \leq 0.10 |
| Alpha-Ketoglutarate | HMDB00208 | 0.52 | 1.79 | 0.0031 | 0.09 | \leq 0.10 |
| B) | | | | | | |
| Uridine diphosphate (UDP)-D-glucuronate | HMDB00935 | 0.57 | 1.94 | 0.0004 | 0.06 | \leq 0.10 |
| Acetoacetate | HMDB00060 | 0.74 | 1.85 | 0.0019 | 0.08 | \leq 0.10 |
| N-Acetylputrescine | HMDB02064 | 0.74 | 1.83 | 0.0024 | 0.08 | \leq 0.10 |
| 2-Oxo-4-methylthiobutanoate | HMDB01553 | 0.61 | 1.80 | 0.0032 | 0.08 | \leq 0.10 |
| Glucono- β -lactone | NA | 0.75 | 1.80 | 0.0034 | 0.08 | \leq 0.10 |
| Phenylpropionate | HMDB02359 | 0.59 | 1.79 | 0.0037 | 0.08 | \leq 0.10 |
| Methylcysteine | HMDB02108 | 0.77 | 1.79 | 0.0041 | 0.08 | \leq 0.10 |
| Fructose-1,6-bisphosphate | HMDB01058 | 0.75 | 1.78 | 0.0044 | 0.08 | \leq 0.10 |
| 3-Hydroxybutyrate | HMDB00357 | 0.54 | 1.77 | 0.0048 | 0.08 | \leq 0.10 |
| Nicotinamide adenine dinucleotide (NAD ⁺) | HMDB00902 | 0.76 | 1.76 | 0.0052 | 0.08 | \leq 0.10 |
| Adenine | HMDB00034 | 0.65 | 1.74 | 0.0063 | 0.09 | \leq 0.10 |
| Inosine | HMDB00195 | 0.73 | 1.73 | 0.0069 | 0.09 | \leq 0.10 |
| Dimethylglycine | HMDB00092 | 0.54 | 1.72 | 0.0072 | 0.09 | \leq 0.10 |

Abbreviations: PLS-DA, Partial Least Square-Discriminant Analysis; NA, not applicable; FC: Fold Change;

SAM, Significance Analysis of Microarrays (metabolites, proteins); VIP, Variable Importance in Projection;

FDR: False discovery rate; HMDB: Human Metabolome Database; h, hours

Next, the statistically significant altered metabolites from PHN 24h and liver 2h were interrogated for overrepresented (enriched) molecular pathways. The alanine, aspartate, and glutamate metabolism was significantly enriched for PHN 24h (table 6A) whereas synthesis and degradation of ketone bodies was overrepresented for the liver 2h (table 6B).

Table 6: Pathway enrichment analyses of significantly altered metabolites (PLS-DA VIP-score \geq 1.0, SAM FDR \leq 0.10, SAM q \leq 0.1) from (A) mouse primary hippocampal neurons treated with ketamine (100 μ M) for 24h (PHN 24h) and (B) the liver 2h after a single injection of ketamine (3 mg kg⁻¹). N=5 mice per group and time point.

| Pathway | p-value | P _{Holm} corrected -value | FDR | Metabolite |
|---|---------|--|-------|--|
| A) | | | | |
| Alanine, aspartate and glutamate metabolism | 0.00004 | 0.003 | 0.003 | Alpha-Ketoglutarate 2-Deoxyglucose-6-phosphate Carbamoyl phosphate |
| B) | | | | |
| Synthesis and degradation of ketone bodies | 0.0004 | 0.036 | 0.036 | Acetoacetate 3-Hydroxybutyrate |

Abbreviations: PLS-DA, Partial Least Square-Discriminant Analysis; FDR: False discovery rate; h: hours;

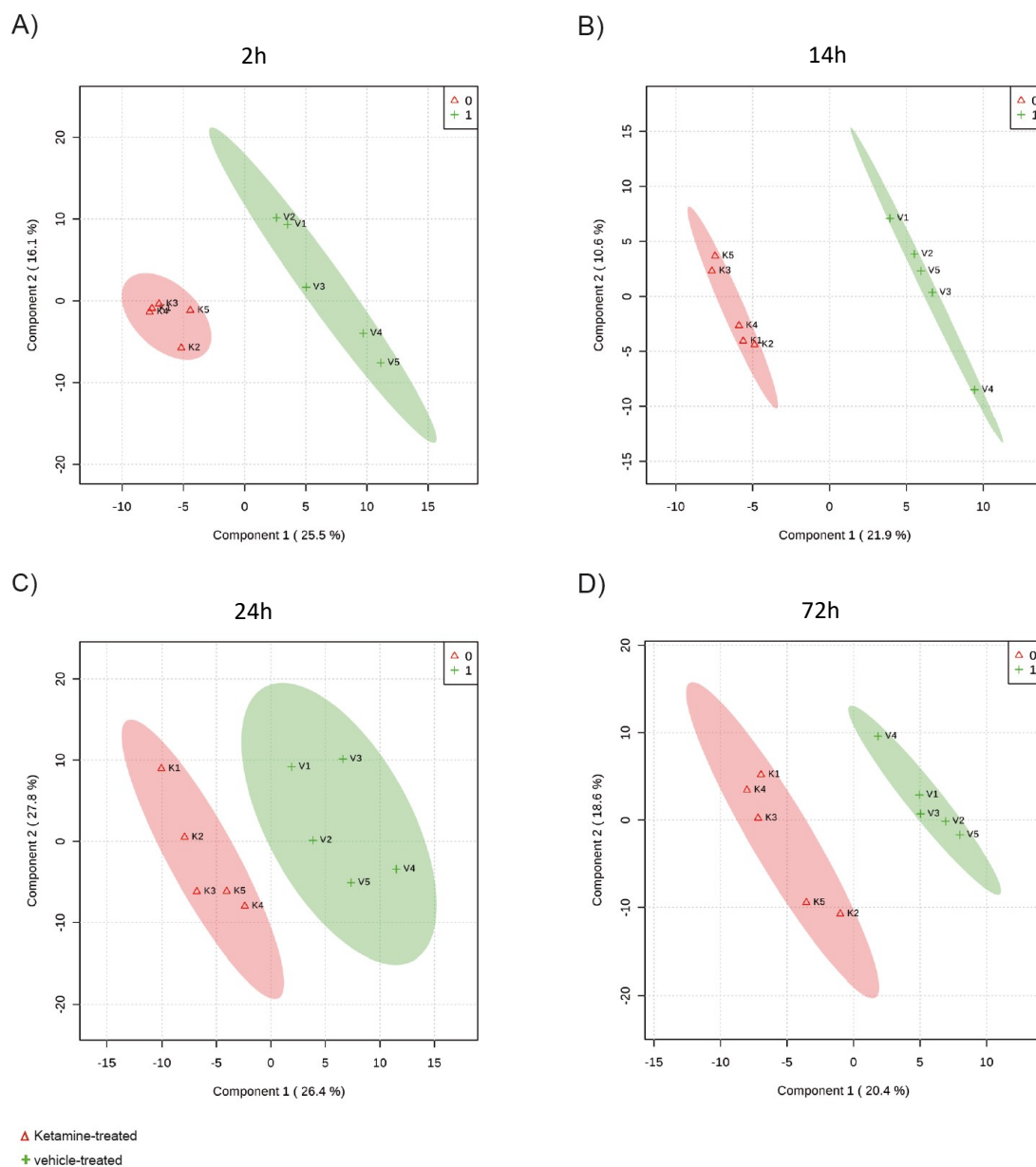
SAM, Significance Analysis of Microarrays (and metabolites); VIP, Variable Importance in Projection.

4.2.1 Time-dependent metabolomics profiling of the hippocampus

The HPC plays a fundamental role in learning and memory which are affected in MDD. Antidepressant drug activity is dependent and mediated by synaptic plasticity mechanisms through the glutamatergic system, involving the NMDAR, BDNF, and the activation of synaptic protein synthesis mediated by mTORC1. The time-dependent hippocampal metabolite profiles 2h, 14h, 24h, and 72h after a single injection of a low dose of ketamine (3 mg kg⁻¹) were analyzed.

A total of 226, 218, 227, and 221 metabolites were quantified in the HPC for the 2h, 14h, 24h, and 72h time points, respectively, after a single injection of ketamine (supplemental table 2).

The metabolite profiles separated ketamine- from vehicle-treated mice using multivariate PLS-DA for all time points (figure 10A-D). The quality criteria (figure 10E) of PLS-DA models were assessed for R², Q² and accuracy values. The time-dependent metabolomics profiling analyses revealed good and robust models for the 2h, 14h, and 24h time points, respectively, but not at the 72h time point. The weak PLS-DA model of the 72h time point can result in false positives. Nevertheless, the results were included as they are an indication of ketamine's fast antidepressant-like effect on the metabolome.



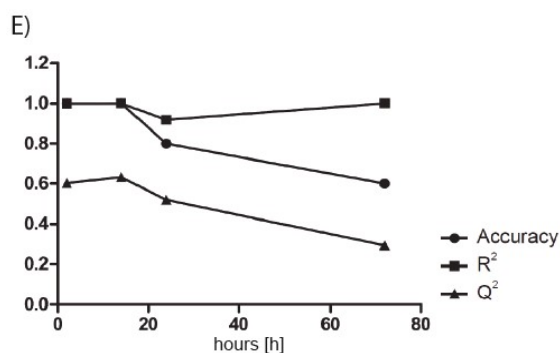


Figure 10: Multivariate partial least squares-discriminant analysis (PLS-DA) of (A) 2h, (B) 14h, (C) 24h and (D) 72h time points comparison after a single injection of a low dose of ketamine (3 mg kg^{-1}) or vehicle using all quantified metabolites. E) Quality criteria assessment (R^2 , Q^2 and accuracy values) of the multivariate data analyses using PLS-DA for the 2h, 14h, 24h and 72h time points indicating good (2h: $R^2=0.99$, $Q^2=0.60$, accuracy=1.0; 14h: $R^2=1.0$, $Q^2=0.63$, accuracy=1.0) and robust (24h: $R^2=0.92$, $Q^2=0.52$, accuracy=0.8) models with the exception of the 72h time point ($R^2=1.0$, $Q^2=0.29$, accuracy=0.6). N=5 mice per group and time point.

For the identification of metabolite changes characteristic for group separation, the VIP-score with values ≥ 1.0 was selected and used for further data analysis. To increase the robustness of the analyses, I again combined the PLS-DA with SAM analysis, to obtain a complete list of metabolites for each time point that significantly contribute to ketamine drug action (table 7).

Table 7: Hippocampal metabolite alterations (A) 2h, (B) 14h and (C) 24h after a single injection of a low dose of ketamine (3 mg kg⁻¹) (PLS-DA VIP-score \geq 1.0, SAM FDR \leq 0.10 and SAM q \leq 0.1). N=5 mice per group and time point.

| Metabolite | HMDB | FC | PLS-DA, VIP-score | SAM, p-value | SAM, q-value | SAM, FDR |
|---------------------------------|-----------|-------|----------------------|-----------------|-----------------|-------------|
| A) | | | | | | |
| Cystathionine | HMDB00099 | 0.80 | 1.80 | 0.004 | 0.052 | \leq 0.05 |
| Glyoxylate | HMDB00119 | 0.59 | 1.78 | 0.002 | 0.052 | \leq 0.05 |
| Fumarate | HMDB00134 | 0.79 | 1.77 | 0.002 | 0.052 | \leq 0.05 |
| Adenine | HMDB00034 | 1.41 | 1.73 | 0.003 | 0.052 | \leq 0.05 |
| Cytosine | HMDB00630 | 1.55 | 1.73 | 0.003 | 0.052 | \leq 0.05 |
| Betaine aldehyde | HMDB01252 | 0.78 | 1.70 | 0.005 | 0.053 | \leq 0.05 |
| Ureidosuccinate | HMDB00828 | 1.23 | 1.69 | 0.005 | 0.053 | \leq 0.05 |
| Cytidine | HMDB00089 | 1.64 | 1.66 | 0.006 | 0.053 | \leq 0.05 |
| 2-Ketoisovalerate | HMDB00019 | 0.81 | 1.64 | 0.007 | 0.053 | \leq 0.10 |
| Pipecolic acid | HMDB00070 | 1.21 | 1.63 | 0.007 | 0.053 | \leq 0.05 |
| Glycerol-3-phosphate | HMDB00126 | 2.47 | 1.63 | 0.017 | 0.067 | \leq 0.10 |
| Citrulline | HMDB00904 | 4.56 | 1.62 | 0.008 | 0.053 | \leq 0.05 |
| Thymidine | HMDB00273 | 0.55 | 1.62 | 0.010 | 0.059 | \leq 0.10 |
| Methylmalonate | HMDB00202 | 1.96 | 1.60 | 0.019 | 0.067 | \leq 0.10 |
| Thiamine pyrophosphate | HMDB01372 | 1.43 | 1.59 | 0.011 | 0.059 | \leq 0.10 |
| Gluconate | HMDB00625 | 0.69 | 1.58 | 0.022 | 0.067 | \leq 0.10 |
| Guanosine-5'-triphosphate (GTP) | HMDB01273 | 1.50 | 1.58 | 0.012 | 0.060 | \leq 0.10 |
| Succinate | HMDB00254 | 1.96 | 1.55 | 0.026 | 0.070 | \leq 0.10 |
| Maleate | HMDB00176 | 0.82 | 1.55 | 0.014 | 0.067 | \leq 0.10 |
| Betaine | HMDB00043 | 0.69 | 1.54 | 0.016 | 0.067 | \leq 0.10 |
| Uridine | HMDB00296 | 0.72 | 1.54 | 0.015 | 0.067 | \leq 0.10 |
| Glutathione | HMDB00125 | 1.16 | 1.52 | 0.019 | 0.067 | \leq 0.10 |
| SBP | NA | 0.69 | 1.49 | 0.019 | 0.067 | \leq 0.10 |
| Putrescine | HMDB01414 | 3.32 | 1.49 | 0.020 | 0.067 | \leq 0.10 |
| OBP | NA | 0.64 | 1.48 | 0.041 | 0.084 | \leq 0.10 |
| Uridine 5'-monophosphate (UMP) | HMDB00288 | 1.28 | 1.46 | 0.022 | 0.067 | \leq 0.10 |
| 5-Methoxytryptophan | HMDB02339 | 0.64 | 1.45 | 0.024 | 0.070 | \leq 0.10 |
| Glycerophosphocholine | HMDB00086 | 1.14 | 1.44 | 0.031 | 0.075 | \leq 0.10 |
| Cyclic AMP (cAMP) | HMDB00058 | 1.36 | 1.44 | 0.026 | 0.070 | \leq 0.10 |
| Indoleacrylic acid | HMDB00734 | 0.76 | 1.44 | 0.035 | 0.080 | \leq 0.10 |
| Phosphoenolpyruvate | HMDB00263 | 1.75 | 1.42 | 0.030 | 0.074 | \leq 0.10 |
| Malate | METPA0049 | 0.82 | 1.42 | 0.030 | 0.074 | \leq 0.10 |
| CDP | HMDB01546 | 0.41 | 1.40 | 0.045 | 0.084 | \leq 0.10 |
| Choline | HMDB00097 | 13.33 | 1.38 | 0.036 | 0.080 | \leq 0.10 |
| Glycerate | HMDB00139 | 0.69 | 1.38 | 0.036 | 0.080 | \leq 0.10 |
| 4-Pyridoxic acid | HMDB00017 | 0.58 | 1.37 | 0.053 | 0.084 | \leq 0.10 |
| Acetyl-Coenzyme A (CoA) | HMDB01206 | 1.49 | 1.36 | 0.044 | 0.084 | \leq 0.10 |
| Xanthurenic acid | HMDB00881 | 0.63 | 1.35 | 0.046 | 0.084 | \leq 0.10 |
| Sedoheptulose-7-phosphate | HMDB01068 | 0.71 | 1.35 | 0.052 | 0.084 | \leq 0.10 |
| Trehalose-6-phosphate | HMDB01124 | 2.38 | 1.35 | 0.043 | 0.084 | \leq 0.10 |
| Argininosuccinate | HMDB00052 | 0.75 | 1.34 | 0.045 | 0.084 | \leq 0.10 |
| Purine | HMDB01366 | 1.35 | 1.34 | 0.050 | 0.084 | \leq 0.10 |
| 2-Deoxyglucose-6-phosphate | HMDB01254 | 1.49 | 1.33 | 0.048 | 0.084 | \leq 0.10 |
| 3-Phosphoglycerate | HMDB00807 | 1.79 | 1.33 | 0.048 | 0.084 | \leq 0.10 |
| Serine | HMDB00187 | 1.14 | 1.32 | 0.049 | 0.084 | \leq 0.10 |

B)

| | | | | | | |
|---|-----------|------|------|-------|-------|--------|
| Erythrose-4-phosphate | HMDB01321 | 0.48 | 1.95 | 0.001 | 0.070 | ≤ 0.05 |
| Thymine | HMDB00262 | 0.81 | 1.87 | 0.002 | 0.070 | ≤ 0.05 |
| Glutamine | HMDB00641 | 0.77 | 1.87 | 0.002 | 0.070 | ≤ 0.05 |
| Malate | HMDB00156 | 0.82 | 1.80 | 0.003 | 0.086 | ≤ 0.05 |
| Acetylphosphate | HMDB01494 | 0.67 | 1.76 | 0.005 | 0.086 | ≤ 0.05 |
| Glyceraldehyde-3-phosphate | HMDB01112 | 0.45 | 1.76 | 0.005 | 0.086 | ≤ 0.05 |
| Fructose-6-phosphate | HMDB00124 | 0.4 | 1.76 | 0.005 | 0.086 | ≤ 0.05 |
| Fructose-1,6-bisphosphate | HMDB01058 | 0.58 | 1.71 | 0.006 | 0.092 | ≤ 0.05 |
| Acetylcarnitine | HMDB00201 | 0.82 | 1.71 | 0.007 | 0.092 | ≤ 0.05 |
| Xanthurenic acid | HMDB00881 | 0.65 | 1.69 | 0.008 | 0.092 | ≤ 0.05 |
| 6-Phospho-D-gluconate | HMDB01316 | 0.65 | 1.69 | 0.011 | 0.092 | ≤ 0.05 |
| Betaine | HMDB00043 | 0.78 | 1.68 | 0.008 | 0.092 | ≤ 0.05 |
| Glucose-6-phosphate | HMDB01401 | 0.53 | 1.68 | 0.010 | 0.092 | ≤ 0.05 |
| N-Acetyl-L-alanine | HMDB00766 | 0.86 | 1.66 | 0.010 | 0.092 | ≤ 0.05 |
| Dihydroxy-acetone-phosphate | HMDB01473 | 0.24 | 1.65 | 0.011 | 0.092 | ≤ 0.05 |
| Deoxyguanosine | HMDB00085 | 0.74 | 1.65 | 0.012 | 0.097 | ≤ 0.05 |
| Nicotinamide | HMDB01406 | 0.6 | 1.61 | 0.013 | 0.097 | ≤ 0.05 |
| Glucosamine-6-phosphate | HMDB01254 | 0.33 | 1.61 | 0.016 | 0.097 | ≤ 0.05 |
| DL-Pipecolic acid | HMDB00070 | 0.78 | 1.60 | 0.017 | 0.097 | ≤ 0.05 |
| Hexose-phosphate | NA | 0.76 | 1.60 | 0.016 | 0.097 | ≤ 0.05 |
| Aminoimidazole carboxamide ribonucleotide | HMDB01517 | 0.74 | 1.60 | 0.018 | 0.097 | ≤ 0.10 |
| Tyrosine | HMDB00158 | 0.75 | 1.55 | 0.019 | 0.100 | ≤ 0.10 |

C)

| | | | | | | |
|---|-----------|------|------|-------|-------|--------|
| Riboflavin | HMDB00244 | 0.70 | 1.98 | 0.000 | 0.038 | ≤ 0.10 |
| Lactate | HMDB00190 | 0.71 | 1.93 | 0.000 | 0.038 | ≤ 0.10 |
| Deoxyguanosine triphosphate (dGTP) | HMDB01440 | 0.63 | 1.77 | 0.002 | 0.068 | ≤ 0.10 |
| Deoxyguanosine diphosphate (dGDP) | HMDB00960 | 0.75 | 1.77 | 0.002 | 0.068 | ≤ 0.10 |
| CoA | HMDB01423 | 0.63 | 1.77 | 0.002 | 0.068 | ≤ 0.10 |
| Adenosine diphosphate (ADP) | HMDB01341 | 0.75 | 1.75 | 0.003 | 0.068 | ≤ 0.10 |
| 5-Thymidylic acid (dTMP) | HMDB01227 | 0.55 | 1.73 | 0.005 | 0.072 | ≤ 0.10 |
| Phenylpropionic acid | HMDB02359 | 0.76 | 1.73 | 0.004 | 0.068 | ≤ 0.10 |
| Adenosine triphosphate (ATP) | HMDB00538 | 0.62 | 1.72 | 0.004 | 0.068 | ≤ 0.10 |
| Cytidine diphosphate (CDP)-Ethanalamine | HMDB01564 | 0.78 | 1.68 | 0.006 | 0.085 | ≤ 0.10 |
| Carbamoyl phosphate | HMDB01096 | 0.83 | 1.66 | 0.007 | 0.098 | ≤ 0.10 |

Abbreviations: PLS-DA, Partial Least Square-Discriminant Analysis; NA, not applicable; FC: Fold Change; h, hour; SAM, Significance Analysis of Microarrays (and metabolites); VIP, Variable Importance in Projection; FDR: False discovery rate; HMDB: Human Metabolome Database

Two hours after a single injection of ketamine 45 metabolite levels were significantly altered, with 21 metabolites reduced and 24 metabolites upregulated when comparing ketamine- with vehicle-treated mice (table 7A). For the 14h and 24h time points, 22 (table 7B) and 11 (table 7C) metabolites, respectively, were detected at lower levels. In agreement with the observation that the PLS-DA model of the 72h time point is not robust, no significant metabolite alterations were found 72h after ketamine treatment.

Next, I examined the statistically significantly altered metabolites obtained by the time-dependent metabolomics analyses of the HPC and performed pathway enrichment analyses for KEGG pathways in order to delineate affected hippocampal biomolecular pathways that are affected by ketamine treatment. A single injection of ketamine significantly enriched the pyrimidine metabolism, the glycolysis/ gluconeogenesis, the alanine, aspartate and glutamate metabolism, the pentose

phosphate pathway, the citrate cycle, the glycine, serine and threonine metabolism and the pyruvate metabolism (table 8).

Table 8: Pathway enrichment analysis for KEGG pathways of significantly altered hippocampal metabolites (PLS-DA VIP-score \geq 1.0, SAM FDR \leq 0.10 and SAM q \leq 0.1) 2h, 14, and 24h after a single injection of ketamine. N=5 mice per group and time point.

| Pathway | p-value | P _{Holm} corrected -value | FDR | Metabolite | Time point |
|---|---------|--|--------|--------------------------------|---------------|
| Pyrimidine metabolism | 0.00001 | 0.0009 | 0.0006 | Ureidosuccinate | 2h |
| | | | | Cytidine | 2h |
| | | | | Thymidine | 2h |
| | | | | Uridine | 2h |
| | | | | Uridine 5'-monophosphate (UMP) | 2h |
| | | | | Cytidine diphosphate (CDP) | 2h |
| | | | | Glutamine | 14h |
| | | | | Thymine | 14h |
| | | | | 5-Thymidylic acid (dTMP) | 24h |
| | | | | Carbamoyl phosphate | 24h |
| | | | | Methylmalonate | 2h |
| Glycolysis/ Gluconeogenesis | 0.00001 | 0.0012 | 0.0006 | Thiamine pyrophosphate | 2h |
| | | | | Phosphoenolpyruvate | 2h |
| | | | | Acetyl-Coenzyme A (CoA) | 2h |
| | | | | Fructose-6-phosphate | 14h |
| | | | | Fructose-1,6-bisphosphate | 14h |
| | | | | Glucose-6-phosphate | 14h |
| | | | | Dihydroxy-acetone-phosphate | 14h |
| | | | | Lactate | 24h |
| | | | | 3-Phosphoglycerate | 2h |
| | | | | Glyceraldehyde-3-phosphate | 14h |
| Alanine, aspartate and glutamate metabolism | 0.00008 | 0.0062 | 0.0021 | Fumarate | 2h |
| | | | | Ureidosuccinate | 2h |
| | | | | Succinate | 2h |
| | | | | Argininosuccinate | 2h |
| | | | | Glutamine | 14h |
| | | | | Glucosamine-6-phosphate | 14h |
| | | | | Carbamoyl phosphate | 24h |
| Pentose phosphate pathway | 0.00016 | 0.0128 | 0.0033 | Glucose-6-phosphate | 14h |
| | | | | 6-Phospho-D-gluconate | 14h |
| | | | | Sedoheptulose-7-phosphate | 2h |
| | | | | Fructose-6-phosphate | 14h |
| | | | | Fructose-1,6-bisphosphate | 14h |
| | | | | Erythrose-4-phosphate | 14h |
| Citrate cycle | 0.00022 | 0.0174 | 0.0037 | Fumarate | 2h |
| | | | | Succinate | 2h |
| | | | | Thiamine pyrophosphate | 2h |
| | | | | Phosphoenolpyruvate | 2h |
| | | | | Acetyl-CoA | 2h |
| | | | | Malate | 2h/ 14h |

All 7 pathways that are statistically significantly enriched are interconnected by shared metabolites based on KEGG database information (figure 11). Several previous analyses by Turck's research group

and others have also shown an involvement of the citrate cycle and glycolysis in psychiatric phenotypes and antidepressant drug action⁴³²⁻⁴³⁴.

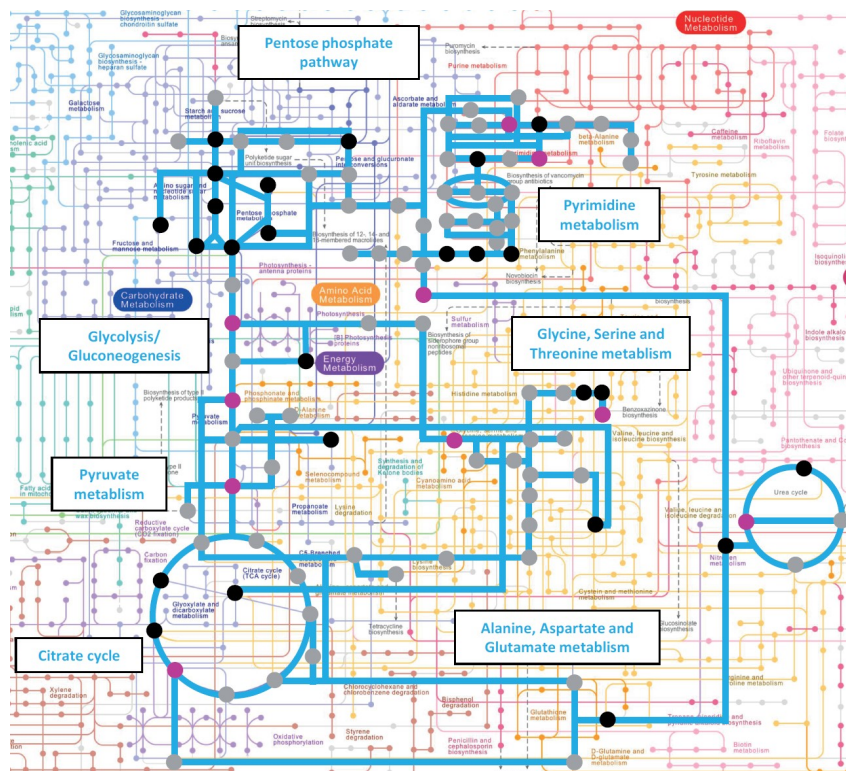


Figure 11: Metabolic KEGG pathways overview highlighting (blue) enriched pathways, calculated based on significantly altered hippocampal metabolites illustrated in either pink (increased fold change (FC) or black (decreased FC) dots (PLS-DA VIP-score ≥ 1.0 , SAM FDR ≤ 0.10 , SAM $q \leq 0.1$) upon ketamine treatment (3 mg kg⁻¹) at 2h, 14h, 24h and 72h time points (cf. table 7 and table 8). Citrate cycle, glycolysis/gluconeogenesis, pentose phosphate pathway, serine, glycine and threonine metabolism and pyrimidine metabolism are interconnected by a shared metabolite in the metabolic KEGG pathway network. Modified pathways are based on <http://www.genome.jp/kegg/>. N=5 mice per group and time point.

The glycolysis and the citrate cycle take place in the cytoplasm and the mitochondria, respectively. These pathways consist of a series of biochemical reactions to generate high levels of energy in form of adenosine triphosphate (ATP) through the connected oxidative phosphorylation (OXPHOS) pathway. The citrate cycle is connected to the OXPHOS through SDHA, the enzyme metabolizing succinate to fumarate. This process is also known as mitochondrial respiration and consists of 5 complexes. These are integrated into the mitochondrial inner membrane and transport electrons from NADH+H⁺ and succinate from the complexes I and II, respectively. The electron transport is driven by pumping H⁺ from the mitochondrial matrix into the intermembrane space of the mitochondria resulting in a mitochondrial membrane potential creating an electrochemical gradient. The energy is then used by complex V to produce ATP from adenosine diphosphate (ADP) by releasing H⁺ back into the mitochondrial matrix⁴³⁵.

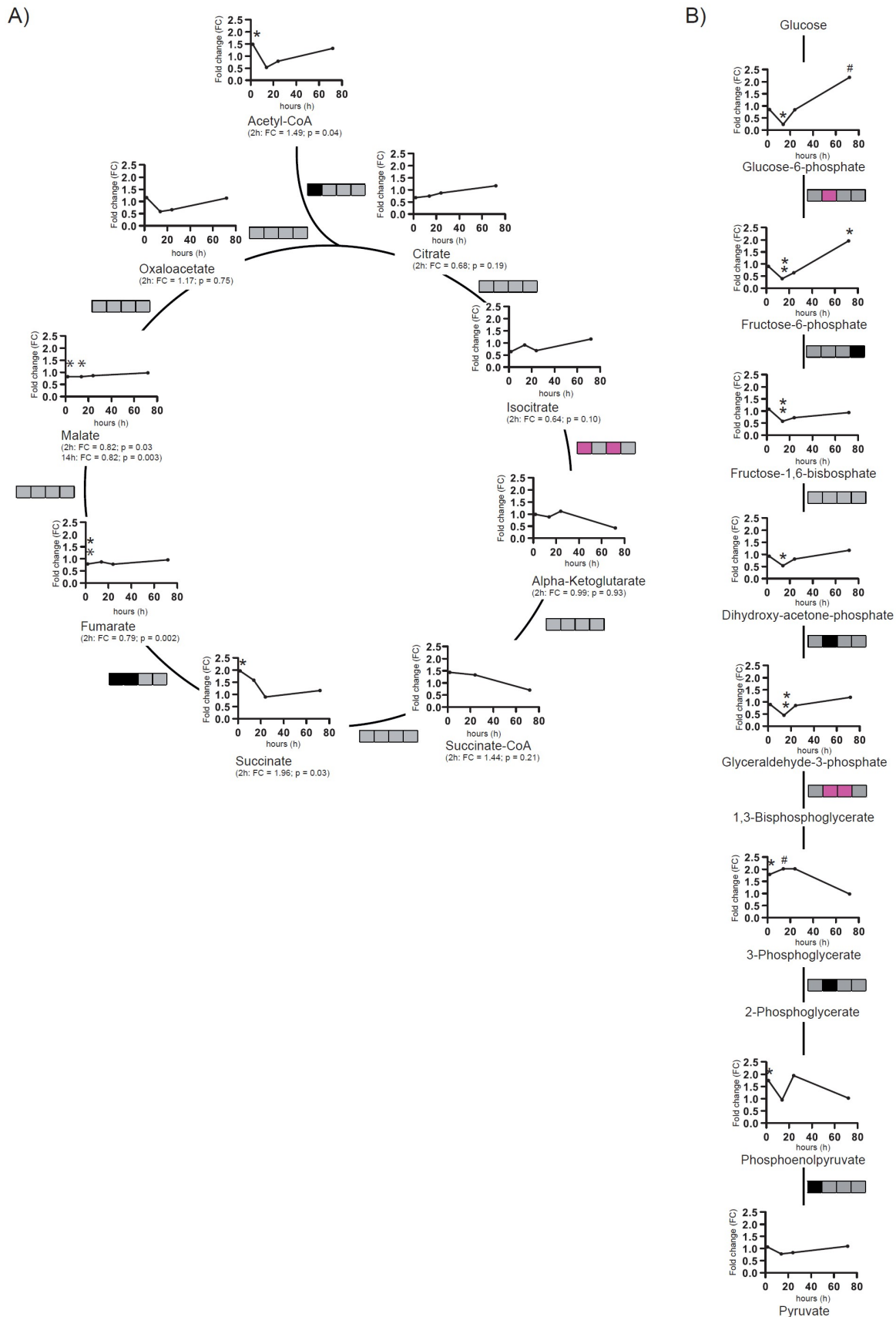


Figure 12: Citrate cycle and glycolysis metabolite levels and metabolite ratios analyses upon ketamine treatment (3 mg kg^{-1}) of 2h, 14h, 24h, and 72h time points. **A)** Citrate cycle and **(B)** glycolysis time course showing metabolite FC and metabolite ratios. Metabolite ratios are indicated by boxes. Each box represents a time point (from left to right 2h, 14h, 24h, and 72h). Significant metabolite ratio differences or trends are illustrated in pink (increased ratio) and black (decreased ratio). N=5 mice per group and time point. # $p \leq 0.10$, * $p \leq 0.05$, ** $p \leq 0.01$. P-values were determined by Student's t-test and SAM.

Already 2h after a single injection of ketamine, the levels of the citrate cycle metabolites thiamine pyrophosphate, acetyl-CoA and succinate were significantly increased. Succinate-CoA showed a high, but not significant fold change (FC) 2h after ketamine treatment. Fumarate levels were significantly reduced 2h after ketamine injection as were malate levels for the 2h and 14h time points.

Isocitrate tended to be downregulated and citrate levels were lower, albeit with no significant FC 2h after a single injection of ketamine. Oxaloacetate and alpha-ketoglutarate levels were unchanged (figure 12A and table 7 and table 8).

The glycolysis/gluconeogenesis pathway was also enriched upon ketamine treatment. Almost all quantified metabolites were significantly altered 14h after a single injection of ketamine (figure 12B and table 4 and table 5). Glucose-6-phosphate, fructose-6-phosphate, fructose-1,6-bisphosphate and dihydroxy-acetone-phosphate were significantly downregulated. In contrast, 3-phosphoglycerate was significantly upregulated at the 2h and 14h time points; phosphoenolpyruvate levels were found to be significantly upregulated 2h after ketamine treatment and pyruvate was unchanged.

Selected pairs of metabolite concentrations (metabolite ratios) can indicate alterations in enzyme activity or expression rate⁴³⁶. Citrate cycle and glycolysis metabolite ratios (figure 12 and figure 13) are indicated by boxes, where each box represents a single time point (from left to right 2h, 14h, 24h, and 72h). Statistical significance or trends of metabolite ratio differences are illustrated in pink (increased ratio) and black (decreased ratio). The citrate/acetyl-CoA ratio is significantly decreased 2h after ketamine treatment. The alpha-ketoglutarate/isocitrate metabolite ratio tended to be increased at the 2h and 24h time points and the fumarate/succinate ratio tended to be lower at 2h and was significantly decreased 14h after a single injection of ketamine (figure 12A and figure 13A).

The fructose-6-phosphate/glucose-6-phosphate ratio tended to be elevated 14h after ketamine treatment. The fructose-1,6-phosphate/fructose-6-phosphate metabolite ratio showed a significant decrease at the 72h time point. However, as the PLS-DA only yielded a weak model for this time point, the decreased fructose-1,6-phosphate/fructose-6-phosphate metabolite ratio could be a false positive finding. The glyceraldehyde-3-phosphate/dihydroxy-acetone-phosphate and phosphoglycerate/glyceraldehyde-3-phosphate ratios were significantly increased 14h after a single injection of ketamine and tended to be upregulated at the 24h time point. The 3-phosphoglycerate/phosphoenolpyruvate and pyruvate/phosphoenolpyruvate ratios were either significantly lower or tended to be lower, respectively (figure 12B and figure 13B).

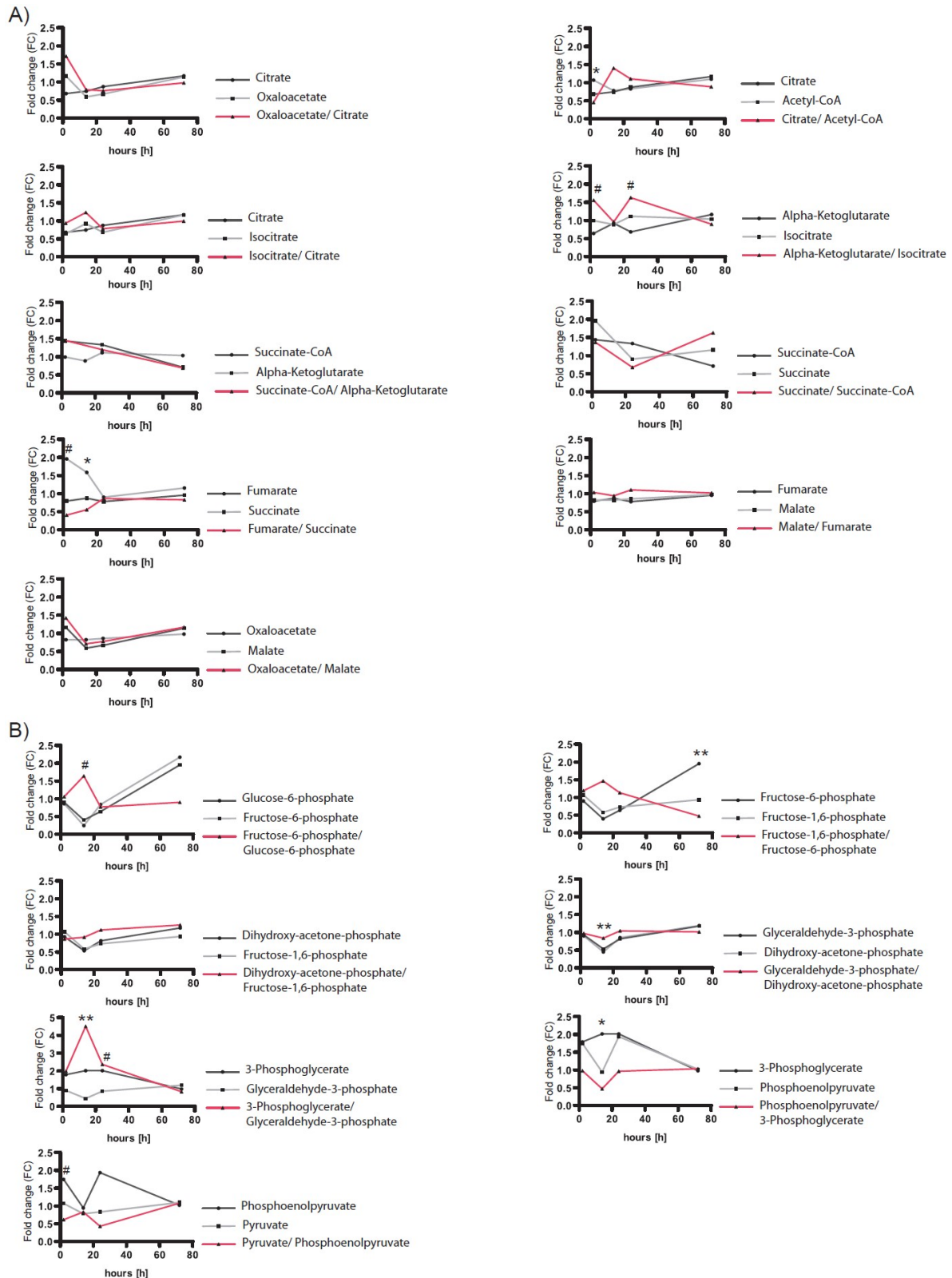


Figure 13: Metabolite ratio analyses of (A) the citrate cycle and (B) the glycolytic pathway. Ratios for selected pairs of metabolites (metabolite ratios) were calculated indicating alterations of enzyme activity or protein expression. N=5 mice per group and time point. # $p \leq 0.10$, * $p \leq 0.05$, ** $p \leq 0.01$. P-values were determined by Student's t-test and SAM.

The altered fumarate/succinate ratio is of particular interest as the enzymatic succinate dehydrogenase subunit A (SDHA) of the complex II metabolizes these metabolites and therefore also connects the citrate cycle with the OXPHOS. Furthermore, fumarate as well as the succinate metabolite intensities strongly correlated with the FST floating time at the 2h time point (figure 14A).

Thus, I hypothesized that the SDHA and most probably also the other complexes of the OXPHOS are involved in ketamine's antidepressant effect. Time-dependent Western blots with an antibody against the SDHA were performed in order to validate that changes in the fumarate/succinate ratio is a result of protein level alterations. The Western blot analyses show that SDHA protein levels are indeed statistically significant increased 14h and 24h after a single injection of ketamine (figure 14B).

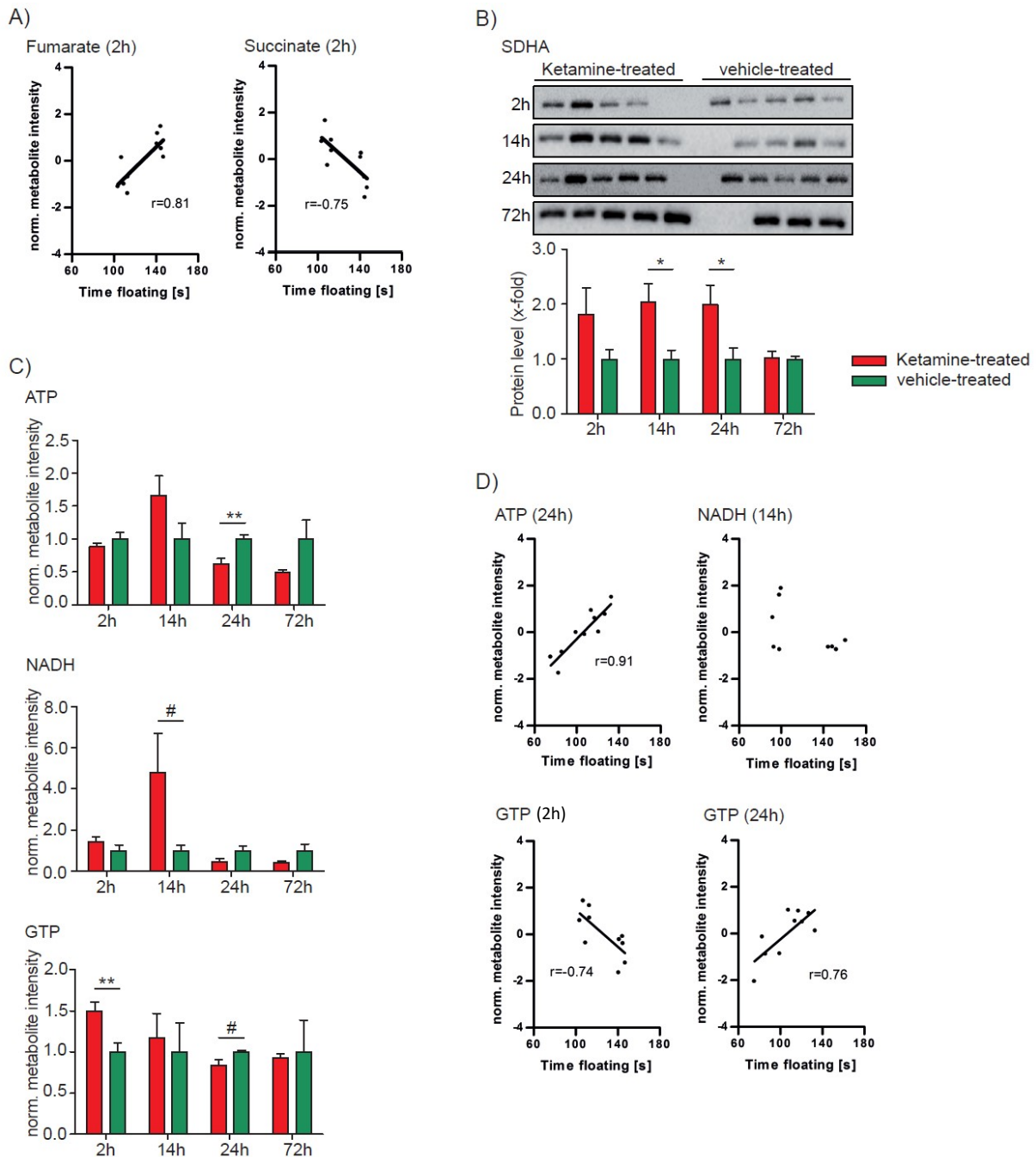


Figure 14: Time-dependent hippocampal protein and metabolite level, metabolite ratio and correlation analyses after a single injection of a low dose of ketamine (3 mg kg^{-1}). **A)** Correlation analyses of fumarate and succinate with the FST floating time 2h after a single injection of ketamine ($p < 0.05$). **B)** SDHA Western blot analyses of the 2h (ketamine-treated, $n=4$; vehicle-treated, $n=5$), 14h (ketamine-treated, $n=5$; vehicle-treated, $n=4$), 24h (ketamine-treated, $n=5$; vehicle-treated, $n=5$), and 72h (ketamine-treated, $n=5$; vehicle-treated, $n=3$) time points. **C)** ATP, GTP, and NADH levels after a single injection of ketamine. **D)** Correlation analyses of ATP (24h, $p < 0.05$), NADH (14h, not significant) and GTP (2h and 24h, $p < 0.05$) with the FST floating time after a single injection of ketamine. The results from ketamine-treated animals are normalized to the ones obtained from vehicle treatment (mean value = 1). $N=5$ mice per group and time point. # $p < 0.10$, * $p < 0.05$, ** $p < 0.01$. P-values were determined by Student's t-test. Error bars represent s.e.m. The correlation coefficient, r , was calculated by Pearson. The linear regression line is only shown for significant ($p < 0.05$) correlation coefficients.

GTP is metabolized through the transformation of succinate-CoA to succinate⁴³⁵. Therefore, the observed elevated complex II SDHA as well as succinate levels might also impact on the energy status. When comparing ketamine- to vehicle-treated mice, ATP levels decrease 24h after a single injection of ketamine, NADH levels tend to increase at the 14h time point and GTP levels first increase and then tend to decrease at the 2h and 24h time points (figure 14C). Moreover, GTP metabolite intensities significantly correlated with the FST floating time at the 2h time point and ATP and GTP also 24h after ketamine treatment. Whereas NADH metabolite intensities did not correlate with the antidepressant-like behavior (figure 14D).

4.2.3 Biomarker discovery for ketamine's antidepressant-like effects

Biomarkers can be differentiated into diagnostic and treatment biomarkers; thus either distinguishing between a health and disease state/ subtype or a biosignature for a specific treatment effect. Moreover, biomarkers could aid in drug development, providing a specific biosignature of a drug effect.

I attempted to identify metabolite biomarkers for a low dose ketamine treatment response. PLS-DA models can be used for biomarker discovery as they rate the metabolite's relevance via the VIP-score. When PLS-DA for the 2h, 14h, 24h, and 72h time points were assessed for quality criteria (figure 10E) all R^2 , Q^2 , and accuracy values indicate good and robust models, with the exception of the 72h time point (cf. section 4.2.1). Based on these results we chose metabolites that are important and stable contributors to group separation with a consistent $VIP\text{-score} \geq 1.0$ for the 2h, 14h, and 24h time points and with $q \leq 0.10$ for at least one of the time points. This resulted in 7 potential metabolite biomarkers: 2-keto-isovalerate, glutathione, maleate, methylmalonate, sedoheptulose-7-phosphate, fumarate and cytosine – candidates for ketamine drug action (figure 15).

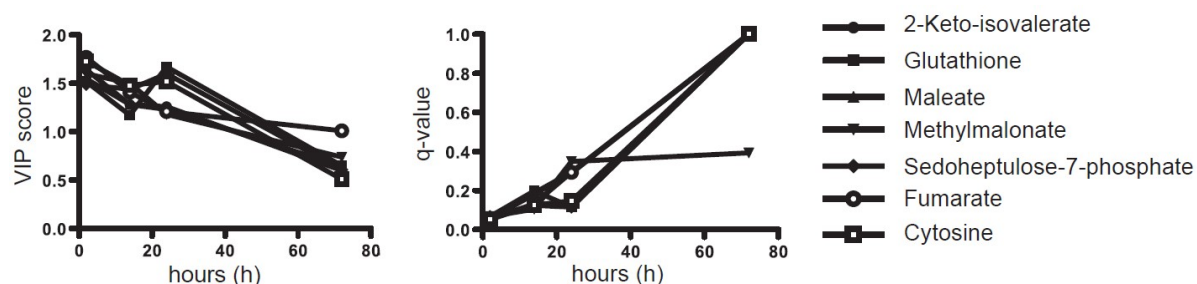


Figure 15: Identification of important metabolites and treatment biomarker candidates contributing to ketamine drug action. Quality criteria (R^2 , Q^2 , and accuracy) assessment of the multivariate data analyses using PLS-DA for the 2h, 14h, 24h, and 72h time points of ketamine treatment (3 mg kg^{-1}). R^2 , Q^2 , and accuracy values indicate good (2h: $R^2=0.99$, $Q^2=0.60$, accuracy=1.0; 14h: $R^2=1.0$, $Q^2=0.63$, accuracy=1.0) and robust (24h: $R^2=0.92$, $Q^2=0.52$, accuracy=0.8) models with the exception of the 72h time point ($R^2=1.0$, $Q^2=0.29$, accuracy=0.6). Important metabolites showed a $VIP\text{-score} \geq 1.0$ for the first three time points and $q \leq 0.1$ for at least one time point. $N=5$ mice per group and time point.

In order to verify biomarker candidates for the antidepressant effect of ketamine, I compared these biomarker candidates to data from a previous metabolomics profiling study of mice treated with the SSRI Paroxetine by Webhofer et al. In this study the antidepressant-like effect measured by the FST became significantly apparent as expected after a chronic treatment for 24 days⁴³². I re-analyzed the metabolomics data obtained from Paroxetine-treated animals and compared the FC, VIP-score, and q-values of the biomarker candidates from the present study for ketamine treatment.

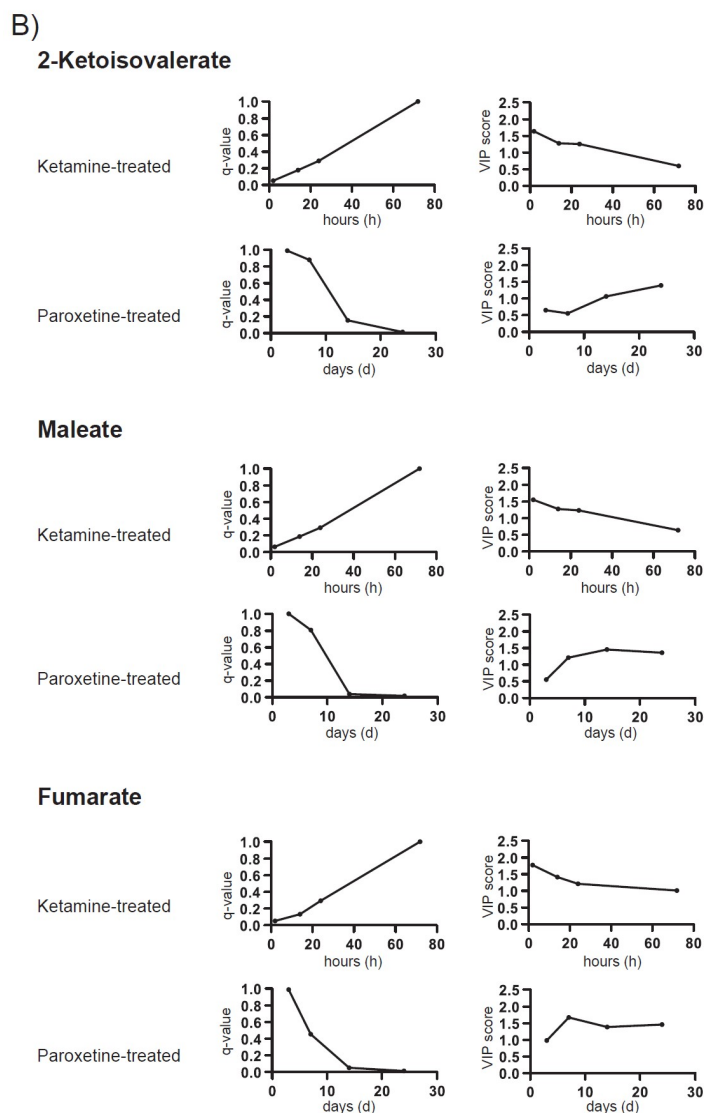
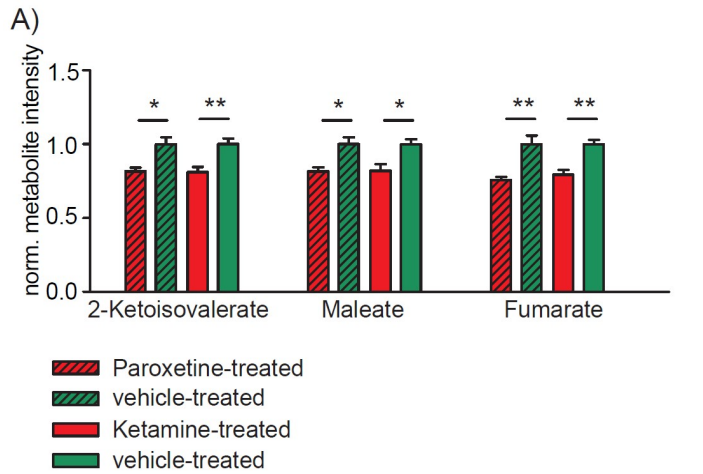


Figure 16: Identification of treatment biomarker candidates for ketamine's antidepressant-like mode of action. Biomarker candidates for ketamine treatment (cf. figure 15) were compared to re-analyzed data obtained by Webhofer et al⁴³². In this study, metabolomics profiling of mice treated with the SSRI antidepressant Paroxetine was performed. The re-analyzed metabolomics data from mice treated with Paroxetine was then compared to the FC, VIP-score, and q-values of the biomarker candidates obtained in the present study for ketamine treatment. **A)** FC comparison of treatment biomarkers of Paroxetine- and ketamine-treated animals compared to vehicle-treated mice. **B)** Q-value and VIP-score comparison of treatment biomarker candidates of Paroxetine- and ketamine-treated animals. Important metabolites showing VIP-score ≥ 1.0 for the first three time points and $q \leq 0.1$ for at least one time point. N=5 mice per group and time point. * $p \leq 0.05$, ** $p \leq 0.01$. P-values were determined by Student's t-test and SAM.

3 out of the 7 biomarker candidates obtained from the present metabolomics profiling study of ketamine-treated animals (2-Keto-isovalerate, maleate, and fumarate) showed similar FCs (figure 16A), VIP-scores, and significant q-values (figure 16B) in the time-dependent metabolomics analyses of Paroxetine treatment. The q-values of the biomarkers for ketamine's antidepressant-like effect are small ($q \leq 0.10$) for the 2h time point and time-dependently increase with the highest value at the 72h time point.

In contrast, with Paroxetine treatment it takes 2 to 4 weeks for the same biomarker candidates to reach the same effect that are seen within hours for ketamine treatment (figure 16B), reflecting the fast antidepressant-like effect of the latter on the biomolecular level. A VIP-score ≥ 1.0 is observed at earlier time points in ketamine-treated animals and decreases over time whereas in Paroxetine-treated animals it takes weeks of the treatment to see the increase (figure 16B). Taken together, 7 biomarkers qualify as treatment biomarkers for ketamine's drug response in the HPC. Out of these 7 biomarkers, 3 also qualify as treatment biomarkers for the antidepressant-like effect of ketamine.

4.3 Time-dependent hippocampal proteome profiling

In addition to the time-dependent HPC metabolome analyses, I performed quantitative proteome profiling analyses 2h and 24h after a single injection of a low dose of ketamine (3 mg kg⁻¹). Five mice per time point and treatment group were chosen based on the FST results (cf. section 4.1). Membrane-associated (MF) and cytoplasmic (CF) proteins from ketamine- and vehicle-treated mice 2h and 24h after ketamine treatment were isolated from the HPC and quantified relatively with ¹⁵N metabolic labelled reference proteins by LC-MS/MS analyses.

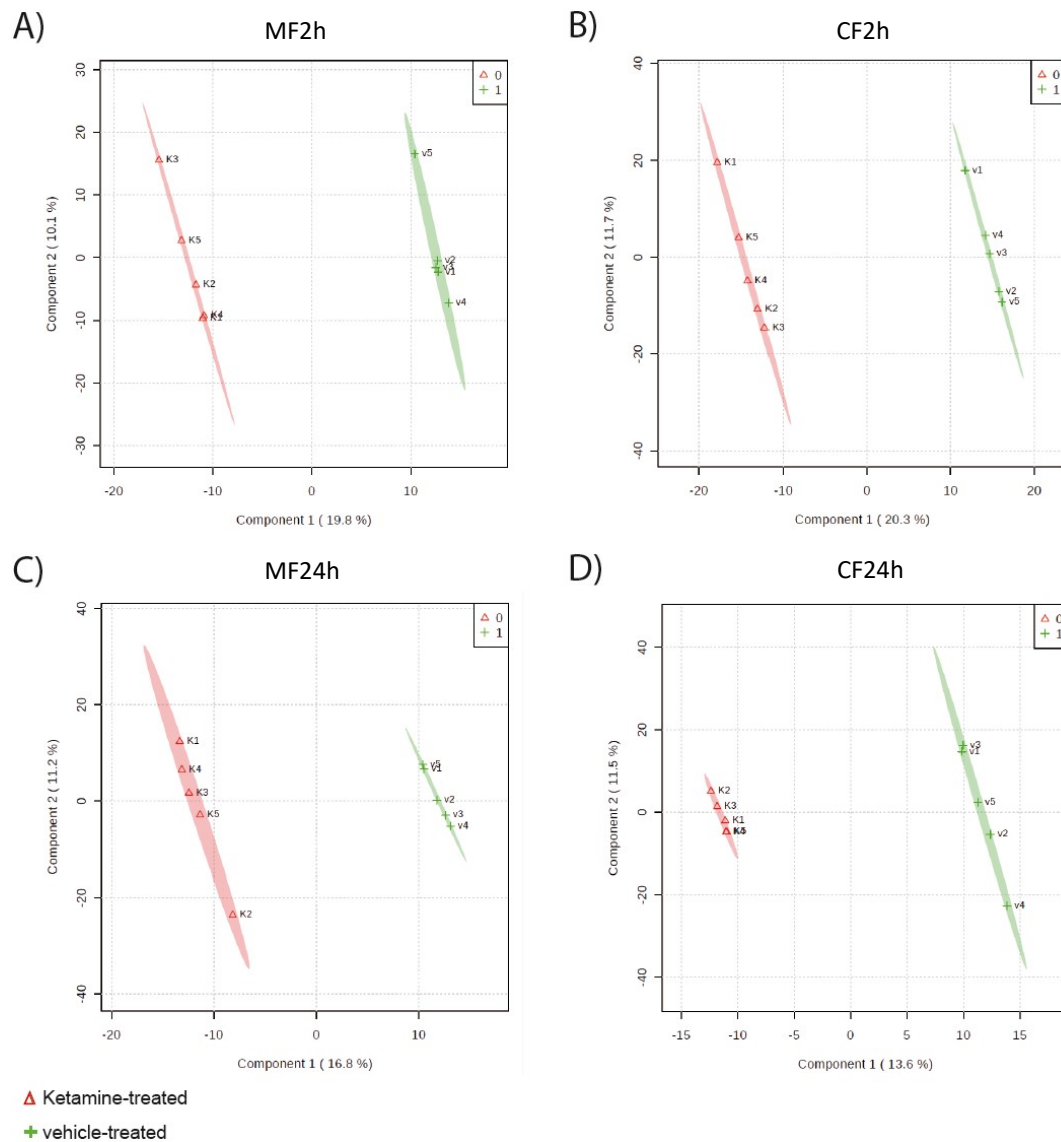


Figure 17: Multivariate partial least squares-discriminant analysis (PLS-DA) of (A) membrane-associated (MF2h) and (B) cytoplasmic (CF2h) proteins of the 2h time point and (C) membrane-associated (MF24h) and (D) cytoplasmic (CF24h) proteins of the 24h time point after a single injection of a low dose of ketamine (3 mg kg⁻¹) or vehicle using all quantified proteins. N=5 mice per group and time point.

After proteomics data processing and missing value imputation (cf. section 4.4), a total of 889 hippocampal MF and 1173 CF proteins were processed by statistical analyses 2h after a single injection of ketamine. 24h after ketamine treatment 1550 MF and 1091 CF relatively quantified proteins were used for further statistical analyses (supplemental table 3). The protein profiles

allowed a separation of ketamine- and vehicle-treated mice using multivariate PLS-DA at both time points (figure 17A–D).

Table 9: Quality criteria assessment (R^2 , Q^2 , and accuracy values) of the multivariate data analyses using PLS-DA for membrane-associated (MF2h) and cytoplasmic (CF2h) proteins 2h after ketamine and vehicle treatment. R^2 , Q^2 and accuracy values indicate good (MF2h: $R^2=0.99$, $Q^2=0.60$, accuracy=1.00; CF2h: $R^2=1.00$, $Q^2=0.64$, accuracy=1.00) and for MF24h and CF24h weak models (MF24h: $R^2=0.90$, $Q^2=0.43$, accuracy=0.90; CF24h: $R^2=0.99$, $Q^2=0.14$, accuracy=0.70). N=5 mice per group and time point.

| | MF2h | CF2h | MF24h | CF24h |
|-------------------------|------|------|-------|-------|
| Accuracy | 1.00 | 1.00 | 0.90 | 0.70 |
| R^2 | 0.99 | 1.00 | 1.00 | 0.99 |
| Q^2 | 0.60 | 0.64 | 0.43 | 0.14 |

Abbreviations: MF proteins, membrane-associated proteins;
CF proteins, cytoplasmic proteins; h, hour

The quality criteria of PLS-DA models were assessed by accuracy, R^2 , and Q^2 values. They indicate good models for the 2h time point in both analyses of MF and CF proteins of ketamine- compared to vehicle-treated animals. However, the PLS-DA models were weak for the 24h time point, which might therefore result in false-positives (table 9).

To increase the robustness of the statistical analyses, I additionally combined the VIP-score of the PLS-DA with SAM analyses, to obtain a reliable list of proteins for MF and CF at the 2h time point, that statistically significant contribute to ketamine's antidepressant action. 61 MF and 95 CF proteins were statistically significant altered at the 2h time point when comparing ketamine- to vehicle-treated mice (table 10).

Table 10: Hippocampal (A) membrane-associated (MF) and (B) cytoplasmic protein (CF) alterations 2h after a single injection of a low dose of ketamine (3 mg kg⁻¹) (PLS-DA VIP-score \geq 1.0, SAM FDR \leq 0.10 and SAM q \leq 0.1). N=5 mice per group and time point.

| Protein ID | Protein name | FC | PLS-DA, VIP-score | SAM, p-value | SAM, q-value | SAM, FDR |
|------------|--|-------|----------------------|-----------------|-----------------|-------------|
| A) | | | | | | |
| Q6DFY8 | BMP/retinoic acid-inducible neural-specific protein 2 | 0.24 | 2.13 | 0.00004 | 0.020 | \leq 0.10 |
| O70622 | Reticulon-2 | 2.52 | 2.13 | 0.00007 | 0.020 | \leq 0.10 |
| P55088 | Aquaporin-4 | 0.41 | 2.12 | 0.00011 | 0.020 | \leq 0.10 |
| P26231 | Catenin alpha-1 | 3.32 | 2.12 | 0.00013 | 0.020 | \leq 0.10 |
| Q9WV34 | MAGUK p55 subfamily member 2 | 4.45 | 2.11 | 0.00016 | 0.020 | \leq 0.10 |
| P41105 | 60S ribosomal protein L28 (Rpl28) | 2.46 | 2.10 | 0.00019 | 0.020 | \leq 0.10 |
| Q8BK72 | 28S ribosomal protein S27, mitochondrial (Mrps27) | 0.58 | 2.06 | 0.00024 | 0.021 | \leq 0.10 |
| P13020 | Gelsolin | 0.16 | 2.06 | 0.00026 | 0.021 | \leq 0.10 |
| Q8BJZ4 | 28S ribosomal protein S35, mitochondrial (Mrps35) | 0.26 | 2.05 | 0.00030 | 0.022 | \leq 0.10 |
| Q9ET43 | Claudin-12 | 3.01 | 2.03 | 0.00039 | 0.025 | \leq 0.10 |
| Q91W43 | Glycine dehydrogenase (decarboxylating), mitochondrial | 0.22 | 2.01 | 0.00047 | 0.027 | \leq 0.10 |
| O35678 | Monoglyceride lipase | 3.81 | 2.00 | 0.00051 | 0.027 | \leq 0.10 |
| Q3U9G9 | Lamin-B receptor | 3.66 | 1.99 | 0.00069 | 0.033 | \leq 0.10 |
| P56371 | Ras-related protein Rab-4A | 0.21 | 1.99 | 0.00073 | 0.033 | \leq 0.10 |
| O09005 | Sphingolipid delta(4)-desaturase DES1 | 3.11 | 1.97 | 0.00087 | 0.036 | \leq 0.10 |
| Q9CWS0 | N(G),N(G)-dimethylarginine dimethylaminohydrolase 1 | 2.59 | 1.96 | 0.00090 | 0.036 | \leq 0.10 |
| P12367 | cAMP-dependent protein kinase type II-alpha regulatory subunit (Prkar2a) | 3.32 | 1.95 | 0.00097 | 0.036 | \leq 0.10 |
| Q9D020 | Cytosolic 5'-nucleotidase 3A | 2.55 | 1.94 | 0.00102 | 0.036 | \leq 0.10 |
| Q921L3 | Transmembrane and coiled-coil domain-containing protein 1 | 0.40 | 1.93 | 0.00120 | 0.040 | \leq 0.10 |
| Q99JY4 | TraB domain-containing protein | 2.56 | 1.92 | 0.00132 | 0.042 | \leq 0.10 |
| O88307 | Sortilin-related receptor | 10.46 | 1.91 | 0.00146 | 0.044 | \leq 0.10 |
| Q5XJY4 | Presenilins-associated rhomboid-like protein, mitochondrial | 4.46 | 1.90 | 0.00153 | 0.044 | \leq 0.10 |
| Q99N87 | 28S ribosomal protein S5, mitochondrial (Mrps5) | 2.49 | 1.89 | 0.00168 | 0.046 | \leq 0.10 |
| O08715 | A-kinase anchor protein 1, mitochondrial (Akap1) | 3.27 | 1.89 | 0.00172 | 0.046 | \leq 0.10 |
| Q8BPN8 | DmX-like protein 2 | 3.22 | 1.88 | 0.00180 | 0.046 | \leq 0.10 |
| Q9CPY7 | Cytosol aminopeptidase | 0.32 | 1.88 | 0.00189 | 0.046 | \leq 0.10 |
| Q8R2Z5 | von Willebrand factor A domain-containing protein 1 | 2.27 | 1.87 | 0.00195 | 0.046 | \leq 0.10 |
| P84099 | 60S ribosomal protein L19 (Rpl19) | 2.99 | 1.87 | 0.00200 | 0.046 | \leq 0.10 |
| Q5SQX6 | Cytoplasmic FMR1-interacting protein 2 | 0.35 | 1.86 | 0.00222 | 0.047 | \leq 0.10 |
| Q9CWG8 | NADH dehydrogenase [ubiquinone] complex I, assembly factor 7 (Ndufa7) | 0.23 | 1.85 | 0.00228 | 0.047 | \leq 0.10 |
| Q9DCF9 | Translocon-associated protein subunit gamma | 1.84 | 1.84 | 0.00242 | 0.047 | \leq 0.10 |
| Q99PU5 | Long-chain-fatty-acid--CoA ligase ACSBG1 | 0.39 | 1.84 | 0.00255 | 0.047 | \leq 0.10 |
| Q9JM63 | ATP-sensitive inward rectifier potassium channel 10 | 0.41 | 1.84 | 0.00261 | 0.047 | \leq 0.10 |
| Q08460 | Calcium-activated potassium channel subunit alpha-1 | 2.65 | 1.83 | 0.00263 | 0.047 | \leq 0.10 |
| Q9D710 | Thioredoxin-related transmembrane protein 2 | 0.51 | 1.83 | 0.00267 | 0.047 | \leq 0.10 |
| Q8BVE3 | V-type proton ATPase subunit H | 0.60 | 1.80 | 0.00327 | 0.056 | \leq 0.10 |
| P60487 | Pyridoxal phosphate phosphatase | 2.48 | 1.79 | 0.00349 | 0.059 | \leq 0.10 |
| Q9D1R1 | Complex I assembly factor TMEM126B, mitochondrial (Tmem126a) | 2.60 | 1.78 | 0.00382 | 0.063 | \leq 0.10 |
| P21995 | Embigin | 0.56 | 1.78 | 0.00395 | 0.063 | \leq 0.10 |
| Q9EQH3 | Vacuolar protein sorting-associated protein 35 | 2.73 | 1.77 | 0.00411 | 0.064 | \leq 0.10 |
| Q8R3T5 | Syntaxin-binding protein 6 | 0.12 | 1.77 | 0.00422 | 0.064 | \leq 0.10 |
| | Cyclin-Y | | | | | \leq 0.10 |
| Q6ZWV3 | 60S ribosomal protein L10 (Rpl10) | 0.49 | 1.75 | 0.00452 | 0.064 | \leq 0.10 |
| P59281 | Rho GTPase-activating protein 39 | 0.57 | 1.75 | 0.00461 | 0.064 | \leq 0.10 |
| Q5IRJ6 | Zinc transporter 9 | 2.52 | 1.74 | 0.00472 | 0.064 | \leq 0.10 |
| Q91VT4 | Carbonyl reductase family member 4 | 0.33 | 1.74 | 0.00475 | 0.064 | \leq 0.10 |
| Q7TQI3 | Ubiquitin thioesterase (Otub1) | 0.37 | 1.73 | 0.00522 | 0.069 | \leq 0.10 |
| O55026 | Ectonucleoside triphosphate diphosphohydrolase 2 | 0.57 | 1.72 | 0.00550 | 0.071 | \leq 0.10 |
| P62717 | 60S ribosomal protein L18a (Rpl18a) | 0.32 | 1.72 | 0.00559 | 0.071 | \leq 0.10 |
| Q8HW98 | IgLON family member 5 | 2.68 | 1.72 | 0.00576 | 0.072 | \leq 0.10 |
| P22892 | AP-1 complex subunit gamma-1 | 0.49 | 1.71 | 0.00607 | 0.075 | \leq 0.10 |
| P20352 | Tissue factor | 0.20 | 1.71 | 0.00638 | 0.077 | \leq 0.10 |
| O89112 | LanC-like protein 1 | 0.44 | 1.70 | 0.00669 | 0.079 | \leq 0.10 |

| | | | | | | |
|--------|--|------|------|---------|-------|--------|
| Q8CBE3 | WD repeat-containing protein 37 | 4.30 | 1.69 | 0.00702 | 0.081 | ≤ 0.10 |
| Q6NZL0 | Protein SOGA3 | 0.33 | 1.69 | 0.00714 | 0.081 | ≤ 0.10 |
| O55023 | Inositol monophosphatase 1 | 2.03 | 1.69 | 0.00739 | 0.083 | ≤ 0.10 |
| Q9Z0V2 | Potassium voltage-gated channel subfamily D member 2 | 4.60 | 1.66 | 0.00862 | 0.095 | ≤ 0.10 |
| P62812 | Gamma-aminobutyric acid receptor subunit alpha-1 (GABA _A R1) | 0.33 | 1.66 | 0.00882 | 0.095 | ≤ 0.10 |
| Q9ERD7 | Tubulin beta-3 chain | 0.80 | 1.66 | 0.00906 | 0.096 | ≤ 0.10 |
| Q9JK42 | [Pyruvate dehydrogenase (acetyl-transferring)] kinase isozyme 2, mitochondrial | 0.47 | 1.65 | 0.00946 | 0.099 | ≤ 0.10 |
| P37040 | NADPH--cytochrome P450 reductase | 0.50 | 1.65 | 0.00962 | 0.099 | ≤ 0.10 |

B)

| | | | | | | |
|--------|--|------|------|---------|-------|--------|
| Q62165 | Dystroglycan | 0.34 | 2.15 | 0.00002 | 0.012 | ≤ 0.10 |
| P23492 | Purine nucleoside phosphorylase | 0.55 | 2.15 | 0.00003 | 0.012 | ≤ 0.10 |
| Q9JLB0 | MAGUK p55 subfamily member 6 | 5.80 | 2.14 | 0.00005 | 0.012 | ≤ 0.10 |
| Q9CS42 | Ribose-phosphate pyrophosphokinase 2 | 0.27 | 2.09 | 0.00007 | 0.012 | ≤ 0.10 |
| O54946 | DnaJ homolog subfamily B member 6 | 5.18 | 2.08 | 0.00009 | 0.012 | ≤ 0.10 |
| Q8VHN8 | Protein syndesmos | 4.99 | 2.07 | 0.00010 | 0.012 | ≤ 0.10 |
| O89029 | Matrilin-4 | 0.33 | 2.06 | 0.00013 | 0.013 | ≤ 0.10 |
| Q9JKB1 | Ubiquitin carboxyl-terminal hydrolase isozyme L3 (Uchl3) | 0.52 | 2.04 | 0.00017 | 0.014 | ≤ 0.10 |
| Q78J03 | Methionine-R-sulfoxide reductase B2, mitochondrial | 0.40 | 2.04 | 0.00019 | 0.014 | ≤ 0.10 |
| Q9CR95 | Adaptin ear-binding coat-associated protein 1 | 1.91 | 2.04 | 0.00020 | 0.014 | ≤ 0.10 |
| Q8K386 | Ras-related protein Rab-15 | 5.90 | 2.02 | 0.00026 | 0.017 | ≤ 0.10 |
| Q91WK5 | Glycine cleavage system H protein, mitochondrial | 0.65 | 1.99 | 0.00032 | 0.018 | ≤ 0.10 |
| Q9ER35 | Fructosamine-3-kinase | 0.32 | 1.99 | 0.00033 | 0.018 | ≤ 0.10 |
| Q61335 | B-cell receptor-associated protein 31 | 2.31 | 1.98 | 0.00042 | 0.021 | ≤ 0.10 |
| P62257 | Ubiquitin-conjugating enzyme E2 H (Ube2h) | 0.63 | 1.95 | 0.00051 | 0.024 | ≤ 0.10 |
| Q9R0X4 | Acyl-coenzyme A thioesterase 9, mitochondrial | 0.42 | 1.93 | 0.00062 | 0.027 | ≤ 0.10 |
| Q99KX1 | Myeloid leukemia factor 2 | 1.72 | 1.92 | 0.00068 | 0.028 | ≤ 0.10 |
| Q9CQE1 | Protein NipSnap homolog 3B | 0.31 | 1.90 | 0.00076 | 0.029 | ≤ 0.10 |
| Q9D6J6 | NADH dehydrogenase [ubiquinone] flavoprotein 2, mitochondrial (Ndufv2) | 1.47 | 1.90 | 0.00081 | 0.030 | ≤ 0.10 |
| P63087 | Serine/threonine-protein phosphatase PP1-gamma catalytic subunit | 0.51 | 1.89 | 0.00084 | 0.030 | ≤ 0.10 |
| P28660 | Nck-associated protein 1 | 1.70 | 1.88 | 0.00100 | 0.033 | ≤ 0.10 |
| Q9JL62 | Glycolipid transfer protein | 0.41 | 1.87 | 0.00113 | 0.033 | ≤ 0.10 |
| Q71M36 | Chondroitin sulfate proteoglycan 5 | 1.50 | 1.87 | 0.00115 | 0.033 | ≤ 0.10 |
| Q3V038 | Tetratricopeptide repeat protein 9A | 0.19 | 1.86 | 0.00119 | 0.033 | ≤ 0.10 |
| Q80TL0 | Protein phosphatase 1E | 1.54 | 1.86 | 0.00121 | 0.033 | ≤ 0.10 |
| Q99PG4 | Regulator of G-protein signaling 18 | 0.41 | 1.87 | 0.00123 | 0.033 | ≤ 0.10 |
| Q9DCM2 | Glutathione S-transferase kappa 1 | 3.99 | 1.86 | 0.00135 | 0.035 | ≤ 0.10 |
| P57759 | Endoplasmic reticulum resident protein 29 | 1.48 | 1.85 | 0.00145 | 0.036 | ≤ 0.10 |
| P51655 | Glypican-4 | 0.33 | 1.84 | 0.00159 | 0.038 | ≤ 0.10 |
| Q8CCK0 | Core histone macro-H2A.2 | 0.43 | 1.84 | 0.00167 | 0.039 | ≤ 0.10 |
| Q8R570 | Synaptosomal-associated protein 47 | 0.25 | 1.83 | 0.00174 | 0.039 | ≤ 0.10 |
| Q9D0M3 | Cytochrome c1, heme protein, mitochondrial (Cyc1) | 2.05 | 1.82 | 0.00212 | 0.046 | ≤ 0.10 |
| Q63829 | COMM domain-containing protein 3 | 0.55 | 1.81 | 0.00228 | 0.047 | ≤ 0.10 |
| Q9D2V7 | Coronin-7 | 0.64 | 1.80 | 0.00233 | 0.047 | ≤ 0.10 |
| Q99J85 | Neuronal pentraxin receptor | 0.40 | 1.80 | 0.00237 | 0.047 | ≤ 0.10 |
| Q99M71 | Mammalian ependymin-related protein 1 | 1.53 | 1.79 | 0.00264 | 0.050 | ≤ 0.10 |
| Q5U3K5 | Rab-like protein 6 | 0.48 | 1.79 | 0.00275 | 0.050 | ≤ 0.10 |
| Q9D1P4 | Cysteine and histidine-rich domain-containing protein 1 | 0.23 | 1.78 | 0.00280 | 0.050 | ≤ 0.10 |
| O35927 | Catenin delta-2 | 1.76 | 1.79 | 0.00284 | 0.050 | ≤ 0.10 |
| Q8BH59 | Calcium-binding mitochondrial carrier protein Aralar1 | 1.94 | 1.78 | 0.00287 | 0.050 | ≤ 0.10 |
| P70195 | Proteasome subunit beta type-7 (Psmb7) | 0.44 | 1.78 | 0.00304 | 0.052 | ≤ 0.10 |
| P46660 | Alpha-internexin | 1.43 | 1.77 | 0.00325 | 0.052 | ≤ 0.10 |
| Q8R0F8 | Acylpyruvase FAHD1, mitochondrial | 0.24 | 1.77 | 0.00332 | 0.052 | ≤ 0.10 |
| Q8R5M8 | Cell adhesion molecule 1 | 1.57 | 1.77 | 0.00333 | 0.052 | ≤ 0.10 |
| Q9DD02 | Protein Hikeshi | 0.55 | 1.77 | 0.00335 | 0.052 | ≤ 0.10 |

| | | | | | | |
|--------|---|------|------|---------|-------|--------|
| Q9DCC4 | Pyrroline-5-carboxylate reductase 3 | 0.16 | 1.75 | 0.00377 | 0.056 | ≤ 0.10 |
| Q9DC71 | 28S ribosomal protein S15, mitochondrial (Mrps15) | 0.55 | 1.75 | 0.00398 | 0.058 | ≤ 0.10 |
| O88485 | Cytoplasmic dynein 1 intermediate chain 1 | 1.46 | 1.75 | 0.00419 | 0.059 | ≤ 0.10 |
| Q91V61 | Sideroflexin-3 | 1.94 | 1.75 | 0.00431 | 0.059 | ≤ 0.10 |
| Q9CY58 | Plasminogen activator inhibitor 1 RNA-binding protein | 0.61 | 1.74 | 0.00436 | 0.059 | ≤ 0.10 |
| P10126 | Elongation factor 1-alpha 1 | 1.52 | 1.74 | 0.00442 | 0.059 | ≤ 0.10 |
| Q3TXS7 | 26S proteasome non-ATPase regulatory subunit 1 (Psm1) | 1.79 | 1.73 | 0.00488 | 0.064 | ≤ 0.10 |
| Q9JKN6 | RNA-binding protein Nova-1 | 0.63 | 1.72 | 0.00507 | 0.065 | ≤ 0.10 |
| P70349 | Histidine triad nucleotide-binding protein 1 | 2.46 | 1.73 | 0.00510 | 0.065 | ≤ 0.10 |
| O88507 | Ciliary neurotrophic factor receptor subunit alpha | 0.25 | 1.72 | 0.00530 | 0.066 | ≤ 0.10 |
| Q99J14 | 26S proteasome non-ATPase regulatory subunit 6 (Psm6) | 1.59 | 1.71 | 0.00546 | 0.066 | ≤ 0.10 |
| Q921F2 | TAR DNA-binding protein 43 | 1.60 | 1.71 | 0.00552 | 0.066 | ≤ 0.10 |
| Q8C5H8 | NAD kinase 2, mitochondrial | 0.55 | 1.71 | 0.00556 | 0.066 | ≤ 0.10 |
| Q9DAK9 | 14 kDa phosphohistidine phosphatase | 0.59 | 1.70 | 0.00589 | 0.068 | ≤ 0.10 |
| O35405 | Phospholipase D3 | 1.84 | 1.70 | 0.00597 | 0.068 | ≤ 0.10 |
| Q8R3Q6 | Coiled-coil domain-containing protein 58 | 0.37 | 1.70 | 0.00610 | 0.068 | ≤ 0.10 |
| Q99L27 | GMP reductase 2 | 0.32 | 1.69 | 0.00616 | 0.068 | ≤ 0.10 |
| Q9DCL9 | Multifunctional protein ADE2 | 8.65 | 1.69 | 0.00621 | 0.068 | ≤ 0.10 |
| P47199 | Quinone oxidoreductase | 0.37 | 1.69 | 0.00631 | 0.068 | ≤ 0.10 |
| Q7TMB8 | Cytoplasmic FMR1-interacting protein 1 | 2.32 | 1.69 | 0.00645 | 0.068 | ≤ 0.10 |
| Q924M7 | Mannose-6-phosphate isomerase | 5.81 | 1.68 | 0.00659 | 0.069 | ≤ 0.10 |
| Q6R891 | Neurabin-2 | 1.80 | 1.68 | 0.00680 | 0.070 | ≤ 0.10 |
| Q9WTT4 | V-type proton ATPase subunit G 2 | 2.91 | 1.68 | 0.00691 | 0.070 | ≤ 0.10 |
| P12658 | Calbindin | 1.45 | 1.68 | 0.00700 | 0.070 | ≤ 0.10 |
| P54728 | UV excision repair protein RAD23 homolog B | 2.64 | 1.68 | 0.00711 | 0.070 | ≤ 0.10 |
| Q8BH95 | Enoyl-CoA hydratase, mitochondrial | 1.37 | 1.67 | 0.00728 | 0.070 | ≤ 0.10 |
| P43006 | Excitatory amino acid transporter 2 | 1.38 | 1.68 | 0.00730 | 0.070 | ≤ 0.10 |
| Q9Z2W9 | Glutamate receptor 3 (Gria3) | 0.65 | 1.67 | 0.00756 | 0.071 | ≤ 0.10 |
| Q8BMK4 | Cytoskeleton-associated protein 4 | 0.62 | 1.66 | 0.00763 | 0.071 | ≤ 0.10 |
| P23819 | Glutamate receptor 2 (Gria2) | 1.61 | 1.66 | 0.00789 | 0.073 | ≤ 0.10 |
| Q9CQW2 | ADP-ribosylation factor-like protein 8B | 5.27 | 1.66 | 0.00812 | 0.073 | ≤ 0.10 |
| O54829 | Regulator of G-protein signaling 7 | 8.96 | 1.66 | 0.00818 | 0.073 | ≤ 0.10 |
| Q9CX56 | 26S proteasome non-ATPase regulatory subunit 8 (Psm8) | 3.32 | 1.66 | 0.00830 | 0.073 | ≤ 0.10 |
| O35621 | Phosphomannomutase 1 | 0.26 | 1.65 | 0.00832 | 0.073 | ≤ 0.10 |
| P51855 | Glutathione synthetase | 3.19 | 1.65 | 0.00900 | 0.078 | ≤ 0.10 |
| Q8BGT8 | Phytanoyl-CoA hydroxylase-interacting protein-like | 1.98 | 1.65 | 0.00909 | 0.078 | ≤ 0.10 |
| O55100 | Synaptogyrin-1 | 1.80 | 1.64 | 0.00939 | 0.078 | ≤ 0.10 |
| Q8BGH4 | Receptor expression-enhancing protein 1 | 5.08 | 1.64 | 0.00940 | 0.078 | ≤ 0.10 |
| Q9R1Z7 | 6-pyruvoyl tetrahydrobiopterin synthase | 0.58 | 1.64 | 0.00945 | 0.078 | ≤ 0.10 |
| P15116 | Cadherin-2 | 3.05 | 1.63 | 0.00997 | 0.081 | ≤ 0.10 |
| P41105 | 60S ribosomal protein L28 (Rpl28) | 0.55 | 1.63 | 0.01017 | 0.082 | ≤ 0.10 |
| Q91WA3 | Histone deacetylase 11 | 0.35 | 1.61 | 0.01154 | 0.092 | ≤ 0.10 |
| Q91YN9 | BAG family molecular chaperone regulator 2 | 0.47 | 1.60 | 0.01173 | 0.092 | ≤ 0.10 |
| Q80ZJ1 | Ras-related protein Rap-2a | 0.54 | 1.60 | 0.01178 | 0.092 | ≤ 0.10 |
| O70310 | Glycylpeptide N-tetradecanoyltransferase 1 | 0.74 | 1.59 | 0.01246 | 0.096 | ≤ 0.10 |
| Q6PGN3 | Serine/threonine-protein kinase DCLK2 | 0.67 | 1.59 | 0.01275 | 0.097 | ≤ 0.10 |
| Q3UFF7 | Lysophospholipase-like protein 1 | 0.23 | 1.59 | 0.01299 | 0.097 | ≤ 0.10 |
| Q9R1Q9 | V-type proton ATPase subunit S1 | 1.43 | 1.59 | 0.01305 | 0.097 | ≤ 0.10 |
| Q9Z1L5 | Voltage-dependent calcium channel subunit alpha-2/delta-3 | 1.77 | 1.58 | 0.01348 | 0.099 | ≤ 0.10 |
| P63044 | Vesicle-associated membrane protein 2 | 1.77 | 1.58 | 0.01370 | 0.100 | ≤ 0.10 |

Abbreviations: PLS-DA, Partial Least Square-Discriminant Analysis; FC: Fold Change; SAM, Significance Analysis of Microarrays (and proteins, metabolites); VIP, Variable Importance in Projection; FDR, False discovery rate; ID, Identification; h, hours

4.3.1 Ketamine's effect on the glutamatergic and GABAergic system

It is assumed that ketamine's antidepressant activity is the result of the drug's blocking of the NMDAR on GABAergic inhibitory interneurons thereby indirectly resulting in an increased synaptic activity of glutamatergic excitatory neurons.

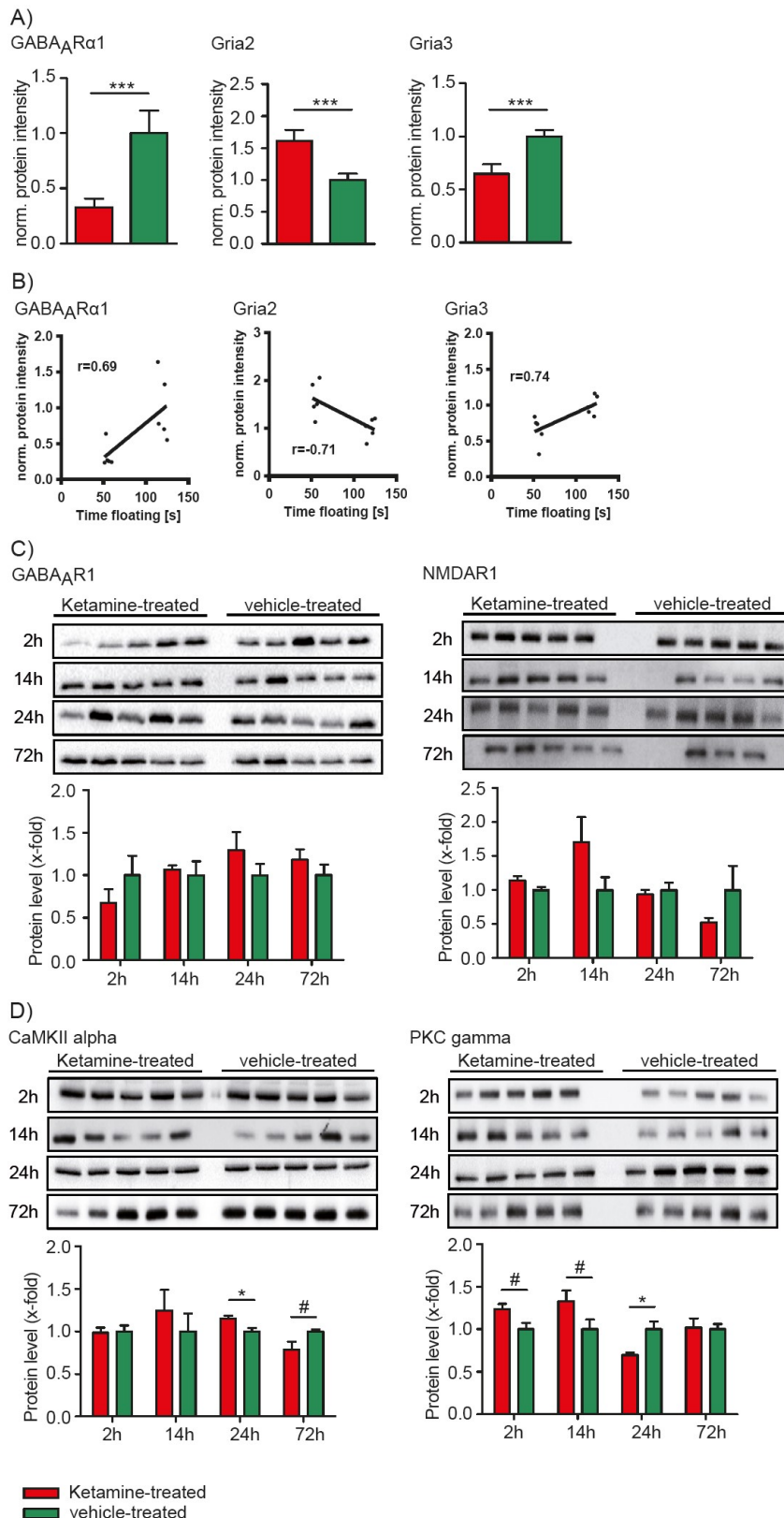


Figure 18: Hippocampal protein level and correlation analyses after a single injection of a low dose of ketamine (3 mg kg^{-1}). **A)** Alterations of GABA_A receptor $\alpha 1$ (GABA_AR $\alpha 1$), and AMPA receptor subunits Gria2 and Gria3 protein levels determined by quantitative proteomics analyses 2h after ketamine treatment. **B)** Correlation analyses of GABA_AR $\alpha 1$, Gria2 and Gria3 protein intensities with the FST floating time ($p \leq 0.05$). **C)** Western blots analysing of GABA_AR1 and NMDAR1 protein levels 2h, 14h, 24h, and 72h after a single injection of ketamine. **D)** CaMKII alpha and PKC gamma protein levels were analyzed by Western blots for the 2h, 14h, 24h, and 72h time points. The results from ketamine-treated animals are normalized to the ones obtained from vehicle treatment (mean value = 1). N=5 mice per group and time point. # $p \leq 0.10$, * $p \leq 0.05$, ** $p \leq 0.01$, *** $p \leq 0.001$. P-values were determined by Student's t-test and SAM. Error bars represent s.e.m. The correlation coefficient, r , was calculated by Pearson. The linear regression line is only shown for significant ($p \leq 0.05$) correlation coefficients.

Alternatively, ketamine's antidepressant effect may result from blocking the NMDAR on the glutamatergic excitatory neurons directly, which, subsequently, stimulates a homeostatic mechanism in the neuronal network trying to keep the original neuronal network activity (cf. chapter 1). In this regard it is interesting to observe that ketamine downregulates GABA_AR α 1 and the AMPA receptor subunit Gria3 protein levels, while increased AMPA receptor subunit Gria2 protein levels are found for the 2h time point (table 10 and figure 18A). Moreover, these proteins also significantly correlated with the FST floating time (figure 18B). The results were further validated by Western blots which showed decreased but not statistically significant GABA_AR1 protein level changes. The observed changes on the glutamatergic receptors seem not to affect NMDAR receptors as Western blot analysis did not show any changes in NMDAR1 protein levels for all time points (figure 18C). Ca²⁺/Calmodulin-dependent protein Kinase (CaMKII) alpha and Protein Kinase C (PKC) gamma mediate AMPA receptor internalization into the synaptic membrane, a mechanism involved in synaptic plasticity such as LTP⁴³⁷. Ketamine statistically significant increased and tended to decrease CaMKII alpha protein levels 24h and 72h after ketamine treatment, respectively (figure 18C). PKC gamma protein levels tended to increase at the 2h and 14h time points and statistically significant decreased 24h after a single injection of ketamine (figure 18D). The observed changes related to the AMPARs are contradictory to the decreased GABA_AR, altered CaMKII alpha and PKC gamma protein levels. They might indicate an induction of synaptic or homeostatic plasticity.

Synaptic plasticity, especially LTP, is promoted by glutamate that is released into the synaptic cleft upon neuronal activity. Once released, glutamate for instance binds and activates AMPARs and NMDARs. In contrast, GABA release into the synaptic cleft by GABAergic inhibitory interneurons inhibits neuronal activity and therefore also synaptic plasticity. Glutamate and GABA are metabolized by glutamine (cf. chapter 1). Therefore, I examined the metabolite ratios and levels of glutamate, glutamine and GABA. When analyzing neurotransmitter ratios I found the GABA/glutamate ratio to be increased 72h after a single injection of ketamine (figure 19A). At 14h the glutamate/glutamine and GABA/glutamine metabolite ratios were increased (figure 19A). GABA levels were upregulated at 72h (figure 19B). For the 14h time point glutamate and glutamine levels were decreased (figure 19B). Putrescine and serine levels, two positive modulators of the NMDAR^{438, 439}, were elevated already 2h after a single injection of ketamine (figure 19C). Furthermore, GABA, glutamate, glutamine, putrescine and serine metabolite intensities statistically significant correlated with the FST floating time at the 72h, 14h and 2h time points, respectively (figure 19D).

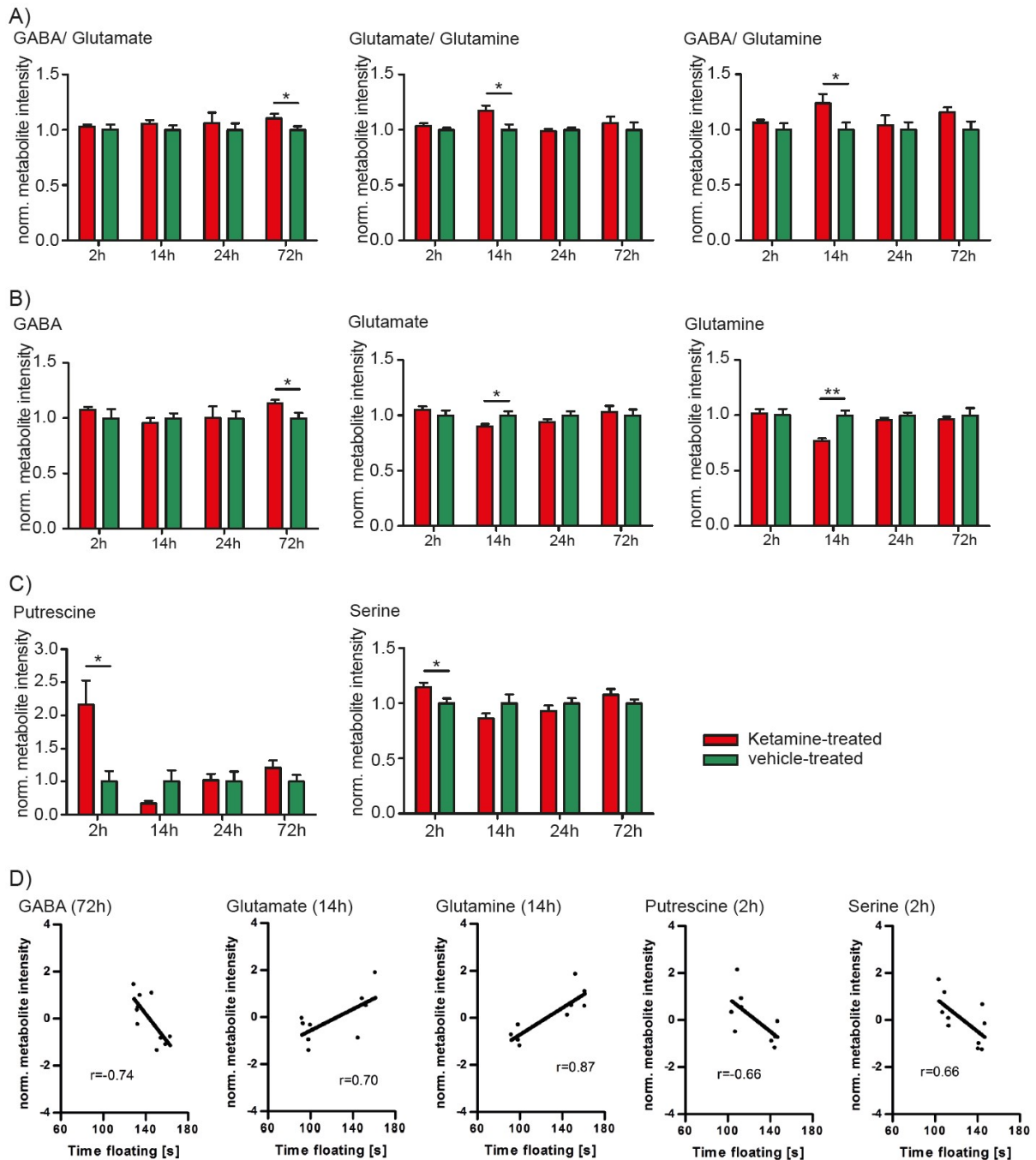


Figure 19: Hippocampal metabolite ratio and metabolite level analyses after a single injection of a low dose of ketamine (3 mg kg^{-1}). **A)** Glutamate/GABA, glutamate/glutamine and GABA/glutamine metabolite ratio analyses determined by time-dependent metabolomics profiling analyses. **B)** Time-dependent metabolite levels of GABA, glutamate, and glutamine. **C)** Time-dependent metabolite level changes of NMDAR positive modulators putrescine and serine. **D)** Correlation analyses of GABA (72h, $p \leq 0.05$), glutamate (14h, $p \leq 0.05$), glutamine (14h, $p \leq 0.05$), putrescine (2h, $p \leq 0.05$) and serine (2h, $p \leq 0.05$) metabolite intensities with the FST floating time. The results from ketamine-treated animals are normalized to the ones obtained from vehicle treatment (mean value = 1). $N=5$ mice per group and time point. * $p \leq 0.05$, ** $p \leq 0.01$. P-values were determined by Student's t-test and SAM. Error bars represent s.e.m. The correlation coefficient, r , was calculated by Pearson. The linear regression line is only shown for significant ($p \leq 0.05$) correlation coefficients.

A loss of HPC volume has been observed for a subset of MDD patients. This process can be reversed by AD treatment which also results in symptom reduction. The volume decline seems to be caused by neuronal atrophy due to weakened and shrunk synaptic connections and seems to be caused by stress. The observed reversal of the volume reduction in MDD patients might result from increased synaptic plasticity (cf. chapter 1).

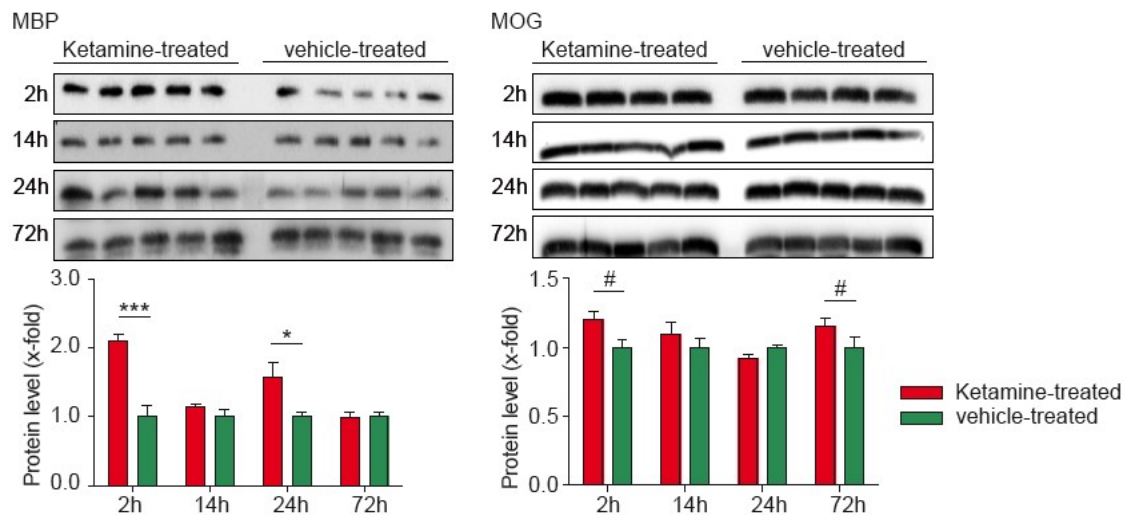


Figure 20: Hippocampal protein level analyses after a single injection of a low dose of ketamine (3 mg kg⁻¹). Time-dependent Western blots for MBP (n=5 mice per group and time point) and MOG (2h: ketamine-treated, n=4; vehicle-treated, n=4; 14h: ketamine-treated, n=5; vehicle-treated, n=5; 24h: ketamine-treated, n=5; vehicle-treated, n=5; 72h: ketamine-treated, n=5; vehicle-treated, n=5). The results from ketamine-treated animals are normalized to the ones obtained from vehicle treatment (mean value = 1). #p<0.10, *p<0.05, **p<0.01, ***p<0.001. P-values were determined by Student's t-test. Error bars represent s.e.m.

The myelin sheath is a protective lipid layer around axons, but not the cell body, produced by glial cells supporting fast neuronal signaling minimizing a loss of information⁴⁴⁰. Therefore, a reversal of the volume reduction observed in a subset of treated MDD patients caused by synaptic plasticity with an outgrowth of synaptic connections should result in an elevated number of myelin proteins. On one hand, a low dose of ketamine has previously been shown to induce synaptic plasticity apparent by newly formed spines in the PFC of rats (cf. chapter 1). On the other hand, when applied at higher doses ketamine is also used as an animal model of schizophrenia where a loss of the myelin sheath is discussed²⁵⁴⁻²⁵⁷. Western blots were conducted for two myelin proteins to gauge their response to ketamine. As expected, ketamine treatment increases myelin basic protein (MBP) levels already 2h and 24h after a single injection (figure 20). Myelin oligodendrocyte glycoprotein (MOG) protein levels tended to be elevated at the 2h and 72h time points (Figure 20). Therefore, I can rule out that the low dose of ketamine that was used in this study produces molecular alterations characteristic for schizophrenia like decreased myelin proteins^{441, 442}.

4.3.2 Ketamine's impact on the mitochondrial energy metabolism, protein damage and quality control system

Several previous analyses and the present study show an impact of major energy metabolism pathways like glycolysis, pyruvate metabolism, citrate cycle and the OXPHOS on psychiatric disorders and AD drug action⁴³²⁻⁴³⁴.

Pathway enrichment analyses for the altered HPC proteins highlight protein processing in endoplasmic reticulum, purine, ribosome, fructose, and mannose metabolism, as expected the OXPHOS, and proteasome (table 11). Furthermore, the altered proteins and identified pathways are in line with the metabolomics profiling results of an affected mitochondrial energy metabolism, especially pointing towards an altered OXPHOS (figures 12, 13 and 14 and tables 10 and 11).

Table 11: Pathway enrichment analysis for KEGG pathways of significantly altered hippocampal proteins (PLS-DA VIP-score \geq 1.0, SAM FDR \leq 0.10, and SAM q \leq 0.10) 2h after a single injection of a low dose of ketamine (3 mg kg⁻¹). N=5 mice per group and time point.

| Pathway | p-value | FDR |
|---|---------|-------|
| Protein processing in endoplasmic reticulum | 0.001 | 0.084 |
| Purine metabolism | 0.001 | 0.084 |
| Ribosome | 0.002 | 0.084 |
| Fructose and mannose metabolism | 0.002 | 0.084 |
| Oxidative phosphorylation (OXPHOS) | 0.002 | 0.084 |
| Proteasome | 0.003 | 0.100 |

Abbreviations: FDR, False discovery rate; h, hours

A low dose of ketamine elevated several OXPHOS protein complexes protein levels including complex I NADH dehydrogenase [ubiquinone] flavoprotein 2 (Ndufv2), Cytochrome c1, heme protein (Cyc1), and complex I assembly factor (Tmem126B) and lead to decreased levels of NADH dehydrogenase [ubiquinone] complex I, assembly factor 7 (Ndufaf7) 2h after a single injection of ketamine (table 10 and figure 21A). Furthermore, the Ndufv2, Cyc1, Ndufaf7 and Tmem126B protein intensities also significantly correlated with the FST floating time (figure 21B). In addition, Western blot analyses revealed that the complex II succinate dehydrogenase subunit B (SDHB) and complex III ubiquinol-cytochrome C reductase core protein II (Uqcrc2) are upregulated 14h and 24h after ketamine treatment, respectively. In contrast, NADH dehydrogenase [ubiquinone] 1 beta subcomplex, 8 (Ndufb8) and ATP synthase, subunit alpha (ATP5a) did not show any differences at the 14h and 24h time points (figure 21C).

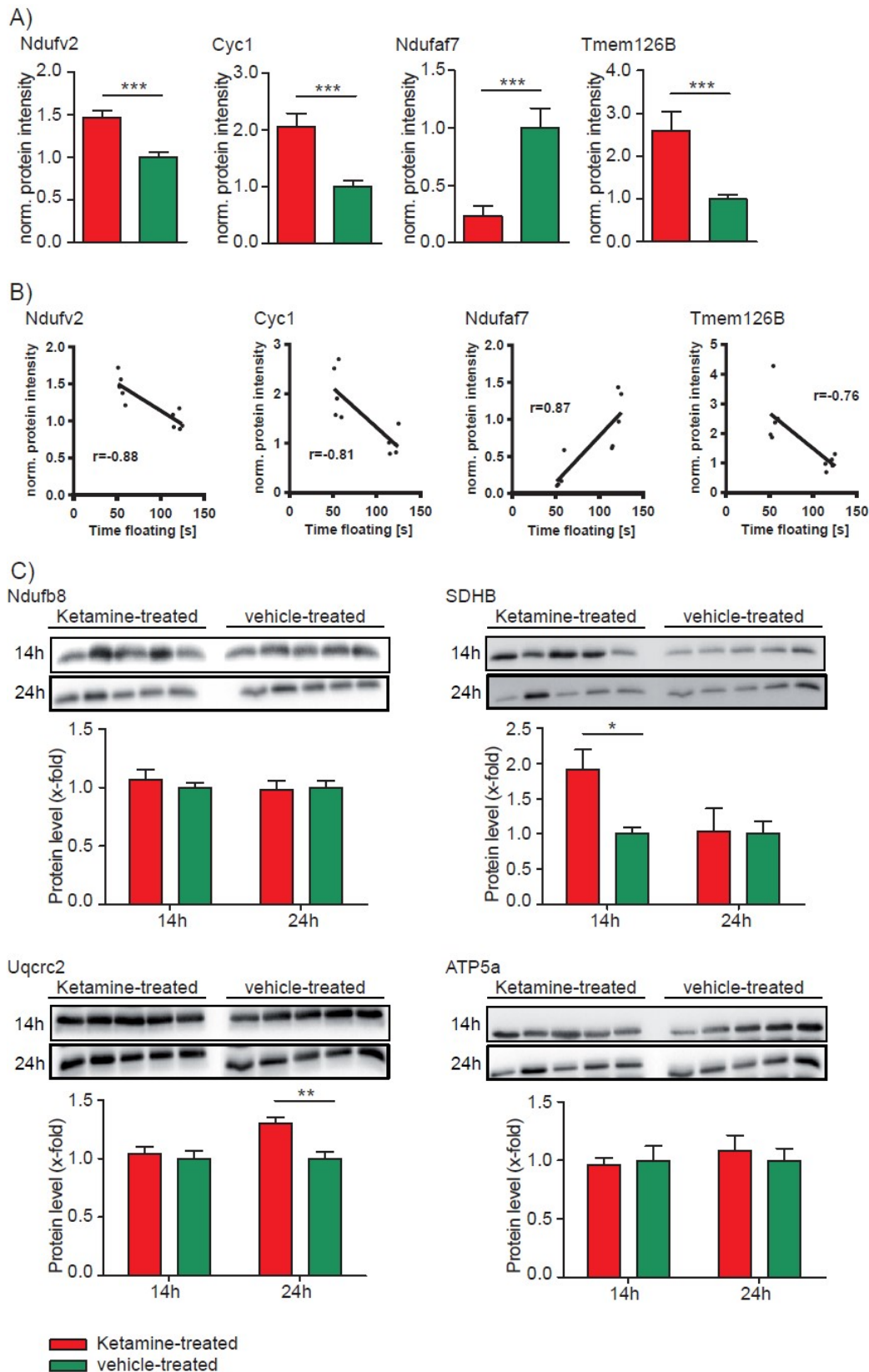
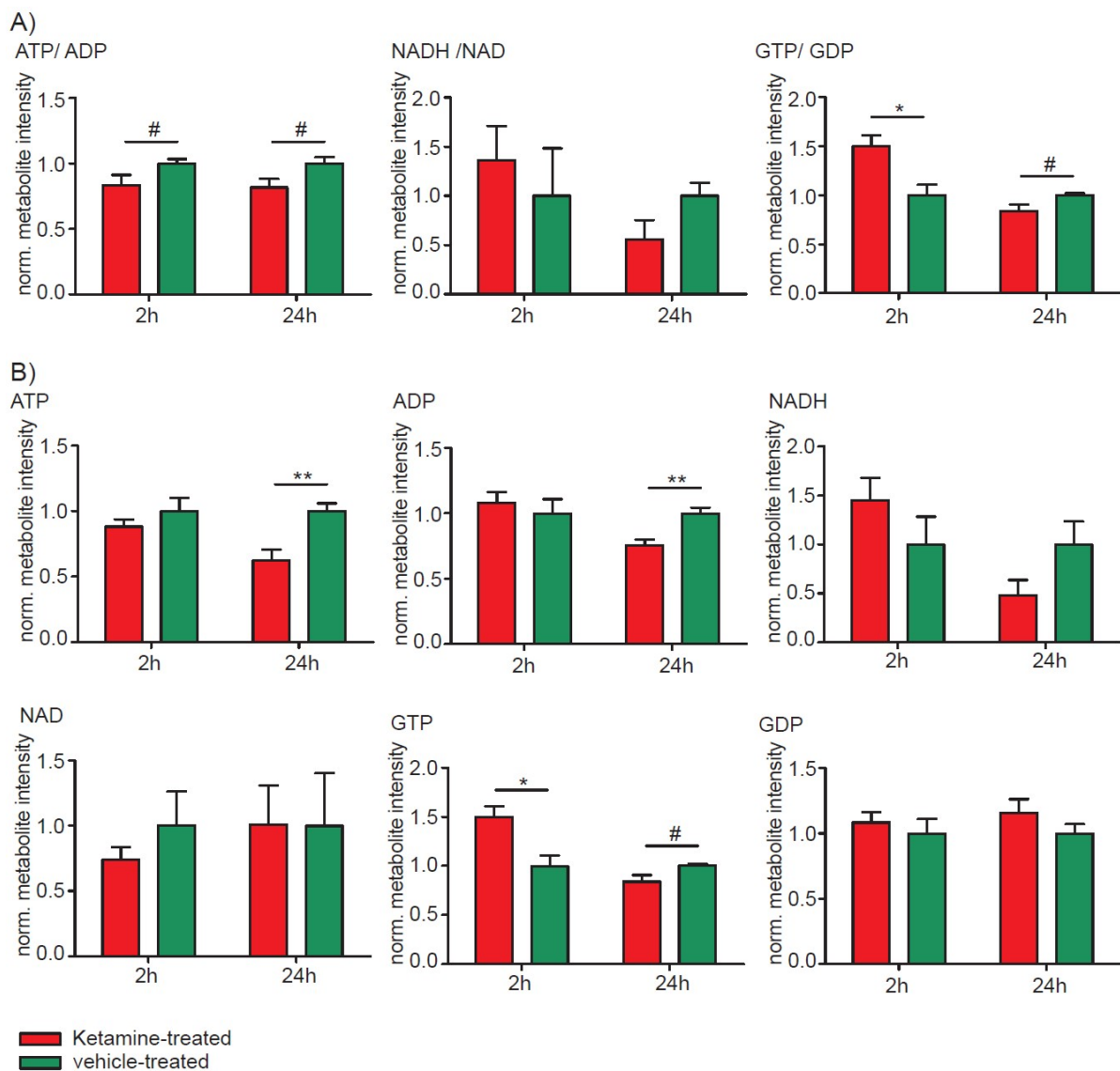


Figure 21: Hippocampal protein level analyses 2h after a single injection of a low dose of ketamine (3 mg kg⁻¹) of (A) the OXPHOS protein levels Ndufv2, Cyc1, Ndufaf7, and Tmem126B, determined by quantitative proteomics profiling analyses. (B) Correlation analyses of Ndufv2, Cyc1, Ndufaf7, and Tmem126B protein intensities with the FST floating time 2h after a single injection of ketamine ($p \leq 0.05$). (C) Western blot analyses of Ndufb8, SDHB, Uqcrc2, and ATP5a protein levels 14h and 24h after ketamine treatment. The results from ketamine-treated animals are normalized to the ones obtained from vehicle treatment (mean value = 1). $N=5$ mice per group and time point. * $p \leq 0.05$, ** $p \leq 0.01$, *** $p \leq 0.001$. P-values were determined by t-test and SAM. Error bars represent s.e.m. The correlation coefficient, r , was calculated by Pearson. The linear regression line is only shown for significant ($p \leq 0.05$) correlation coefficients.

I further investigated the consequences of the observed protein level changes related to the OXPHOS protein complexes on the associated energy equivalents: ATP, ADP, NADH, NAD, GTP, and GDP. The ATP/ADP metabolite ratio tends to be down for both time points (figure 22A). The metabolite levels of both ATP and ADP showed no significant differences for the 2h time point, but a statistically significant decrease for both metabolite levels 24h after ketamine treatment (figure 22B). Neither the NADH/NAD metabolite ratio nor the NADH and NAD metabolite levels are statistically significant altered after ketamine treatment (figures 22A and 22B). A single injection of ketamine statistically significant increases the GTP/GDP metabolite ratio at 2h, but it tends to decrease at the 24h time point (figure 22A). In line with this observation, GTP metabolite levels were statistically significant increased 2h and also tend to decrease 24h upon ketamine treatment, whereas the GDP levels do not show any significant differences at any time point (figure 22B). Moreover, correlation analyses of ATP, ADP and GTP for the respective time points where significant metabolite level alterations were found revealed that they significantly correlated with the FST floating time (figure 22C).



C)

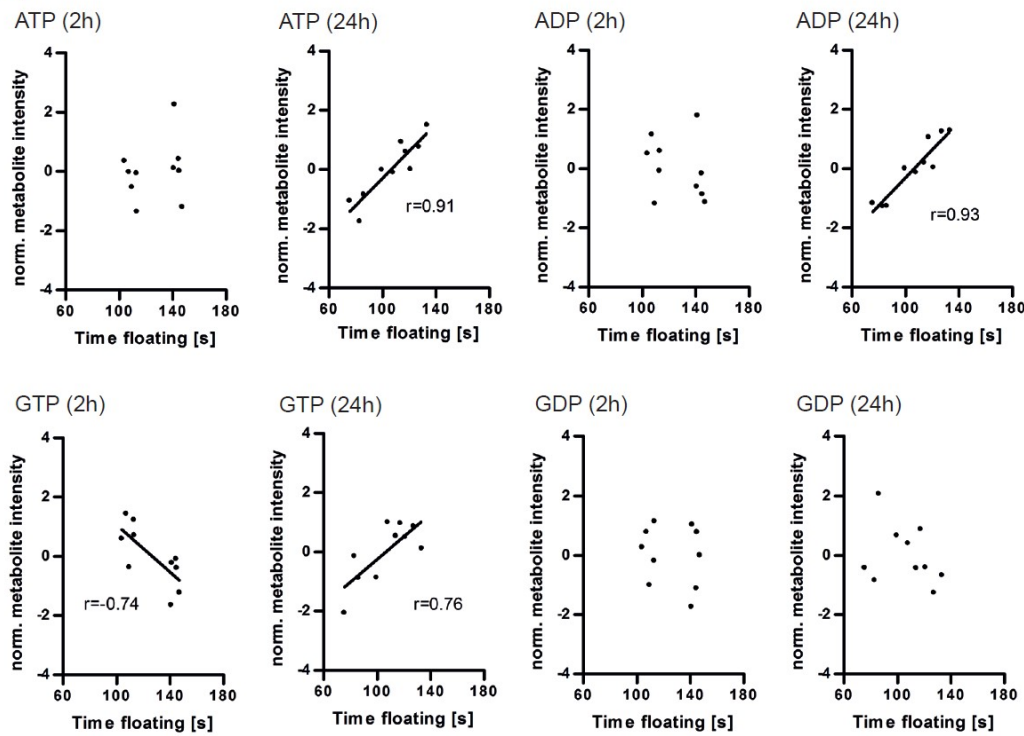


Figure 22: Time-dependent hippocampal metabolite ratio and metabolite level analyses. **A)** ATP/ADP, NADH/NAD, and GTP/GDP metabolite ratio analyses of the 2h and 24h time points determined by time-dependent metabolomics profiling analyses. **B)** Time-dependent ATP, ADP, NADH, NAD, GTP, and GDP levels at the 2h and 24h time points. **C)** Correlation analyses of ATP (2h, not significant; 24h, $p \leq 0.05$), ADP (2h, not significant; 24h, $p \leq 0.05$), GTP (2h and 24h, $p \leq 0.05$) and GDP (2h and 24h, not significant) with the FST floating time. The results from ketamine-treated animals are normalized to the ones obtained from vehicle treatment (mean value = 1). $N=5$ mice per group and time point. # $p \leq 0.10$, * $p \leq 0.05$, ** $p \leq 0.01$. P-values were determined by Student's t-test and SAM. Error bars represent s.e.m. The correlation coefficient, r , was calculated by Pearson. The linear regression line is only shown for significant ($p \leq 0.05$) correlation coefficients.

Synaptic plasticity, especially LTP, is a process of high ATP consumption. AMP activated protein Kinase (AMPK) is the major energy status sensor that promotes catabolic pathways to generate ATP and inhibits anabolic pathways that consume ATP. AMPK is activated by high AMP and ADP levels whereas increased levels of ATP inhibit AMPK⁴⁴³⁻⁴⁴⁹. I time-dependently analyzed AMPK protein levels as well as the phosphorylation (active state of AMPK) status of the protein kinase (pAMPK) by Western blots. The overall AMPK protein levels stay relatively constant at a slightly lowered level, however statistically this only reaches trend level at 14 and 24h (figure 23A). PAMPK protein levels statistically significant increase at the 24h time point (figure 23A), ultimately leading to an elevated ratio of pAMPK/AMPK 24h after a single injection of ketamine (figure 23B). Activation of the AMPK leads to the conclusion that ketamine treatment results in an energy deficit that needs to be regulated by promoting catabolic pathways⁴⁴³⁻⁴⁵¹. In general, neurons either might cope with higher energy demands by increasing mitochondrial proteins as shown by the obtained results (cf. figure 21), the number of mitochondria, also termed mitochondrial biogenesis and/or by regulating the local position of mitochondria to the synapses where energy is needed.

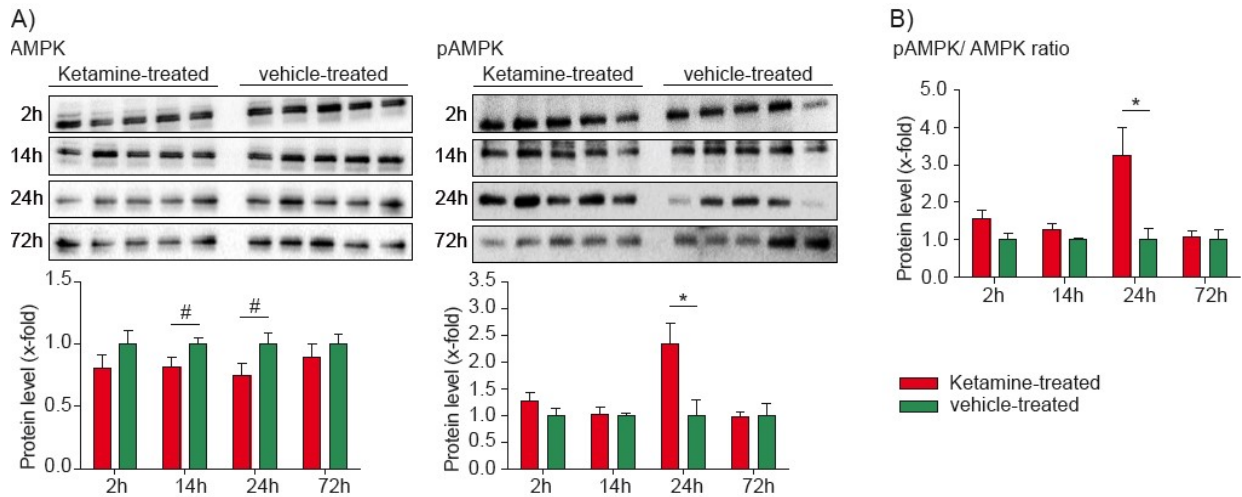


Figure 23: Hippocampal protein level analyses after a single injection of a low dose of ketamine (3 mg kg⁻¹). **A)** Time-dependent Western blot analysis of AMPK and pAMPK protein levels. **B)** Ratio of the pAMPK to AMPK protein levels to determine the activated related to the non-activated form of the enzyme. The results from ketamine-treated animals are normalized to the ones obtained from vehicle treatment (mean value = 1). N=5 mice per group and time point. #p<0.10, *p<0.05. P-values were determined by Student's t-test. Error bars represent s.e.m.

Mitochondrial biogenesis is achieved by an elevation of mitochondrial transcription factors ultimately resulting in elevated mitochondrial protein levels, especially for the mitochondrial ETC complexes of the OXPHOS. Mitochondrial proteins are not only expressed in the nucleus, but also in the mitochondria as they contain their own mitochondrial DNA. Nuclear encoded mitochondrial proteins are transcribed in the nucleus, the mRNA is then transported and imported into the mitochondria where they are finally translated⁴⁵²⁻⁴⁵⁴. I therefore analyzed mitochondrial transcription factors and mitochondrial import protein levels by Western blots. The peroxisome proliferator-activated receptor gamma coactivator 1-alpha (PGC1 α) protein levels tended to be decreased in the cytoplasm 2h after a single injection of ketamine.

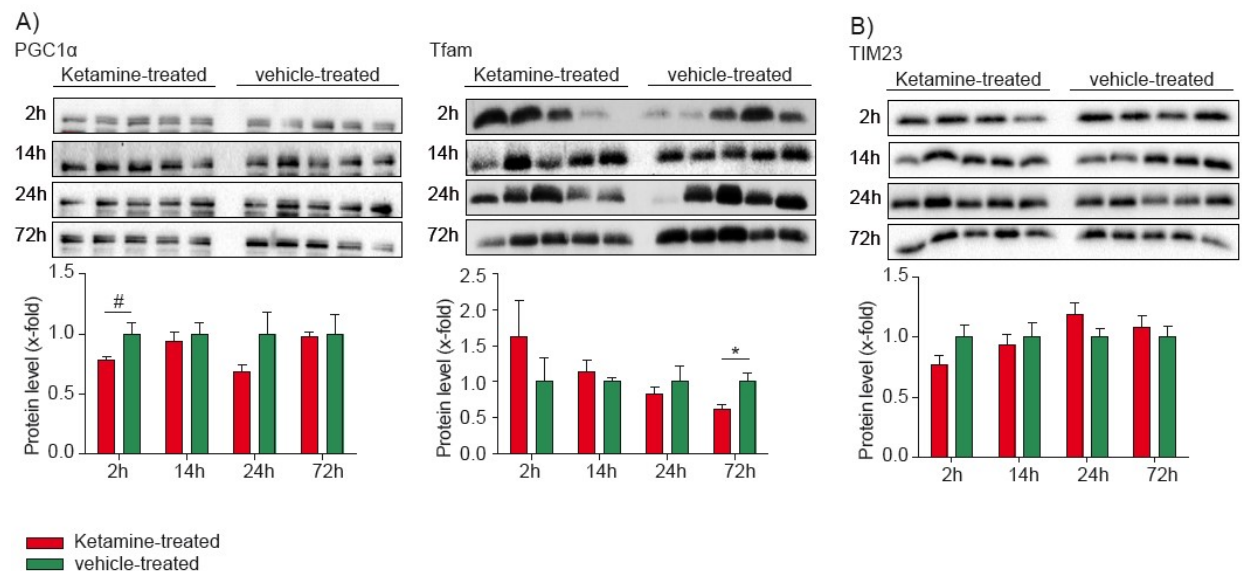


Figure 24: Hippocampal protein level analyses after a single injection of a low dose of ketamine (3 mg kg⁻¹). **A)** Time-dependent Western blot analyses of PGC1 α and Tfam protein levels. **B)** Time-dependent Western blot analysis of TIM23 protein levels. The results from ketamine-treated animals are normalized to the ones obtained from vehicle treatment (mean value = 1). N=5 mice per group and time point. #p<0.10, *p<0.05, P-values were determined by Student's t-test. Error bars represent s.e.m.

Mitochondrial transcription factor A (Tfam) protein levels were statistically significant reduced at the 72h time point (figure 24A). No protein level changes were observed for the mitochondrial import protein translocase of inner membrane 23 (TIM23) (figure 24B).

Oxidative stress describes an imbalance in the amount of reactive oxygen species (ROS) and the cellular defense system including molecules like antioxidants and enzymes such as Peroxiredoxins (Prdxs). Both, the antioxidants and the Prdxs have an antioxidant capacity and counteract ROS⁴⁵⁵⁻⁴⁵⁹.

Therefore, I next analyzed the effects of the altered OXPHOS protein levels on oxidative stress. I performed Western Blots of cytoplasmic Prdx1 and mitochondrial Prdx3 and analyzed the total antioxidant capacity (TAC) 2h, 14h, 24h, and 72h after a single injection of a low dose of ketamine (3 mg kg⁻¹). Cytoplasmic Prdx1 protein levels were statistically significant downregulated at the 2h time point. Furthermore, the mitochondrial Prdx3 protein levels were reduced 72h after ketamine treatment (figure 25A). Ketamine not only downregulated levels of enzymes combating ROS, but also decreases the TAC 72h after a single injection (figure 25B).

Oxidative stress can lead to cellular damage as ROS radicals react with DNA, RNA, lipids, and also proteins⁴⁶⁰. Therefore, I continued to analyze ROS mediated damaged (carbonylated) protein levels by OxyBlot. Protein carbonylation can be caused by abatement in the antioxidant defense system, increased production of ROS during standard metabolic processes, failure to remove oxidized proteins e.g. by the proteasome, or an increased vulnerability to oxidative attack^{461, 462}. The results indicate that ketamine has an influence on protein carbonylation leading to statistically significant level reductions 72h after ketamine treatment (figure 25C)⁴⁶³.

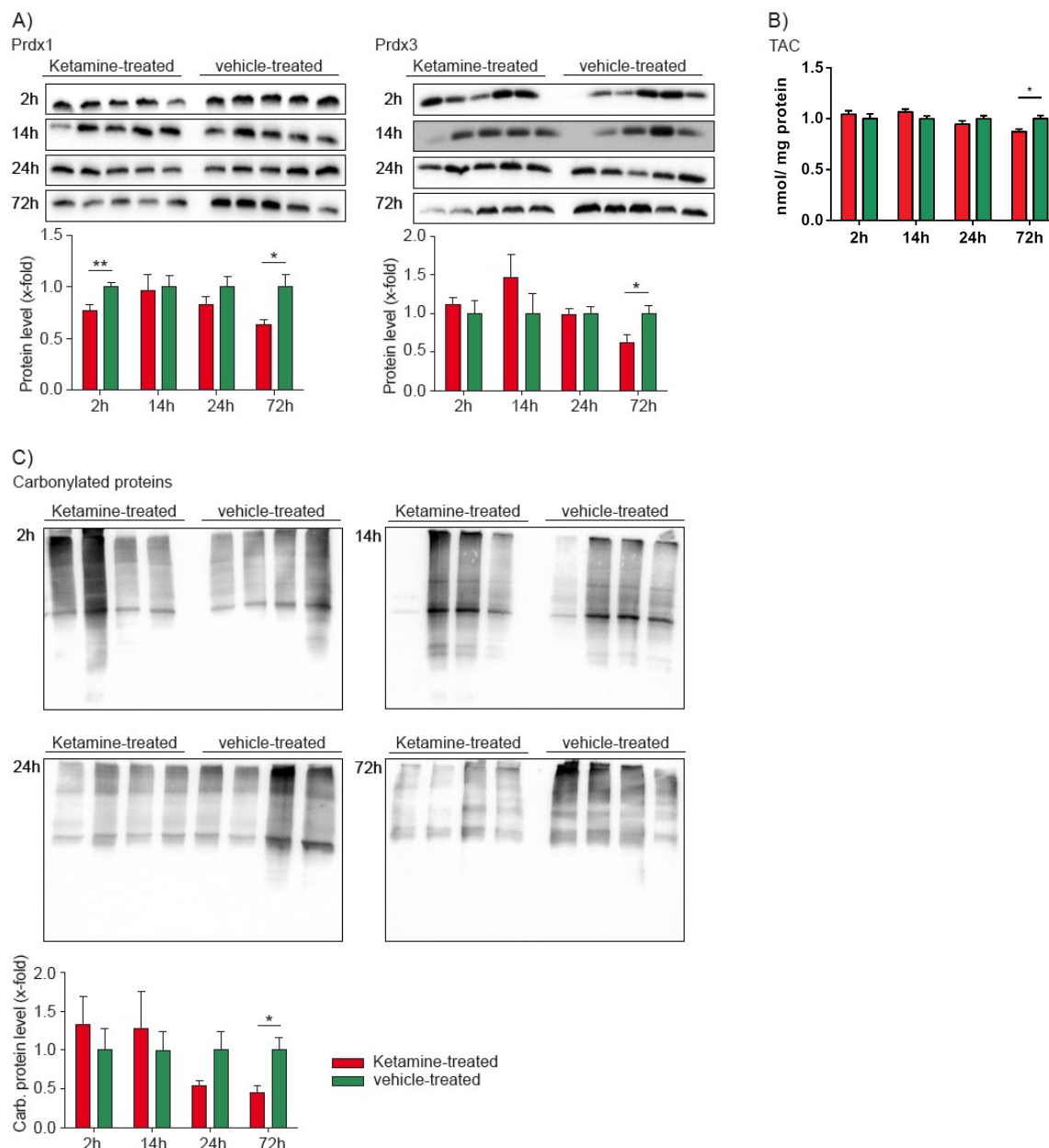


Figure 25: Hippocampal protein level analyses after a single injection of a low dose of ketamine (3 mg kg⁻¹). **A)** Time-dependent Western blot analysis of Prdx1 and Prdx3. N=5 mice per group and time point. **B)** TAC analyses to determine the antioxidant capacity of the HPC. N=5 mice per group and time point. **C)** OxyBlot analysis of the time-dependent protein damage by protein carbonylation in the HPC after ketamine treatment. N=4 mice per group and time point⁴⁶³. The results from ketamine-treated animals are normalized to the ones obtained from vehicle treatment (mean value = 1). *p<0.05, **p<0.01. P-values were determined by Student's t-test. Error bars represent s.e.m.

The pathway enrichment analyses also revealed an involvement of the proteasome at the 72h time point (table 11). The proteasome is a multicatalytic proteinase complex which is characterized by its ability to cleave unneeded or damaged proteins. The addition of ubiquitin to a substrate protein is called ubiquitination or ubiquitylation. Ubiquitination can affect proteins in many ways: it can signal for their degradation via the proteasome, alter their cellular location, affect their activity, or promote or prevent protein interactions^{461, 462}.

The quantitative proteomics profiling analyses revealed that ketamine statistically significant decreased Ubiquitin carboxyl-terminal hydrolase 8 (Otub1), Ubiquitin-conjugating enzyme E2 H (Ube2h) and Ubiquitin carboxyl-terminal hydrolase isozyme (Uchl3) as well as 26S proteasome subunit beta type-7 (Psmb7) protein levels at the 2h time point (figure 26A and 26B).

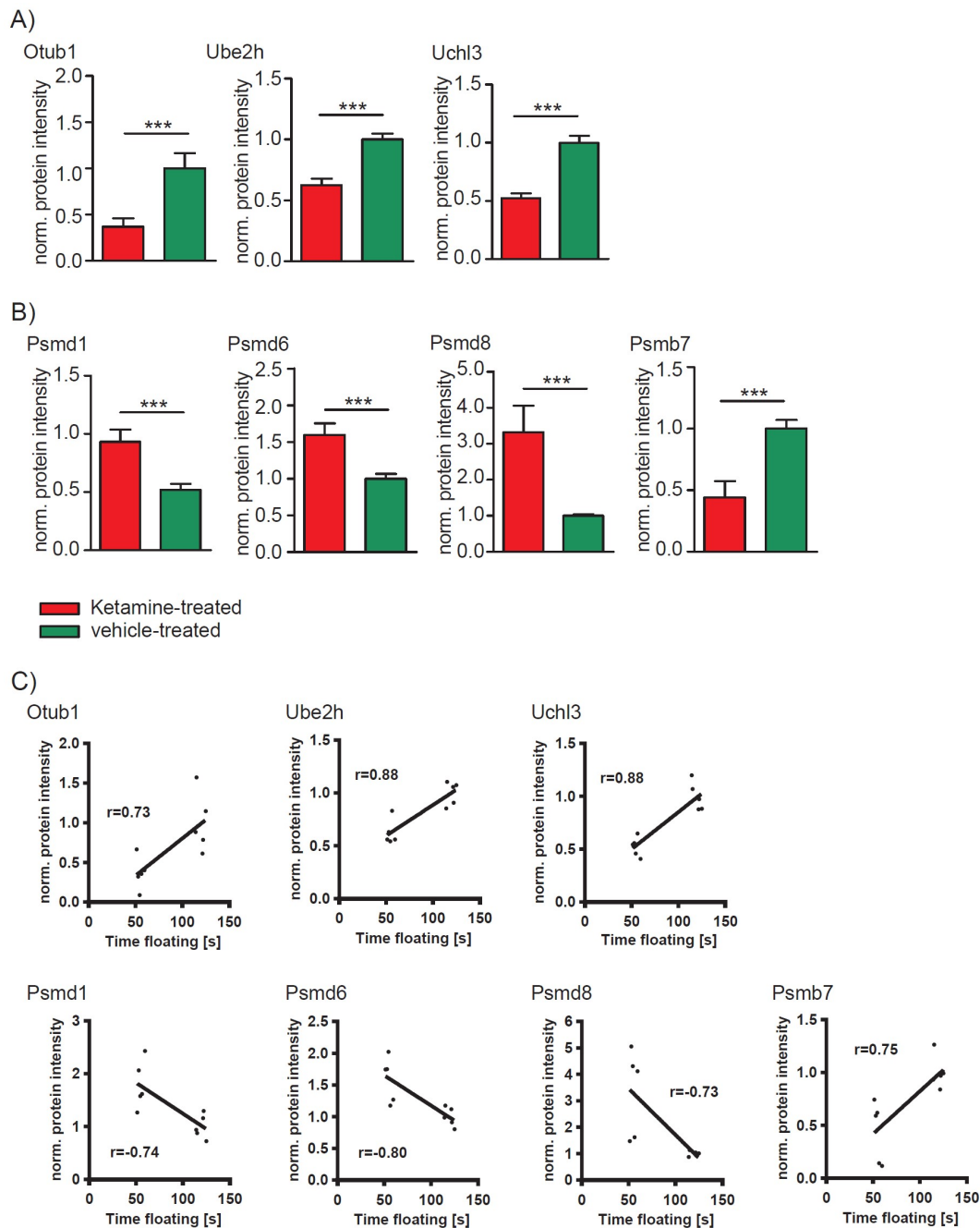


Figure 26: Hippocampal protein level analyses of the ubiquitin and proteasome systems determined by quantitative proteomics profiling analyses 2h after a single injection of a low dose of ketamine (3 mg kg⁻¹) of (A) Ubiquitin carboxyl-terminal hydrolase 8 (Otub1), Ubiquitin-conjugating enzyme E2 H (Ube2h), Ubiquitin carboxyl-terminal hydrolase isozyme (Uchl3), (B) 26S proteasome non-ATPase regulatory subunit 1 (Psm1), 26S proteasome non-ATPase regulatory subunit 6 (Psm6), 26S proteasome non-ATPase regulatory subunit 8 (Psm8) and 26S proteasome subunit beta type-7 (Psm7) protein levels. (C) Correlation analyses of Otub1, Ube2h, Uchl3, Psm1, Psm8 and Psm7 protein intensities with the FST floating time 2h after a single injection of ketamine ($p \leq 0.05$). The results from ketamine-treated animals are normalized to the ones obtained from vehicle treatment (mean value = 1). N=5 mice per group and time point. *** $p \leq 0.001$. P-values were determined by Student's t-test and SAM. Error bars represent s.e.m. The correlation coefficient, r , was calculated by Pearson. The linear regression line is only shown for significant ($p \leq 0.05$) correlation coefficients.

In contrast, the 26S proteasome non-ATPase regulatory subunit 1 (Psm1), 26S proteasome non-ATPase regulatory subunit 6 (Psm6) and 26S proteasome non-ATPase regulatory subunit 8 (Psm8) protein levels are statistically significant up-regulated 2h after a single injection of ketamine (table 10 and figure 26B). Furthermore, Otub1, Ube2h, Uchl3, Psm1, Psm6, Psm8 and Psm7 protein intensities significantly correlated with the antidepressant-like FST floating behavior (figure 26C).

Otub1 is a hydrolase that can remove conjugated ubiquitin from proteins and therefore plays an important regulatory role at the level of protein turnover by preventing degradation⁴⁶⁴. Ube2h accepts ubiquitin and catalyzes its covalent attachment to other proteins⁴⁶⁵. Uchl3 is a deubiquitinating enzyme that controls levels of cellular ubiquitin through processing of ubiquitin precursors and ubiquitinated proteins^{466, 467}. Psmb7 of the proteasome has an ATP-dependent proteolytic activity. This unit is responsible for the trypsin-like activity of the proteasome. Psmd1, Psmd6, and Psmd8 are regulatory subunits of the proteasome⁴⁶⁸⁻⁴⁷³.

4.3.3 A potential signaling cascade for ketamine drug action

Next I focused on ketamine's cellular signaling cascade with regard to its effects on mitochondria. The Protein Kinase A (PKA) gets only activated in the presence of cyclic adenosine 3',5'-monophosphate (cAMP).

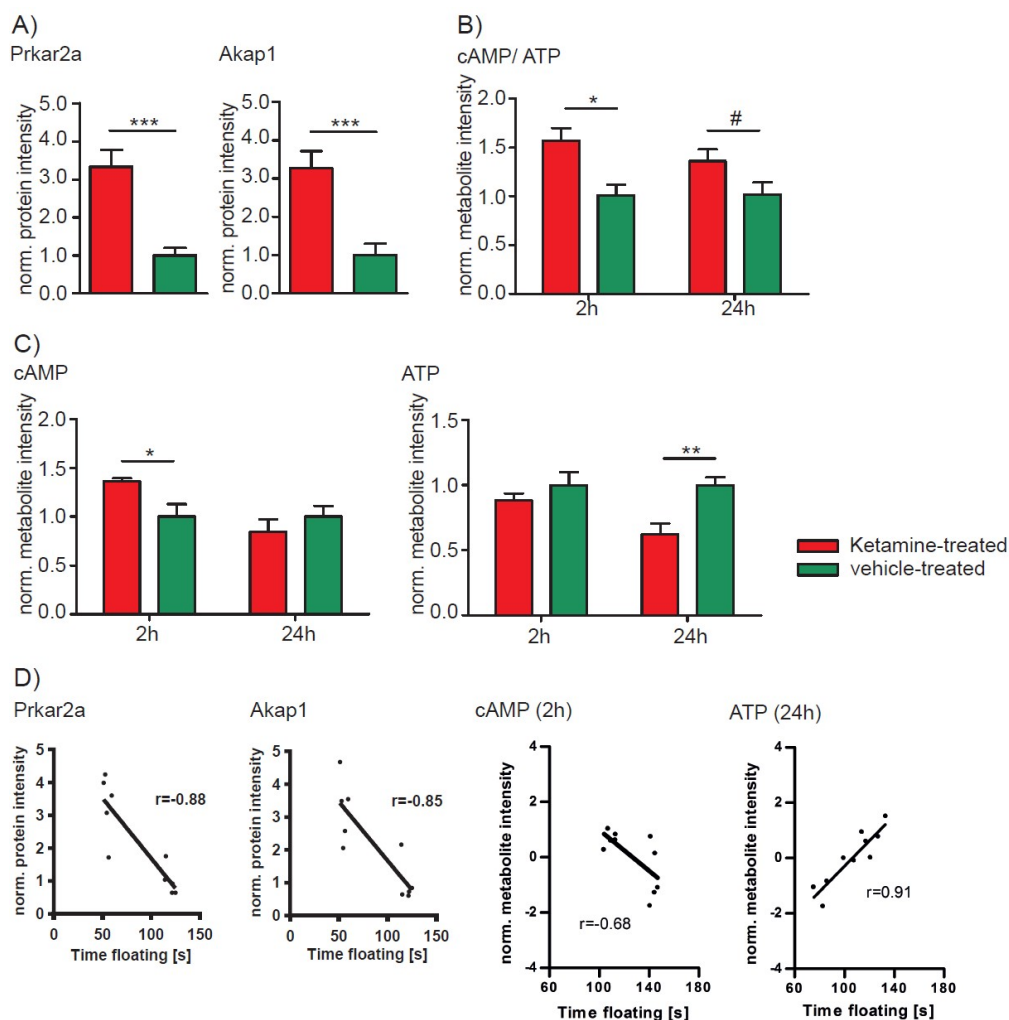


Figure 27: Hippocampal protein and metabolite level as well as metabolite ratio analyses 2h and 24h after a single injection of a low dose of ketamine (3 mg kg⁻¹). **A)** PKA and AKAP1 protein level alterations were determined by quantitative proteomics analyses. **B)** cAMP/ATP metabolite ratio analyses. **C)** cAMP and ATP metabolite level analyses. **D)** Correlation analyses of Prkar2a (2h, p<0.05), Akap1 (2h, p<0.05), cAMP (2h, p<0.05) and ATP (24h, p<0.05) protein and metabolite intensities with the antidepressant-like FST floating behaviour. The results from ketamine-treated animals are normalized to the ones obtained from vehicle treatment (mean value = 1). N=5 mice per group and time point. #p<0.10, *p<0.05, **p<0.01, ***p<0.001. P-values were determined by Student's t-test and SAM. Error bars represent s.e.m. The correlation coefficient, r, was calculated by Pearson. The linear regression line is only shown for significant (p<0.05) correlation coefficients.

Both have previously been described to play a role in MDD pathobiology. cAMP is catalyzed by Adenylyl cyclases converting ATP to cAMP^{112, 474}. The regulatory subunit II of PKA (Prkar2a) binds to A-kinase anchor protein 1 (AKAP1) that tethers the PKA to mitochondria. Thereby AKAP1 allows to specifically targets substrates regulated by PKA phosphorylation to the mitochondria⁴⁷⁵⁻⁴⁷⁷. The proteomics data showed that Prkar2a and AKAP1 are statistically significant upregulated and correlated with the antidepressant-like FST floating behavior 2h after a single injection of ketamine (figure 27A and 27D). I further analyzed the metabolite ratios and levels connected to PKA activity. Ketamine treatment statistically significant elevates or tends to increase cAMP/ATP metabolite ratios at the 2h and 24h time points, respectively (table 10 and figure 27B). cAMP metabolite levels were statistically up-regulated and correlated with the FST floating time at the 2h time point, whereas ATP metabolite levels were downregulated and also correlated with the FST floating time 24h after ketamine injection (figure 27C and 27D).

4.4 Analyses of mitochondrial OXPHOS protein complexes with blue native-polyacrylamide gel electrophoresis (BN-PAGE)

The metabolome and proteome profiling analyses revealed that ketamine has an impact on mitochondrial energy metabolism pathways including glycolysis, citrate cycle, and the OXPHOS. A time-dependent increase of the mitochondrial OXPHOS protein complexes I and II were observed. Ketamine might time-dependently increase the enzymatic activity of the OXPHOS protein complexes in order to cope with a possible higher energy demand at activated synapses. In order to test this hypothesis several methods first had to be established:

- Enrichment and isolation of mitochondria and solubilization of native mitochondrial membrane protein complexes
- Separation of native mitochondrial membrane protein complexes with BN-PAGE
- In-gel enzymatic activity measurement of the OXPHOS protein complexes

4.4.1 Isolation of mitochondria

Mitochondria from brain tissue were enriched in order to analyze the enzymatic activity of the OXPHOS protein complexes. Mitochondria were then fractionated and isolated through gradient centrifugation containing 20%, 36%, and 50% sucrose. After the centrifugation 3 fractions were visible with the third expected to contain mitochondria (figure 28A). The fractions were collected, resolved and a Western blot was performed to verify the mitochondrial fraction. All obtained fractions from the sucrose gradient centrifugation as well as a cytoplasmic protein fraction as a control were analyzed with antibodies against a mitochondrial membrane marker (porin), a mitochondrial matrix marker (Prdx3), and a cytoplasmic marker (β -actin). The results of the Western blots revealed that fraction 1 and the cytoplasmic protein fraction contain β -Actin but almost no mitochondrial proteins. Fraction 2 contains mitochondrial proteins, but also β -Actin. Fraction 3 contains almost no β -Actin, but shows the highest concentration of the mitochondrial marker proteins (figure 28B). Therefore, fraction 3 was used for further analyses⁴⁷⁸.

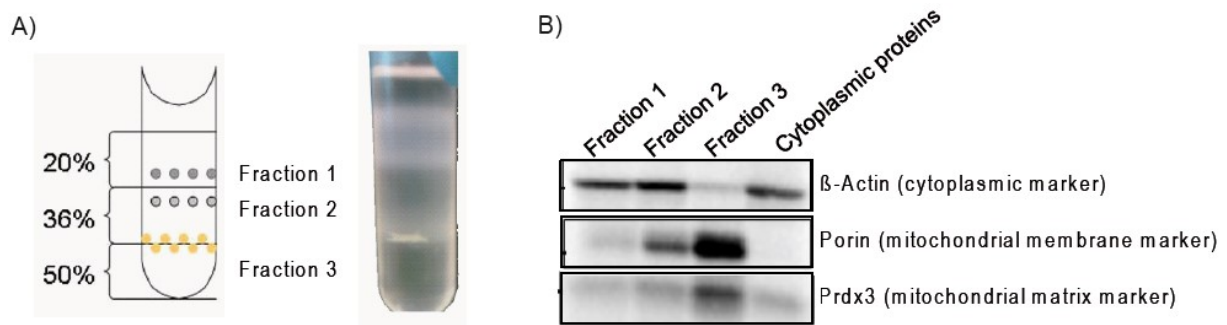


Figure 28: Isolation of mitochondria. **A)** Fractionation of enriched mitochondria through gradient centrifugation with 20%, 36% and 50% sucrose. Schematic and original picture of the three fractions revealed by sucrose gradient centrifugation. **B)** Western blot determination of the different fractions from the sucrose gradient centrifugation as well as from the cytoplasmic fraction as a control with antibodies against a mitochondrial membrane marker (Anti-porin), mitochondrial matrix marker (Anti-Prdx3), and a cytoplasmic marker (Anti-β-actin)⁴⁷⁸.

4.4.2 Separation and identification of the OXPHOS protein complexes with BN-PAGE and LC-MS/MS analyses

OXPHOS protein complexes can be separated with BN-PAGE. This method allows a separation of protein complexes in their native and functional form.

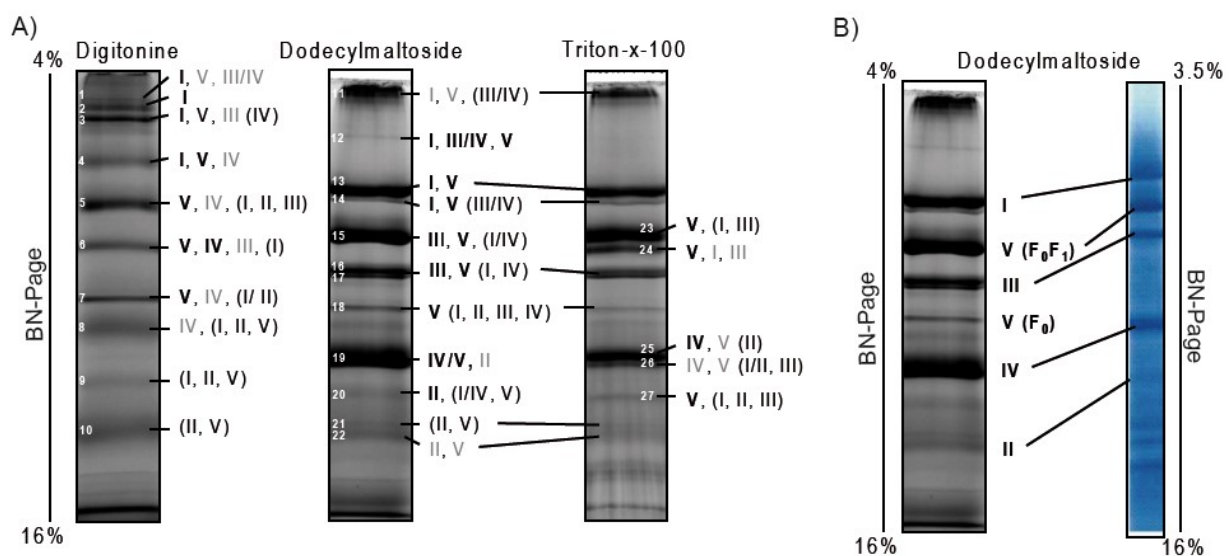


Figure 29: BN-PAGE separating mitochondrial membrane protein complexes solubilized with Digitonine, DDM and TX-100. **A)** Separation of mitochondrial membrane protein complexes that were previously solubilized with Digitonine, DDM or TX-100. OXPHOS protein complexes were identified by LC-MS/MS analyses. Bold: Protein complex with most of the subunits identified. Grey: ~8 subunits of a complex were identified. In parentheses: ≤5 subunits of a complex identified. **B)** OXPHOS protein complexes and bands used for further enzymatic in-gel activity measurements and comparison with already published BN-PAGE from Wittig et al^{478, 479}.

However, mitochondrial protein complexes first have to be solubilized from the membrane. Therefore, three different mild detergents were tested: Digitonine, Dodecylmaltoside (DDM), and Triton-x-100. The solubilized mitochondrial membrane protein complexes were then separated by BN-PAGE and mitochondrial OXPHOS protein complexes identified with LC-MS/MS-analyses (figure 29A). DDM and Triton-x-100 showed a very similar band pattern in contrast to the milder detergent Digitonine (figure 29A). There is a very clear separation and no double bands are visible with digitonine solubilization compared to DDM and Triton-x-100 (figure 29A).

The OXPHOS protein complexes were identified by LC-MS/MS-analyses and showed very similar results when comparing the bands from the three solubilizations. Furthermore, the band pattern is similar to the one published by Wittig and colleagues (figure 29B)^{478 479}.

Every band contained subunits of different mitochondrial OXPHOS protein complexes. However, the more subunits were identified the more abundant the protein complex. The upper bands 1–3, 4, 12, 13/14 mainly contained subunits of complex I and V. Bands 5, 15, 23 and 24 mainly consist of complex V subunits, but also complexes III and IV subunits and less of complex I and II. Bands 6 and 16/17 had subunits of complexes III, IV and V. Bands 7 and 18 mainly contained complex V subunits and bands 8, 19 and 25/26 mainly complexes IV subunits and less complex V subunits. Furthermore, they also contained complex II subunits. The other bands (9, 20, 27, 10, and 21/22) mainly consist of subunits of the complex II and V (figure 29A).

The identification of different subunits of OXPHOS complexes might be due to the formation of so-called supercomplexes, a complex formation made up of different OXPHOS complexes. However, only the individual OXPHOS complexes and not the supercomplexes are of interest and, therefore, considered for further enzymatic OXPHOS protein complex in-gel activity measurements. The mitochondrial membrane OXPHOS protein complexes were solubilized with DDM for further enzymatic in-gel activity measurements. The bands with the most subunits of a specific complex were chosen for the in-gel enzymatic activity analyses. The related bands were cut out of the gel after BN-gel electrophoresis and the activity of the related OXPHOS complex was measured⁴⁷⁸.

4.4.3 OXPHOS protein complex in-gel-enzymatic activity measurement

The goal was to analyze the mitochondrial OXPHOS protein complex activity in ketamine- compared to vehicle-treated mice. However, the method first needed to be established. Different protein amounts of solubilized mitochondrial membrane protein complexes were separated by BN-PAGE and the enzymatic activity of each OXPHOS complex was measured inside the gel. Linearity of protein amount with Coomassie staining in the BN-gel and OXPHOS protein complex enzymatic activity was then determined with colored chemical substrate reaction (cf. chapter 3).

The optimal fitting curves to all measurements were linear, except for complex V (F_1) where an exponential fit was used. The regression R^2 values all indicate very good fits with values ranging from 0.95 to 0.98 for the Coomassie-stained proteins of the BN-gel and from 0.91 to 0.97 for the enzymatic activity measurements of the ETC complexes, with the exception of the ETC complex activity of the F_1F_0 holo-enzyme (figure 30) where only $R^2=0.62$ was reached. The enzymatic activity of complex II could not be determined⁴⁷⁸.

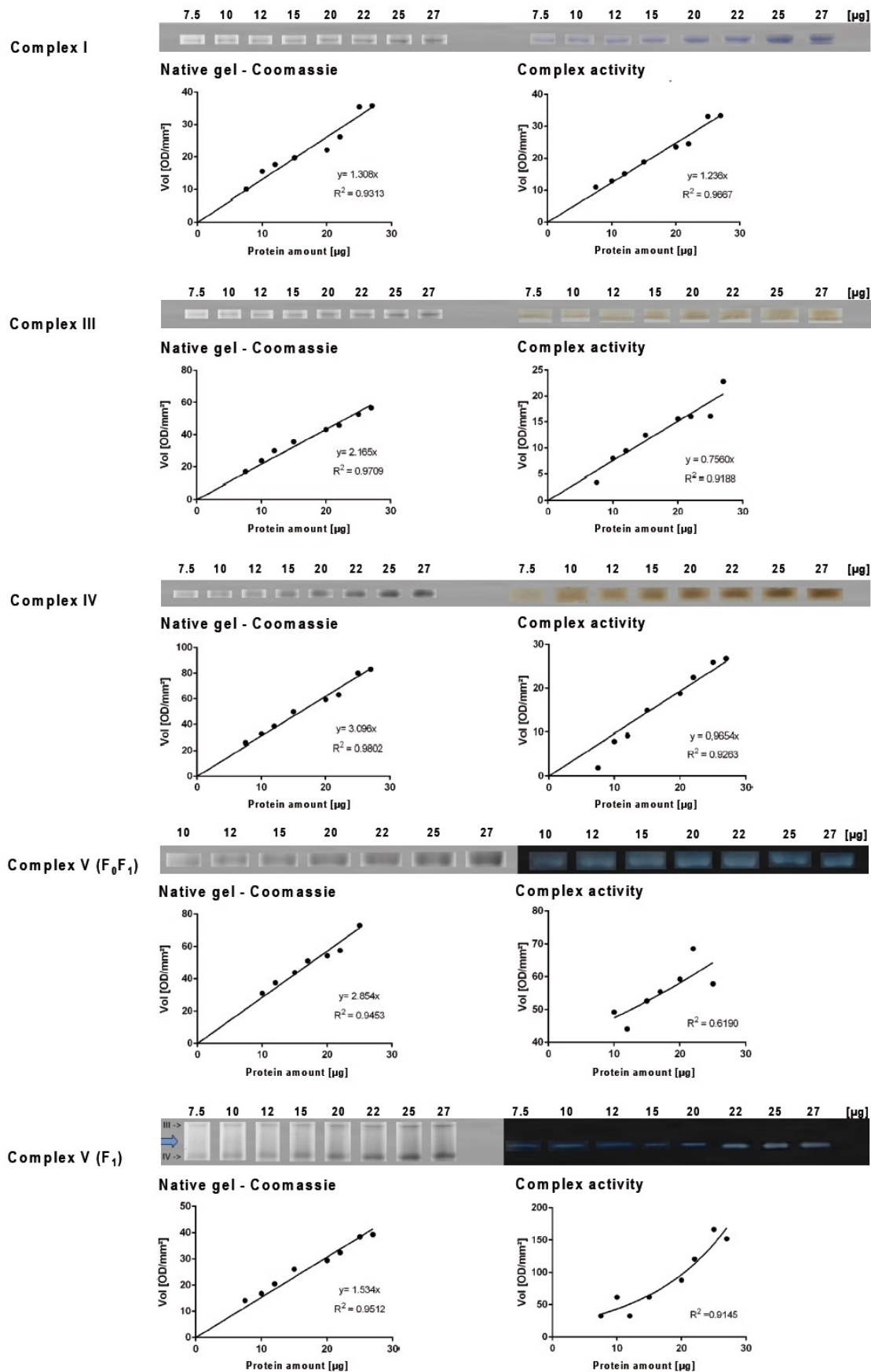


Figure 30: Linearity analyses of the OXPHOS protein complex enzymatic activity measurements. Different amounts of mitochondrial membrane protein complexes were separated with BN-PAGE and the enzymatic activity of each OXPHOS protein complex was measured. The protein amount of the OXPHOS complexes I to V (F_0F_1 and F_1) and their enzymatic activity were determined by the Coomassie-stained proteins and chemical reactions, respectively, as described in chapter 3. The R^2 of the regression was calculated for all analyses⁴⁷⁸.

Next, the OXPHOS complex enzymatic activity of ketamine- and vehicle-treated mouse brains was measured using 12µg of mitochondrial proteins. There were no statistically significant differences in OXPHOS protein complex activity comparing ketamine- with vehicle-treated mice (figure 31)⁴⁷⁸.

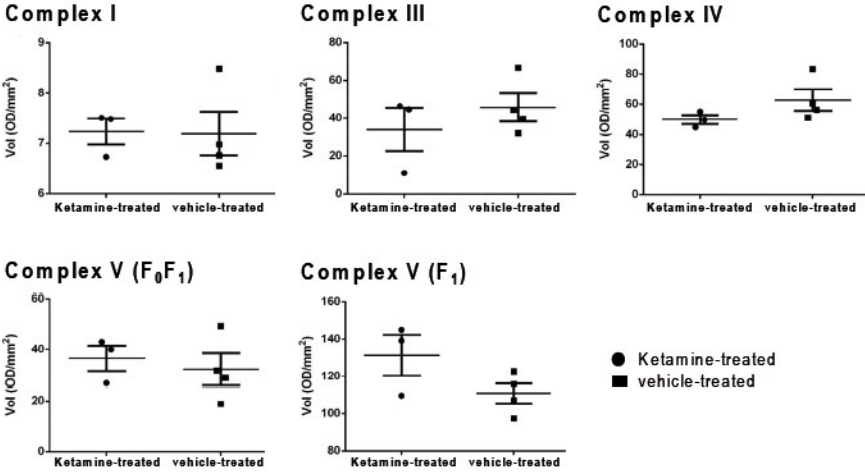


Figure 31: In-gel enzymatic activity measurements of the mitochondrial OXPHOS protein complexes by BN-PAGE. The enzymatic activity of the complexes I–V (except complex II) were analyzed comparing ketamine- (3 mg kg⁻¹, n=3) and vehicle-treated (n=4) mice⁴⁷⁸.

5.0 Discussion

MDD is a devastating psychiatric disorder with approximately 350 million people suffering worldwide. Conventional treatment options include ADs that take 2 to 4 weeks until a therapeutic effect becomes apparent⁸. Unfortunately, approximately one third of the patients does not respond to conventional AD treatment and thus suffer from TRD. To date, ketamine is the only fast-acting medication used in the clinic being effective between 2h and 4h – especially for patients suffering from TRD (cf. chapter 1). Research on biomolecular mechanisms involved in ketamine's fast antidepressant effect mainly focuses on synaptic plasticity, which seems to be induced through mTORC1 and BDNF (cf. chapter 1). However, the exact mechanisms still remain elusive. In order to understand the biomolecular pathways and cellular mechanism underlying ketamine's mode of action as well as to aid at developing fast acting ADs, time-dependent metabolomics and proteomics profiling analyses and treatment response biomarker discovery were performed. Furthermore, I focused on several pathways that were significantly enriched in my –omics data, especially mitochondrial energy metabolism. To the best of my knowledge, this is the first study that identifies metabolome and proteome alterations, affected pathways and biomarker candidates for the ketamine treatment response in mice.

In humans, ketamine is used as an antidepressant by injecting 0.5 mg kg⁻¹, whereas anesthesia is already introduced by 1-5 mg kg⁻¹ ^{251, 480, 481}. In contrast, mice are anaesthetized with doses of 50-200 mg kg⁻¹ of ketamine^{482, 483}. In addition, ketamine is not only used to study the fast antidepressant-like effects in mice, but also as an animal model for schizophrenia thereby already analyzing the effects of 6 mg kg⁻¹ of ketamine²⁵⁴⁻²⁵⁷. In the present study, a low dose of 3 mg kg⁻¹ of ketamine was used as described in Autry et al., in contrast to other researchers mostly treating mice with 10 mg kg⁻¹ of ketamine (cf. chapter 1).

5.1 Ketamine's fast antidepressant-like effects

The first part of the thesis is focused on the time-dependent antidepressant-like effect of a low-dose of ketamine (3 mg kg⁻¹). The FST revealed time-dependent antidepressant-like effects, starting already after 2h and lasting up to 72h, thereby reflecting the fast antidepressant-like effect of the drug. The FST is the most widely used behavioral test and highly reliable for predicting the therapeutic potential of a compound. No other behavioral assays were performed since they might affect the animals' metabolome and proteome and skew the data. However, repeating this study with an animal model of depression would add further relevance to the human situation. For further –omics and validation analyses 3 to 5 mice were chosen around the FST mean behavior, especially not considering behavioral extremes in order to analyze ketamine's general biomolecular effects in mice.

5.2 A comparative metabolomics profiling analyses

The second part of my thesis focused on metabolomics profiling analyses of different mouse tissues, BP and PHN. Metabolomics provides an analytical tool for the identification of pathway alterations and drug targets.

Ketamine had a statistically significant metabolomic effect on the liver, PHNs and the HPC, but not the CRBL, BP and most surprisingly not the PFC. In addition, the results obtained from the profiling analyses of the liver and the CRBL can also be considered as an evidence for the methodical validity of metabolomics study. Ketamine is degraded in the liver. Therefore, metabolite changes were to be expected. In contrast, and in line with the results obtained in this present study, no drug effects were expected in the CRBL as this brain region does not seem to play a significant role in MDD.

Biomarkers are useful in drug development efforts by providing information of a biological state or drug effect. Drug development would benefit from biomarkers or a biosignature of ketamine to predict a treatment effect for newly developed ADs. Biomarker discovery favors BP as it is easy to obtain. Unfortunately, my metabolomics profiling analyses did not reveal any statistical significant alterations in the BP. Repeating this study with a mouse model of depression would probably be more effective for a biomarker discovery in the BP. Stress *per se* already causes many biomolecular alterations that are reflected in the blood and could be reversed by AD treatment (cf. chapter 1) and thus might also generate biomarkers for ketamine's antidepressant-like effects.

Mouse PHN also showed significant metabolome alterations. In order to verify the best ketamine concentration used for PHN treatment and subsequent metabolomics profiling analysis, different ketamine concentrations were first tested by the MTT assay. This assay is a toxicity test measuring the metabolic activity of the cells and therefore indirectly cellular viability. In general, ketamine treatment in PHNs exhibits three different stages with increasing concentrations of the drug. At first, the metabolic activity drops, then increases again and finally drops again until nearly all cells show no cellular activity. Ketamine's mode of action is dose-dependent at high doses resulting in apoptosis. Metabolomics results obtained from ketamine treatment of PHN were in line with findings observed in the HPC that will be described below. In both analyses – the PHN and HPC metabolomics profiling – the alanine, aspartate and glutamate metabolism was overrepresented. However, carbamoylphosphate and deoxyglucose-6 phosphate which were significantly altered in PHN and HPC showed different FCs. This difference could be explained due to the fact that ketamine might also affect NMDARs at glial cells including astrocytes, oligodendrocytes and microglia⁴⁸⁴. In addition, ketamine's drug effect might also be dependent on the presence of a complete neuronal network as present in the brain.

The PFC is discussed to play a significant role in MDD development, conventional AD treatment effects and also ketamine's fast antidepressant mode of action (cf. chapter 1). Several reasons might explain why in this study ketamine did not show significant PFC metabolomics alterations: The PFC is a brain region responsible for goal-directed behavior which involves action planning and executive functions. The amygdala plays a primary role in the processing of memory, decision-making, and emotional reactions, which is believed to be important for MDD development. The PFC regulates the emotional reactions of the amygdala, a process which is perturbed in patients suffering from MDD. Several lines of evidence points to a PFC, HPC volume decline and amygdala volume increase in a subset of depressed patients due to stressful life events. In rodents, stress leads to neuronal atrophy of the PFC and HPC, whereas the amygdala shows an increase in synaptic plasticity^{24, 25, 30, 35-45, 208, 485, 486}. Therefore, the PFC's regulatory role over the amygdala's emotional reactions is inhibited, most probably leading to the MDD symptoms in humans. ADs as well as ketamine seem to reverse neuronal atrophy (cf. chapter 1). In the present thesis, non-stressed mice were treated with ketamine. Therefore, no dysregulation of the PFC or amygdala was caused by stress and could be reversed by the drug. Although ketamine should also block NMDARs in the PFC and therefore observable biomolecular alterations might have occurred in less than 2h after ketamine treatment¹⁷⁹. This could also be a reason why no statistically significant metabolome changes were found.

5.3 Time-dependent hippocampal metabolomics and proteomics profiling analyses

The most interesting results were obtained by the time-dependent metabolomics and proteomics profiling analyses of the HPC. The following discussion will focus on the results obtained from the HPC analyses. They not only showed a very good time-dependent separation of ketamine- and vehicle-treated mice with a good quality assessment of the PLS-DA, but also many statistically significant metabolite and protein level and metabolite ratio alterations as well as overrepresented pathways. In addition, PLS-DA and VIP-score analyses obtained by the metabolomics analyses revealed that 2-Keto-isovalerate, maleate and fumarate qualified as antidepressant treatment response biomarkers. They could be used for the development of alternative faster acting ADs with a similar mode of action as ketamine, however, with fewer side effects.

5.3.1 Ketamine's impact on the mitochondrial energy metabolism

The HPC metabolomics profiling analyses indicate statistically significant metabolite level and metabolite ratio changes that are part of several pathways including citrate cycle and glycolysis. Mitochondrial abnormalities including alterations in energy metabolism have previously been implicated in the pathobiology of affective disorders⁴³²⁻⁴³⁴. Several metabolite level and metabolite ratio changes of the citrate cycle and glycolysis were observed already 2h and 14h after ketamine treatment, thereby reflecting the fast antidepressant-like effect of the drug. Moreover, it is interesting to note, that the citrate cycle and glycolysis are connected pathways ultimately producing energy in form of ATP through the OXPHOS. Glycolysis is a major catabolic cytoplasmic pathway where glucose is degraded to pyruvate, which is further metabolized by pyruvate dehydrogenase complex to Acetyl-CoA that enters the citrate cycle. The latter is a mitochondrial matrix pathway that is coupled to the mitochondrial OXPHOS⁴³⁵. Almost all metabolites of the glycolytic pathway showed lower levels 14h after ketamine injection, with the exception of 3-phosphoglycerate and phosphoenolpyruvate that were upregulated at the 2h time point. The observed changes might be caused by an inhibitory feedback mechanism of the citrate cycle probably observable by the metabolite ratio changes of the citrate cycle and glycolysis pathway thereby indicating altered enzyme activities or protein expression⁴³⁵. Whereas in the present study reduced metabolite levels of the glycolysis pathway after ketamine treatment were found, a previous study has shown an elevation of glycolytic metabolites following SSRI treatment, suggesting that the two drug types have very different modes of action⁴³². In line with this hypothesis is the observation that neither conventional ADs such as imipramine and fluoxetine acutely or chronically administered nor electroconvulsive shock activate mTORC1. Moreover, it was observed that the SSRI sertraline inhibits mTORC1¹⁷⁹. All these findings might explain the delayed onset of conventional ADs and the opposite findings with regard to pathway activity between conventional ADs and ketamine.

The connecting metabolites of the citrate cycle to the OXPHOS, succinate and fumarate, as well as the metabolite ratio of succinate/fumarate showed statistically significant differences and the metabolites strongly correlated with the antidepressant-like FST floating behavior. Metabolite ratio changes might indicate protein level changes of the OXPHOS enzymatic subunit SDHA of the complex II transforming these metabolites⁴³⁶. As expected SDHA protein levels were indeed upregulated 14h and 24h after a single injection of ketamine. In addition, the correlated metabolites, succinate and fumarate, as well as the observed upregulated SDHA protein levels led to the hypothesis that the

mitochondrial energy metabolism plays an important role in transducing the antidepressant-like effect of ketamine.

The energy equivalents GTP and NADH are produced through the citrate cycle and ATP via the connected OXPHOS pathway. GTP is generated during the transformation of succinate-CoA to succinate⁴³⁵. Statistically significant higher levels of succinate were observed after ketamine treatment possibly resulting in the observed elevated GTP levels at the same time point which are also well correlated with the FST floating time. Mitochondria are usually bound to microtubules of axons and dendrites. Ca^{2+} rises after synaptic activation at excitatory glutamatergic neurons and separates the mitochondria from the microtubule. The mitochondrial separation from microtubules is required to enrich these organelles in the synaptic density in order to increase ATP levels at the activated synapses. Furthermore, pyruvate dehydrogenase, isocitrate dehydrogenase, a citrate cycle enzyme, and the complex II of the OXPHOS are also regulated by Ca^{2+} ^{453, 475, 487, 488}. Ketamine's increased influx of Ca^{2+} at activated synapses also results in an uptake into the mitochondria, which ultimately could be the cause for the here observed metabolite level, metabolite ratio and protein level alterations. Decreased isocitrate/alpha-Ketoglutarate and succinate/fumarate ratios as well as increased OXPHOS complex II SDHA and SDHB protein levels further support this hypothesis. In addition, the correlation of succinate, fumarate and GTP with the behavioral effects measured by the FST sets the observed metabolite changes in a relation with ketamine's antidepressant-like effects.

Ketamine was shown to phosphorylate and therefore activate mTORC1 which not only leads to increased synthesis of synaptic proteins, but also increased mitochondrial metabolism^{176, 177, 179}. This study describes an involvement of the mitochondrial energy metabolism, especially the OXPHOS that is most probably upregulated in order to generate energy in form of ATP to compensate for the higher energy demand at activated synapses. My metabolomics and proteomics profiling as well as further Western blot analyses results support this assumption. Ketamine treatment affects the OXPHOS pathway and several ETC complex protein levels including complex I Ndufv2, Cyc1 and Tmem126B were time-dependently altered and also correlated with the FST floating time. Further Western Blot analyses revealed that complex II SDHA and SDHB and complex III Uqcrc2 are time-dependently upregulated, too. In addition, also ADP levels were downregulated and significantly correlated with the FST behavior 24h after a single injection of ketamine as well as the ATP/ADP ratio tended to be lower at the 2h and 24h time points. Presumably more ATP is consumed than can be produced from ADP at the OXPHOS complex V, most probably because of the high energy demand at activated synapses. An increase of OXPHOS complex protein levels should result in increased ATP levels and indeed the at first lowered ATP levels turned back to the same FC observed for vehicle-treated animals at the 72h time point.

Furthermore, results from previous studies have shown that treatment with ADs alters ATP levels. Phosphorous-31 magnetic resonance spectroscopy data have shown decreased NPT levels (mainly ATP) in the brain of depressed patients. Another magnetic resonance spectroscopy study could demonstrate lower NPT levels (mainly ATP) in fluoxetine responders compared with non-responders^{489, 490}. These inconsistent findings make it difficult to know whether the observations of decreased ATP levels contribute to the ketamine antidepressant-like effect. However, the correlation analyses of ATP and ADP also create a relation of the drug treatment and the herein before mentioned observed antidepressant-like effects of ketamine.

A low ATP/ADP ratio activates and phosphorylates the AMPK (pAMPK), the major energy sensor of the cell. pAMPK decreases and increases the activity of pathways that consume a lot of energy (anabolic pathways) and produce energy (catabolic pathways), respectively⁴⁴³⁻⁴⁴⁹. Previous data from a study in rats suggested that ketamine's antidepressant-like effects are mediated by an increased

anabolic rate, thereby inducing cell growth and differentiation¹⁷⁹. An elevated anabolism seems to come along with a higher energy demand, which I assume is the case during the first 24h after ketamine treatment. As expected, the pAMPK/AMPK ratio is elevated while ATP levels and ATP/ADP ratio are lower at the 24h time point. pAMPK activates mitochondrial biogenesis through PGC1 α , inhibits mTORC1 and thereby decreases mitochondrial metabolism, promotes autophagy and glucose uptake^{174, 491-495}. As expected, no mitochondrial changes apparent by altered metabolite levels, ratios and protein levels are observed 72h after a single injection of ketamine. Furthermore, the PLS-DA quality criteria for the 72h time point indicated a weak model and all changes observed related to glycolysis, citrate cycle and OXPHOS returned to normal levels. I conclude that the first 24h after ketamine treatment is an important time window that is critical for the fast antidepressant-like effects. However, ketamine's behavioral effect during the FST is still present at the 72h time point. In this regard Autry et al. showed antidepressant-like effects lasting up to 1 week after a single injection of ketamine²⁴³. Therefore, I would propose that ketamine's mode of action could probably be divided into an acute and a more sustained effect inducing and stabilizing synaptic plasticity, respectively. The acute effect might be dependent on the activation of mTORC1, BDNF, synaptic protein synthesis and mitochondrial energy metabolism.

An increase of the pAMPK/AMPK ratio led to the assumption that mitochondrial biogenesis is induced by PGC1 α activation. Tfam, a mitochondrial transcription factor, is translated upon PGC1 α activation. Further nuclear encoded mitochondrial proteins are then imported into the mitochondria by import proteins including TIM23. Activation of mTORC1, but also AMPK, results in the relocation of PGC1 α from the cytoplasm into the nucleus^{173, 174, 495}. Ketamine activates mTORC1 within the first 30min of treatment¹⁷⁹ whereas my results show an activation of AMPK at the 24h time point. Therefore, and as expected, Western blot analyses showed alterations of PGC1 α protein levels at the 2h and 24h time points. However, the method used in the present study only isolates cytoplasmic proteins and not proteins from the nucleus (cf. chapter 3). This could explain the decreased PGC1 α protein levels. Ketamine might lead to the translocation of PGC1 α into the nucleus. Further studies analyzing the nuclear protein fraction upon ketamine treatment for PGC1 α would elucidate this research question. Tfam protein levels were decreased at the 72h time point after a single injection of ketamine.

Probably, earlier measurements as in this study as well as during the 24h and 72h time point would result in a more detailed understanding of ketamine's biomolecular effects at the mitochondrial biogenesis and metabolism regulation. Western blot analyses of TIM23 did not show any significant differences. Ketamine's effects on mitochondrial biogenesis, especially the transcription and import require further analyses at different time points.

5.3.2 Ketamine's effects on the antioxidant defense and quality control system

An increased protein expression and elevated activity of OXPHOS protein complexes may also lead to an elevated production of ROS. These radicals when at high levels may damage proteins, DNA and lipids and therefore result in oxidative stress. ROS are difficult to measure since oxygen radicals are highly reactive towards other molecules. One of the most popular indirect ROS assessments is protein damage, specifically the analysis of carbonylated (damaged) proteins (cf. chapter 3)⁴⁵⁵. Protein damage time-dependently decreases and is statistically significant reduced at the 72h time point. Either ROS levels decrease over time or the cellular defense system is activated. The cellular defense system includes antioxidant molecules and enzymes such as Prdxs that combat ROS. In

addition, a protein quality control system that degrades damaged proteins counteracts oxidative stress. The main function of the proteasome is to degrade damaged or unneeded proteins that are tagged for proteolysis by ubiquitin^{456-459, 462, 470}. The TAC and cytoplasmic Prdx1 levels were decreased at the 2h and 72h time points and mitochondrial Prdx3 levels 72h after a single injection of ketamine. Therefore, the antioxidant defense system might not be needed suggesting that ROS levels were not increased at any time point. However, the downregulated carbonylated protein levels might also be indicative of an increased activity of the protein quality control system. The proteomics profiling analyses revealed that the proteasome pathway was overrepresented 2h after ketamine treatment. However, the results are somewhat contradictory. Ketamine treatment significantly decreased Otub1, a hydrolase that can remove conjugated ubiquitin from proteins and therefore plays an important regulatory role at the level of protein turnover by preventing proteasomal degradation. Uchl3, a deubiquitinating enzyme that controls cellular ubiquitin levels through processing of ubiquitin precursors and ubiquitinated proteins is also decreased upon ketamine treatment. Furthermore, the 26S proteasome non-ATPase regulatory subunits Psmd1, Psmd6 and Psmd8 protein levels are significantly upregulated 2h after a single injection of ketamine. In contrast, Ube2h, that accepts ubiquitin and catalyzes its covalent attachment to proteins, as well as the proteasomal subunit Psmb7 protein levels were decreased at the 2h time point⁴⁶⁴⁻⁴⁷³. Moreover, these proteins showed a significant correlation with the FST floating time. The antioxidant defense system might not get activated since ROS levels were not elevated at any time point of ketamine treatment. In conclusion, ketamine treatment might lead to an increased degradation of damaged proteins and therefore in a decrease in protein damage, TAC as well as antioxidant Prdx1 and Prdx3 protein levels eventually resulting in an homeostatic redox adjustment which promotes the antidepressant-like effects of ketamine.

5.3.3 A potential novel signaling cascade for ketamine's antidepressant-like effects

The present study results suggest a mitochondrial impact of ketamine's mode of action. However, the downstream effect promoting mitochondrial metabolism might not only be through an activation of mTORC1, but also involves the regulatory subunit of PKA and Akap1. PKA has previously been shown to play a role in MDD and is required for hippocampal memory formation mediated by LTP. Multiple chemical neurotransmitters, hormones, and other signaling substances use cAMP as an intracellular second messenger through activation of G protein coupled receptors. The cAMP/PKA signaling pathway critically regulates molecular components underlying LTP and long-term memory. In the postsynaptic neuron PKA targets include NMDARs and AMPARs and the transcription factor CREB that has been implicated in BDNF synthesis⁴⁹⁶. PKA binds with its regulatory subunits to AKAPs and phosphorylates target proteins. The regulatory subunit Prkar2a of PKA binds to AKAP1, a protein that is found on the outer mitochondrial membrane^{238, 475, 476, 497-499}. Prkar2a and AKAP1 as well as cAMP/ATP ratio levels were elevated suggesting an increased activation of the PKA. Furthermore, Prkar2a, AKAP1, cAMP and ATP significantly correlated with the FST floating time. AKAP1 not only recruits PKA, but also mRNA, suggesting a role in supporting mitochondrial biosynthesis. Results from a previous study showed that overexpression of wild-type AKAP1 increased mitochondrial membrane potential, while expression of AKAP1ΔPKA reduced mitochondrial membrane potential below control levels. In conclusion, AKAP1/PKA play an important role in ATP synthesis as this process is dependent on a high mitochondrial membrane potential. PKA-dependent substrate phosphorylation due to increased cAMP levels can result in mitochondrial elongation as well as more efficient ATP

production. In addition, the AKAP1/PKA response protects mitochondria from degradation and support mitochondrial network integrity and neuronal survival^{475, 476, 500}. Therefore, I propose that during LTP, PKA not only targets NMDARs, AMPARs and CREB, but also mitochondria, thereby supporting energy supply resulting in the herein before mentioned antidepressant-like effects.

Besides PKA, CamKII and PKC are promoting downstream effects upon LTP and both proteins are activated by Ca^{2+} ^{144, 437}. In addition, CaMKII and PKC are involved in the insertion of additional AMPARs into the postsynaptic membrane. CaMKII alpha protein levels were slightly increased and tended to be decreased 24h and 72h after ketamine treatment. PKC protein levels tended to be increased at the 2h and 14h time points, whereas decreased levels were observed at 24h. Future studies should analyze the phosphorylation status of these proteins as they indicate their enzymatic activity.

5.3.4 Ketamine's effects on the glutamatergic and GABAergic system

Ketamine decreases GABA_AR1 levels and AMPAR subunit Gria3 and elevates AMPAR subunit Gria2 protein levels, changing AMPAR composition in favor of Gria2. Furthermore, the observed protein intensities also significantly correlated with the FST floating behavior. In the mammalian central nervous system, AMPA-type glutamate receptors mediate the vast majority of fast excitatory synaptic transmission. The AMPAR Gria2 subunit dictates the critical biophysical properties of the receptor, strongly influences receptor assembly and trafficking, and plays pivotal roles in a number of forms of long-term synaptic plasticity. Gria2 is a critical subunit for determining mammalian AMPAR function⁵⁰¹.

Homeostatic synaptic plasticity is distinct from input-specific Hebbian forms of synaptic plasticity such as LTP, and is most readily induced by chronically blocking neuronal activity or glutamatergic transmission in cultured neurons⁵⁰²⁻⁵⁰⁴. An increase in Gria1, but not Gria2, protein expression is observed in response to NMDAR activity blockade, and this appears to be primarily due to a selective increase in dendritic protein synthesis of the Gria1 subunit. 10 mg kg⁻¹ of ketamine also increased Gria1 as well as further synaptic protein levels, induced LTP and increased the spine number in the PFC of rats; thereby supporting the hypothesis that ketamine might be the cause of a homeostatic plasticity mechanism¹⁷⁹. On the other hand, Zanos et al. recently has shown that 10 mg kg⁻¹ of ketamine increased Gria1 and Gria2 protein levels in the HPC, but not in the PFC²⁶². The results of the present study in which an even lower dose of ketamine (3 mg kg⁻¹) was used, showed an elevation of AMPAR Gria2 subunit protein levels, thereby favoring the most popular hypothesis of ketamine drug action, the input-specific Hebbian forms of plasticity such as LTP.

In summary, it seems that a low dose of 3 mg kg⁻¹ of ketamine more likely blocks NMDARs on GABAergic inhibitory neurons thereby resulting in an increased activation of glutamatergic excitatory neurons promoting LTP (cf. chapter 1). In addition, the lower GABA_AR1 protein levels might thereby further decrease the inhibitory function of GABAergic interneurons and the increase of AMPAR Gria2 subunit protein levels ultimately promote an increased activity at excitatory glutamatergic synapses.

This increased synaptic plasticity ought to be observable by changes of the neurotransmitter GABA and glutamate transducing the inhibitory and excitatory effects, respectively (cf. chapter 1).

Glutamate and GABA metabolite levels were decreased and increased in the 14h and 72h time points, respectively. The latter result might be a false positive as the PLS-DA quality assessment indicated a weak model for this time point. However, the GABA as well as glutamate levels correlated very well with the antidepressant-like effects measured by the FST. Glutamate and GABA are

metabolized by glutamine and recycled in the respective glutamate/glutamine and GABA/glutamine cycle (cf. chapter 1). Glutamine metabolite levels are decreased and the glutamate/glutamine and GABA/glutamine ratios were increased 14h after ketamine treatment. In addition, glutamine levels also significantly correlated with the FST floating time. In conclusion, the results obtained from the present study appear contradictory to previous analyses showing an increased glutamate outflow in the PFC (cf. chapter 1). Therefore, opposite neurotransmitter levels of glutamate and GABA would be more likely to be expected in this study. A blockage of NMDARs present at inhibitory GABAergic neurons would lead to increased and lowered levels of glutamate and GABA levels in the synaptic cleft, respectively. In addition, my results indicate disturbances in the glutamate/glutamine and GABA/glutamine cycles. However, the GABA/glutamine ratio was only decreased at the 72h time point. Despite from the at first site appearing contradictory results of the present study, it is more likely that glutamate and GABA release will be different depending on the activity of inhibitory and excitatory neurons. The observed neurotransmitter changes only represent the total pool of glutamate, GABA and glutamine and not the released neurotransmitter levels. Therefore, microdialysate measurements are more suitable and should be used in future experiments thereby revealing the actual released pool of glutamate and GABA into the synaptic cleft by neuronal activation and inhibition.

Two positive modulators of the NMDAR, serine and putrescine, are elevated and significantly correlated with the FST floating time 2h after a single injection of ketamine. The fast antidepressant-like effects of ketamine might be even more pronounced by an augmentation therapy with these NMDAR modulators. In this regard putrescine has already been shown to exhibit a fast antidepressant effect in the FST⁴³⁹.

Ketamine treatment causes LTP with synaptic spine outgrowth, which further support the hypothesis that the observed HPC and PFC volume reductions in a subset of MDD patients is rescued by synaptic plasticity (cf. chapter 1)⁴³. The myelin sheath is an isolating lipid layer around axons in order to preserve fast neuronal signaling and minimizing information loss⁴⁴⁰. Therefore, a reversal of the volume reduction observed in a subset of treated MDD patients caused by synaptic plasticity with an outgrowth of synaptic connections should result in an elevated number of myelin proteins. As expected, ketamine treatment at low doses (3 mg kg⁻¹) also results in increased MBP protein levels at the 2h and 24h time points and tended to elevate MOG protein levels at 2h and 72h time points. In contrast, when applied at higher, but still subanaesthetic doses, ketamine (6 mg kg⁻¹) is also used as an animal model of schizophrenia, where a loss of the myelin sheath is discussed²⁵⁴⁻²⁵⁷. Therefore, I can also rule out that a low dose of ketamine as used in this study produces molecular alterations characteristic for schizophrenia like decreased myelin proteins^{441, 442}.

A possible explanation for the different ketamine treatment effects observed for an acute, chronic, low and high dosage might be the involvement of different receptor types as well as the fact that ketamine at higher doses might block NMDARs universally and not only at inhibitory interneurons. Acute low doses of ketamine treatment has been reported to only block NMDARs on GABAergic interneurons, whereas chronic treatment with high doses not only blocks NMDARs universally but also nicotinic acetylcholine receptors (cf. chapter 1)²⁵⁵.

Alterations in metabolite, transcript and protein levels in *post-mortem* tissue from schizophrenic patients have been reported for glycolysis, citrate cycle and OXPHOS, the same pathways observed to be affected in the present study⁵⁰⁵⁻⁵⁰⁷. As ketamine at higher doses can induce schizophrenia-like symptoms, it is conceivable that certain molecular pathways are shared between the antidepressant

and psychotic effects. At the same time there must be differences in other affected pathways responsible for the opposite effects of the drug.

5.4 An additional and novel model for Ketamine's antidepressant effect

Taken together, my results do not provide an ultimate answer to the question, which of the previously described hypotheses for ketamine drug action are the correct one albeit there are some hints that rather promote the LTP-like process. In fact, the obtained results fit to the indirect as well as the direct hypothesis of ketamine's antidepressant-like drug action either leading to a synaptic LTP-like process or homeostatic synaptic mechanism, respectively (cf. chapter 1). In addition, to the best of my knowledge the results of the present study are the first to connect the antidepressant-like effects observed for ketamine with the mitochondrial energy metabolism. In order to link the previously stated hypotheses with the obtained results of the present thesis, I especially considered the findings obtained pointing towards an altered mitochondrial energy metabolism: Thus, I postulate an additional and novel model for ketamine's antidepressant effect with an important impact of the mitochondrial energy metabolism. The proposed model suggests that ketamine increases synaptic plasticity as it also increases synaptic activity.

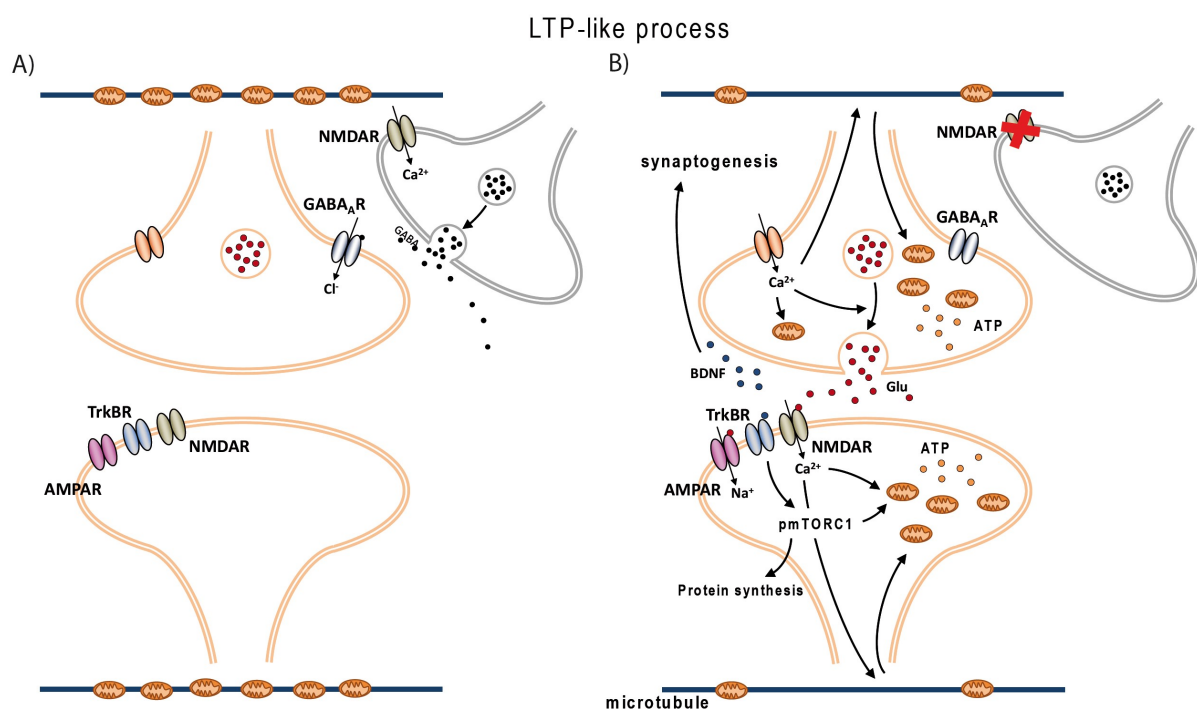


Figure 32: Schematic representation of a novel and additional model of the antidepressant LTP-like process mediated by ketamine drug action on excitatory glutamatergic and inhibitory GABAergic interneurons. Previous studies showed that pharmacological treatment with ketamine results in a glutamate burst, increased BDNF levels, TrkB receptor and mTORC1 activation (pmTORC1), elevated synaptic protein synthesis and integration of AMPARs into the synaptic membrane. These processes strengthen glutamatergic synapses resulting in synaptogenesis (cf. chapter 1). **A)** Synapses without ketamine treatment. Glutamatergic neurons are inhibited by active GABAergic inhibitory neurons. **B)** Ketamine's indirect inhibition of excitatory pyramidal neurons inhibiting NMDARs at GABAergic inhibitory interneurons, thereby resulting in an LTP-like process. The novel finding for ketamine's antidepressant-like effect implicates an impact of the mitochondrial energy metabolism, especially mitochondrial enrichment in synaptic compartments as well as increased synthesis of OXPHOS protein complexes. The proposed novel model describes that an elevation of synaptic Ca^{2+} leads to mitochondrial enrichment of mitochondria into the active synaptic compartment. Furthermore, pmTORC1 induces mitochondrial metabolism and promotes ATP production to cope for the high energy demand in activated synapses.

Therefore, an elevation of synaptic Ca^{2+} firstly leads to a mitochondrial enrichment into the active synaptic compartment, secondly, to an activation and increased protein expression of mitochondrial enzymes including OXPHOS complex II SDHA and SDHB.

In addition, pmTORC1 and pAMPK induce mitochondrial metabolism and promote ATP production to cope for the high energy demand in activated synapses. Overall, ketamine might especially promote its antidepressant effect by an increased mitochondrial energy metabolism in synaptic compartments, increased synthesis of OXPHOS protein complexes as well as synaptogenesis (figure 32B and 33B). The results obtained by the present study also provide novel drug targets – besides the NMDAR – for faster acting antidepressants with a similar mode of action as ketamine, like mitochondria and related enzymes of the energy metabolism.

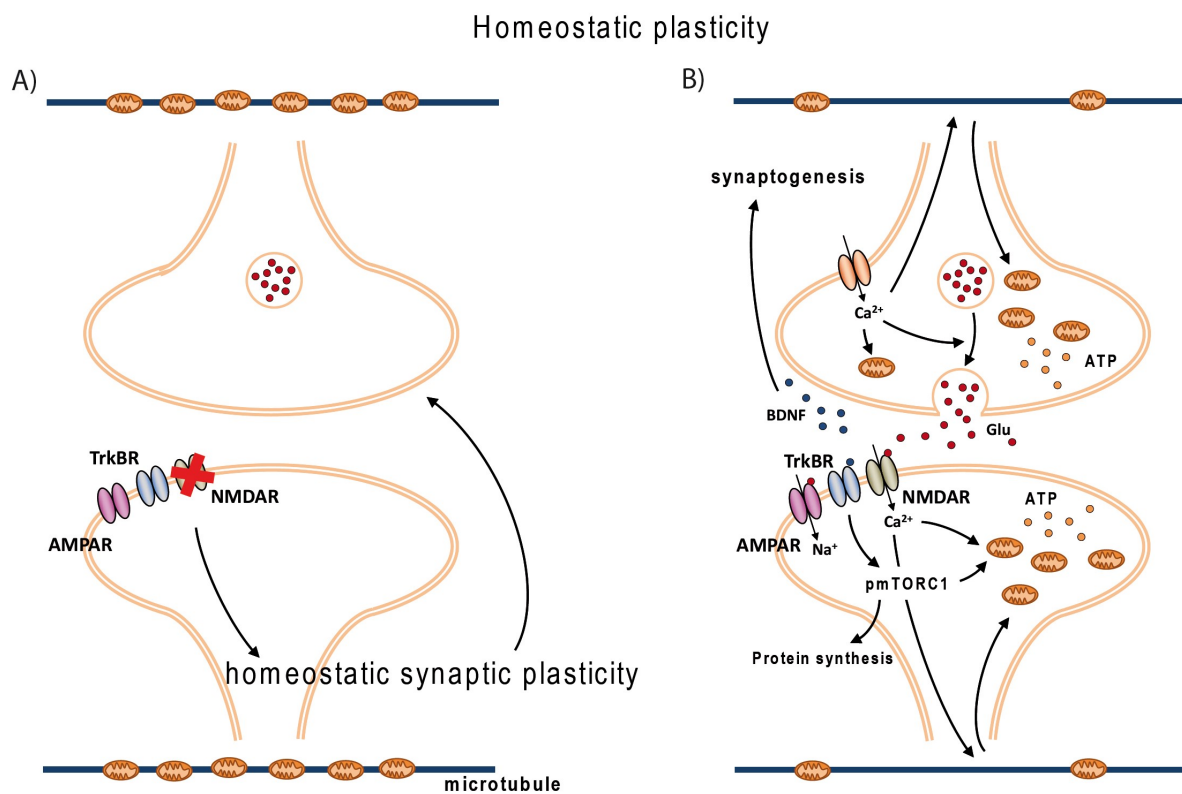


Figure 33: Schematic representation of a novel and additional model of the antidepressant drug effect mediated by a synaptic homeostatic plasticity mechanism of the excitatory glutamatergic neurons induced by ketamine. Previous studies showed that pharmacological treatment with ketamine results in a glutamate burst, increased BDNF levels, TrkB receptor and mTORC1 activation (pmTORC1), elevated synaptic protein synthesis and integration of AMPARs into the synaptic membrane. These processes strengthen glutamatergic synapses resulting in synaptogenesis (cf. chapter 1). **A)** Ketamine blocks NMDARs at excitatory glutamatergic neurons thereby inducing a homeostatic synaptic plasticity mechanism. **B)** The direct inhibition of NMDARs and the induced homeostatic synaptic plasticity results after the degradation of ketamine to an increased activity of glutamatergic excitatory neurons. The novel finding for ketamine's antidepressant-like effect implicates an impact of the mitochondrial energy metabolism, especially mitochondrial enrichment in synaptic compartments as well as increased synthesis of OXPHOS protein complexes. The proposed novel model describes that an elevation of synaptic Ca^{2+} leads to mitochondrial enrichment of mitochondria into the active synaptic compartment. Furthermore, pmTORC1 induces mitochondrial metabolism and promotes ATP production to cope for the high energy demand in activated synapses.

5.4 Clinical relevance

Several previous studies have shown an involvement of mitochondria in MDD pathobiology^{432, 487, 508}. In addition, mitochondrial respiration in peripheral blood mononuclear cells from depressed patients was lower compared to control subjects and correlated with depressive symptom severity⁵⁰⁹. In addition, patients with mitochondrial disorders are very often co-morbid for psychiatric illnesses including MDD. These patients suffer from primary impairment of mitochondrial functioning through either nuclear or mitochondrial DNA mutations of the mitochondrial genome. Mitochondrial impairment mostly affects high energy consuming organs like muscles and the brain. MDD symptoms and molecular findings are apparent by depressed mood, fatigue, cognitive decline, elevated blood lactate levels and atrophy, most of them explainable by mitochondrial dysfunction. Patients are mostly first diagnosed with MDD and the mitochondrial disorder is only recognized later in life. Conventional ADs are mostly not effective and these patients suffer from TRD. Moreover, traditional ADs seem to worsen the effects as SSRIs and TCAs inhibit mitochondrial OXPHOS ETC protein complexes^{510, 511}. Ketamine is especially effective in MDD patients suffering from TRD and my results indicate an increase of the mitochondrial energy metabolism after a single injection of a low dose of ketamine. For all these reasons I submit that mitochondria play a critical role in the development of MDD as well as AD treatment response, at least in a subset of patients with a defined symptomatology.

6.0 Literature

- 1 J. Olesen, M. G. Baker, T. Freund, M. di Luca, J. Mendlewicz, I. Ragan and M. Westphal, 'Consensus document on European brain research', *J Neurol Neurosurg Psychiatry*, 77 Suppl 1, Aug 2006, i1-49.
- 2 C. J. Murray and A. D. Lopez, 'Alternative projections of mortality and disability by cause 1990-2020: Global Burden of Disease Study', *Lancet*, 349: 9064, May 1997, 1498-1504.
- 3 Y. Agid, G. Buzsáki, D. M. Diamond, R. Frackowiak, J. Giedd, J. A. Girault, A. Grace, J. J. Lambert, H. Manji, H. Mayberg, M. Popoli, A. Prochiantz, G. Richter-Levin, P. Somogyi, M. Spedding, P. Svenningsson and D. Weinberger, 'How can drug discovery for psychiatric disorders be improved?', *Nat Rev Drug Discov*, 6: 3, Mar 2007, 189-201.
- 4 R. C. Kessler, S. Aguilar-Gaxiola, J. Alonso, S. Chatterji, S. Lee, J. Ormel, T. B. Ustün and P. S. Wang, 'The global burden of mental disorders: an update from the WHO World Mental Health (WMH) surveys', *Epidemiol Psychiatr Soc*, 18: 1, 2009 Jan-Mar 2009, 23-33.
- 5 R. C. Kessler, 'Epidemiology of women and depression', *J Affect Disord*, 74: 1, Mar 2003, 5-13.
- 6 World Health Organization, 'Depression', www.who.int/mediacentre/factsheets/fs369/en/, 2016.
- 7 M. H. Trivedi, A. J. Rush, S. R. Wisniewski, A. A. Nierenberg, D. Warden, L. Ritz, G. Norquist, R. H. Howland, B. Lebowitz, P. J. McGrath, K. Shores-Wilson, M. M. Biggs, G. K. Balasubramani, M. Fava and STAR*D Study Team, 'Evaluation of outcomes with citalopram for depression using measurement-based care in STAR*D: implications for clinical practice', *Am J Psychiatry*, 163: 1, Jan 2006, 28-40.
- 8 C. M. Sonnenberg, D. J. Deeg, H. C. Comijs, W. van Tilburg and A. T. Beekman, 'Trends in antidepressant use in the older population: results from the LASA-study over a period of 10 years', *J Affect Disord*, 111: 2-3, Dec 2008, 299-305.
- 9 G. Racagni and M. Popoli, 'Cellular and molecular mechanisms in the long-term action of antidepressants', *Dialogues Clin Neurosci*, 10: 42008, 385-400.
- 10 R. C. Kessler, P. Berglund, O. Demler, R. Jin, D. Koretz, K. R. Merikangas, A. J. Rush, E. E. Walters, P. S. Wang and National Comorbidity Survey Replication, 'The epidemiology of major depressive disorder: results from the National Comorbidity Survey Replication (NCS-R)', *JAMA*, 289: 23, Jun 2003, 3095-3105.
- 11 E. J. Nestler, M. Barrot, R. J. DiLeone, A. J. Eisch, S. J. Gold and L. M. Monteggia, 'Neurobiology of depression', *Neuron*, 34: 1, Mar 2002, 13-25.
- 12 J. F. Cryan, A. Markou and I. Lucki, 'Assessing antidepressant activity in rodents: recent developments and future needs', *Trends Pharmacol Sci*, 23: 5, May 2002, 238-245.
- 13 P. Hamet and J. Tremblay, 'Genetics and genomics of depression', *Metabolism*, 54: 5 Suppl 1, May 2005, 10-15.
- 14 C. Hammen, J. Davila, G. Brown, A. Ellicott and M. Gitlin, 'Psychiatric history and stress: predictors of severity of unipolar depression', *J Abnorm Psychol*, 101: 1, Feb 1992, 45-52.
- 15 G. W. Brown, A. Bifulco and T. O. Harris, 'Life events, vulnerability and onset of depression: some refinements', *Br J Psychiatry*, 150, Jan 1987, 30-42.
- 16 B. J. Casey, N. Craddock, B. N. Cuthbert, S. E. Hyman, F. S. Lee and K. J. Ressler, 'DSM-5 and RDoC: progress in psychiatry research?', *Nat Rev Neurosci*, 14: 11, Nov 2013, 810-814.
- 17 S. E. Lakhan, K. Vieira and E. Hamlat, 'Biomarkers in psychiatry: drawbacks and potential for misuse', *Int Arch Med*, 32010, 1.
- 18 World Health Organization, 'International Statistical Classification of Diseases and Related Health Problems', <http://apps.who.int/classifications/icd10/browse/2016/en#/F30-F39>, 2016.
- 19 American Psychiatric Association, *Diagnostic and Statistical Manual of Mental Disorders, 4th Edition*, 1994.
- 20 American Psychiatric Association, *Diagnostic and Statistical Manual of Mental Disorders, 4th Edition*, 1994.

- 21 National Institutes of Health, 'Research Domain Criteria', <https://www.nimh.nih.gov/research-priorities/rdoc/index.shtml>.
- 22 H. Sun, P. J. Kennedy and E. J. Nestler, 'Epigenetics of the depressed brain: role of histone acetylation and methylation', *Neuropsychopharmacology*, 38: 1, Jan 2013, 124-137.
- 23 E. K. Miller, D. J. Freedman and J. D. Wallis, 'The prefrontal cortex: categories, concepts and cognition', *Philos Trans R Soc Lond B Biol Sci*, 357: 1424, Aug 2002, 1123-1136.
- 24 Y. Yang and A. Raine, 'Prefrontal structural and functional brain imaging findings in antisocial, violent, and psychopathic individuals: a meta-analysis', *Psychiatry Res*, 174: 2, Nov 2009, 81-88.
- 25 C. G. DeYoung, J. B. Hirsh, M. S. Shane, X. Papademetris, N. Rajeevan and J. R. Gray, 'Testing predictions from personality neuroscience. Brain structure and the big five', *Psychol Sci*, 21: 6, Jun 2010, 820-828.
- 26 The University of Texas, 'Chapter 5: The Limbic System: The Hippocampus', <http://neuroscience.uth.tmc.edu/s4/chapter05.html>.
- 27 B. Y. Hayden and M. L. Platt, 'Neurons in anterior cingulate cortex multiplex information about reward and action', *J Neurosci*, 30: 9, Mar 2010, 3339-3346.
- 28 'Cingulate binds learning', *Trends Cogn Sci*, 1: 1, Apr 1997, 2.
- 29 K. A. Hadland, M. F. Rushworth, D. Gaffan and R. E. Passingham, 'The effect of cingulate lesions on social behaviour and emotion', *Neuropsychologia*, 41: 82003, 919-931.
- 30 K. Amunts, O. Kedo, M. Kindler, P. Pieperhoff, H. Mohlberg, N. J. Shah, U. Habel, F. Schneider and K. Zilles, 'Cytoarchitectonic mapping of the human amygdala, hippocampal region and entorhinal cortex: intersubject variability and probability maps', *Anat Embryol (Berl)*, 210: 5-6, Dec 2005, 343-352.
- 31 Eve A. Gallman James Weyhenmeyer, *Rapid Review Neuroscience*, 2006.
- 32 I. G. Cameron, M. Watanabe, G. Pari and D. P. Munoz, 'Executive impairment in Parkinson's disease: response automaticity and task switching', *Neuropsychologia*, 48: 7, Jun 2010, 1948-1957.
- 33 V. S. Chakravarthy, D. Joseph and R. S. Bapi, 'What do the basal ganglia do? A modeling perspective', *Biol Cybern*, 103: 3, Sep 2010, 237-253.
- 34 A. Stocco, C. Lebiere and J. R. Anderson, 'Conditional routing of information to the cortex: a model of the basal ganglia's role in cognitive coordination', *Psychol Rev*, 117: 2, Apr 2010, 541-574.
- 35 G. MacQueen and T. Frodl, 'The hippocampus in major depression: evidence for the convergence of the bench and bedside in psychiatric research?', *Mol Psychiatry*, 16: 3, Mar 2011, 252-264.
- 36 G. Rajkowska, J. J. Miguel-Hidalgo, J. Wei, G. Dille, S. D. Pittman, H. Y. Meltzer, J. C. Overholser, B. L. Roth and C. A. Stockmeier, 'Morphometric evidence for neuronal and glial prefrontal cell pathology in major depression', *Biol Psychiatry*, 45: 9, May 1999, 1085-1098.
- 37 B. S. McEwen, 'The ever-changing brain: cellular and molecular mechanisms for the effects of stressful experiences', *Dev Neurobiol*, 72: 6, Jun 2012, 878-890.
- 38 R. S. Duman, 'Pathophysiology of depression and innovative treatments: remodeling glutamatergic synaptic connections', *Dialogues Clin Neurosci*, 16: 1, Mar 2014, 11-27.
- 39 W. C. Drevets, J. L. Price, J. R. Simpson, R. D. Todd, T. Reich, M. Vannier and M. E. Raichle, 'Subgenual prefrontal cortex abnormalities in mood disorders', *Nature*, 386: 6627, Apr 1997, 824-827.
- 40 Y. I. Sheline, P. W. Wang, M. H. Gado, J. G. Csernansky and M. W. Vannier, 'Hippocampal atrophy in recurrent major depression', *Proc Natl Acad Sci U S A*, 93: 9, Apr 1996, 3908-3913.
- 41 Y. I. Sheline, M. Sanghavi, M. A. Mintun and M. H. Gado, 'Depression duration but not age predicts hippocampal volume loss in medically healthy women with recurrent major depression', *J Neurosci*, 19: 12, Jun 1999, 5034-5043.
- 42 M. J. Kempton, Z. Salvador, M. R. Munafò, J. R. Geddes, A. Simmons, S. Frangou and S. C. Williams, 'Structural neuroimaging studies in major depressive disorder. Meta-analysis and comparison with bipolar disorder', *Arch Gen Psychiatry*, 68: 7, Jul 2011, 675-690.
- 43 S. Campbell and G. Macqueen, 'The role of the hippocampus in the pathophysiology of major depression', *J Psychiatry Neurosci*, 29: 6, Nov 2004, 417-426.

- 44 A. Vyas, R. Mitra, B. S. Shankaranarayana Rao and S. Chattarji, 'Chronic stress induces contrasting patterns of dendritic remodeling in hippocampal and amygdaloid neurons', *J Neurosci*, 22: 15, Aug 2002, 6810-6818.
- 45 A. Vyas, A. G. Pillai and S. Chattarji, 'Recovery after chronic stress fails to reverse amygdaloid neuronal hypertrophy and enhanced anxiety-like behavior', *Neuroscience*, 128: 42004, 667-673.
- 46 C. A. Stockmeier, G. J. Mahajan, L. C. Konick, J. C. Overholser, G. J. Jurjus, H. Y. Meltzer, H. B. Uylings, L. Friedman and G. Rajkowska, 'Cellular changes in the postmortem hippocampus in major depression', *Biol Psychiatry*, 56: 9, Nov 2004, 640-650.
- 47 G. Eisenhofer, I. J. Kopin and D. S. Goldstein, 'Catecholamine metabolism: a contemporary view with implications for physiology and medicine', *Pharmacol Rev*, 56: 3, Sep 2004, 331-349.
- 48 P. Riederer, L. Lachenmayer and G. Laux, 'Clinical applications of MAO-inhibitors', *Curr Med Chem*, 11: 15, Aug 2004, 2033-2043.
- 49 P. Blier and C. de Montigny, 'Current advances and trends in the treatment of depression', *Trends Pharmacol Sci*, 15: 7, Jul 1994, 220-226.
- 50 S. M. Stahl, 'Basic psychopharmacology of antidepressants, part 1: Antidepressants have seven distinct mechanisms of action', *J Clin Psychiatry*, 59 Suppl 41998, 5-14.
- 51 B. E. Leonard, 'Psychopathology of depression', *Drugs Today (Barc)*, 43: 10, Oct 2007, 705-716.
- 52 P. J. Kenny, F. Gasparini and A. Markou, 'Group II metabotropic and alpha-amino-3-hydroxy-5-methyl-4-isoxazole propionate (AMPA)/kainate glutamate receptors regulate the deficit in brain reward function associated with nicotine withdrawal in rats', *J Pharmacol Exp Ther*, 306: 3, Sep 2003, 1068-1076.
- 53 C. J. Swanson, M. Bures, M. P. Johnson, A. M. Linden, J. A. Monn and D. D. Schoepp, 'Metabotropic glutamate receptors as novel targets for anxiety and stress disorders', *Nat Rev Drug Discov*, 4: 2, Feb 2005, 131-144.
- 54 S. Chaki, R. Yoshikawa, S. Hirota, T. Shimazaki, M. Maeda, N. Kawashima, T. Yoshimizu, A. Yasuhara, K. Sakagami, S. Okuyama, S. Nakanishi and A. Nakazato, 'MGS0039: a potent and selective group II metabotropic glutamate receptor antagonist with antidepressant-like activity', *Neuropharmacology*, 46: 4, Mar 2004, 457-467.
- 55 H. Jourdi, Y. T. Hsu, M. Zhou, Q. Qin, X. Bi and M. Baudry, 'Positive AMPA receptor modulation rapidly stimulates BDNF release and increases dendritic mRNA translation', *J Neurosci*, 29: 27, Jul 2009, 8688-8697.
- 56 J. C. Lauterborn, G. Lynch, P. Vanderklisch, A. Arai and C. M. Gall, 'Positive modulation of AMPA receptors increases neurotrophin expression by hippocampal and cortical neurons', *J Neurosci*, 20: 1, Jan 2000, 8-21.
- 57 F. Bai, M. Bergeron and D. L. Nelson, 'Chronic AMPA receptor potentiator (LY451646) treatment increases cell proliferation in adult rat hippocampus', *Neuropharmacology*, 44: 8, Jun 2003, 1013-1021.
- 58 T. Mele, M. Carman-Krzan and D. M. Juric, 'Regulatory role of monoamine neurotransmitters in astrocytic NT-3 synthesis', *Int J Dev Neurosci*, 28: 1, Feb 2010, 13-19.
- 59 M. A. Kurian, P. Gissen, M. Smith, S. Heales and P. T. Clayton, 'The monoamine neurotransmitter disorders: an expanding range of neurological syndromes', *Lancet Neurol*, 10: 8, Aug 2011, 721-733.
- 60 A. Meneses and G. Liy-Salmeron, 'Serotonin and emotion, learning and memory', *Rev Neurosci*, 23: 5-62012, 543-553.
- 61 I. S. Bazan and W. H. Fares, 'Review of the Ongoing Story of Appetite Suppressants, Serotonin Pathway, and Pulmonary Vascular Disease', *Am J Cardiol*, 117: 10, May 2016, 1691-1696.
- 62 C. M. Portas, B. Bjorvatn and R. Ursin, 'Serotonin and the sleep/wake cycle: special emphasis on microdialysis studies', *Prog Neurobiol*, 60: 1, Jan 2000, 13-35.
- 63 H. A. Mitchell and D. Weinschenker, 'Good night and good luck: norepinephrine in sleep pharmacology', *Biochem Pharmacol*, 79: 6, Mar 2010, 801-809.

- 64 A. Adell, C. Garcia-Marquez, A. Armario and E. Gelpi, 'Chronic stress increases serotonin and noradrenaline in rat brain and sensitizes their responses to a further acute stress', *J Neurochem*, 50: 6, Jun 1988, 1678-1681.
- 65 G. R. Heninger, P. L. Delgado and D. S. Charney, 'The revised monoamine theory of depression: a modulatory role for monoamines, based on new findings from monoamine depletion experiments in humans', *Pharmacopsychiatry*, 29: 1, Jan 1996, 2-11.
- 66 F. Sulser, 'New perspectives on the molecular pharmacology of affective disorders', *Eur Arch Psychiatry Neurol Sci*, 238: 5-6/1989, 231-239.
- 67 S. P. Banerjee, L. S. Kung, S. J. Riggi and S. K. Chanda, 'Development of beta-adrenergic receptor subsensitivity by antidepressants', *Nature*, 268: 5619, Aug 1977, 455-456.
- 68 S. E. Hyman and E. J. Nestler, 'Initiation and adaptation: a paradigm for understanding psychotropic drug action', *Am J Psychiatry*, 153: 2, Feb 1996, 151-162.
- 69 D. De Cesare, G. M. Fimia and P. Sassone-Corsi, 'Signaling routes to CREM and CREB: plasticity in transcriptional activation', *Trends Biochem Sci*, 24: 7, Jul 1999, 281-285.
- 70 D. J. Nutt, 'The neuropharmacology of serotonin and noradrenaline in depression', *Int Clin Psychopharmacol*, 17 Suppl 1, Jun 2002, S1-12.
- 71 I. M. Anderson and B. M. Tomenson, 'The efficacy of selective serotonin re-uptake inhibitors in depression: a meta-analysis of studies against tricyclic antidepressants', *J Psychopharmacol*, 8: 4, Jan 1994, 238-249.
- 72 L. Altshuler, L. Kiriakos, J. Calcagno, R. Goodman, M. Gitlin, M. Frye and J. Mintz, 'The impact of antidepressant discontinuation versus antidepressant continuation on 1-year risk for relapse of bipolar depression: a retrospective chart review', *J Clin Psychiatry*, 62: 8, Aug 2001, 612-616.
- 73 D. Lacroix, P. Blier, O. Curet and C. de Montigny, 'Effects of long-term desipramine administration on noradrenergic neurotransmission: electrophysiological studies in the rat brain', *J Pharmacol Exp Ther*, 257: 3, Jun 1991, 1081-1090.
- 74 T. H. Svensson and T. Usdin, 'Feedback inhibition of brain noradrenaline neurons by tricyclic antidepressants: alpha-receptor mediation', *Science*, 202: 4372, Dec 1978, 1089-1091.
- 75 S. T. Szabo and P. Blier, 'Effect of the selective noradrenergic reuptake inhibitor reboxetine on the firing activity of noradrenaline and serotonin neurons', *Eur J Neurosci*, 13: 11, Jun 2001, 2077-2087.
- 76 D. N. Thomas, D. Nutt and R. B. Holman, 'Regionally specific changes in extracellular noradrenaline following chronic idazoxan as revealed by in vivo microdialysis', *Eur J Pharmacol*, 261: 1-2, Aug 1994, 53-57.
- 77 D. J. Nutt, M. D. Lallies, L. A. Lione and A. L. Hudson, 'Noradrenergic mechanisms in the prefrontal cortex', *J Psychopharmacol*, 11: 2/1997, 163-168.
- 78 A. N. Schoffelmeer and A. H. Mulder, '3H-Noradrenaline and 3H-5-hydroxytryptamine release from rat brain slices and its presynaptic alpha-adrenergic modulation after long-term desipramine pretreatment', *Naunyn Schmiedeberg's Arch Pharmacol*, 318: 3, Feb 1982, 173-180.
- 79 I. C. Campbell and R. M. McKernan, 'Clorgyline and desipramine alter the sensitivity of [3H]noradrenaline release to calcium but not to clonidine', *Brain Res*, 372: 2, May 1986, 253-259.
- 80 G. Sacchetti, M. Bernini, M. Gobbi, S. Parini, L. Pirona, T. Mennini and R. Samanin, 'Chronic treatment with desipramine facilitates its effect on extracellular noradrenaline in the rat hippocampus: studies on the role of presynaptic alpha2-adrenoceptors', *Naunyn Schmiedeberg's Arch Pharmacol*, 363: 1, Jan 2001, 66-72.
- 81 M. V. Puig, P. Celada and F. Artigas, '[Serotonergic control of prefrontal cortex]', *Rev Neurol*, 39: 6, 2004 Sep 16-30 2004, 539-547.
- 82 K. Rickels, J. Amsterdam, C. Clary, J. Hassman, J. London, G. Puzzuoli and E. Schweizer, 'Buspirone in depressed outpatients: a controlled study', *Psychopharmacol Bull*, 26: 2/1990, 163-167.
- 83 S. M. Stahl, L. Kaiser, J. Roeschen, J. M. Keppel Hesselink and J. Orazem, 'Effectiveness of ipsapirone, a 5-HT-1A partial agonist, in major depressive disorder: support for the role of 5-HT-1A receptors in the mechanism of action of serotonergic antidepressants', *Int J Neuropsychopharmacol*, 1: 1, Jul 1998, 11-18.

- 84 P. Blier and C. de Montigny, 'Modification of 5-HT neuron properties by sustained administration of the 5-HT_{1A} agonist gepirone: electrophysiological studies in the rat brain', *Synapse*, 1: 51987, 470-480.
- 85 S. Hjorth, C. S. Suchowski and M. P. Galloway, 'Evidence for 5-HT autoreceptor-mediated, nerve impulse-independent, control of 5-HT synthesis in the rat brain', *Synapse*, 19: 3, Mar 1995, 170-176.
- 86 A. M. Gardier, I. Malagié, A. C. Trillat, C. Jacquot and F. Artigas, 'Role of 5-HT_{1A} autoreceptors in the mechanism of action of serotonergic antidepressant drugs: recent findings from in vivo microdialysis studies', *Fundam Clin Pharmacol*, 10: 11996, 16-27.
- 87 N. Bel and F. Artigas, 'Chronic treatment with fluvoxamine increases extracellular serotonin in frontal cortex but not in raphe nuclei', *Synapse*, 15: 3, Nov 1993, 243-245.
- 88 J. J. Rutter, C. Gundlach and S. B. Auerbach, 'Increase in extracellular serotonin produced by uptake inhibitors is enhanced after chronic treatment with fluoxetine', *Neurosci Lett*, 171: 1-2, Apr 1994, 183-186.
- 89 J. Vetulani and F. Sulser, 'Action of various antidepressant treatments reduces reactivity of noradrenergic cyclic AMP-generating system in limbic forebrain', *Nature*, 257: 5526, Oct 1975, 495-496.
- 90 G. B. Baker and A. J. Greenshaw, 'Effects of long-term administration of antidepressants and neuroleptics on receptors in the central nervous system', *Cell Mol Neurobiol*, 9: 1, Mar 1989, 1-44.
- 91 S. F. Gao and A. M. Bao, 'Corticotropin-releasing hormone, glutamate, and γ -aminobutyric acid in depression', *Neuroscientist*, 17: 1, Feb 2011, 124-144.
- 92 C. E. Detillion, T. K. Craft, E. R. Glasper, B. J. Prendergast and A. C. DeVries, 'Social facilitation of wound healing', *Psychoneuroendocrinology*, 29: 8, Sep 2004, 1004-1011.
- 93 A. M. Bao, G. Meynen and D. F. Swaab, 'The stress system in depression and neurodegeneration: focus on the human hypothalamus', *Brain Res Rev*, 57: 2, Mar 2008, 531-553.
- 94 D. F. Swaab, A. M. Bao and P. J. Lucassen, 'The stress system in the human brain in depression and neurodegeneration', *Ageing Res Rev*, 4: 2, May 2005, 141-194.
- 95 P. Sobocki, B. Jönsson, J. Angst and C. Rehnberg, 'Cost of depression in Europe', *J Ment Health Policy Econ*, 9: 2, Jun 2006, 87-98.
- 96 L. Jacobson and R. Sapolsky, 'The role of the hippocampus in feedback regulation of the hypothalamic-pituitary-adrenocortical axis', *Endocr Rev*, 12: 2, May 1991, 118-134.
- 97 I. Liberzon, M. Krstov and E. A. Young, 'Stress-restress: effects on ACTH and fast feedback', *Psychoneuroendocrinology*, 22: 6, Aug 1997, 443-453.
- 98 M. J. Owens and C. B. Nemeroff, 'Physiology and pharmacology of corticotropin-releasing factor', *Pharmacol Rev*, 43: 4, Dec 1991, 425-473.
- 99 D. K. Grammatopoulos and G. P. Chrousos, 'Functional characteristics of CRH receptors and potential clinical applications of CRH-receptor antagonists', *Trends Endocrinol Metab*, 13: 10, Dec 2002, 436-444.
- 100 C. M. Pariante, 'Depression, stress and the adrenal axis', *J Neuroendocrinol*, 15: 8, Aug 2003, 811-812.
- 101 E. J. Nestler, 'Antidepressant treatments in the 21st century', *Biol Psychiatry*, 44: 7, Oct 1998, 526-533.
- 102 C. Anacker, P. A. Zunszain, L. A. Carvalho and C. M. Pariante, 'The glucocorticoid receptor: pivot of depression and of antidepressant treatment?', *Psychoneuroendocrinology*, 36: 3, Apr 2011, 415-425.
- 103 H. Dam, 'Dexamethasone suppression test', *Acta Psychiatr Scand Suppl*, 345: 1988, 38-44.
- 104 F. Holsboer and N. Barden, 'Antidepressants and hypothalamic-pituitary-adrenocortical regulation', *Endocr Rev*, 17: 2, Apr 1996, 187-205.
- 105 R. T. Rubin, J. J. Phillips, T. F. Sadow and J. T. McCracken, 'Adrenal gland volume in major depression. Increase during the depressive episode and decrease with successful treatment', *Arch Gen Psychiatry*, 52: 3, Mar 1995, 213-218.
- 106 ME and Howland Thase, R, *Biological processes in depression: updated review and integration.*, 1995.

- 107 S. C. Ribeiro, R. Tandon, L. Grunhaus and J. F. Greden, 'The DST as a predictor of outcome in depression: a meta-analysis', *Am J Psychiatry*, 150: 11, Nov 1993, 1618-1629.
- 108 G. N. Neigh and C. B. Nemeroff, 'Reduced glucocorticoid receptors: consequence or cause of depression?', *Trends Endocrinol Metab*, 17: 4, 2006 May-Jun 2006, 124-125.
- 109 M. J. Webster, M. B. Knable, J. O'Grady, J. Orthmann and C. S. Weickert, 'Regional specificity of brain glucocorticoid receptor mRNA alterations in subjects with schizophrenia and mood disorders', *Mol Psychiatry*, 7: 92002, 985-994, 924.
- 110 C. M. Pariante and S. L. Lightman, 'The HPA axis in major depression: classical theories and new developments', *Trends Neurosci*, 31: 9, Sep 2008, 464-468.
- 111 M. Banasr, J. M. Dwyer and R. S. Duman, 'Cell atrophy and loss in depression: reversal by antidepressant treatment', *Curr Opin Cell Biol*, 23: 6, Dec 2011, 730-737.
- 112 C. Pittenger and R. S. Duman, 'Stress, depression, and neuroplasticity: a convergence of mechanisms', *Neuropsychopharmacology*, 33: 1, Jan 2008, 88-109.
- 113 G. E. Wood, L. T. Young, L. P. Reagan, B. Chen and B. S. McEwen, 'Stress-induced structural remodeling in hippocampus: prevention by lithium treatment', *Proc Natl Acad Sci U S A*, 101: 11, Mar 2004, 3973-3978.
- 114 S. D. Norrholm and C. C. Ouimet, 'Altered dendritic spine density in animal models of depression and in response to antidepressant treatment', *Synapse*, 42: 3, Dec 2001, 151-163.
- 115 T. Hajszan, A. Dow, J. L. Warner-Schmidt, K. Szigeti-Buck, N. L. Sallam, A. Parducz, C. Leranth and R. S. Duman, 'Remodeling of hippocampal spine synapses in the rat learned helplessness model of depression', *Biol Psychiatry*, 65: 5, Mar 2009, 392-400.
- 116 J. M. Bessa, D. Ferreira, I. Melo, F. Marques, J. J. Cerqueira, J. A. Palha, O. F. Almeida and N. Sousa, 'The mood-improving actions of antidepressants do not depend on neurogenesis but are associated with neuronal remodeling', *Mol Psychiatry*, 14: 8, Aug 2009, 764-773, 739.
- 117 R. S. Duman and L. M. Monteggia, 'A neurotrophic model for stress-related mood disorders', *Biol Psychiatry*, 59: 12, Jun 2006, 1116-1127.
- 118 V. Krishnan and E. J. Nestler, 'The molecular neurobiology of depression', *Nature*, 455: 7215, Oct 2008, 894-902.
- 119 M. A. Smith, S. Makino, R. Kvetnanský and R. M. Post, 'Effects of stress on neurotrophic factor expression in the rat brain', *Ann N Y Acad Sci*, 771, Dec 1995, 234-239.
- 120 G. Aicardi, E. Argilli, S. Cappello, S. Santi, M. Riccio, H. Thoenen and M. Canossa, 'Induction of long-term potentiation and depression is reflected by corresponding changes in secretion of endogenous brain-derived neurotrophic factor', *Proc Natl Acad Sci U S A*, 101: 44, Nov 2004, 15788-15792.
- 121 A. Balkowiec and D. M. Katz, 'Cellular mechanisms regulating activity-dependent release of native brain-derived neurotrophic factor from hippocampal neurons', *J Neurosci*, 22: 23, Dec 2002, 10399-10407.
- 122 J. L. Banko, F. Poulin, L. Hou, C. T. DeMaria, N. Sonenberg and E. Klann, 'The translation repressor 4E-BP2 is critical for eIF4F complex formation, synaptic plasticity, and memory in the hippocampus', *J Neurosci*, 25: 42, Oct 2005, 9581-9590.
- 123 A. Citri and R. C. Malenka, 'Synaptic plasticity: multiple forms, functions, and mechanisms', *Neuropsychopharmacology*, 33: 1, Jan 2008, 18-41.
- 124 M. Costa-Mattioli, W. S. Sossin, E. Klann and N. Sonenberg, 'Translational control of long-lasting synaptic plasticity and memory', *Neuron*, 61: 1, Jan 2009, 10-26.
- 125 C. A. Hoeffer and E. Klann, 'mTOR signaling: at the crossroads of plasticity, memory and disease', *Trends Neurosci*, 33: 2, Feb 2010, 67-75.
- 126 W. J. McEntee and T. H. Crook, 'Glutamate: its role in learning, memory, and the aging brain', *Psychopharmacology (Berl)*, 111: 41993, 391-401.
- 127 L. Pessoa, 'On the relationship between emotion and cognition', *Nat Rev Neurosci*, 9: 2, Feb 2008, 148-158.
- 128 A. Holtmaat and K. Svoboda, 'Experience-dependent structural synaptic plasticity in the mammalian brain', *Nat Rev Neurosci*, 10: 9, Sep 2009, 647-658.

- 129 J. R. Whitlock, A. J. Heynen, M. G. Shuler and M. F. Bear, 'Learning induces long-term potentiation in the hippocampus', *Science*, 313: 5790, Aug 2006, 1093-1097.
- 130 P. J. Carlson, J. B. Singh, C. A. Zarate, W. C. Drevets and H. K. Manji, 'Neural circuitry and neuroplasticity in mood disorders: insights for novel therapeutic targets', *NeuroRx*, 3: 1, Jan 2006, 22-41.
- 131 I. Hindmarch, 'Expanding the horizons of depression: beyond the monoamine hypothesis', *Hum Psychopharmacol*, 16: 3, Apr 2001, 203-218.
- 132 F. Orrego and S. Villanueva, 'The chemical nature of the main central excitatory transmitter: a critical appraisal based upon release studies and synaptic vesicle localization', *Neuroscience*, 56: 3, Oct 1993, 539-555.
- 133 G. E. Hardingham and H. Bading, 'Synaptic versus extrasynaptic NMDA receptor signalling: implications for neurodegenerative disorders', *Nat Rev Neurosci*, 11: 10, Oct 2010, 682-696.
- 134 M. Erecińska and I. A. Silver, 'Metabolism and role of glutamate in mammalian brain', *Prog Neurobiol*, 35: 41990, 245-296.
- 135 J. Cartmell and D. D. Schoepp, 'Regulation of neurotransmitter release by metabotropic glutamate receptors', *J Neurochem*, 75: 3, Sep 2000, 889-907.
- 136 J. P. Pin and R. Duvoisin, 'The metabotropic glutamate receptors: structure and functions', *Neuropharmacology*, 34: 1, Jan 1995, 1-26.
- 137 D. D. Schoepp, 'Unveiling the functions of presynaptic metabotropic glutamate receptors in the central nervous system', *J Pharmacol Exp Ther*, 299: 1, Oct 2001, 12-20.
- 138 F. Bordi and A. Ugolini, 'Group I metabotropic glutamate receptors: implications for brain diseases', *Prog Neurobiol*, 59: 1, Sep 1999, 55-79.
- 139 F. Ferraguti and R. Shigemoto, 'Metabotropic glutamate receptors', *Cell Tissue Res*, 326: 2, Nov 2006, 483-504.
- 140 Y. Shigeri, R. P. Seal and K. Shimamoto, 'Molecular pharmacology of glutamate transporters, EAATs and VGLUTs', *Brain Res Brain Res Rev*, 45: 3, Jul 2004, 250-265.
- 141 J. A. Blendy, 'The role of CREB in depression and antidepressant treatment', *Biol Psychiatry*, 59: 12, Jun 2006, 1144-1150.
- 142 H. Bito, K. Deisseroth and R. W. Tsien, 'CREB phosphorylation and dephosphorylation: a Ca(2+)- and stimulus duration-dependent switch for hippocampal gene expression', *Cell*, 87: 7, Dec 1996, 1203-1214.
- 143 A. Ghosh, D. D. Ginty, H. Bading and M. E. Greenberg, 'Calcium regulation of gene expression in neuronal cells', *J Neurobiol*, 25: 3, Mar 1994, 294-303.
- 144 J. Kasahara, K. Fukunaga and E. Miyamoto, 'Activation of calcium/calmodulin-dependent protein kinase IV in long term potentiation in the rat hippocampal CA1 region', *J Biol Chem*, 276: 26, Jun 2001, 24044-24050.
- 145 B. Lee, G. Q. Butcher, K. R. Hoyt, S. Impey and K. Obrietan, 'Activity-dependent neuroprotection and cAMP response element-binding protein (CREB): kinase coupling, stimulus intensity, and temporal regulation of CREB phosphorylation at serine 133', *J Neurosci*, 25: 5, Feb 2005, 1137-1148.
- 146 D. Tardito, E. Tiraboschi, J. Kasahara, G. Racagni and M. Popoli, 'Reduced CREB phosphorylation after chronic lithium treatment is associated with down-regulation of CaM kinase IV in rat hippocampus', *Int J Neuropsychopharmacol*, 10: 4, Aug 2007, 491-496.
- 147 E. Tiraboschi, D. Tardito, J. Kasahara, S. Moraschi, P. Pruneri, M. Gennarelli, G. Racagni and M. Popoli, 'Selective phosphorylation of nuclear CREB by fluoxetine is linked to activation of CaM kinase IV and MAP kinase cascades', *Neuropsychopharmacology*, 29: 10, Oct 2004, 1831-1840.
- 148 E. R. Kandel, 'The molecular biology of memory storage: a dialogue between genes and synapses', *Science*, 294: 5544, Nov 2001, 1030-1038.
- 149 P. T. Pang, H. K. Teng, E. Zaitsev, N. T. Woo, K. Sakata, S. Zhen, K. K. Teng, W. H. Yung, B. L. Hempstead and B. Lu, 'Cleavage of proBDNF by tPA/plasmin is essential for long-term hippocampal plasticity', *Science*, 306: 5695, Oct 2004, 487-491.
- 150 B. Mayr and M. Montminy, 'Transcriptional regulation by the phosphorylation-dependent factor CREB', *Nat Rev Mol Cell Biol*, 2: 8, Aug 2001, 599-609.

- 151 A. E. West, E. C. Griffith and M. E. Greenberg, 'Regulation of transcription factors by neuronal activity', *Nat Rev Neurosci*, 3: 12, Dec 2002, 921-931.
- 152 B. E. Lonze and D. D. Ginty, 'Function and regulation of CREB family transcription factors in the nervous system', *Neuron*, 35: 4, Aug 2002, 605-623.
- 153 W. A. Carlezon, R. S. Duman and E. J. Nestler, 'The many faces of CREB', *Trends Neurosci*, 28: 8, Aug 2005, 436-445.
- 154 K. Deisseroth, H. Bito and R. W. Tsien, 'Signaling from synapse to nucleus: postsynaptic CREB phosphorylation during multiple forms of hippocampal synaptic plasticity', *Neuron*, 16: 1, Jan 1996, 89-101.
- 155 W. G. Chen, Q. Chang, Y. Lin, A. Meissner, A. E. West, E. C. Griffith, R. Jaenisch and M. E. Greenberg, 'Derepression of BDNF transcription involves calcium-dependent phosphorylation of MeCP2', *Science*, 302: 5646, Oct 2003, 885-889.
- 156 K. Martinowich, H. Manji and B. Lu, 'New insights into BDNF function in depression and anxiety', *Nat Neurosci*, 10: 9, Sep 2007, 1089-1093.
- 157 J. O. Groves, 'Is it time to reassess the BDNF hypothesis of depression?', *Mol Psychiatry*, 12: 12, Dec 2007, 1079-1088.
- 158 J. W. Wang, A. Dranovsky and R. Hen, 'The when and where of BDNF and the antidepressant response', *Biol Psychiatry*, 63: 7, Apr 2008, 640-641.
- 159 M. Roceri, F. Cirulli, C. Pessina, P. Peretto, G. Racagni and M. A. Riva, 'Postnatal repeated maternal deprivation produces age-dependent changes of brain-derived neurotrophic factor expression in selected rat brain regions', *Biol Psychiatry*, 55: 7, Apr 2004, 708-714.
- 160 A. E. West, W. G. Chen, M. B. Dalva, R. E. Dolmetsch, J. M. Kornhauser, A. J. Shaywitz, M. A. Takasu, X. Tao and M. E. Greenberg, 'Calcium regulation of neuronal gene expression', *Proc Natl Acad Sci U S A*, 98: 20, Sep 2001, 11024-11031.
- 161 E. Tongiorgi, L. Domenici and M. Simonato, 'What is the biological significance of BDNF mRNA targeting in the dendrites? Clues from epilepsy and cortical development', *Mol Neurobiol*, 33: 1, Feb 2006, 17-32.
- 162 A. Gärtner and V. Staiger, 'Neurotrophin secretion from hippocampal neurons evoked by long-term-potential-inducing electrical stimulation patterns', *Proc Natl Acad Sci U S A*, 99: 9, Apr 2002, 6386-6391.
- 163 M. Hartmann, R. Heumann and V. Lessmann, 'Synaptic secretion of BDNF after high-frequency stimulation of glutamatergic synapses', *EMBO J*, 20: 21, Nov 2001, 5887-5897.
- 164 I. J. Lever, E. J. Bradbury, J. R. Cunningham, D. W. Adelson, M. G. Jones, S. B. McMahon, J. C. Marvizón and M. Malcangio, 'Brain-derived neurotrophic factor is released in the dorsal horn by distinctive patterns of afferent fiber stimulation', *J Neurosci*, 21: 12, Jun 2001, 4469-4477.
- 165 C. T. Drake, T. A. Milner and S. L. Patterson, 'Ultrastructural localization of full-length trkB immunoreactivity in rat hippocampus suggests multiple roles in modulating activity-dependent synaptic plasticity', *J Neurosci*, 19: 18, Sep 1999, 8009-8026.
- 166 C. Aoki, K. Wu, A. Elste, G. Len, S. Lin, G. McAuliffe and I. B. Black, 'Localization of brain-derived neurotrophic factor and TrkB receptors to postsynaptic densities of adult rat cerebral cortex', *J Neurosci Res*, 59: 3, Feb 2000, 454-463.
- 167 H. Husi, M. A. Ward, J. S. Choudhary, W. P. Blackstock and S. G. Grant, 'Proteomic analysis of NMDA receptor-adhesion protein signaling complexes', *Nat Neurosci*, 3: 7, Jul 2000, 661-669.
- 168 Y. Ji, P. T. Pang, L. Feng and B. Lu, 'Cyclic AMP controls BDNF-induced TrkB phosphorylation and dendritic spine formation in mature hippocampal neurons', *Nat Neurosci*, 8: 2, Feb 2005, 164-172.
- 169 A. Yoshii and M. Constantine-Paton, 'BDNF induces transport of PSD-95 to dendrites through PI3K-AKT signaling after NMDA receptor activation', *Nat Neurosci*, 10: 6, Jun 2007, 702-711.
- 170 A. Yoshii and M. Constantine-Paton, 'Postsynaptic localization of PSD-95 is regulated by all three pathways downstream of TrkB signaling', *Front Synaptic Neurosci*, 6: 2014, 6.
- 171 S. Biffo, N. Offenhäuser, B. D. Carter and Y. A. Barde, 'Selective binding and internalisation by truncated receptors restrict the availability of BDNF during development', *Development*, 121: 8, Aug 1995, 2461-2470.

- 172 K. Hashimoto, E. Shimizu and M. Iyo, 'Critical role of brain-derived neurotrophic factor in mood disorders', *Brain Res Brain Res Rev*, 45: 2, May 2004, 104-114.
- 173 J. T. Cunningham, J. T. Rodgers, D. H. Arlow, F. Vazquez, V. K. Mootha and P. Puigserver, 'mTOR controls mitochondrial oxidative function through a YY1-PGC-1 α transcriptional complex', *Nature*, 450: 7170, Nov 2007, 736-740.
- 174 P. Puigserver and B. M. Spiegelman, 'Peroxisome proliferator-activated receptor- γ coactivator 1 α (PGC-1 α): transcriptional coactivator and metabolic regulator', *Endocr Rev*, 24: 1, Feb 2003, 78-90.
- 175 K. Düvel, J. L. Yecies, S. Menon, P. Raman, A. I. Lipovsky, A. L. Souza, E. Triantafellow, Q. Ma, R. Gorski, S. Cleaver, M. G. Vander Heiden, J. P. MacKeigan, P. M. Finan, C. B. Clish, L. O. Murphy and B. D. Manning, 'Activation of a metabolic gene regulatory network downstream of mTOR complex 1', *Mol Cell*, 39: 2, Jul 2010, 171-183.
- 176 P. Polak and M. N. Hall, 'mTOR and the control of whole body metabolism', *Curr Opin Cell Biol*, 21: 2, Apr 2009, 209-218.
- 177 S. M. Schieke, D. Phillips, J. P. McCoy, A. M. Aponte, R. F. Shen, R. S. Balaban and T. Finkel, 'The mammalian target of rapamycin (mTOR) pathway regulates mitochondrial oxygen consumption and oxidative capacity', *J Biol Chem*, 281: 37, Sep 2006, 27643-27652.
- 178 P. Bekinschtein, C. Katche, L. N. Slipczuk, L. M. Igaz, M. Cammarota, I. Izquierdo and J. H. Medina, 'mTOR signaling in the hippocampus is necessary for memory formation', *Neurobiol Learn Mem*, 87: 2, Feb 2007, 303-307.
- 179 N. Li, B. Lee, R. J. Liu, M. Banasr, J. M. Dwyer, M. Iwata, X. Y. Li, G. Aghajanian and R. S. Duman, 'mTOR-dependent synapse formation underlies the rapid antidepressant effects of NMDA antagonists', *Science*, 329: 5994, Aug 2010, 959-964.
- 180 H. Yang, D. G. Rudge, J. D. Koos, B. Vaidialingam, H. J. Yang and N. P. Pavletich, 'mTOR kinase structure, mechanism and regulation', *Nature*, 497: 7448, May 2013, 217-223.
- 181 N. Li, R. J. Liu, J. M. Dwyer, M. Banasr, B. Lee, H. Son, X. Y. Li, G. Aghajanian and R. S. Duman, 'Glutamate N-methyl-D-aspartate receptor antagonists rapidly reverse behavioral and synaptic deficits caused by chronic stress exposure', *Biol Psychiatry*, 69: 8, Apr 2011, 754-761.
- 182 F. Karege, G. Vaudan, M. Schwald, N. Perroud and R. La Harpe, 'Neurotrophin levels in postmortem brains of suicide victims and the effects of antemortem diagnosis and psychotropic drugs', *Brain Res Mol Brain Res*, 136: 1-2, May 2005, 29-37.
- 183 M. Korte, P. Carroll, E. Wolf, G. Brem, H. Thoenen and T. Bonhoeffer, 'Hippocampal long-term potentiation is impaired in mice lacking brain-derived neurotrophic factor', *Proc Natl Acad Sci U S A*, 92: 19, Sep 1995, 8856-8860.
- 184 J. M. Gatt, C. B. Nemeroff, C. Dobson-Stone, R. H. Paul, R. A. Bryant, P. R. Schofield, E. Gordon, A. H. Kemp and L. M. Williams, 'Interactions between BDNF Val66Met polymorphism and early life stress predict brain and arousal pathways to syndromal depression and anxiety', *Mol Psychiatry*, 14: 7, Jul 2009, 681-695.
- 185 O. Berton, C. A. McClung, R. J. Dileone, V. Krishnan, W. Renthal, S. J. Russo, D. Graham, N. M. Tsankova, C. A. Bolanos, M. Rios, L. M. Monteggia, D. W. Self and E. J. Nestler, 'Essential role of BDNF in the mesolimbic dopamine pathway in social defeat stress', *Science*, 311: 5762, Feb 2006, 864-868.
- 186 M. Adachi, M. Barrot, A. E. Autry, D. Theobald and L. M. Monteggia, 'Selective loss of brain-derived neurotrophic factor in the dentate gyrus attenuates antidepressant efficacy', *Biol Psychiatry*, 63: 7, Apr 2008, 642-649.
- 187 Y. Shirayama, A. C. Chen, S. Nakagawa, D. S. Russell and R. S. Duman, 'Brain-derived neurotrophic factor produces antidepressant effects in behavioral models of depression', *J Neurosci*, 22: 8, Apr 2002, 3251-3261.
- 188 V. Pencea, K. D. Bingaman, S. J. Wiegand and M. B. Luskin, 'Infusion of brain-derived neurotrophic factor into the lateral ventricle of the adult rat leads to new neurons in the parenchyma of the striatum, septum, thalamus, and hypothalamus', *J Neurosci*, 21: 17, Sep 2001, 6706-6717.
- 189 T. Zigova, V. Pencea, S. J. Wiegand and M. B. Luskin, 'Intraventricular administration of BDNF increases the number of newly generated neurons in the adult olfactory bulb', *Mol Cell Neurosci*, 11: 4, Jul 1998, 234-245.

- 190 S. L. Patterson, T. Abel, T. A. Deuel, K. C. Martin, J. C. Rose and E. R. Kandel, 'Recombinant BDNF rescues deficits in basal synaptic transmission and hippocampal LTP in BDNF knockout mice', *Neuron*, 16: 6, Jun 1996, 1137-1145.
- 191 H. Kang, A. A. Welcher, D. Shelton and E. M. Schuman, 'Neurotrophins and time: different roles for TrkB signaling in hippocampal long-term potentiation', *Neuron*, 19: 3, Sep 1997, 653-664.
- 192 P. Bekinschtein, M. Cammarota, L. M. Izquierdo, L. R. Bevilaqua, I. Izquierdo and J. H. Medina, 'Persistence of long-term memory storage requires a late protein synthesis- and BDNF- dependent phase in the hippocampus', *Neuron*, 53: 2, Jan 2007, 261-277.
- 193 W. J. Tyler and L. D. Pozzo-Miller, 'BDNF enhances quantal neurotransmitter release and increases the number of docked vesicles at the active zones of hippocampal excitatory synapses', *J Neurosci*, 21: 12, Jun 2001, 4249-4258.
- 194 D. Ongür, W. C. Drevets and J. L. Price, 'Glial reduction in the subgenual prefrontal cortex in mood disorders', *Proc Natl Acad Sci U S A*, 95: 22, Oct 1998, 13290-13295.
- 195 D. Cotter, D. Mackay, S. Landau, R. Kerwin and I. Everall, 'Reduced glial cell density and neuronal size in the anterior cingulate cortex in major depressive disorder', *Arch Gen Psychiatry*, 58: 6, Jun 2001, 545-553.
- 196 M. P. Bowley, W. C. Drevets, D. Ongür and J. L. Price, 'Low glial numbers in the amygdala in major depressive disorder', *Biol Psychiatry*, 52: 5, Sep 2002, 404-412.
- 197 B. Moghaddam, 'Stress preferentially increases extraneuronal levels of excitatory amino acids in the prefrontal cortex: comparison to hippocampus and basal ganglia', *J Neurochem*, 60: 5, May 1993, 1650-1657.
- 198 J. Bagley and B. Moghaddam, 'Temporal dynamics of glutamate efflux in the prefrontal cortex and in the hippocampus following repeated stress: effects of pretreatment with saline or diazepam', *Neuroscience*, 77: 1, Mar 1997, 65-73.
- 199 C. Venero and J. Borrell, 'Rapid glucocorticoid effects on excitatory amino acid levels in the hippocampus: a microdialysis study in freely moving rats', *Eur J Neurosci*, 11: 7, Jul 1999, 2465-2473.
- 200 M. T. Lowy, L. Gault and B. K. Yamamoto, 'Adrenalectomy attenuates stress-induced elevations in extracellular glutamate concentrations in the hippocampus', *J Neurochem*, 61: 5, Nov 1993, 1957-1960.
- 201 Y. Watanabe, E. Gould and B. S. McEwen, 'Stress induces atrophy of apical dendrites of hippocampal CA3 pyramidal neurons', *Brain Res*, 588: 2, Aug 1992, 341-345.
- 202 J. M. Gorman and J. P. Docherty, 'A hypothesized role for dendritic remodeling in the etiology of mood and anxiety disorders', *J Neuropsychiatry Clin Neurosci*, 22: 32010, 256-264.
- 203 A. Holmes and C. L. Wellman, 'Stress-induced prefrontal reorganization and executive dysfunction in rodents', *Neurosci Biobehav Rev*, 33: 6, Jun 2009, 773-783.
- 204 B. S. McEwen and A. M. Magarinos, 'Stress and hippocampal plasticity: implications for the pathophysiology of affective disorders', *Hum Psychopharmacol*, 16: S1, Jan 2001, S7-S19.
- 205 B. S. McEwen, 'Glucocorticoids, depression, and mood disorders: structural remodeling in the brain', *Metabolism*, 54: 5 Suppl 1, May 2005, 20-23.
- 206 R. M. Shansky and J. H. Morrison, 'Stress-induced dendritic remodeling in the medial prefrontal cortex: effects of circuit, hormones and rest', *Brain Res*, 1293, Oct 2009, 108-113.
- 207 R. M. Shansky, C. Hamo, P. R. Hof, B. S. McEwen and J. H. Morrison, 'Stress-induced dendritic remodeling in the prefrontal cortex is circuit specific', *Cereb Cortex*, 19: 10, Oct 2009, 2479-2484.
- 208 D. M. Diamond, A. M. Campbell, C. R. Park, J. Halonen and P. R. Zoladz, 'The temporal dynamics model of emotional memory processing: a synthesis on the neurobiological basis of stress-induced amnesia, flashbulb and traumatic memories, and the Yerkes-Dodson law', *Neural Plast*, 20072007, 60803.
- 209 C. A. Altamura, M. C. Mauri, A. Ferrara, A. R. Moro, G. D'Andrea and F. Zamberlan, 'Plasma and platelet excitatory amino acids in psychiatric disorders', *Am J Psychiatry*, 150: 11, Nov 1993, 1731-1733.
- 210 K. Hashimoto, A. Sawa and M. Iyo, 'Increased levels of glutamate in brains from patients with mood disorders', *Biol Psychiatry*, 62: 11, Dec 2007, 1310-1316.

- 211 W. C. Drevets, 'Neuroimaging studies of mood disorders', *Biol Psychiatry*, 48: 8, Oct 2000, 813-829.
- 212 G. Sanacora, R. Gueorguieva, C. N. Epperson, Y. T. Wu, M. Appel, D. L. Rothman, J. H. Krystal and G. F. Mason, 'Subtype-specific alterations of gamma-aminobutyric acid and glutamate in patients with major depression', *Arch Gen Psychiatry*, 61: 7, Jul 2004, 705-713.
- 213 G. Sanacora, C. A. Zarate, J. H. Krystal and H. K. Manji, 'Targeting the glutamatergic system to develop novel, improved therapeutics for mood disorders', *Nat Rev Drug Discov*, 7: 5, May 2008, 426-437.
- 214 M. Maes, R. Verkerk, E. Vandoolaeghe, A. Lin and S. Scharpé, 'Serum levels of excitatory amino acids, serine, glycine, histidine, threonine, taurine, alanine and arginine in treatment-resistant depression: modulation by treatment with antidepressants and prediction of clinical responsivity', *Acta Psychiatr Scand*, 97: 4, Apr 1998, 302-308.
- 215 C. Altamura, M. Maes, J. Dai and H. Y. Meltzer, 'Plasma concentrations of excitatory amino acids, serine, glycine, taurine and histidine in major depression', *Eur Neuropsychopharmacol*, 5 Suppl1995, 71-75.
- 216 M. Castillo, L. Kwock, H. Courvoisier and S. R. Hooper, 'Proton MR spectroscopy in children with bipolar affective disorder: preliminary observations', *AJNR Am J Neuroradiol*, 21: 5, May 2000, 832-838.
- 217 N. Michael, A. Erfurth, P. Ohrmann, V. Arolt, W. Heindel and B. Pfeleiderer, 'Metabolic changes within the left dorsolateral prefrontal cortex occurring with electroconvulsive therapy in patients with treatment resistant unipolar depression', *Psychol Med*, 33: 7, Oct 2003, 1277-1284.
- 218 D. P. Auer, B. Pütz, E. Kraft, B. Lipinski, J. Schill and F. Holsboer, 'Reduced glutamate in the anterior cingulate cortex in depression: an in vivo proton magnetic resonance spectroscopy study', *Biol Psychiatry*, 47: 4, Feb 2000, 305-313.
- 219 Y. Mirza, J. Tang, A. Russell, S. P. Banerjee, R. Bhandari, J. Ivey, M. Rose, G. J. Moore and D. R. Rosenberg, 'Reduced anterior cingulate cortex glutamatergic concentrations in childhood major depression', *J Am Acad Child Adolesc Psychiatry*, 43: 3, Mar 2004, 341-348.
- 220 D. R. Rosenberg, F. P. Macmaster, Y. Mirza, J. M. Smith, P. C. Easter, S. P. Banerjee, R. Bhandari, C. Boyd, M. Lynch, M. Rose, J. Ivey, R. A. Villafuerte, G. J. Moore and P. Renshaw, 'Reduced anterior cingulate glutamate in pediatric major depression: a magnetic resonance spectroscopy study', *Biol Psychiatry*, 58: 9, Nov 2005, 700-704.
- 221 B. Pfeleiderer, N. Michael, A. Erfurth, P. Ohrmann, U. Hohmann, M. Wolgast, M. Fiebich, V. Arolt and W. Heindel, 'Effective electroconvulsive therapy reverses glutamate/glutamine deficit in the left anterior cingulum of unipolar depressed patients', *Psychiatry Res*, 122: 3, Apr 2003, 185-192.
- 222 G. Bonanno, R. Giambelli, L. Raiteri, E. Tiraboschi, S. Zappettini, L. Musazzi, M. Raiteri, G. Racagni and M. Popoli, 'Chronic antidepressants reduce depolarization-evoked glutamate release and protein interactions favoring formation of SNARE complex in hippocampus', *J Neurosci*, 25: 13, Mar 2005, 3270-3279.
- 223 A. Bouron and J. Y. Chatton, 'Acute application of the tricyclic antidepressant desipramine presynaptically stimulates the exocytosis of glutamate in the hippocampus', *Neuroscience*, 90: 3, Mar 1999, 729-736.
- 224 P. V. Choudary, M. Molnar, S. J. Evans, H. Tomita, J. Z. Li, M. P. Vawter, R. M. Myers, W. E. Bunney, H. Akil, S. J. Watson and E. G. Jones, 'Altered cortical glutamatergic and GABAergic signal transmission with glial involvement in depression', *Proc Natl Acad Sci U S A*, 102: 43, Oct 2005, 15653-15658.
- 225 R. M. Tordera, Q. Pei and T. Sharp, 'Evidence for increased expression of the vesicular glutamate transporter, VGLUT1, by a course of antidepressant treatment', *J Neurochem*, 94: 4, Aug 2005, 875-883.
- 226 L. Moutsimilli, S. Farley, S. Dumas, S. El Mestikawy, B. Giros and E. T. Zavara, 'Selective cortical VGLUT1 increase as a marker for antidepressant activity', *Neuropharmacology*, 49: 6, Nov 2005, 890-900.

- 227 R. E. McCullumsmith and J. H. Meador-Woodruff, 'Striatal excitatory amino acid transporter transcript expression in schizophrenia, bipolar disorder, and major depressive disorder', *Neuropsychopharmacology*, 26: 3, Mar 2002, 368-375.
- 228 A. J. Law and J. F. Deakin, 'Asymmetrical reductions of hippocampal NMDAR1 glutamate receptor mRNA in the psychoses', *Neuroreport*, 12: 13, Sep 2001, 2971-2974.
- 229 R. E. McCullumsmith, L. V. Kristiansen, M. Beneyto, E. Scarr, B. Dean and J. H. Meador-Woodruff, 'Decreased NR1, NR2A, and SAP102 transcript expression in the hippocampus in bipolar disorder', *Brain Res*, 1127: 1, Jan 2007, 108-118.
- 230 E. Scarr, G. Pavey, S. Sundram, A. MacKinnon and B. Dean, 'Decreased hippocampal NMDA, but not kainate or AMPA receptors in bipolar disorder', *Bipolar Disord*, 5: 4, Aug 2003, 257-264.
- 231 C. Toro and J. F. Deakin, 'NMDA receptor subunit NR1 and postsynaptic protein PSD-95 in hippocampus and orbitofrontal cortex in schizophrenia and mood disorder', *Schizophr Res*, 80: 2-3, Dec 2005, 323-330.
- 232 C. Rocher, M. Spedding, C. Munoz and T. M. Jay, 'Acute stress-induced changes in hippocampal/prefrontal circuits in rats: effects of antidepressants', *Cereb Cortex*, 14: 2, Feb 2004, 224-229.
- 233 A. C. Shakesby, R. Anwyl and M. J. Rowan, 'Overcoming the effects of stress on synaptic plasticity in the intact hippocampus: rapid actions of serotonergic and antidepressant agents', *J Neurosci*, 22: 9, May 2002, 3638-3644.
- 234 J. C. Von Frijtag, A. Kamal, L. G. Reijmers, L. H. Schrama, R. van den Bos and B. M. Spruijt, 'Chronic imipramine treatment partially reverses the long-term changes of hippocampal synaptic plasticity in socially stressed rats', *Neurosci Lett*, 309: 3, Aug 2001, 153-156.
- 235 H. Qi, F. Mailliet, M. Spedding, C. Rocher, X. Zhang, P. Delagrangé, B. McEwen, T. M. Jay and P. Svenningsson, 'Antidepressants reverse the attenuation of the neurotrophic MEK/MAPK cascade in frontal cortex by elevated platform stress; reversal of effects on LTP is associated with GluA1 phosphorylation', *Neuropharmacology*, 56: 1, Jan 2009, 37-46.
- 236 R. Martínez-Turrillas, D. Frechilla and J. Del Río, 'Chronic antidepressant treatment increases the membrane expression of AMPA receptors in rat hippocampus', *Neuropharmacology*, 43: 8, Dec 2002, 1230-1237.
- 237 J. Du, N. A. Gray, C. Falke, P. Yuan, S. Szabo and H. K. Manji, 'Structurally dissimilar antimanic agents modulate synaptic plasticity by regulating AMPA glutamate receptor subunit GluR1 synaptic expression', *Ann N Y Acad Sci*, 1003, Nov 2003, 378-380.
- 238 J. Du, N. A. Gray, C. A. Falke, W. Chen, P. Yuan, S. T. Szabo, H. Einat and H. K. Manji, 'Modulation of synaptic plasticity by antimanic agents: the role of AMPA glutamate receptor subunit 1 synaptic expression', *J Neurosci*, 24: 29, Jul 2004, 6578-6589.
- 239 J. Du, R. Machado-Vieira, S. Maeng, K. Martinowich, H. K. Manji and C. A. Zarate, 'Enhancing AMPA to NMDA throughput as a convergent mechanism for antidepressant action', *Drug Discov Today Ther Strateg*, 3: 42006, 519-526.
- 240 S. Maeng, C. A. Zarate, J. Du, R. J. Schloesser, J. McCammon, G. Chen and H. K. Manji, 'Cellular mechanisms underlying the antidepressant effects of ketamine: role of alpha-amino-3-hydroxy-5-methylisoxazole-4-propionic acid receptors', *Biol Psychiatry*, 63: 4, Feb 2008, 349-352.
- 241 I. A. Paul and P. Skolnick, 'Glutamate and depression: clinical and preclinical studies', *Ann N Y Acad Sci*, 1003, Nov 2003, 250-272.
- 242 P. A. Boyer, P. Skolnick and L. H. Fossom, 'Chronic administration of imipramine and citalopram alters the expression of NMDA receptor subunit mRNAs in mouse brain. A quantitative in situ hybridization study', *J Mol Neurosci*, 10: 3, Jun 1998, 219-233.
- 243 A. E. Autry, M. Adachi, E. Nosyreva, E. S. Na, M. F. Los, P. F. Cheng, E. T. Kavalali and L. M. Monteggia, 'NMDA receptor blockade at rest triggers rapid behavioural antidepressant responses', *Nature*, 475: 7354, Jul 2011, 91-95.
- 244 R. M. Berman, A. Cappiello, A. Anand, D. A. Oren, G. R. Heninger, D. S. Charney and J. H. Krystal, 'Antidepressant effects of ketamine in depressed patients', *Biol Psychiatry*, 47: 4, Feb 2000, 351-354.

- 245 K. Hirota and D. G. Lambert, 'Ketamine: its mechanism(s) of action and unusual clinical uses', *Br J Anaesth*, 77: 4, Oct 1996, 441-444.
- 246 J. H. Krystal, D. C. D'Souza, I. L. Petrakis, A. Belger, R. M. Berman, D. S. Charney, W. Abi-Saab and S. Madonick, 'NMDA agonists and antagonists as probes of glutamatergic dysfunction and pharmacotherapies in neuropsychiatric disorders', *Harv Rev Psychiatry*, 7: 3, 1999 Sep-Oct 1999, 125-143.
- 247 J. H. Krystal, G. Sanacora, H. Blumberg, A. Anand, D. S. Charney, G. Marek, C. N. Epperson, A. Goddard and G. F. Mason, 'Glutamate and GABA systems as targets for novel antidepressant and mood-stabilizing treatments', *Mol Psychiatry*, 7 Suppl 12002, S71-80.
- 248 J. H. Krystal, G. Sanacora and R. S. Duman, 'Rapid-acting glutamatergic antidepressants: the path to ketamine and beyond', *Biol Psychiatry*, 73: 12, Jun 2013, 1133-1141.
- 249 K. Kashiwagi, T. Masuko, C. D. Nguyen, T. Kuno, I. Tanaka, K. Igarashi and K. Williams, 'Channel blockers acting at N-methyl-D-aspartate receptors: differential effects of mutations in the vestibule and ion channel pore', *Mol Pharmacol*, 61: 3, Mar 2002, 533-545.
- 250 S. E. Kotermanski and J. W. Johnson, 'Mg²⁺ imparts NMDA receptor subtype selectivity to the Alzheimer's drug memantine', *J Neurosci*, 29: 9, Mar 2009, 2774-2779.
- 251 M. aan het Rot, K. A. Collins, J. W. Murrough, A. M. Perez, D. L. Reich, D. S. Charney and S. J. Mathew, 'Safety and efficacy of repeated-dose intravenous ketamine for treatment-resistant depression', *Biol Psychiatry*, 67: 2, Jan 2010, 139-145.
- 252 N. Diazgranados, L. Ibrahim, N. E. Brutsche, A. Newberg, P. Kronstein, S. Khalife, W. A. Kammerer, Z. Quezado, D. A. Luckenbaugh, G. Salvatore, R. Machado-Vieira, H. K. Manji and C. A. Zarate, 'A randomized add-on trial of an N-methyl-D-aspartate antagonist in treatment-resistant bipolar depression', *Arch Gen Psychiatry*, 67: 8, Aug 2010, 793-802.
- 253 G. L. Larkin and A. L. Beautrais, 'A preliminary naturalistic study of low-dose ketamine for depression and suicide ideation in the emergency department', *Int J Neuropsychopharmacol*, 14: 8, Sep 2011, 1127-1131.
- 254 M. Chatterjee, S. Ganguly, M. Srivastava and G. Palit, 'Effect of 'chronic' versus 'acute' ketamine administration and its 'withdrawal' effect on behavioural alterations in mice: implications for experimental psychosis', *Behav Brain Res*, 216: 1, Jan 2011, 247-254.
- 255 M. Chatterjee, R. Verma, S. Ganguly and G. Palit, 'Neurochemical and molecular characterization of ketamine-induced experimental psychosis model in mice', *Neuropharmacology*, 63: 6, Nov 2012, 1161-1171.
- 256 N. R. Swerdlow, N. Taaid, J. L. Oostwegel, E. Randolph and M. A. Geyer, 'Towards a cross-species pharmacology of sensorimotor gating: effects of amantadine, bromocriptine, pergolide and ropinirole on prepulse inhibition of acoustic startle in rats', *Behav Pharmacol*, 9: 5-6, Sep 1998, 389-396.
- 257 J. Cilia, P. Hatcher, C. Reavill and D. N. Jones, '(+/-) Ketamine-induced prepulse inhibition deficits of an acoustic startle response in rats are not reversed by antipsychotics', *J Psychopharmacol*, 21: 3, May 2007, 302-311.
- 258 D. C. Javitt and S. R. Zukin, 'Recent advances in the phencyclidine model of schizophrenia', *Am J Psychiatry*, 148: 10, Oct 1991, 1301-1308.
- 259 L. S. Garcia, C. M. Comim, S. S. Valvassori, G. Z. Réus, L. M. Barbosa, A. C. Andreazza, L. Stertz, G. R. Fries, E. C. Gavioli, F. Kapczinski and J. Quevedo, 'Acute administration of ketamine induces antidepressant-like effects in the forced swimming test and increases BDNF levels in the rat hippocampus', *Prog Neuropsychopharmacol Biol Psychiatry*, 32: 1, Jan 2008, 140-144.
- 260 L. S. Garcia, C. M. Comim, S. S. Valvassori, G. Z. Réus, L. Stertz, F. Kapczinski, E. C. Gavioli and J. Quevedo, 'Ketamine treatment reverses behavioral and physiological alterations induced by chronic mild stress in rats', *Prog Neuropsychopharmacol Biol Psychiatry*, 33: 3, Apr 2009, 450-455.
- 261 H. Koike, M. Iijima and S. Chaki, 'Involvement of AMPA receptor in both the rapid and sustained antidepressant-like effects of ketamine in animal models of depression', *Behav Brain Res*, 224: 1, Oct 2011, 107-111.
- 262 P. Zanos, R. Moaddel, P. J. Morris, P. Georgiou, J. Fischell, G. I. Elmer, M. Alkondon, P. Yuan, H. J. Pribut, N. S. Singh, K. S. Dossou, Y. Fang, X. P. Huang, C. L. Mayo, I. W. Wainer, E. X. Albuquerque,

- S. M. Thompson, C. J. Thomas, C. A. Zarate and T. D. Gould, 'NMDAR inhibition-independent antidepressant actions of ketamine metabolites', *Nature*, 533: 7604, May 2016, 481-486.
- 263 B. Voleti, A. Navarria, R. J. Liu, M. Banasr, N. Li, R. Terwilliger, G. Sanacora, T. Eid, G. Aghajanian and R. S. Duman, 'Scopolamine rapidly increases mammalian target of rapamycin complex 1 signaling, synaptogenesis, and antidepressant behavioral responses', *Biol Psychiatry*, 74: 10, Nov 2013, 742-749.
- 264 E. Beurel, L. Song and R. S. Jope, 'Inhibition of glycogen synthase kinase-3 is necessary for the rapid antidepressant effect of ketamine in mice', *Mol Psychiatry*, 16: 11, Nov 2011, 1068-1070.
- 265 H. Homayoun and B. Moghaddam, 'NMDA receptor hypofunction produces opposite effects on prefrontal cortex interneurons and pyramidal neurons', *J Neurosci*, 27: 43, Oct 2007, 11496-11500.
- 266 B. Moghaddam, B. Adams, A. Verma and D. Daly, 'Activation of glutamatergic neurotransmission by ketamine: a novel step in the pathway from NMDA receptor blockade to dopaminergic and cognitive disruptions associated with the prefrontal cortex', *J Neurosci*, 17: 8, Apr 1997, 2921-2927.
- 267 O. H. Miller, J. T. Moran and B. J. Hall, 'Two cellular hypotheses explaining the initiation of ketamine's antidepressant actions: Direct inhibition and disinhibition', *Neuropharmacology*, 100, Jan 2016, 17-26.
- 268 O. H. Miller, L. Yang, C. C. Wang, E. A. Hargroder, Y. Zhang, E. Delpire and B. J. Hall, 'GluN2B-containing NMDA receptors regulate depression-like behavior and are critical for the rapid antidepressant actions of ketamine', *Elife*, 32014, e03581.
- 269 S. H. Preskorn, B. Baker, S. Kolluri, F. S. Menniti, M. Krams and J. W. Landen, 'An innovative design to establish proof of concept of the antidepressant effects of the NR2B subunit selective N-methyl-D-aspartate antagonist, CP-101,606, in patients with treatment-refractory major depressive disorder', *J Clin Psychopharmacol*, 28: 6, Dec 2008, 631-637.
- 270 C. C. Wang, R. G. Held, S. C. Chang, L. Yang, E. Delpire, A. Ghosh and B. J. Hall, 'A critical role for GluN2B-containing NMDA receptors in cortical development and function', *Neuron*, 72: 5, Dec 2011, 789-805.
- 271 C. C. Wang, R. G. Held and B. J. Hall, 'SynGAP regulates protein synthesis and homeostatic synaptic plasticity in developing cortical networks', *PLoS One*, 8: 122013, e83941.
- 272 J. A. Gray, Y. Shi, H. Usui, M. J. Doring, K. Sakimura and R. A. Nicoll, 'Distinct modes of AMPA receptor suppression at developing synapses by GluN2A and GluN2B: single-cell NMDA receptor subunit deletion in vivo', *Neuron*, 71: 6, Sep 2011, 1085-1101.
- 273 R. G. Paredes and A. Agmo, 'GABA and behavior: the role of receptor subtypes', *Neurosci Biobehav Rev*, 16: 21992, 145-170.
- 274 G. Sanacora, G. F. Mason and J. H. Krystal, 'Impairment of GABAergic transmission in depression: new insights from neuroimaging studies', *Crit Rev Neurobiol*, 14: 12000, 23-45.
- 275 A. R. Calver, C. H. Davies and M. Pangalos, 'GABA(B) receptors: from monogamy to promiscuity', *Neurosignals*, 11: 6, 2002 Nov-Dec 2002, 299-314.
- 276 M. J. Millan, 'The neurobiology and control of anxious states', *Prog Neurobiol*, 70: 2, Jun 2003, 83-244.
- 277 P. Brambilla, J. Perez, F. Barale, G. Schettini and J. C. Soares, 'GABAergic dysfunction in mood disorders', *Mol Psychiatry*, 8: 8, Aug 2003, 721-737, 715.
- 278 H. M. Emrich, D. von Zerssen, W. Kissling, H. J. Möller and A. Windorfer, 'Effect of sodium valproate on mania. The GABA-hypothesis of affective disorders', *Arch Psychiatr Nervenkr (1970)*, 229: 11980, 1-16.
- 279 M. Otsuka, L. L. Iversen, Z. W. Hall and E. A. Kravitz, 'Release of gamma-aminobutyric acid from inhibitory nerves of lobster', *Proc Natl Acad Sci U S A*, 56: 4, Oct 1966, 1110-1115.
- 280 B. Meldrum, 'GABA and acute psychoses', *Psychol Med*, 12: 1, Feb 1982, 1-5.
- 281 B. Meldrum, 'Pharmacology of GABA', *Clin Neuropharmacol*, 5: 31982, 293-316.
- 282 A. Guidotti, M. G. Corda, B. C. Wise, F. Vaccarino and E. Costa, 'GABAergic synapses. Supramolecular organization and biochemical regulation', *Neuropharmacology*, 22: 12B, Dec 1983, 1471-1479.

- 283 F. Petty, 'GABA and mood disorders: a brief review and hypothesis', *J Affect Disord*, 34: 4, Aug 1995, 275-281.
- 284 C. Boudaba, L. A. Schrader and J. G. Tasker, 'Physiological evidence for local excitatory synaptic circuits in the rat hypothalamus', *J Neurophysiol*, 77: 6, Jun 1997, 3396-3400.
- 285 C. Boudaba, K. Szabó and J. G. Tasker, 'Physiological mapping of local inhibitory inputs to the hypothalamic paraventricular nucleus', *J Neurosci*, 16: 22, Nov 1996, 7151-7160.
- 286 J. P. Herman, A. Renda and B. Bodie, 'Norepinephrine-gamma-aminobutyric acid (GABA) interaction in limbic stress circuits: effects of reboxetine on GABAergic neurons', *Biol Psychiatry*, 53: 2, Jan 2003, 166-174.
- 287 L. Peng, L. Hertz, R. Huang, U. Sonnewald, S. B. Petersen, N. Westergaard, O. Larsson and A. Schousboe, 'Utilization of glutamine and of TCA cycle constituents as precursors for transmitter glutamate and GABA', *Dev Neurosci*, 15: 3-5, 1993, 367-377.
- 288 A. Schousboe, N. Westergaard, U. Sonnewald, S. B. Petersen, R. Huang, L. Peng and L. Hertz, 'Glutamate and glutamine metabolism and compartmentation in astrocytes', *Dev Neurosci*, 15: 3-5, 1993, 359-366.
- 289 L. A. Borden, 'GABA transporter heterogeneity: pharmacology and cellular localization', *Neurochem Int*, 29: 4, Oct 1996, 335-356.
- 290 M. M. Durkin, K. E. Smith, L. A. Borden, R. L. Weinshank, T. A. Branchek and E. L. Gustafson, 'Localization of messenger RNAs encoding three GABA transporters in rat brain: an in situ hybridization study', *Brain Res Mol Brain Res*, 33: 1, Oct 1995, 7-21.
- 291 M. Eder, G. Rammes, W. Zieglgänsberger and H. U. Dodt, 'GABA(A) and GABA(B) receptors on neocortical neurons are differentially distributed', *Eur J Neurosci*, 13: 5, Mar 2001, 1065-1069.
- 292 E. Costa, J. Auta, D. R. Grayson, K. Matsumoto, G. D. Pappas, X. Zhang and A. Guidotti, 'GABAA receptors and benzodiazepines: a role for dendritic resident subunit mRNAs', *Neuropharmacology*, 43: 6, Nov 2002, 925-937.
- 293 J. Bormann, 'Electrophysiology of GABAA and GABAB receptor subtypes', *Trends Neurosci*, 11: 3, Mar 1988, 112-116.
- 294 R. L. Macdonald, R. E. Twyman, T. Ryan-Jastrow and T. P. Angelotti, 'Regulation of GABAA receptor channels by anticonvulsant and convulsant drugs and by phosphorylation', *Epilepsy Res Suppl*, 9, 1992, 265-277.
- 295 E. W. Karbon, R. S. Duman and S. J. Enna, 'GABAB receptors and norepinephrine-stimulated cAMP production in rat brain cortex', *Brain Res*, 306: 1-2, Jul 1984, 327-332.
- 296 M. Chebib and G. A. Johnston, 'The 'ABC' of GABA receptors: a brief review', *Clin Exp Pharmacol Physiol*, 26: 11, Nov 1999, 937-940.
- 297 M. Chebib, 'GABAC receptor ion channels', *Clin Exp Pharmacol Physiol*, 31: 11, Nov 2004, 800-804.
- 298 N. G. Bowery, B. Bettler, W. Froestl, J. P. Gallagher, F. Marshall, M. Raiteri, T. I. Bonner and S. J. Enna, 'International Union of Pharmacology. XXXIII. Mammalian gamma-aminobutyric acid(B) receptors: structure and function', *Pharmacol Rev*, 54: 2, Jun 2002, 247-264.
- 299 L. Hertz, 'The Glutamate-Glutamine (GABA) Cycle: Importance of Late Postnatal Development and Potential Reciprocal Interactions between Biosynthesis and Degradation', *Front Endocrinol (Lausanne)*, 4, 2013, 59.
- 300 G. X. Liu, G. Q. Cai, Y. Q. Cai, Z. J. Sheng, J. Jiang, Z. Mei, Z. G. Wang, L. Guo and J. Fei, 'Reduced anxiety and depression-like behaviors in mice lacking GABA transporter subtype 1', *Neuropsychopharmacology*, 32: 7, Jul 2007, 1531-1539.
- 301 K. G. Lloyd, F. Thuret and A. Pilc, 'Upregulation of gamma-aminobutyric acid (GABA) B binding sites in rat frontal cortex: a common action of repeated administration of different classes of antidepressants and electroshock', *J Pharmacol Exp Ther*, 235: 1, Oct 1985, 191-199.
- 302 N. Motohashi, K. Ikawa and T. Kariya, 'GABAB receptors are up-regulated by chronic treatment with lithium or carbamazepine. GABA hypothesis of affective disorders?', *Eur J Pharmacol*, 166: 1, Jul 1989, 95-99.

- 303 N. Motohashi, 'GABA receptor alterations after chronic lithium administration. Comparison with carbamazepine and sodium valproate', *Prog Neuropsychopharmacol Biol Psychiatry*, 16: 4, Jul 1992, 571-579.
- 304 P. D. Suzdak and G. Gianutsos, 'Parallel changes in the sensitivity of gamma-aminobutyric acid and noradrenergic receptors following chronic administration of antidepressant and GABAergic drugs. A possible role in affective disorders', *Neuropharmacology*, 24: 3, Mar 1985, 217-222.
- 305 B. E. Suranyi-Cadotte, T. V. Dam and R. Quirion, 'Antidepressant--anxiolytic interaction: decreased density of benzodiazepine receptors in rat brain following chronic administration of antidepressants', *Eur J Pharmacol*, 106: 3, Nov 1984, 673-675.
- 306 M. L. Barbaccia, L. Ravizza and E. Costa, 'Maprotiline: an antidepressant with an unusual pharmacological profile', *J Pharmacol Exp Ther*, 236: 2, Feb 1986, 307-312.
- 307 A. Bouthillier and C. de Montigny, 'Long-term antidepressant treatment reduces neuronal responsiveness to flurazepam: an electrophysiological study in the rat', *Neurosci Lett*, 73: 3, Jan 1987, 271-275.
- 308 A. Pilc and K. G. Lloyd, 'Chronic antidepressants and GABA "B" receptors: a GABA hypothesis of antidepressant drug action', *Life Sci*, 35: 21, Nov 1984, 2149-2154.
- 309 J. R. Kimber, J. A. Cross and R. W. Horton, 'Benzodiazepine and GABAA receptors in rat brain following chronic antidepressant drug administration', *Biochem Pharmacol*, 36: 23, Dec 1987, 4173-4175.
- 310 K. F. McKenna, D. J. McManus, G. B. Baker and R. T. Coutts, 'Chronic administration of the antidepressant phenelzine and its N-acetyl analogue: effects on GABAergic function', *J Neural Transm Suppl*, 41/1994, 115-122.
- 311 K. G. Todd, D. J. McManus and G. B. Baker, 'Chronic administration of the antidepressants phenelzine, desipramine, clomipramine, or maprotiline decreases binding to 5-hydroxytryptamine_{2A} receptors without affecting benzodiazepine binding sites in rat brain', *Cell Mol Neurobiol*, 15: 3, Jun 1995, 361-370.
- 312 A. M. Szekely, M. L. Barbaccia and E. Costa, 'Effect of a protracted antidepressant treatment on signal transduction and [3H](-)baclofen binding at GABAB receptors', *J Pharmacol Exp Ther*, 243: 1, Oct 1987, 155-159.
- 313 J. A. Cross and R. W. Horton, 'Are increases in GABAB receptors consistent findings following chronic antidepressant administration?', *Eur J Pharmacol*, 141: 1, Sep 1987, 159-162.
- 314 D. J. McManus and A. J. Greenshaw, 'Differential effects of antidepressants on GABAB and beta-adrenergic receptors in rat cerebral cortex', *Biochem Pharmacol*, 42: 8, Sep 1991, 1525-1528.
- 315 A. H. Engelbrecht, V. A. Russell and J. J. Taljaard, 'Lack of effect of bilateral locus coeruleus lesion and antidepressant treatment on gamma-aminobutyric acid_B receptors in the rat frontal cortex', *Neurochem Res*, 19: 9, Sep 1994, 1119-1123.
- 316 P. D. Suzdak and G. Gianutsos, 'Effect of chronic imipramine or baclofen on GABA-B binding and cyclic AMP production in cerebral cortex', *Eur J Pharmacol*, 131: 1, Nov 1986, 129-133.
- 317 G. D. Pratt and N. G. Bowery, 'Repeated administration of desipramine and a GABAB receptor antagonist, CGP 36742, discretely up-regulates GABAB receptor binding sites in rat frontal cortex', *Br J Pharmacol*, 110: 2, Oct 1993, 724-735.
- 318 Y. Nakagawa, T. Ishima, Y. Ishibashi, T. Yoshii and T. Takashima, 'Involvement of GABA(B) receptor systems in action of antidepressants: baclofen but not bicuculline attenuates the effects of antidepressants on the forced swim test in rats', *Brain Res*, 709: 2, Feb 1996, 215-220.
- 319 Y. Nakagawa, T. Ishima, Y. Ishibashi, M. Tsuji and T. Takashima, 'Involvement of GABAB receptor systems in action of antidepressants. II: Baclofen attenuates the effect of desipramine whereas muscimol has no effect in learned helplessness paradigm in rats', *Brain Res*, 728: 2, Jul 1996, 225-230.
- 320 Y. Nakagawa, T. Ishima, Y. Ishibashi, M. Tsuji and T. Takashima, 'Involvement of GABAB receptor systems in experimental depression: baclofen but not bicuculline exacerbates helplessness in rats', *Brain Res*, 741: 1-2, Nov 1996, 240-245.

- 321 P. Martin, P. Pichat, J. Massol, P. Soubrié, K. G. Lloyd and A. J. Puech, 'Decreased GABA B receptors in helpless rats: reversal by tricyclic antidepressants', *Neuropsychobiology*, 22: 41989, 220-224.
- 322 F. Petty, G. L. Kramer, C. M. Gullion and A. J. Rush, 'Low plasma gamma-aminobutyric acid levels in male patients with depression', *Biol Psychiatry*, 32: 4, Aug 1992, 354-363.
- 323 R. H. Gerner and T. A. Hare, 'CSF GABA in normal subjects and patients with depression, schizophrenia, mania, and anorexia nervosa', *Am J Psychiatry*, 138: 8, Aug 1981, 1098-1101.
- 324 K. Kasa, S. Otsuki, M. Yamamoto, M. Sato, H. Kuroda and N. Ogawa, 'Cerebrospinal fluid gamma-aminobutyric acid and homovanillic acid in depressive disorders', *Biol Psychiatry*, 17: 8, Aug 1982, 877-883.
- 325 A. Roy, J. Dejong and T. Ferraro, 'CSF GABA in depressed patients and normal controls', *Psychol Med*, 21: 3, Aug 1991, 613-618.
- 326 F. Petty, J. Steinberg, G. L. Kramer, M. Fulton and F. G. Moeller, 'Desipramine does not alter plasma GABA in patients with major depression', *J Affect Disord*, 29: 1, Sep 1993, 53-56.
- 327 F. Petty, G. L. Kramer, M. Fulton, L. Davis and A. J. Rush, 'Stability of plasma GABA at four-year follow-up in patients with primary unipolar depression', *Biol Psychiatry*, 37: 11, Jun 1995, 806-810.
- 328 A. Rode, A. Bidziński and S. Puzyński, '[GABA levels in the plasma of patients with endogenous depression and during the treatment with thymoleptics]', *Psychiatr Pol*, 25: 3-4, 1991 May-Aug 1991, 4-7.
- 329 F. Petty and M. A. Schlessler, 'Plasma GABA in affective illness. A preliminary investigation', *J Affect Disord*, 3: 4, Dec 1981, 339-343.
- 330 F. Petty and A. D. Sherman, 'Plasma GABA levels in psychiatric illness', *J Affect Disord*, 6: 2, Apr 1984, 131-138.
- 331 F. Petty, G. L. Kramer, D. Dunnam and A. J. Rush, 'Plasma GABA in mood disorders', *Psychopharmacol Bull*, 26: 21990, 157-161.
- 332 F. Petty and G. Kramer, 'Stability of plasma gamma-aminobutyric acid with time in healthy controls', *Biol Psychiatry*, 31: 7, Apr 1992, 743-745.
- 333 W. H. Berrettini, J. I. Nurnberger, T. A. Hare, S. Simmons-Alling, E. S. Gershon and R. M. Post, 'Reduced plasma and CSF gamma-aminobutyric acid in affective illness: effect of lithium carbonate', *Biol Psychiatry*, 18: 2, Feb 1983, 185-194.
- 334 R. H. Gerner, L. Fairbanks, G. M. Anderson, J. G. Young, M. Scheinin, M. Linnoila, T. A. Hare, B. A. Shaywitz and D. J. Cohen, 'CSF neurochemistry in depressed, manic, and schizophrenic patients compared with that of normal controls', *Am J Psychiatry*, 141: 12, Dec 1984, 1533-1540.
- 335 B. I. Gold, M. B. Bowers, R. H. Roth and D. W. Sweeney, 'GABA levels in CSF of patients with psychiatric disorders', *Am J Psychiatry*, 137: 3, Mar 1980, 362-364.
- 336 R. Zimmer, A. W. Teelken, K. D. Meier, M. Ackenheil and K. J. Zander, 'Preliminary studies on CSF gamma-aminobutyric acid levels in psychiatric patients before and during treatment with different psychotropic drugs', *Prog Neuropsychopharmacol*, 4: 61980, 613-620.
- 337 W. H. Berrettini, J. I. Nurnberger, T. A. Hare, S. Simmons-Alling and E. S. Gershon, 'CSF GABA in euthymic manic-depressive patients and controls', *Biol Psychiatry*, 21: 8-9, Jul 1986, 844-846.
- 338 G. Sanacora, G. F. Mason, D. L. Rothman, K. L. Behar, F. Hyder, O. A. Petroff, R. M. Berman, D. S. Charney and J. H. Krystal, 'Reduced cortical gamma-aminobutyric acid levels in depressed patients determined by proton magnetic resonance spectroscopy', *Arch Gen Psychiatry*, 56: 11, Nov 1999, 1043-1047.
- 339 Z. Bhagwagar, M. Wylezinska, P. Jezard, J. Evans, E. Boorman, P. M. Matthews and P. J. Cowen, 'Low GABA concentrations in occipital cortex and anterior cingulate cortex in medication-free, recovered depressed patients', *Int J Neuropsychopharmacol*, 11: 2, Mar 2008, 255-260.
- 340 G. Hasler, J. W. van der Veen, T. Tumonis, N. Meyers, J. Shen and W. C. Drevets, 'Reduced prefrontal glutamate/glutamine and gamma-aminobutyric acid levels in major depression determined using proton magnetic resonance spectroscopy', *Arch Gen Psychiatry*, 64: 2, Feb 2007, 193-200.

- 341 E. K. Perry, P. H. Gibson, G. Blessed, R. H. Perry and B. E. Tomlinson, 'Neurotransmitter enzyme abnormalities in senile dementia. Choline acetyltransferase and glutamic acid decarboxylase activities in necropsy brain tissue', *J Neurol Sci*, 34: 2, Nov 1977, 247-265.
- 342 S. H. Fatemi, S. Hossein Fatemi, J. M. Stary, J. A. Earle, M. Araghi-Niknam and E. Eagan, 'GABAergic dysfunction in schizophrenia and mood disorders as reflected by decreased levels of glutamic acid decarboxylase 65 and 67 kDa and Reelin proteins in cerebellum', *Schizophr Res*, 72: 2-3, Jan 2005, 109-122.
- 343 H. Biela, J. Steiner, C. Mawrin, K. Trübner, R. Brisch, G. Meyer-Lotz, M. Brodhun, H. Dobrowolny, B. Baumann, T. Gos, H. G. Bernstein and B. Bogerts, 'Dysregulation of GABAergic neurotransmission in mood disorders: a postmortem study', *Ann N Y Acad Sci*, 1096, Jan 2007, 157-169.
- 344 S. C. Cheetham, M. R. Crompton, C. L. Katona, S. J. Parker and R. W. Horton, 'Brain GABAA/benzodiazepine binding sites and glutamic acid decarboxylase activity in depressed suicide victims', *Brain Res*, 460: 1, Sep 1988, 114-123.
- 345 G. N. Pandey, R. R. Conley, S. C. Pandey, S. Goel, R. C. Roberts, C. A. Tamminga, D. Chute and J. Smialek, 'Benzodiazepine receptors in the post-mortem brain of suicide victims and schizophrenic subjects', *Psychiatry Res*, 71: 3, Aug 1997, 137-149.
- 346 Z. Merali, L. Du, P. Hrdina, M. Palkovits, G. Faludi, M. O. Poulter and H. Anisman, 'Dysregulation in the suicide brain: mRNA expression of corticotropin-releasing hormone receptors and GABA(A) receptor subunits in frontal cortical brain region', *J Neurosci*, 24: 6, Feb 2004, 1478-1485.
- 347 G. Sanacora and A. Saricicek, 'GABAergic contributions to the pathophysiology of depression and the mechanism of antidepressant action', *CNS Neurol Disord Drug Targets*, 6: 2, Apr 2007, 127-140.
- 348 L. L. Carpenter, J. M. Schecter, A. R. Tyrka, A. F. Mello, M. F. Mello, R. Haggarty and L. H. Price, 'Open-label tiagabine monotherapy for major depressive disorder with anxiety', *J Clin Psychiatry*, 67: 1, Jan 2006, 66-71.
- 349 A. Urani, S. Chourbaji and P. Gass, 'Mutant mouse models of depression: candidate genes and current mouse lines', *Neurosci Biobehav Rev*, 29: 4-52005, 805-828.
- 350 E. J. Nestler and S. E. Hyman, 'Animal models of neuropsychiatric disorders', *Nat Neurosci*, 13: 10, Oct 2010, 1161-1169.
- 351 P. Willner and P. J. Mitchell, 'The validity of animal models of predisposition to depression', *Behav Pharmacol*, 13: 3, May 2002, 169-188.
- 352 H. Anisman and K. Matheson, 'Stress, depression, and anhedonia: caveats concerning animal models', *Neurosci Biobehav Rev*, 29: 4-52005, 525-546.
- 353 B. Vollmayr, M. M. Mahlstedt and F. A. Henn, 'Neurogenesis and depression: what animal models tell us about the link', *Eur Arch Psychiatry Clin Neurosci*, 257: 5, Aug 2007, 300-303.
- 354 E. J. Nestler, E. Gould, H. Manji, M. Buncan, R. S. Duman, H. K. Greshenfeld, R. Hen, S. Koester, I. Lederhendler, M. Meaney, T. Robbins, L. Winsky and S. Zalcman, 'Preclinical models: status of basic research in depression', *Biol Psychiatry*, 52: 6, Sep 2002, 503-528.
- 355 R. D. Porsolt, A. Bertin and M. Jalfre, 'Behavioral despair in mice: a primary screening test for antidepressants', *Arch Int Pharmacodyn Ther*, 229: 2, Oct 1977, 327-336.
- 356 R. D. Porsolt, M. Le Pichon and M. Jalfre, 'Depression: a new animal model sensitive to antidepressant treatments', *Nature*, 266: 5604, Apr 1977, 730-732.
- 357 R. D. Porsolt, A. Bertin and M. Jalfre, '"Behavioural despair" in rats and mice: strain differences and the effects of imipramine', *Eur J Pharmacol*, 51: 3, Oct 1978, 291-294.
- 358 R. D. Porsolt, G. Anton, N. Blavet and M. Jalfre, 'Behavioural despair in rats: a new model sensitive to antidepressant treatments', *Eur J Pharmacol*, 47: 4, Feb 1978, 379-391.
- 359 J. F. Cryan and C. Mombereau, 'In search of a depressed mouse: utility of models for studying depression-related behavior in genetically modified mice', *Mol Psychiatry*, 9: 4, Apr 2004, 326-357.
- 360 J. F. Cryan, C. Mombereau and A. Vassout, 'The tail suspension test as a model for assessing antidepressant activity: review of pharmacological and genetic studies in mice', *Neurosci Biobehav Rev*, 29: 4-52005, 571-625.

- 361 I. Lucki, A. Dalvi and A. J. Mayorga, 'Sensitivity to the effects of pharmacologically selective antidepressants in different strains of mice', *Psychopharmacology (Berl)*, 155: 3, May 2001, 315-322.
- 362 B. Petit-Demouliere, F. Chenu and M. Bourin, 'Forced swimming test in mice: a review of antidepressant activity', *Psychopharmacology (Berl)*, 177: 3, Jan 2005, 245-255.
- 363 L. Steru, R. Chermat, B. Thierry and P. Simon, 'The tail suspension test: a new method for screening antidepressants in mice', *Psychopharmacology (Berl)*, 85: 31985, 367-370.
- 364 A. Dalvi and I. Lucki, 'Murine models of depression', *Psychopharmacology (Berl)*, 147: 1, Nov 1999, 14-16.
- 365 V. Krishnan and E. J. Nestler, 'Animal models of depression: molecular perspectives', *Curr Top Behav Neurosci*, 72011, 121-147.
- 366 M. E. Seligman and G. Beagley, 'Learned helplessness in the rat', *J Comp Physiol Psychol*, 88: 2, Feb 1975, 534-541.
- 367 M. E. Seligman, R. A. Rosellini and M. J. Kozak, 'Learned helplessness in the rat: time course, immunization, and reversibility', *J Comp Physiol Psychol*, 88: 2, Feb 1975, 542-547.
- 368 N. Haddjeri, P. Blier and C. de Montigny, 'Long-term antidepressant treatments result in a tonic activation of forebrain 5-HT_{1A} receptors', *J Neurosci*, 18: 23, Dec 1998, 10150-10156.
- 369 F. A. Henn and B. Vollmayr, 'Stress models of depression: forming genetically vulnerable strains', *Neurosci Biobehav Rev*, 29: 4-52005, 799-804.
- 370 N. K. Dess, J. Raizer, C. D. Chapman and J. Garcia, 'Stressors in the learned helplessness paradigm: effects on body weight and conditioned taste aversion in rats', *Physiol Behav*, 44: 4-51988, 483-490.
- 371 L. Greenberg, E. Edwards and F. A. Henn, 'Dexamethasone suppression test in helpless rats', *Biol Psychiatry*, 26: 5, Sep 1989, 530-532.
- 372 A. D. Sherman, J. L. Sacquitne and F. Petty, 'Specificity of the learned helplessness model of depression', *Pharmacol Biochem Behav*, 16: 3, Mar 1982, 449-454.
- 373 W. T. McKinney, 'Electroconvulsive therapy and animal models of depression', *Ann N Y Acad Sci*, 4621986, 65-69.
- 374 M. P. Boyle, J. A. Brewer, M. Funatsu, D. F. Wozniak, J. Z. Tsien, Y. Izumi and L. J. Muglia, 'Acquired deficit of forebrain glucocorticoid receptor produces depression-like changes in adrenal axis regulation and behavior', *Proc Natl Acad Sci U S A*, 102: 2, Jan 2005, 473-478.
- 375 Q. Wei, E. K. Hebda-Bauer, A. Pletsch, J. Luo, M. T. Hoversten, A. J. Osetek, S. J. Evans, S. J. Watson, A. F. Seasholtz and H. Akil, 'Overexpressing the glucocorticoid receptor in forebrain causes an aging-like neuroendocrine phenotype and mild cognitive dysfunction', *J Neurosci*, 27: 33, Aug 2007, 8836-8844.
- 376 S. L. Gourley, D. D. Kiraly, J. L. Howell, P. Olausson and J. R. Taylor, 'Acute hippocampal brain-derived neurotrophic factor restores motivational and forced swim performance after corticosterone', *Biol Psychiatry*, 64: 10, Nov 2008, 884-890.
- 377 C. B. Nemeroff, E. Widerlöv, G. Bissette, H. Walléus, I. Karlsson, K. Eklund, C. D. Kilts, P. T. Loosen and W. Vale, 'Elevated concentrations of CSF corticotropin-releasing factor-like immunoreactivity in depressed patients', *Science*, 226: 4680, Dec 1984, 1342-1344.
- 378 M. B. Müller and F. Holsboer, 'Mice with mutations in the HPA-system as models for symptoms of depression', *Biol Psychiatry*, 59: 12, Jun 2006, 1104-1115.
- 379 B. J. Kolber, M. P. Boyle, L. Wiczorek, C. L. Kelley, C. C. Onwuzurike, S. A. Nettles, S. K. Vogt and L. J. Muglia, 'Transient early-life forebrain corticotropin-releasing hormone elevation causes long-lasting anxiogenic and despair-like changes in mice', *J Neurosci*, 30: 7, Feb 2010, 2571-2581.
- 380 S. J. Mathew, H. K. Manji and D. S. Charney, 'Novel drugs and therapeutic targets for severe mood disorders', *Neuropsychopharmacology*, 33: 9, Aug 2008, 2080-2092.
- 381 P. Willner, 'Chronic mild stress (CMS) revisited: consistency and behavioural-neurobiological concordance in the effects of CMS', *Neuropsychobiology*, 52: 22005, 90-110.
- 382 T. Strekalova, R. Spanagel, D. Bartsch, F. A. Henn and P. Gass, 'Stress-induced anhedonia in mice is associated with deficits in forced swimming and exploration', *Neuropsychopharmacology*, 29: 11, Nov 2004, 2007-2017.

- 383 S. V. Argyropoulos and D. J. Nutt, 'Anhedonia and chronic mild stress model in depression', *Psychopharmacology (Berl)*, 134: 4, Dec 1997, 333-336; discussion 371-337.
- 384 C. Broekkamp, 'Predictive validity and the robustness criterion for animal models', *Psychopharmacology (Berl)*, 134: 4, Dec 1997, 341-343; discussion 371-347.
- 385 M. N. Jayatissa, C. Bisgaard, A. Tingström, M. Papp and O. Wiborg, 'Hippocampal cytogenesis correlates to escitalopram-mediated recovery in a chronic mild stress rat model of depression', *Neuropsychopharmacology*, 31: 11, Nov 2006, 2395-2404.
- 386 T. Strelakova, N. Gorenkova, E. Schunk, O. Dolgov and D. Bartsch, 'Selective effects of citalopram in a mouse model of stress-induced anhedonia with a control for chronic stress', *Behav Pharmacol*, 17: 3, May 2006, 271-287.
- 387 R. J. Katz, K. A. Roth and B. J. Carroll, 'Acute and chronic stress effects on open field activity in the rat: implications for a model of depression', *Neurosci Biobehav Rev*, 5: 21981, 247-251.
- 388 S. Pothion, J. C. Bizot, F. Trovero and C. Belzung, 'Strain differences in sucrose preference and in the consequences of unpredictable chronic mild stress', *Behav Brain Res*, 155: 1, Nov 2004, 135-146.
- 389 D. F. Avgustinovich, I. L. Kovalenko and N. N. Kudryavtseva, 'A model of anxious depression: persistence of behavioral pathology', *Neurosci Behav Physiol*, 35: 9, Nov 2005, 917-924.
- 390 E. Malatynska and R. J. Knapp, 'Dominant-submissive behavior as models of mania and depression', *Neurosci Biobehav Rev*, 29: 4-52005, 715-737.
- 391 H. E. Covington and K. A. Miczek, 'Intense cocaine self-administration after episodic social defeat stress, but not after aggressive behavior: dissociation from corticosterone activation', *Psychopharmacology (Berl)*, 183: 3, Dec 2005, 331-340.
- 392 Manuela Martinez, Angels Calvo-Torrent and Maria Angeles Pico-Alfonso, 'Social defeat and subordination as models of social stress in laboratory rodents: a review.', In: Faculty of Psychology Area of Psychobiology, University of Valencia, Valencia, Spain, ed, *Aggressive Behavior*, 1998, 241-256.
- 393 V. Krishnan, M. H. Han, D. L. Graham, O. Berton, W. Renthal, S. J. Russo, Q. Laplant, A. Graham, M. Lutter, D. C. Lagace, S. Ghose, R. Reister, P. Tannous, T. A. Green, R. L. Neve, S. Chakravarty, A. Kumar, A. J. Eisch, D. W. Self, F. S. Lee, C. A. Tamminga, D. C. Cooper, H. K. Gershenfeld and E. J. Nestler, 'Molecular adaptations underlying susceptibility and resistance to social defeat in brain reward regions', *Cell*, 131: 2, Oct 2007, 391-404.
- 394 C. Becker, B. Zeau, C. Rivat, A. Blugeot, M. Hamon and J. J. Benoliel, 'Repeated social defeat-induced depression-like behavioral and biological alterations in rats: involvement of cholecystokinin', *Mol Psychiatry*, 13: 12, Dec 2008, 1079-1092.
- 395 R. Rygula, N. Abumaria, U. Havemann-Reinecke, E. Rütther, C. Hiemke, G. Zernig, E. Fuchs and G. Flügge, 'Pharmacological validation of a chronic social stress model of depression in rats: effects of reboxetine, haloperidol and diazepam', *Behav Pharmacol*, 19: 3, May 2008, 183-196.
- 396 H. C. Yan, H. D. Qu, L. R. Sun, S. J. Li, X. Cao, Y. Y. Fang, W. Jie, J. C. Bean, W. K. Wu, X. H. Zhu and T. M. Gao, 'Fuzi polysaccharide-1 produces antidepressant-like effects in mice', *Int J Neuropsychopharmacol*, 13: 5, Jun 2010, 623-633.
- 397 N. M. Tsankova, O. Berton, W. Renthal, A. Kumar, R. L. Neve and E. J. Nestler, 'Sustained hippocampal chromatin regulation in a mouse model of depression and antidepressant action', *Nat Neurosci*, 9: 4, Apr 2006, 519-525.
- 398 A. V. Kalueff, D. F. Avgustinovich, N. N. Kudryavtseva and D. L. Murphy, 'BDNF in anxiety and depression', *Science*, 312: 5780, Jun 2006, 1598-1599; author reply 1598-1599.
- 399 N. N. Kudryavtseva, I. V. Bakshtanovskaya and L. A. Koryakina, 'Social model of depression in mice of C57BL/6J strain', *Pharmacol Biochem Behav*, 38: 2, Feb 1991, 315-320.
- 400 S. C. Dulawa and R. Hen, 'Recent advances in animal models of chronic antidepressant effects: the novelty-induced hypophagia test', *Neurosci Biobehav Rev*, 29: 4-52005, 771-783.
- 401 D. L. Wallace, M. H. Han, D. L. Graham, T. A. Green, V. Vialou, S. D. Iñiguez, J. L. Cao, A. Kirk, S. Chakravarty, A. Kumar, V. Krishnan, R. L. Neve, D. C. Cooper, C. A. Bolaños, M. Barrot, C. A. McClung and E. J. Nestler, 'CREB regulation of nucleus accumbens excitability mediates social isolation-induced behavioral deficits', *Nat Neurosci*, 12: 2, Feb 2009, 200-209.

- 402 M. B. Wilkinson, G. Xiao, A. Kumar, Q. LaPlant, W. Renthal, D. Sikder, T. J. Kodadek and E. J. Nestler, 'Imipramine treatment and resiliency exhibit similar chromatin regulation in the mouse nucleus accumbens in depression models', *J Neurosci*, 29: 24, Jun 2009, 7820-7832.
- 403 F. Fumagalli, R. Molteni, G. Racagni and M. A. Riva, 'Stress during development: Impact on neuroplasticity and relevance to psychopathology', *Prog Neurobiol*, 81: 4, Mar 2007, 197-217.
- 404 S. J. Lupien, B. S. McEwen, M. R. Gunnar and C. Heim, 'Effects of stress throughout the lifespan on the brain, behaviour and cognition', *Nat Rev Neurosci*, 10: 6, Jun 2009, 434-445.
- 405 Biomarkers Definitions Working Group., 'Biomarkers and surrogate endpoints: preferred definitions and conceptual framework', *Clin Pharmacol Ther*, 69: 3, Mar 2001, 89-95.
- 406 R. M. Benca, W. H. Obermeyer, R. A. Thisted and J. C. Gillin, 'Sleep and psychiatric disorders. A meta-analysis', *Arch Gen Psychiatry*, 49: 8, Aug 1992, 651-668; discussion 669-670.
- 407 E. Castrén and T. Rantamäki, 'The role of BDNF and its receptors in depression and antidepressant drug action: Reactivation of developmental plasticity', *Dev Neurobiol*, 70: 5, Apr 2010, 289-297.
- 408 H. D. Schmidt and R. S. Duman, 'The role of neurotrophic factors in adult hippocampal neurogenesis, antidepressant treatments and animal models of depressive-like behavior', *Behav Pharmacol*, 18: 5-6, Sep 2007, 391-418.
- 409 H. D. Schmidt and R. S. Duman, 'Peripheral BDNF produces antidepressant-like effects in cellular and behavioral models', *Neuropsychopharmacology*, 35: 12, Nov 2010, 2378-2391.
- 410 A. H. Miller, V. Maletic and C. L. Raison, 'Inflammation and its discontents: the role of cytokines in the pathophysiology of major depression', *Biol Psychiatry*, 65: 9, May 2009, 732-741.
- 411 A. H. Miller, E. Haroon, C. L. Raison and J. C. Felger, 'Cytokine targets in the brain: impact on neurotransmitters and neurocircuits', *Depress Anxiety*, 30: 4, Apr 2013, 297-306.
- 412 H. Hendrickx, B. S. McEwen and F. Ouderaa, 'Metabolism, mood and cognition in aging: the importance of lifestyle and dietary intervention', *Neurobiol Aging*, 26 Suppl 1, Dec 2005, 1-5.
- 413 Y. Dowlati, N. Herrmann, W. Swardfager, H. Liu, L. Sham, E. K. Reim and K. L. Lancôt, 'A meta-analysis of cytokines in major depression', *Biol Psychiatry*, 67: 5, Mar 2010, 446-457.
- 414 J. Hannestad, N. DellaGioia and M. Bloch, 'The effect of antidepressant medication treatment on serum levels of inflammatory cytokines: a meta-analysis', *Neuropsychopharmacology*, 36: 12, Nov 2011, 2452-2459.
- 415 C. L. Raison, J. M. Lin and W. C. Reeves, 'Association of peripheral inflammatory markers with chronic fatigue in a population-based sample', *Brain Behav Immun*, 23: 3, Mar 2009, 327-337.
- 416 A. Anand, D. S. Charney, D. A. Oren, R. M. Berman, X. S. Hu, A. Cappiello and J. H. Krystal, 'Attenuation of the neuropsychiatric effects of ketamine with lamotrigine: support for hyperglutamatergic effects of N-methyl-D-aspartate receptor antagonists', *Arch Gen Psychiatry*, 57: 3, Mar 2000, 270-276.
- 417 M. M. Bradford, 'A rapid and sensitive method for the quantitation of microgram quantities of protein utilizing the principle of protein-dye binding', *Anal Biochem*, 72, May 1976, 248-254.
- 418 O. H. LOWRY, N. J. ROSEBROUGH, A. L. FARR and R. J. RANDALL, 'Protein measurement with the Folin phenol reagent', *J Biol Chem*, 193: 1, Nov 1951, 265-275.
- 419 Thermo Fisher, 'LTQ Orbitrap XL', <http://planetorbitrap.com/ltq-orbitrap-xl#.V1M7jjWLRaQ>.
- 420 Thermo Fisher, 'Q Exactive Quadrupole Orbitrap', <http://planetorbitrap.com/q-exactive#tab:schematic>.
- 421 C. G. Dotti, C. A. Sullivan and G. A. Banker, 'The establishment of polarity by hippocampal neurons in culture', *J Neurosci*, 8: 4, Apr 1988, 1454-1468.
- 422 Thermo Fisher, '5500 QTrap', <http://www.chromacademy.com/essential-guide/dec2011/figure-12.jpg>.
- 423 M. Yuan, S. B. Breitkopf, X. Yang and J. M. Asara, 'A positive/negative ion-switching, targeted mass spectrometry-based metabolomics platform for bodily fluids, cells, and fresh and fixed tissue', *Nat Protoc*, 7: 5, May 2012, 872-881.
- 424 Xia Lab, 'Metaboanalyst', <http://www.metaboanalyst.ca/faces/docs/About.xhtml>.

- 425 J. Xia, N. Psychogios, N. Young and D. S. Wishart, 'MetaboAnalyst: a web server for metabolomic data analysis and interpretation', *Nucleic Acids Res*, 37: Web Server issue, Jul 2009, W652-660.
- 426 V. G. Tusher, R. Tibshirani and G. Chu, 'Significance analysis of microarrays applied to the ionizing radiation response', *Proc Natl Acad Sci U S A*, 98: 9, Apr 2001, 5116-5121.
- 427 Wold Svante, Sjöströma Michael and Eriksson Lennart, 'PLS-regression: a basic tool of chemometrics', *Chemometrics and Intelligent Laboratory Systems*, 2001, 109-130.
- 428 STRING Consortium 2016, 'STRING', <http://www.string-db.org>, 2016.
- 429 D. A. Hosack, G. Dennis, B. T. Sherman, H. C. Lane and R. A. Lempicki, 'Identifying biological themes within lists of genes with EASE', *Genome Biol*, 4: 102003, R70.
- 430 R. Kaddurah-Daouk and K. R. Krishnan, 'Metabolomics: a global biochemical approach to the study of central nervous system diseases', *Neuropsychopharmacology*, 34: 1, Jan 2009, 173-186.
- 431 O. Fiehn, 'Metabolomics--the link between genotypes and phenotypes', *Plant Mol Biol*, 48: 1-2, Jan 2002, 155-171.
- 432 C. Webhofer, P. Gormanns, S. Reckow, M. Lebar, G. Maccarrone, T. Ludwig, B. Pütz, J. M. Asara, F. Holsboer, I. Sillaber, W. Zieglgänsberger and C. W. Turck, 'Proteomic and metabolomic profiling reveals time-dependent changes in hippocampal metabolism upon paroxetine treatment and biomarker candidates', *J Psychiatr Res*, 47: 3, Mar 2013, 289-298.
- 433 M. D. Filiou, Y. Zhang, L. Teplytska, S. Reckow, P. Gormanns, G. Maccarrone, E. Frank, M. S. Kessler, B. Hamsch, M. Nussbaumer, M. Bunck, T. Ludwig, A. Yassouridis, F. Holsboer, R. Landgraf and C. W. Turck, 'Proteomics and metabolomics analysis of a trait anxiety mouse model reveals divergent mitochondrial pathways', *Biol Psychiatry*, 70: 11, Dec 2011, 1074-1082.
- 434 G. Scaini, P. M. Santos, J. Benedet, N. Rochi, L. M. Gomes, L. S. Borges, G. T. Rezin, D. P. Pezente, J. Quevedo and E. L. Streck, 'Evaluation of Krebs cycle enzymes in the brain of rats after chronic administration of antidepressants', *Brain Res Bull*, 82: 3-4, May 2010, 224-227.
- 435 John L Tymoczko Jeremy M Berg, and Lubert Stryer, *Biochemistry. 5th edition*, 2002.
- 436 A. K. Petersen, J. Krumsiek, B. Wägele, F. J. Theis, H. E. Wichmann, C. Gieger and K. Suhre, 'On the hypothesis-free testing of metabolite ratios in genome-wide and metabolome-wide association studies', *BMC Bioinformatics*, 13:2012, 120.
- 437 University California Santa Cruz, 'Emotions', <http://courses.pbsci.ucsc.edu/mcdb/bio125/lecture17.pdf>.
- 438 O. Malkesman, D. R. Austin, T. Tragon, G. Wang, G. Rompala, A. B. Hamidi, Z. Cui, W. S. Young, K. Nakazawa, C. A. Zarate, H. K. Manji and G. Chen, 'Acute D-serine treatment produces antidepressant-like effects in rodents', *Int J Neuropsychopharmacol*, 15: 8, Sep 2012, 1135-1148.
- 439 A. D. Zomkowski, A. R. Santos and A. L. Rodrigues, 'Putrescine produces antidepressant-like effects in the forced swimming test and in the tail suspension test in mice', *Prog Neuropsychopharmacol Biol Psychiatry*, 30: 8, Dec 2006, 1419-1425.
- 440 Mark F. Bear, Connors, Barry W., Paradiso, Michael A., *Neurowissenschaften: Ein grundlegendes Lehrbuch für Biologie, Medizin und Psychologie*, 2009.
- 441 M. D. Filiou, L. Teplytska, D. M. Otte, A. Zimmer and C. W. Turck, 'Myelination and oxidative stress alterations in the cerebellum of the G72/G30 transgenic schizophrenia mouse model', *J Psychiatr Res*, 46: 10, Oct 2012, 1359-1365.
- 442 S. W. Flynn, D. J. Lang, A. L. Mackay, V. Goghari, I. M. Vavasour, K. P. Whittall, G. N. Smith, V. Arango, J. J. Mann, A. J. Dwork, P. Falkai and W. G. Honer, 'Abnormalities of myelination in schizophrenia detected in vivo with MRI, and post-mortem with analysis of oligodendrocyte proteins', *Mol Psychiatry*, 8: 9, Sep 2003, 811-820.
- 443 G. A. Amodeo, M. J. Rudolph and L. Tong, 'Crystal structure of the heterotrimer core of *Saccharomyces cerevisiae* AMPK homologue SNF1', *Nature*, 449: 7161, Sep 2007, 492-495.
- 444 J. M. Corton, J. G. Gillespie, S. A. Hawley and D. G. Hardie, '5-aminoimidazole-4-carboxamide ribonucleoside. A specific method for activating AMP-activated protein kinase in intact cells?', *Eur J Biochem*, 229: 2, Apr 1995, 558-565.

- 445 R. Townley and L. Shapiro, 'Crystal structures of the adenylate sensor from fission yeast AMP-activated protein kinase', *Science*, 315: 5819, Mar 2007, 1726-1729.
- 446 B. Xiao, R. Heath, P. Saiu, F. C. Leiper, P. Leone, C. Jing, P. A. Walker, L. Haire, J. F. Eccleston, C. T. Davis, S. R. Martin, D. Carling and S. J. Gamblin, 'Structural basis for AMP binding to mammalian AMP-activated protein kinase', *Nature*, 449: 7161, Sep 2007, 496-500.
- 447 B. Xiao, M. J. Sanders, E. Underwood, R. Heath, F. V. Mayer, D. Carmena, C. Jing, P. A. Walker, J. F. Eccleston, L. F. Haire, P. Saiu, S. A. Howell, R. Aasland, S. R. Martin, D. Carling and S. J. Gamblin, 'Structure of mammalian AMPK and its regulation by ADP', *Nature*, 472: 7342, Apr 2011, 230-233.
- 448 B. Xiao, M. J. Sanders, D. Carmena, N. J. Bright, L. F. Haire, E. Underwood, B. R. Patel, R. B. Heath, P. A. Walker, S. Hallen, F. Giordanetto, S. R. Martin, D. Carling and S. J. Gamblin, 'Structural basis of AMPK regulation by small molecule activators', *Nat Commun*, 42013, 3017.
- 449 K. Barnes, J. C. Ingram, O. H. Porras, L. F. Barros, E. R. Hudson, L. G. Fryer, F. Foufelle, D. Carling, D. G. Hardie and S. A. Baldwin, 'Activation of GLUT1 by metabolic and osmotic stress: potential involvement of AMP-activated protein kinase (AMPK)', *J Cell Sci*, 115: Pt 11, Jun 2002, 2433-2442.
- 450 A. Bonen, X. X. Han, D. D. Habets, M. Febbraio, J. F. Glatz and J. J. Luiken, 'A null mutation in skeletal muscle FAT/CD36 reveals its essential role in insulin- and AICAR-stimulated fatty acid metabolism', *Am J Physiol Endocrinol Metab*, 292: 6, Jun 2007, E1740-1749.
- 451 S. Chen, J. Murphy, R. Toth, D. G. Campbell, N. A. Morrice and C. Mackintosh, 'Complementary regulation of TBC1D1 and AS160 by growth factors, insulin and AMPK activators', *Biochem J*, 409: 2, Jan 2008, 449-459.
- 452 A. Cheng, Y. Hou and M. P. Mattson, 'Mitochondria and neuroplasticity', *ASN Neuro*, 2: 52010, e00045.
- 453 A. F. MacAskill and J. T. Kittler, 'Control of mitochondrial transport and localization in neurons', *Trends Cell Biol*, 20: 2, Feb 2010, 102-112.
- 454 A. F. MacAskill, T. A. Atkin and J. T. Kittler, 'Mitochondrial trafficking and the provision of energy and calcium buffering at excitatory synapses', *Eur J Neurosci*, 32: 2, Jul 2010, 231-240.
- 455 V. I. Lushchak, 'FREE RADICALS, REACTIVE OXYGEN SPECIES, OXIDATIVE STRESSES AND THEIR CLASSIFICATIONS', *Ukr Biochem J*, 87: 6, 2015 Nov-Dec 2015, 11-18.
- 456 J. Ruszkiewicz and J. Albrecht, 'Changes in the mitochondrial antioxidant systems in neurodegenerative diseases and acute brain disorders', *Neurochem Int*, 88, Sep 2015, 66-72.
- 457 J. C. Begara-Morales, B. Sánchez-Calvo, M. Chaki, R. Valderrama, C. Mata-Pérez, M. N. Padilla, F. J. Corpas and J. B. Barroso, 'Antioxidant Systems are Regulated by Nitric Oxide-Mediated Post-translational Modifications (NO-PTMs)', *Front Plant Sci*, 72016, 152.
- 458 X. Wang and C. Hai, 'Novel insights into redox system and the mechanism of redox regulation', *Mol Biol Rep*, Jun 2016.
- 459 S. G. Rhee, 'Overview on Peroxiredoxin', *Mol Cells*, 39: 1, Jan 2016, 1-5.
- 460 L. A. Rowe, N. Degtyareva and P. W. Doetsch, 'DNA damage-induced reactive oxygen species (ROS) stress response in *Saccharomyces cerevisiae*', *Free Radic Biol Med*, 45: 8, Oct 2008, 1167-1177.
- 461 T. Nyström, 'Role of oxidative carbonylation in protein quality control and senescence', *EMBO J*, 24: 7, Apr 2005, 1311-1317.
- 462 M. Kastle and T. Grune, 'Protein oxidative modification in the aging organism and the role of the ubiquitin proteasomal system', *Curr Pharm Des*, 17: 36, Dec 2011, 4007-4022.
- 463 Jamie L. Iannace, 'Protein Carbonylation Analysis in Ketamine Treated Mice ', 2015.
- 464 M. J. Edelmann, A. Iphöfer, M. Akutsu, M. Altun, K. di Gleria, H. B. Kramer, E. Fiebigler, S. Dhe-Paganon and B. M. Kessler, 'Structural basis and specificity of human otubain 1-mediated deubiquitination', *Biochem J*, 418: 2, Mar 2009, 379-390.
- 465 P. Kaiser, W. Seufert, L. Höfferer, B. Kofler, C. Sachsenmaier, H. Herzog, S. Jentsch, M. Schweiger and R. Schneider, 'A human ubiquitin-conjugating enzyme homologous to yeast UBC8', *J Biol Chem*, 269: 12, Mar 1994, 8797-8802.
- 466 M. F. Navarro, L. Carmody, O. Romo-Fewell, M. E. Lokensgard and J. J. Love, 'Characterizing substrate selectivity of ubiquitin C-terminal hydrolase-L3 using engineered α -linked ubiquitin substrates', *Biochemistry*, 53: 51, Dec 2014, 8031-8042.

- 467 J. Kwon, 'The new function of two ubiquitin C-terminal hydrolase isozymes as reciprocal modulators of germ cell apoptosis', *Exp Anim*, 56: 2, Apr 2007, 71-77.
- 468 S. Murata, H. Yashiroda and K. Tanaka, 'Molecular mechanisms of proteasome assembly', *Nat Rev Mol Cell Biol*, 10: 2, Feb 2009, 104-115.
- 469 H. C. Tai and E. M. Schuman, 'Ubiquitin, the proteasome and protein degradation in neuronal function and dysfunction', *Nat Rev Neurosci*, 9: 11, Nov 2008, 826-838.
- 470 O. Coux, K. Tanaka and A. L. Goldberg, 'Structure and functions of the 20S and 26S proteasomes', *Annu Rev Biochem*, 65:1996, 801-847.
- 471 V. O. Kyrychenko, V. S. Nagibin, L. V. Tumanovska, D. O. Pashevin, V. L. Gurianova, A. A. Moibenko, V. E. Dosenko and D. J. Klionsky, 'Knockdown of PSMB7 induces autophagy in cardiomyocyte cultures: possible role in endoplasmic reticulum stress', *Pathobiology*, 81: 12014, 8-14.
- 472 H. Ryu, S. P. Gygi, Y. Azuma, A. Arnaoutov and M. Dasso, 'SUMOylation of Psmd1 controls Adrm1 interaction with the proteasome', *Cell Rep*, 7: 6, Jun 2014, 1842-1848.
- 473 X. Wang, C. F. Chen, P. R. Baker, P. L. Chen, P. Kaiser and L. Huang, 'Mass spectrometric characterization of the affinity-purified human 26S proteasome complex', *Biochemistry*, 46: 11, Mar 2007, 3553-3565.
- 474 R. S. Duman and B. Voleti, 'Signaling pathways underlying the pathophysiology and treatment of depression: novel mechanisms for rapid-acting agents', *Trends Neurosci*, 35: 1, Jan 2012, 47-56.
- 475 R. A. Merrill and S. Strack, 'Mitochondria: a kinase anchoring protein 1, a signaling platform for mitochondrial form and function', *Int J Biochem Cell Biol*, 48, Mar 2014, 92-96.
- 476 F. W. Herberg, A. Maleszka, T. Eide, L. Vossebein and K. Tasken, 'Analysis of A-kinase anchoring protein (AKAP) interaction with protein kinase A (PKA) regulatory subunits: PKA isoform specificity in AKAP binding', *J Mol Biol*, 298: 2, Apr 2000, 329-339.
- 477 M. S. Kapiloff, R. V. Schillace, A. M. Westphal and J. D. Scott, 'mAKAP: an A-kinase anchoring protein targeted to the nuclear membrane of differentiated myocytes', *J Cell Sci*, 112 (Pt 16), Aug 1999, 2725-2736.
- 478 Alexandra Knorr, 'Auswirkungen von Ketamin auf die oxidative Phosphorylierung - Untersuchung mitochondrialer Atmungskettenkomplexe mittels BN-PAGE ', 2013.
- 479 I. Wittig, H. P. Braun and H. Schägger, 'Blue native PAGE', *Nat Protoc*, 1: 12006, 418-428.
- 480 Bernhard M, Bein B, Böttiger BW, Bohn A, Fischer M, Gräsner JT, Hinkelbein J, Kill C, Lott C, Popp E, Roessler M, Schaumberg A, Wenzel V and Hossfeld B, 'Handlungsempfehlung zur prähospitalen Notfallnarkose beim Erwachsenen', 2015.
- 481 J. W. Murrough and D. S. Charney, 'Cracking the moody brain: lifting the mood with ketamine', *Nat Med*, 16: 12, Dec 2010, 1384-1385.
- 482 Albert Einstein College of Medicine Institute for Animal Studies, 'Recommended Methods of Anesthesia, Analgesia, and Euthanasia for Laboratory Animal Species'.
- 483 Q. Xu, Z. Ming, A. M. Dart and X. J. Du, 'Optimizing dosage of ketamine and xylazine in murine echocardiography', *Clin Exp Pharmacol Physiol*, 34: 5-6, 2007 May-Jun 2007, 499-507.
- 484 D. Dzamba, P. Honsa and M. Anderova, 'NMDA Receptors in Glial Cells: Pending Questions', *Curr Neuropharmacol*, 11: 3, May 2013, 250-262.
- 485 W. C. Drevets, 'Functional anatomical abnormalities in limbic and prefrontal cortical structures in major depression', *Prog Brain Res*, 126:2000, 413-431.
- 486 W. C. Drevets, J. L. Price and M. L. Furey, 'Brain structural and functional abnormalities in mood disorders: implications for neurocircuitry models of depression', *Brain Struct Funct*, 213: 1-2, Sep 2008, 93-118.
- 487 B. Glancy and R. S. Balaban, 'Role of mitochondrial Ca²⁺ in the regulation of cellular energetics', *Biochemistry*, 51: 14, Apr 2012, 2959-2973.
- 488 Z. Li, K. Okamoto, Y. Hayashi and M. Sheng, 'The importance of dendritic mitochondria in the morphogenesis and plasticity of spines and synapses', *Cell*, 119: 6, Dec 2004, 873-887.

- 489 C. M. Moore, J. D. Christensen, B. Lafer, M. Fava and P. F. Renshaw, 'Lower levels of nucleoside triphosphate in the basal ganglia of depressed subjects: a phosphorous-31 magnetic resonance spectroscopy study', *Am J Psychiatry*, 154: 1, Jan 1997, 116-118.
- 490 H. P. Volz, R. Rzanny, S. Riehemann, S. May, H. Hegewald, B. Preussler, G. Hübner, W. A. Kaiser and H. Sauer, '31P magnetic resonance spectroscopy in the frontal lobe of major depressed patients', *Eur Arch Psychiatry Clin Neurosci*, 248: 61998, 289-295.
- 491 D. M. Gwinn, D. B. Shackelford, D. F. Egan, M. M. Mihaylova, A. Mery, D. S. Vasquez, B. E. Turk and R. J. Shaw, 'AMPK phosphorylation of raptor mediates a metabolic checkpoint', *Mol Cell*, 30: 2, Apr 2008, 214-226.
- 492 K. Inoki, T. Zhu and K. L. Guan, 'TSC2 mediates cellular energy response to control cell growth and survival', *Cell*, 115: 5, Nov 2003, 577-590.
- 493 V. A. Narkar, M. Downes, R. T. Yu, E. Emblar, Y. X. Wang, E. Banayo, M. M. Mihaylova, M. C. Nelson, Y. Zou, H. Juguilon, H. Kang, R. J. Shaw and R. M. Evans, 'AMPK and PPARdelta agonists are exercise mimetics', *Cell*, 134: 3, Aug 2008, 405-415.
- 494 W. W. Winder, B. F. Holmes, D. S. Rubink, E. B. Jensen, M. Chen and J. O. Holloszy, 'Activation of AMP-activated protein kinase increases mitochondrial enzymes in skeletal muscle', *J Appl Physiol (1985)*, 88: 6, Jun 2000, 2219-2226.
- 495 S. Jäger, C. Handschin, J. St-Pierre and B. M. Spiegelman, 'AMP-activated protein kinase (AMPK) action in skeletal muscle via direct phosphorylation of PGC-1alpha', *Proc Natl Acad Sci U S A*, 104: 29, Jul 2007, 12017-12022.
- 496 V. A. Skeberdis, V. Chevaleyre, C. G. Lau, J. H. Goldberg, D. L. Pettit, S. O. Suadicani, Y. Lin, M. V. Bennett, R. Yuste, P. E. Castillo and R. S. Zukin, 'Protein kinase A regulates calcium permeability of NMDA receptors', *Nat Neurosci*, 9: 4, Apr 2006, 501-510.
- 497 C. Anacker, P. A. Zunszain, A. Cattaneo, L. A. Carvalho, M. J. Garabedian, S. Thuret, J. Price and C. M. Pariante, 'Antidepressants increase human hippocampal neurogenesis by activating the glucocorticoid receptor', *Mol Psychiatry*, 16: 7, Jul 2011, 738-750.
- 498 P. Svenningsson, H. Bateup, H. Qi, K. Takamiya, R. L. Huganir, M. Spedding, B. L. Roth, B. S. McEwen and P. Greengard, 'Involvement of AMPA receptor phosphorylation in antidepressant actions with special reference to tianeptine', *Eur J Neurosci*, 26: 12, Dec 2007, 3509-3517.
- 499 N. Tartaglia, J. Du, W. J. Tyler, E. Neale, L. Pozzo-Miller and B. Lu, 'Protein synthesis-dependent and -independent regulation of hippocampal synapses by brain-derived neurotrophic factor', *J Biol Chem*, 276: 40, Oct 2001, 37585-37593.
- 500 H. Otera, N. Ishihara and K. Mihara, 'New insights into the function and regulation of mitochondrial fission', *Biochim Biophys Acta*, 1833: 5, May 2013, 1256-1268.
- 501 J. T. Isaac, M. C. Ashby and C. J. McBain, 'The role of the GluR2 subunit in AMPA receptor function and synaptic plasticity', *Neuron*, 54: 6, Jun 2007, 859-871.
- 502 G. G. Turrigiano, K. R. Leslie, N. S. Desai, L. C. Rutherford and S. B. Nelson, 'Activity-dependent scaling of quantal amplitude in neocortical neurons', *Nature*, 391: 6670, Feb 1998, 892-896.
- 503 G. G. Turrigiano and S. B. Nelson, 'Thinking globally, acting locally: AMPA receptor turnover and synaptic strength', *Neuron*, 21: 5, Nov 1998, 933-935.
- 504 G. G. Turrigiano and S. B. Nelson, 'Homeostatic plasticity in the developing nervous system', *Nat Rev Neurosci*, 5: 2, Feb 2004, 97-107.
- 505 D. Martins-de-Souza, W. F. Gattaz, A. Schmitt, C. Rewerts, G. Maccarrone, E. Dias-Neto and C. W. Turck, 'Prefrontal cortex shotgun proteome analysis reveals altered calcium homeostasis and immune system imbalance in schizophrenia', *Eur Arch Psychiatry Clin Neurosci*, 259: 3, Apr 2009, 151-163.
- 506 S. Prabakaran, J. E. Swatton, M. M. Ryan, S. J. Huffaker, J. T. Huang, J. L. Griffin, M. Wayland, T. Freeman, F. Dudbridge, K. S. Lilley, N. A. Karp, S. Hester, D. Tkachev, M. L. Mimmack, R. H. Yolken, M. J. Webster, E. F. Torrey and S. Bahn, 'Mitochondrial dysfunction in schizophrenia: evidence for compromised brain metabolism and oxidative stress', *Mol Psychiatry*, 9: 7, Jul 2004, 684-697, 643.
- 507 C. A. Altar, L. W. Jurata, V. Charles, A. Lemire, P. Liu, Y. Bukhman, T. A. Young, J. Bullard, H. Yokoe, M. J. Webster, M. B. Knable and J. A. Brockman, 'Deficient hippocampal neuron expression of

proteasome, ubiquitin, and mitochondrial genes in multiple schizophrenia cohorts', *Biol Psychiatry*, 58: 2, Jul 2005, 85-96.

508 C. Webhofer, P. Gormanns, V. Tolstikov, W. Zieglgänsberger, I. Sillaber, F. Holsboer and C. W. Turck, 'Metabolite profiling of antidepressant drug action reveals novel drug targets beyond monoamine elevation', *Transl Psychiatry*, 12011, e58.

509 A. Karabatsiakos, C. Böck, J. Salinas-Manrique, S. Kolassa, E. Calzia, D. E. Dietrich and I. T. Kolassa, 'Mitochondrial respiration in peripheral blood mononuclear cells correlates with depressive subsymptoms and severity of major depression', *Transl Psychiatry*, 42014, e397.

510 R. E. Anglin, S. L. Garside, M. A. Tarnopolsky, M. F. Mazurek and P. I. Rosebush, 'The psychiatric manifestations of mitochondrial disorders: a case and review of the literature', *J Clin Psychiatry*, 73: 4, Apr 2012, 506-512.

511 R. E. Anglin, M. A. Tarnopolsky, M. F. Mazurek and P. I. Rosebush, 'The psychiatric presentation of mitochondrial disorders in adults', *J Neuropsychiatry Clin Neurosci*, 24: 42012, 394-409

7.0 Acknowledgements

First I would like to thank Prof. Dr. Christoph Turck, for giving me the opportunity to work in his group and most importantly for the overall interesting topic and freedom he has given me to develop a great independence, scientific self-confidence and my own ideas. I greatly appreciate his support as well as all the scientific as well as non-scientific inputs that have helped pursuing my own interests as well as my maturation. In addition, I really enjoyed the unconventional conversations and opinions as well as I will not forget the year 2023!

I am very grateful for the scientific input during the TAC meetings from Prof. Dr. Rainer Landgraf and Prof. Dr. Dr. Dr. Felix Tretter as well as my collaborators from the MPI of Psychiatry and the University of Cambridge.

A special thank goes to Hans-Joerg Schaeffer and his team from the IMPRS-LS coordination office, who are great, lovely and always very helpful!

Thanks to all I shared my daily “lab-life” with and thanks for the “anecdotic” memories:

Luis Rodrigues: “meat and too much negativity” – made me smile!

Chi-ya Kao: I thank her for not only sharing the “lab-life”, but also the daily one at our home. Thank you for the many nice days with cheese, wine and the even more yammi food!

Christiane Rewerts: “Gute Zeiten, schlechte Zeiten”, organization, laughther and “bear”.

Frederick Dethloff: “STARK”. I guess nothing more to say...

Dongik Park: Thanks for all the fruitful and interesting discussions with a consensus about life and work.

Alex Knorr: She is a lovely, enthusiastic, and great “workaholic”. I especially thank her for the work on the establishment of several protocols and further experiments on the mitochondrial enrichment, BN-PAGE and in-gel-OXPHOS activity measurements!

Jamie Iannace: She is an intelligent, lovely, and curious person. I am thankful for all the interesting conversations and new ideas. I especially thank her for working on the OxyBlots.

Monika Zaba: We were not sharing our “lab-life”, but also our daily one...I am happy that our research groups fused after some time as enjoyed the many conversations and inputs I gained from the psychologist and psychiatric point of views. I am thankful for her being sometimes a dreamer, curious, life-loving, eating, travelling, philosophic talking and thinking: for being unconventional, free and liberal thinking.

Thanks also to the other members of the RG Turck, especially to Giuseppina Maccarone and Michaela Filiou for their discussions and support! Thanks to Ulrike Schmidt and her research group for wonderful discussions and coffee/tea!

I will miss all of them and hope to stay in contact!

Finally, I would like to thank some very special people that have been (and always be) part of my life, without whom I would not have been the person I am now: My parents Hannelore and Siegfried, my sister Susanne and my friends Andrea and Nadine.

Curriculum Vitae

Katja Weckmann

Wilhelmsstraße 16, 55128 Mainz

Katja_Weckmann@yahoo.de

+49 (0) 177 318 1151



Professional and educational history

Research experience

| | |
|-----------------------------|---|
| Mar 2012 to Apr 2016 | Max Planck Institute of Psychiatry, Dept. of Translational research in Psychiatry, Research Group: Proteomics and Biomarkers, Munich |
| PhD student | Ketamine's fast antidepressant drug response: Biosignatures and pathways |
| Supervisor | Prof. Dr. C. W. Turck |
| Sep to Dec 2011 | Max Planck Institute of Psychiatry, Dept. of Translational research in Psychiatry, Research Group: Proteomics and Biomarkers, Munich |
| Internship | Analyses of oxidative stress mediated protein carbonylation levels of a trait anxiety mouse model |
| Supervisor | Prof. Dr. C. W. Turck |
| Jan to Dec 2010 | Institute for Molecular Bio Sciences at Goethe University, Frankfurt/Main |
| Diploma thesis | The biological regulation of the Lon protease in <i>P. anserina</i> |
| Supervisor | Prof. Dr. H. D. Osiewacz |
| Feb to Mar 2009 | Neuroscience Centre of Medical School at Goethe University, Frankfurt/Main |
| Internship | Transcriptome & Proteome Survey of A53T-SNCA overexpressing mice |
| Supervisor | Prof. Dr. G. Auburger |
| Jul to Dec 2008 | Institute for Molecular Bio Sciences at Goethe University, Frankfurt/Main |
| Student assistant | Aging-related research on the mitochondrial protein quality control system, specifically on the Lon protease in <i>P. anserina</i> |
| Supervisor | Prof. Dr. H. D. Osiewacz |
| May to Jun 2008 | Interdisciplinary Centre for Neuroscience at Goethe University, Frankfurt/Main |
| Student assistant | Research on Juvenile Neuronal Ceroid Lipofuscinosis |
| Supervisor | Dr. M. Ruonala |

| | |
|------------------------|---|
| Mar to Apr 2008 | Interdisciplinary Centre for Neuroscience at Goethe University, Frankfurt/ Main |
| Internship | Visualization initial events of EGFR signaling <i>in situ</i> , an application of MELC Technology |
| Supervisor | Dr. M. Ruonala |
| Jan to Feb 2008 | Institute for Molecular Bio Sciences at Goethe University, Frankfurt/ Main |
| Internship | Generation of a proteasomal β 1-subunit over-expression in <i>P. anserina</i> |
| Supervisor | Prof. H. D. Osiewacz |

University Education

| | |
|---------------------|---|
| 2005 to 2010 | Goethe University in Frankfurt/ Main, Germany |
| | Pre-Diploma (equivalent to a B.Sc.) with honours in Biology in 2007 |
| Final grade | 2.4 (good) |
| | Diploma (equivalent to a M.Sc.) with honours in December 2010 |
| Main subjects | Genetics, Neurobiology, and Cell and Developmental biology |
| Final grade | 1.7 (good) |

Pre-university Education

| | |
|---------------------|---|
| 2002 to 2005 | Hessenkolleg in Wiesbaden, Germany |
| | Equivalent to 'A' levels. Focus on biology, english, social studies. |
| Final grade | 2.2 (good) |
| 1999 to 2002 | Gläser GmbH & Co. KG in Bad Kreuznach, Germany |
| | Formal business and economics training to become an industrial management assistant. Business and economics traineeship including: purchasing department, sales division, accounts department, operations management and customer services. |
| 1995 to 1999 | Alfred-Delp-Schule (equivalent to a secondary school) in Hargesheim, Germany |

Scientific methods and techniques

Specialized techniques

- Proteomics including the identification, characterization and quantification of proteins with mass spectrometry
- Metabolomics and proteomic data analyses
- Isolation of mitochondria
- Confocal microscopy

Standard techniques

- DNA: DNA isolation, Southern Blot
- RNA: RNA isolation, PCR, quantitative RT-PCR
- Proteins: Protein isolation, Western blot, "OxyBlot", 1D and 2D SDS-Page electrophoresis
- Cell culture: Fibroblasts, HeLa cells, primary neurons

Computer skills

- Standard: MicroSoft Office Software (Word, Excel, Powerpoint)
- Graphic and design: Adobe Photoshop, Adobe Illustrator, Image J
- Citation: EndNote
- Data analysis: Quantity One, Image Lab, GraphPrism, SSPS, Metaboanalyst

Languages

- German: Mother tongue
- English: very good, both oral and written
- French: moderate, basic communication

Conferences attended (selected)

| | |
|-------------|---|
| 2015 | Poster presentation: "Time-dependent metabolomic profiling of Ketamine drug action reveals hippocampal pathway alterations and Biomarker candidates", 11 th International Conference of the Metabolomics society, Burlingame, USA |
| 2015 | Poster presentation: "Time-dependent metabolomics and proteomics profiling of Ketamine drug action reveals potential targets for fast-acting antidepressants", NPC Progress Meeting, Utrecht, Netherlands |
| 2014 | Poster presentation: "Time-dependent metabolomic profiling of Ketamine drug action reveals hippocampal pathway alterations", SFN, Society for Neuroscience, Annual meeting, Washington DC, USA |
| 2014 | Oral presentation: "Exploring molecular correlates and affected pathways of Ketamine drug action", 4 th Annual PRIME-XS meeting, Avila, Spain |
| 2008 | Poster presentation: "Exploring the Toponome of Juvenile Neuronal Ceroid Lipofuscinosis", ICNF-Symposium "Neuroscience in Frankfurt", Frankfurt/ Main, Germany |

Academic achievements

Publication

Weckmann K et al., Time-dependent metabolomics profiling of Ketamine drug action reveals hippocampal pathway alterations and biomarker candidates, Translational Psychiatry, 2014

Honours and Awards

- 2015** Mifek-Kirschner award, Max Planck Institute of Psychiatry, Munich
- 2015** Travel grant for the 11th International Conference of the Metabolomics Society in San Francisco, USA
- 2015** Travel grant for the NPC progress meeting in Utrecht, The Netherlands
- 2013** PRIME-XS, a European Union funded access to an infrastructure of state-of-the-art proteomics technology. Collaboration with the PRIME-XS access site of Cambridge Centre for Proteomics, Cambridge, UK

Ph.D. fellowship

- 2012 to 2016** International Max Planck Research School for Molecular and Cellular Life Sciences: From Biology to Medicine (IMPRS-LS)

Supervision

-
- May to Sep 2013** B.Sc. student

Advanced and specialized methods training

Project management skills

- Time and project management

Communication and soft skills

- Scientific Writing
- Power point presentation
- Poster Design
- Career Mentoring & Management
- Conflict Management

Methods training

- Advanced proteomics course for molecular biologists and clinicians
- Introduction to Statistics

Voluntary work and social contribution

-
- Ph.D. representative of the Max Planck Institute of Psychiatry, Munich, Germany
 - Co-founder of the Window of Life foundation in Germany. The foundation supports a local organization in Uganda that runs a Babies home and finances the education of talented children from Uganda and Rwanda

Referees

-
- Prof. Dr. C. Turck, Max Planck Institute of Psychiatry, Munich, +49 (0) 89 30622 317
 - Prof. Dr. H. D. Osiewacz, Goethe University in Frankfurt/ Main, +49 (0) 69 79829 263
 - Dr. M. Ruonala, Goethe University in Frankfurt/ Main, +49 (0) 69 79829 463333